National Library of Canada
Bibliothèque nationale du Canada

Canadian Theses Service
Service des thèses canadiennes

Ottawa, Canada
K1A 0N4

NOTICE

The quality of this microform is heavily dependent upon the quality of the original thesis submitted for microfilming. Every effort has been made to ensure the highest quality of reproduction possible.

If pages are missing, contact the university which granted the degree.

Some pages may have indistinct print especially if the original pages were typed with a poor typewriter ribbon or if the university sent us an inferior photocopy.

Reproduction in full or in part of this microform is governed by the Canadian Copyright Act, R.S.C. 1970, c. C-30, and subsequent amendments.

AVIS

La qualité de cette microforme dépend grandement de la qualité de la thèse soumise au microfilmage. Nous avons tout fait pour assurer une qualité supérieure de reproduction.

S'il manque des pages, veuillez communiquer avec l'université qui a conféré le grade.

La qualité d'impression de certaines pages peut laisser à désirer, surtout si les pages originales ont été dactylographiées à l'aide d'un ruban usé ou si l'université nous a fait parvenir une photocopie de qualité inférieure.

La reproduction, même partielle, de cette microforme est soumise à la Loi canadienne sur le droit d'auteur, SRC 1970, c. C-30, et ses amendements subséquents.

NL-339 (r. 88/04) c

Canada

UNIVERSITY OF ALBERTA

GAS-PHASE REACTIONS OF SULFUR ATOMS WITH ALKENES

BY

JYOTHI MARY JOSEPH

A THESIS

SUBMITTED TO THE FACULTY OF GRADUATE STUDIES AND RESEARCH IN PARTIAL FULFILLMENT OF THE REQUIREMENTS FOR THE DEGREE OF DOCTOR OF PHILOSOPHY

DEPARTMENT OF CHEMISTRY

EDMONTON, ALBERTA

SPRING, 1991

National Library of Canada
Bibliothèque nationale du Canada

Canadian Theses Service
Service des thèses canadiennes

Ottawa, Canada
K1A 0N4

The author has granted an irrevocable non-exclusive licence allowing the National Library of Canada to reproduce, loan, distribute or sell copies of his/her thesis by any means and in any form or format, making this thesis available to interested persons.

The author retains ownership of the copyright in his/her thesis. Neither the thesis nor substantial extracts from it may be printed or otherwise reproduced without his/her permission.

L'auteur a accordé une licence irrévocable et non exclusive permettant à la Bibliothèque nationale du Canada de reproduire, prêter, distribuer ou vendre des copies de sa thèse de quelque manière et sous quelque forme que ce soit pour mettre des exemplaires de cette thèse à la disposition des personnes intéressées.

L'auteur conserve la propriété du droit d'auteur qui protège sa thèse. Ni la thèse ni des extraits substantiels de celle-ci ne doivent être imprimés ou autrement reproduits sans son autorisation.

ISBN 0-315-66831-8

Canada

University of Alberta
Edmonton
Canada T6G 2G2

Department of Chemistry
Faculty of Science
E3-44 Chemistry Bldg., Tel. (403) 492-3254 Fax (403) 492-8231

PUBLICATIONS DIVISION
MAR 5 1991

March 01, 1991

Permissions Editor
American Chemical Society
1155 Sixteenth Street N.W.
Washington, D.C.
20036
U.S.A.

BOOKS & JOURNALS DIVISION
1155 - 16th St., N.W.
Washington, D.C. 20036
3-5-91

PERMISSION TO REPRINT IS GRANTED BY THE AMERICAN CHEMICAL SOCIETY
ACS COPYRIGHT CREDIT LINE REQUIRED. Please follow this sample: Reprinted with permission from (full journal reference). Copyright (year) American Chemical Society.
Barbara F. Blansky
Copyright Administrator

Dear Sir:

I would like to request permission to reproduce Figure 7 from "Stereospecificity of the S(^3P_J) + Butene-2 Reaction and the NMR Spectra of the 1,2-Dimethylthiiranes: An Experimental and Theoretical Study", J. Am. Chem. Soc., V. 112, pp. 8670-8678 (1990) by J. Joseph, R.K. Gosavi, A. Otter, G. Kotovych, E.M. Lown and O.P. Strausz in my Ph.D. Thesis to be submitted to the UNIVERSITY OF ALBERTA, Edmonton, Alberta, Canada.

Thanking you in advance, I remain,

Yours sincerely,

Jm Joseph

Jyothi M. Joseph

P.S. Please send the copyright release form to me at the following address: Department of Science, Grande Prairie Regional College, 10726 - 106 Ave., Grande Prairie, Alta., Can. T8V 4C4

P.P.S. I have the permission from the co-authors.

UNIVERSITY OF ALBERTA

RELEASE FORM

NAME OF AUTHOR:	JYOTHI MARY JOSEPH
TITLE OF THESIS:	GAS-PHASE REACTIONS OF SULFUR ATOMS WITH ALKENES
DEGREE:	Ph.D.
YEAR THIS DEGREE GRANTED:	1991

PERMISSION IS HEREBY GRANTED TO THE UNIVERSITY OF ALBERTA LIBRARY TO REPRODUCE SINGLE COPIES OF THIS THESIS AND TO LEND OR SELL SUCH COPIES FOR PRIVATE, SCHOLARLY OR SCIENTIFIC RESEARCH PURPOSES ONLY.

THE AUTHOR RESERVES OTHER PUBLICATION RIGHTS, AND NEITHER THE THESIS NOR EXTENSIVE EXTRACTS FROM IT MAY BE PRINTED OR OTHERWISE REPRODUCED WITHOUT THE AUTHOR'S WRITTEN PERMISSION.

J.M. Joseph

17311 - 81 Avenue
Edmonton, Alberta
T5T 0B8

Date: April 22, 1991

UNIVERSITY OF ALBERTA

FACULTY OF GRADUATE STUDIES AND RESEARCH

THE UNDERSIGNED CERTIFY THEY HAVE READ , AND RECOMMEND TO THE FACULTY OF GRADUATE STUDIES AND RESEARCH FOR ACCEPTANCE, A THESIS ENTITLED "GAS-PHASE REACTIONS OF SULFUR ATOMS WITH ALKENES."
SUBMITTED BY JYOTHI MARY JOSEPH
IN PARTIAL FULFILLMENT OF THE REQUIREMENTS FOR THE DEGREE OF DOCTOR OF PHILOSOPHY IN CHEMISTRY.

O.P. Strausz - Supervisor

L.G. Hepler

G. Kotovych

J. Takats

P. Sporns - Food Science

M. Back - University of Ottawa

Date: Jan. 7 1991

To my family and friends

ABSTRACT

The gas-phase reactions of ground ($^3P_{2,1,0}$) and lowest excited state ($^1D_2$) sulfur atoms with tetrahydrothiophene, 2-fluoropropene and the cis and trans isomers of 2-butene, 1,2-difluoroethylene and 1,2-dichloroethylene, have been studied.

With tetrahydrothiophene at pressures <104 Torr, the products at short conversions were CS_2, n-C_4H_9SH, H_2S and C_2H_4, due to fragmentation of either a vibrationally excited tetrahydrothiophene thiosulfoxide or of the isomerized 1,2-dithiane, formed from the S(^1D, ^3P) atom attack on the S atom of tetrahydrothiophene. 1,2-Dithiane was not detected.

With 2-fluoropropene, S($^1D_2$) atoms add to the double bond and insert into the C–H bonds to give the three novel compounds: 2-fluoro-2-methylthiirane, 2-fluoro-2-propene-1-thiol and Z-2-fluoro-1-propenethiol, as identified by their NMR, IR and mass spectra. E-2-fluoro-1-propenethiol was not detected.

The products obtained for the S(^3P) + cis- and trans-2-butene and cis- and trans-1,2-difluoroethylene reactions were identified by NMR and mass spectra. S(^3P) atoms were found to react stereospecifically with cis- and trans-2-butene, cis-1,2-difluoroethylene and trans-1,2-dichloroethylene. This is the only divalent species known to react stereospecifically in the triplet state. Ab initio m.o. calculations on the S(^3P) + C_2H_4 reaction predict the lowest triplet state thiirane to be the initial product via a spin, state and orbital symmetry allowed concerted process. The energy released in the reaction (~60 kcal mol^{-1}) is not sufficient to drive rotation about the C–C bond in the triplet thiirane, which has a rotational barrier of ~5.4 kcal mol^{-1} and an excitation energy of 54.0 kcal mol^{-1}. In triplet state dimethylthiirane the rotational barrier is expected to be even higher, hence the observed stereospecificity.

With increasing conversion, the stereoselectivity of the S(^3P) + cis- and trans-2-butene reactions decreases due to isomerization of the 2-butenes caused by the reversible

addition of the triplet 2,3-dimethylthiiranes to the butenes and to photodecomposition, polymerization and desulfurization of the thiirane products. No isomerization of cis- and trans-1,2-difluoroethylene and 1,2-dichloroethylene was detected.

The $S(^3P)$ + trans-1,2-difluoroethylene reaction was found to be ~87% stereoselective and the $S(^3P)$ + cis-1,2-dichloroethylene, ~91% stereoselective.

Since 2,3-difluorothiiranes and 2,3-dichlorothiiranes were not found to mediate the isomerization of cis- and trans-1,2-difluoroethylene and 1,2-dichloroethylene, respectively, dimethylthiiranes were photolyzed ($\lambda > 225$ nm) in the presence of difluoroethylenes. Again no isomerization of the difluoroethylenes was detected. Trans-2,3-difluorothiirane when photolyzed in the presence of cis-2-butene did not effect isomerization of the latter.

ACKNOWLEDGEMENTS

The author wishes firstly, to express her sincere appreciation to Dr. O.P. Strausz for his patient supervision, enlightening comments and monetary as well as moral support. It has been a pleasant working and learning experience.

I would also like to express heartfelt gratitude to Dr. E.M. Lown who has read and edited my thesis several times and has painstakingly drawn all the structures therein.

I would like to express my sincere gratitude to the following people who have imparted to me their knowledge and skills: to Mr. Andrew Jodhan who taught me glassblowing and later ran g.c. mass spectra for me, to Dr. Toshi Yokota who assisted me with the construction of my vacuum system, to Drs. Manuel Torres, Deane McIntyre and George Kotovych who assisted me with the interpretation of NMR data, to Dr. Alvin Otter who performed computer simulations of NMR spectra, to Dr. R.K. Gosavi who carried out theoretical calculations to augment my experimental results, and my special thanks to Mr. Alan Clement who assisted me with the modification of my vacuum system and helped in countless other ways when I was carrying out initial experiments.

I would also like to thank Mrs. Lillian Eastman, who has always cheerfully and speedily typed up documents for me, and the other members of my research group who were always ready and willing to provide assistance.

I would also like to express my appreciation of all the services rendered by members of the technical and secretarial staff. They were always friendly and efficient, and it has been a pleasure to work with them.

I am grateful to have had the opportunity of associating with the academic staff who were excellent in teaching and carrying out research and who were very personable. I hope to emulate to some degree the people I have appreciated and learned from. I thank the members of my committee for their valuable evaluations.

I don't know if I would have made it without the compassion and friendship of some very special people, especially my best friend, Marei Griffith who, with her family, has stuck with me through many unpleasant as well as happy situations. I have also appreciated the friendships of Angelina Morales, Patricia Rose, Patrica Lane-Bell, Jed Harrison, Margaret-Ann Vaughan, John Crerar and that of many people who worked on the 3rd Floor, West Wing, as well as that of people in the rest of the department. The warmth of the people from China has been very refreshing.

I thank my parents, Mr. and Mrs. Jesudasan Ipe and my brothers, Joshi and Jith for their encouragement and for making it possible for me to attend the University of Alberta. I also thank my uncle and aunt, Mr. and Mrs. S. Zachariah and my cousins, Shaju, Saly and Sheena, who have been my family and have provided the love and support I needed in Edmonton. I have also appreciated the friendships of the Malayalee people in Edmonton and that of the congregation of Meadowlark-Westland Baptist Church.

I thank my supervisor, Dr. O.P. Strausz and the Department of Chemistry, University of Alberta, for the financial assistance to conduct research pertaining to my thesis.

Last but not least I would like to thank June Kylor Gibson for her perseverance, speed and cheerfulness in typing the thesis before you.

All Glory, Laud and Honor to the Lord for His Grace, Mercy and Faithfulness.

TABLE OF CONTENTS

Page

ABSTRACT

ACKNOWLEDGEMENTS

LIST OF TABLES

LIST OF FIGURES

CHAPTER I: INTRODUCTION 1

A. The Sulfur Atom [Ne]$3s^2 3p^4$ 2

B. Carbonyl Sulfide – A Good Source of Sulfur Atoms 3

C. Gas-Phase Reactions of ($^1D_2$) and (^3P_J) S Atoms with COS 6

D. Reactions of Group VIA Atoms 10

(a) with alkanes 10

(i) S(^{1}D) Atom Reactions 10

(ii) O(^{1}D) Atom Reactions 13

(iii) Se(^{1}D) and Te(^{1}D) Atom Reactions 15

(iv) S(^{3}P) Atom Reactions 16

(v) O(^{3}P) Atom Reactions 16

(vi) Se(^{3}P) and Te(^{3}P) Atom Reactions 17

(vii) S-Atom Reactions in the Liquid Phase 18

(viii) S-Atom Reactions in Low Temperature Matrices 19

(ix) S($^1S_0$) Atom Reactions 20

(b) with alkenes 20

(i) S(^{1}D) Atom Reactions 20

(ii) O(^{1}D) Atom Reactions 23

(iii) Se(^{1}D) and Te(^{1}D) Atom Reactions 24

(iv) S(^{3}P) Atom Reactions 24

(v) O(^{3}P) Atom Reactions 29

(vi) Se(^{3}P) and Te(^{3}P) Atom Reactions 32

(vii) S-Atom Reactions in the Liquid Phase 33

(viii) S- and O-Atom Reactions in Low Temperature Matrices 33

Page

(ix) $S(^1S_0)$ Atom Reactions 34
(c) with alkynes 34
(i) $S(^1D)$ Atom Reactions 34
(ii) $O(^1D)$ Atom Reactions 37
(iii) $Se(^1D)$ and $Te(^1D)$ Atom Reactions 38
(iv) $S(^3P)$ Atom Reactions 38
(v) $O(^3P)$ Atom Reactions 39
(vi) $Se(^3P)$ and $Te(^3P)$ Atom Reactions 41
(vii) S-Atom Reactions in the Condensed Phases 41
(viii) $S(^1S_0)$ Atom Reactions 41
(d) with dienes 42
(i) $S(^1D,^3P)$ Atom Reactions 42
(ii) $O(^1D,^3P)$ Atom Reactions 45
(iii) Se and Te Atom Reactions 49
(e) with aromatics 49
(i) S-Atom Reactions 49
(ii) $O(^3P)$ Atom Reactions 50
(f) with thioethers 52
(i) $S(^1D,^3P)$ Atom Reactions 52
(ii) $O(^3P)$ Atom Reactions 54
E. Other Gas-Phase Reactions and Quenching Interactions of S Atoms 57
(a) with hydrogen 57
(b) with oxygen 58
(c) with NO_2 59
(d) with N_2O 60
(e) with CO_2 60
(f) with NO 61
(g) with CS_2, SO_2 and H_2S 61
(h) with CO, N_2, Xe, Kr, Ar, Ne, He and SF_6 62
(i) with silanes, boranes and carboranes 63
F. Aim of the Present Investigation 63

Page

CHAPTER II: EXPERIMENTAL 71
A. High-Vacuum System 71
B. Photolytic Assembly 73
C. Materials Used and Their Purification 73
D. Operating Procedures 74
E. Analytical Techniques 75

CHAPTER III: REACTIONS OF SULFUR ATOMS WITH TETRAHYDROTHIOPHENE 85
A. Results 85
(a) UV absorption of tetrahydrothiophene 85
(b) Reaction Products 85
B. Discussion 86

CHAPTER IV: REACTIONS OF SULFUR ATOMS WITH 2-FLUOROPROPENE 91
A. Results 91
(a) Reaction Products 91
(i) Identifications 91
(ii) Properties of products **1**, **2** and **3** 97
(b) Variation in Product Yields as a Function of Irradiation Time and Pressure 98
B. Discussion 98

CHAPTER V: REACTIONS OF SULFUR ATOMS WITH CIS- AND TRANS-ALKENES 113
A. Results 113
1. $S(^3P)$ + Cis- and Trans-2-butene 113
(a) Reaction Products 113
(i) Identifications 113
(ii) Properties of the C_4H_8S isomers 116
(b) Retention of Stereospecificity in the Products and Extent of Isomerization of the Reactants 117

Page

2. S + Cis- and Trans-1,2-difluoroethylene 117
(a) Reaction Products 117
(i) Identifications 118
(ii) Properties of the reaction products 120
(b) Effect of Photolysis Time and Increasing $C_2H_2F_2$ Pressure on Product Yields and Distributions in the $S(^3P) + C_2H_2F_2$ Reaction 121
(c) Effect of Photolysis Time and Increasing $C_2H_2F_2$ Pressure on Product Yields and Distributions in the $S(^1D,^3P) + C_2H_2F_2$ Reaction 121
3. S + Cis- and Trans-1,2-dichloroethylene 123
(a) Reaction Products 123
(b) Effect of Photolysis Time on the Yields and Mole Fractions of the $C_2H_2Cl_2S$ Products from the $S + C_2H_2Cl_2$ Reactions 124
B. Discussion 125
1. $S(^3P)$ + Trans- and Cis-2-butene 126
2. S + Trans- and Cis-difluoroethylene 140
(a) $S(^3P)$ + trans- and cis-difluoroethylene 140
(b) $S(^1D,^3P)$ + trans- and cis-DFE 145
3. S + Cis- and Trans-1,2-dichloroethylene 151
(a) $S(^3P)$ + trans- and cis-dichloroethylene 151
(b) $S(^1D,^3P)$ + trans- and cis-DClE 153

CHAPTER VI: ISOMERIZATION OF ALKENES BY THIIRANE DERIVATIVES 185
A. Results 185
B. Discussion 185

CHAPTER VII: SUMMARY AND CONCLUSIONS 191

BIBLIOGRAPHY 197

		Page
APPENDIX		211
A	Extinction Coefficient Values, $\varepsilon(10 \times cm^{-1} Torr^{-1})$	211
B-1	Mass Spectral Data for C_3H_5FS Isomers	212
B-2	Mass Spectral Data for C_4H_8S Isomers	213
B-3	Mass Spectral Data for $C_2H_2F_2S$ Isomers	214
B-4	Mass Spectral Data for $C_2H_2Cl_2S$ Isomers	215

LIST OF TABLES

Table		Page
I–1	Atomic Energy Levels of Ground and Lower Excited States of the Group VIA Atoms	65
I–2	Some Photochemical Sources of the Group VIA Atoms in the Gas Phase	66
I–3	Rate Constants at 298 K and Rate Parameters for $S(^3P_J)$ and $O(^3P_J)$ Reactions with Selected Alkenes	67
I–4	Rate Constants at 298 K and Rate Parameters for $Se(^3P_J)$ and $Te(^3P_J)$ Reactions with Selected Alkenes	68
I–5	Rate Constants for the Deactivation of $S(^1D_2)$ and $S(^1S_0)$ Atoms by Various Molecules	69
II–1	Columns and Conditions Used	79
II–2	Retention Times of Reactants and Products under Given Conditions on Given Columns	80
IV–1	Variation in Product Yields from the $S(^1D, ^3P)$ + 2-Fluoropropene Reaction as a Function of Irradiation Time	104
IV–2	Variation in Product Yields from the $S(^1D, ^3P)$ + C_3H_5F Reaction as a Function of C_3H_5F Pressure	105
V–1	Effect of Increasing Photolysis Time on the Product Yields from the $S(^3P)$ + Trans-2-butene Reaction	156
V–2	Effect of Increasing Photolysis Time on the Product Yields from the $S(^3P)$ + Cis-2-butene Reaction	157

V–3	Product Recoveries in the $S(^3P)$ + Trans-2-butene Reaction	158
V–4	Effect of Increasing Photolysis Time on the Product Yields from the $S(^3P)$ + Cis-1,2-difluoroethylene Reaction	159
V–5	Effect of Increasing Photolysis Time on the Product Yields from the $S(^3P)$ + Trans-1,2-difluoroethylene Reaction	160
V–6	Effect of Increasing Trans-1,2-difluoroethylene Pressure on the Product Yields from the $S(^3P)$ + Trans-1,2-difluoroethylene Reaction	161
V–7	Effect of Increasing Cis-1,2-difluoroethylene Pressure on the Product Yields from the $S(^3P)$ + Cis-1,2-difluoroethylene Reaction	162
V–8	Effect of Increasing Photolysis Time on the Product Yields from the $S(^1D,^3P)$ + Cis-1,2-difluoroethylene Reactions	163
V–9	Effect of Increasing Trans-1,2-difluoroethylene Pressure on the Product Yields from the $S(^1D,^3P)$ + Trans-1,2-difluoroethylene Reaction	164
V–10	Effect of Increasing Cis-1,2-difluoroethylene Pressure on the Product Yields from the $S(^1D,^3P)$ + Cis-1,2-difluoroethylene Reaction	165
V–11	Effect of Increasing Photolysis Time on the $C_2H_2Cl_2S$ Yields from the S + Trans-1,2-dichloroethylene Reaction	166
V–12	Effect of Increasing Photolysis Time on the $C_2H_2Cl_2S$ Yields from the S + Cis-1,2-dichloroethylene Reaction	167
VI–1	Mole Fractions of Reactants and Some Products from the Reactions between Substituted Ethylenes and Triplet-State Thiirane Derivatives	190

LIST OF FIGURES

Figure		Page
I–1	CO Yield as a Function of Increasing 1-Butene Pressure in the COS + 1-C_4H_8 Reaction	70
II–1a	The Mercury-free Section of the High Vacuum System	82
II–1b	The Non-mercury-free Part of the High Vacuum System	83
II–2	Lamp Profile (Δ) and Absorbance Profile of: 80 Torr COS, 2 Vycor Filters (○) and 100 Torr COS, 3 Vycor Filters (●)	84
IV–1	^1H and ^{19}F NMR Spectra of Product **1**	106
IV–2	^{13}C NMR Spectrum of Product **1**	107
IV–3	Infrared Spectra of Products **1**, **2** and **3**	108
IV–4	^1H and ^{19}F NMR Spectra of Product **2**	109
IV–5	^1H and ^{19}F NMR Spectra of Product **3**	110
IV–6	Rates of Formation of Products **1**, **2** and **3** as a Function of CO yield.	111
IV–7	Variation in the Yields of CO and Products **1**, **2** and **3** as a Function of 2-Fluoropropene Pressure	112
V–1	^1H NMR Spectra of Trans- and Cis-2,3-dimethylthiirane.	168
V–2	Mole Fractions of Trans-C_4H_8 and Trans-C_4H_8S as a Function of CO in the $S(^3P)$ + Trans-C_4H_8 Reaction	169

V–3	Mole Fractions of Cis-C_4H_8 and Cis-C_4H_8S as a Function of CO in the $S(^3P)$ + Cis-C_4H_8 Reaction	170
V–4	Rates of C_4H_8S Formation as a Function of CO Yield for the $S(^3P)$ + Trans- and Cis-C_4H_8 Reactions	171
V–5	^1H and ^{19}F NMR Spectra of Trans-2,3-difluorothiirane	172
V–6	^1H and ^{19}F NMR Spectra of Cis-2,3-difluorothiirane	173
V–7	Mole Fractions of the Stereoselective Product in the $S(^3P)$ + Trans- and Cis-$C_2H_2F_2$ Reactions as a Function of CO Yield	174
V–8	Rates of Product Formation as a Function of CO Yield in the $S(^3P)$ + Trans- and Cis-$C_2H_2F_2$ Reactions	175
V–9	Mole Fractions of Trans- and Cis-$C_2H_2F_2S$ as a Function of $C_2H_2F_2$ Pressure.	176
V–10	Rates of Product Formation as a Function of $C_2H_2F_2$ Pressure in the $S(^3P)$ + Trans- and Cis-$C_2H_2F_2$ Reactions	177
V–11	Rates of Product Formation as a Function of CO Yield for the $S(^1D, ^3P)$ + Cis-$C_2H_2F_2$ Reaction	178
V–12	Mole Fraction of Cis-$C_2H_2F_2S$ as a Function of CO Yield for the $S(^1D, ^3P)$ + Cis-$C_2H_2F_2$ Reaction	179
V–13	Mole Fractions of $C_2H_2F_2S$ Products from the $S(^1D, ^3P)$ + Trans- and Cis-$C_2H_2F_2$ Reactions as a Function of $C_2H_2F_2$ Pressure	180
V–14	Variation in Product Yields as a Function of $C_2H_2F_2$ Pressure in the $S(^1D, ^3P)$ + Trans- and Cis-$C_2H_2F_2$ Reactions	181

V–15 Mole Fractions of the Stereoselective $C_2H_2Cl_2S$ Products in the S + Trans- and Cis-$C_2H_2Cl_2$ Reactions as a Function of CO Yield, in the Presence (•), and in the Absence (○) of 1200 Torr CO_2 182

V–16 Rates of Product Formation as a Function of CO Yield for the S + Trans- and Cis-$C_2H_2Cl_2$ Reactions, in the Presence (•,▲), and in the Absence (○,△) of 1200 Torr CO_2 183

V–17 Reaction Surface for the $S(^3P)$ and $S(^1D)$ Addition to C_2H_4 (^1A_g) 184

CHAPTER I

INTRODUCTION

The world around us comprises a little over one hundred elements as building blocks, most of which have been studied down to the atomic level. Knowledge of the atomic structure and the chemical behavior patterns of the elements has facilitated the arrangement of the elements into the Periodic Table, where elements with similar chemical reactivities, due to their similar configuration of valence electrons, fall in the same group. The atomic reactions of elements are quite different from their molecular reactions and small differences in the atomic reactivities and properties of elements in the same group may result in significant differences in reactivities at the molecular level. In this study the gas-phase reactions of sulfur atoms in the ground state and the lowest excited state are examined further and are compared to the atomic reactions of the other group VIA elements.

Except for the noble gases, the atoms of most elements are not present in nature as such because of their free radical character, i.e. they have an incomplete outer shell of electrons, which renders them highly reactive. Metal atoms were among the first to be studied in the early 1900's since they could be easily formed thermally, by heating the metal surface.[1] By 1912 Langmuir had generated hydrogen atoms,[2] but it was not until the 1950's that most metal and non-metal atom reactions began to be studied extensively, when convenient methods of generation of the atoms were discovered. The reactions of oxygen atoms became of particular interest when they were found to be continuously generated in the atmosphere by the stratospheric photolysis of molecular oxygen and ozone. This prompted the study of the reactions of the atoms of the next group VIA element, sulfur, especially when the photolysis of carbonyl sulfide (COS) was found to be a good source of sulfur atoms.[3] Over the last ten years it has come to light that a small amount of sulfur atoms, about 5.3×10^{10} g y^{-1} globally,[4] are formed in the stratosphere by the photolysis of

COS, which is present in a constant proportion in the earth's atmosphere.[4,5] So reactions of sulfur atoms are of even more interest now.

A. The Sulfur Atom [Ne] $3s^2 3p^4$

The sulfur atom ($^{32}_{16}S$ - 95.02%, $^{34}_{16}S$ - 4.21%), like the other atoms of the group VIA elements, oxygen, selenium, tellurium, and the radioactive element polonium, has six valence electrons leading to a ground state electronic configuration of ns^2np^4, where n = 3. These valence electrons are arranged around the sulfur atom in an approximately tetrahedral configuration as two lone pairs and two unpaired electrons. If the latter have parallel spins a triplet state results, where $S = {}^1/_2 + {}^1/_2 = 1$. A singlet state corresponds to antiparallel spins i.e. $S = {}^1/_2 - {}^1/_2 = 0$. The triplet state comprises three levels corresponding to $J = |L + S| \ldots |L - S| = L + 1, L + 0$ and $L - 1$, which are very close in energy, whereas a singlet state consists of only one energy level, $J = L + 0$. From the ns^2np^4 electronic configuration, the following allowed spectroscopic states are obtained for the group VIA atoms: $^3P_{2,1,0}$, $^1D_2$ and $^1S_0$,[6] the ground state being the $^3P_2$ state according to Hund's rule of maximum multiplicity, maximum L value and maximum J value if the outermost filled subshell is more than half full.[7] The relative energies of the ground and the lower excited states of the group VIA atoms are presented in Table I–1.[8] The energy separations between the ^3P levels in the oxygen and sulfur atoms are very small and until recently it has not been possible to distinguish the reactivities of the three ^3P levels in these atoms. Recently, however, Black[9] reported the detection of electronically hot $^3P_1$ and $^3P_0$ sulfur atoms and monitored their collisionally-induced decay to the thermal equilibrium population. Similar findings have been reported for selenium and tellurium atoms.[10] Under the conditions used in the present study the $^3P_{2,1,0}$ states of the sulfur atom may be considered collectively as the ^3P_J state.[11]

The $^1D_2$ state is the lowest excited state since it has a higher L value than the $^1S_0$ state. The major selection rules governing radiative transitions between electronic states are:

$$\Delta L = \pm 1,\ \Delta S = 0 \text{ and } \Delta J = \pm 1, 0$$

So although a transition between the $^1D_2$ and the $^1S_0$ states is spin allowed, the $\Delta L = \pm 1$ and the $\Delta J = \pm 1, 0$ rules are not met. Transitions between these excited states and the ^3P states are spin forbidden, and only collisional relaxation occurs to the ^3P states. So both the excited states are metastable and have relatively long lifetimes.

B. Carbonyl Sulfide – A Good Source of Sulfur Atoms

To form sulfur atoms thermally from sulfur vapor, the latter has to be heated to 2500 K at a pressure of about 10^{-5} atmospheres, due to the associative tendency of the sulfur atoms. Electrical or microwave discharges passed through sulfur vapor can also produce sulfur atoms.[12] The most convenient method of forming sulfur atoms and the other group VIA atoms is by the photolysis or photosensitization of simple organic or inorganic sulfides, oxides, selenides and tellurides. Table I–2 lists some possible photochemical sources of group VIA atoms. Marquart et al. suggest that there is potential for the thermal production of selenium and tellurium atoms, although this avenue has not been widely pursued.[10]

A good source of atoms should:

1) be readily available, relatively cheap and easy to handle;
2) photolyze in a convenient region of the spectrum, and
3) dissociate in a simple manner to give the required atom in a known spectroscopic state, and the other fragments formed should not interfere with the reactions of the atom.

The photolysis of COS (m.w. = 60.07 g mol^{-1}, m.p. = –138.2 °C, b.p. = –50.2 °C)[32] in the ultraviolet region, using a medium-pressure mercury lamp, is a more convenient source of sulfur atoms than CS_2 or H_2S, which are cheaper, mainly because the other photofragment formed in the photolysis of COS is the stable, neutral, relatively unreactive CO molecule which can also act as an internal actinometer to measure how much photolysis actually took place. Furthermore, unlike COS, CS_2 is not very volatile[32] and would be difficult to separate from the products, and the generation of sulfur atoms from H_2S requires a 2-photon dissociation[22] which entails more sophisticated instrumentation. COS is commercially available at about 96% purity.

Since it is a non-symmetrical linear molecule with $C_{\infty v}$ symmetry, it has absorptions in the UV region with maxima at 152.7 nm (ε = 41 840 L mol^{-1} cm^{-1}), 166.7 nm (ε = 8980 L mol^{-1} cm^{-1}) and 223.7 nm (ε = 81.6 L mol^{-1} cm^{-1})[33] corresponding to the $^1\Sigma^+ \leftarrow {}^1\Sigma^+$ transition in the 142 to 156 nm region, the $^1\Pi \leftarrow {}^1\Sigma^+$ transition in the 156 to 195 nm region and $^1\Delta \leftarrow {}^1\Sigma^+$ transition in the 195 to 270 nm region, respectively.[33, 34] Below 142 nm a series of Rydberg transitions are seen.[33]

The molecular orbital configuration of COS in the ground state is $(6\sigma)^2(7\sigma)^2(8\sigma)^2(2\pi)^4(9\sigma)^2(3\pi)^4(4\pi)^0(10\sigma)^0(11\sigma)^0$.[18,33,34]

When COS absorbs in the 142–156 nm region, giving rise to an intense structured band corresponding to the colinear $^1\Sigma^+ \leftarrow {}^1\Sigma^+$ transition[33] due to a $3\pi \rightarrow 4\pi$ excitation,[34] the sulfur atoms formed are in the $^1S_0$ state in good yield:[14]

$$O{=}C{=}S\ (X^1\Sigma^+) + h\upsilon\ (142 - 156\ nm) \longrightarrow CO(^1\Sigma^+) + S(^1S_0)\ \Phi > 0.8 \qquad [1]$$

In the 156 – 195 nm region, COS absorbs to give a broad diffuse band with vibrational structure corresponding to a transition from a linear $^1\Sigma^+$ state to a bent $^1\Pi$ state,[34] which is due to a $9\sigma \rightarrow 4\pi$ excitation.[18,33,34] Sulfur atoms in both the $^1D_2$ and $^1S_0$ states are formed in this region.[14]

$$COS\ (^1\Sigma^+) + h\upsilon(156 - 195\ nm) \longrightarrow CO(^1\Sigma^+) + S(^1D_2, {}^1S_0) \quad [2]$$

The weak broad band in the 195 to 270 nm region is due to the forbidden linear $^1\Delta \leftarrow {}^1\Sigma^+$ transition ($\Delta\Lambda = +2$), which is made possible by the Herzberg-Teller coupling of the electronic motion with a bending vibration.[35] The bending splits the doubly degenerate $^1\Delta$ state into the $^1A'$ ($^1\Delta$) and $^1A''$ ($^1\Delta$) non-degenerate states[35,36] (also known as the Renner-Teller components of the $^1\Delta$ state),[15] and transitions to both states have been observed.[15] These transitions are also due to the $3\pi \rightarrow 4\pi$ excitation, which gives rise to the $^1\Sigma^+$, $^1\Delta$ and $^1\Sigma^-$ excited states. The absorption of COS in this region yields $^1D_2$ sulfur atoms.[15]

$$COS\ (^1\Sigma^+) + h\upsilon(195 - 270\ nm) \longrightarrow CO(^1\Sigma^+) + S(^1D_2) \quad [3]$$

To obtain sulfur atoms in the ground state, a 10- to 15-fold excess of CO_2 collisionally deactivates the $^1D_2$ sulfur atoms initially produced.[16]

$$S(^1D_2) + \text{excess } CO_2 \longrightarrow CO_2^* + S(^3P_J) \quad [4]$$

Almost no ^3P_J sulfur atoms are formed from the primary photochemical decomposition of $COS(^1\Sigma^+)$[15] due to the spin conservation rule.

The minimum energy required to form sulfur atoms in the $^1S_0$, $^1D_2$ and ^3P_J states from COS can be calculated from the expression:

$$\Delta H^0_f\ (CO) + \Delta H^0_f\ (S) - \Delta H^0_f\ (COS)$$

Since ΔH^0_f (CO) = –26.42 kcal mol^{-1},[32] ΔH^0_f (COS) = –33.96 kcal mol^{-1},[32] $\Delta H^0_f\ [S(^3P_J)]$ = 66.636 kcal mol^{-1},[32] $S(^3P_2) \rightarrow S(^1D_2)$ = 26.42 kcal mol^{-1}, and

$S(^3P_2) \rightarrow S(^1S_0) = 63.42$ kcal mol^{-1}, the minimum energy required to form a $^1D_2$ state sulfur atom from COS is:

$$[(-26.42) + 66.636 + 26.42 - (-33.96)] \text{ kcal mol}^{-1} = 100.60 \text{ kcal mol}^{-1}$$

This energy corresponds to the energy of electromagnetic radiation of wavelength $\lambda = 284.2$ nm. Similar calculations using $E = h\upsilon$ give a maximum wavelength of 385.4 nm for the production of ^3P-state sulfur atoms from COS, but the latter has almost negligible absorption in the 284 to 385 nm region[37] at room temperature, although the absorption increases slightly with increasing temperature.[38] For the production of $^1S_0$ state sulfur atoms, COS must be photolyzed at wavelengths shorter than 207.8 nm.

C. Gas-Phase Reactions of ($^1D_2$) and (^3P_J) S Atoms with COS

The photochemical reactions that occur on photolysis of pure COS in the 200 to 260 nm region are as follows:

$$\text{COS } (^1\Sigma^+) + h\upsilon \longrightarrow \text{CO}(^1\Sigma^+) + S(^1D_2) \quad [3a]$$

$$\longrightarrow \text{CO}(^1\Sigma^+) + S(^3P_{2,1,0}) \quad [3b]$$

$$\text{COS } (^1\Sigma^+) + S(^1D) \longrightarrow \text{CO}(^1\Sigma^+) + S_2(X^3\Sigma_g^-) \quad [5a]$$

$$\longrightarrow \text{CO}(^1\Sigma^+) + S_2(\tilde{a}\ ^1\Delta_g) \quad [5b]$$

$$\text{COS } (^1\Sigma^+) + S(^1D) \longrightarrow \text{COS}(^1\Sigma^+) + S(^3P_J) \quad [6]$$

$$\text{COS } (^1\Sigma^+) + S(^3P_J) \longrightarrow \text{CO}(^1\Sigma^+) + S_2(^3\Sigma_g^-) \quad [7]$$

$$S(^3P_J) + S(^3P_J) + M \longrightarrow S_2(^3\Sigma_g^-) + M^* \quad [8a]$$

$$S(^3P_J) + S(^3P_J) \xrightarrow{\text{wall}} S_2(^3\Sigma_g^-) \quad [8b]$$

$$S_2(\tilde{a}\ ^1\Delta_g) + M \longrightarrow S_2(^3\Sigma_g^-) + M^* \quad [9]$$

$$S(^3P_J) + S_2(^3\Sigma_g^-) \longrightarrow S_3, \text{etc.} \quad [10]$$

That the S atoms formed initially from the long-wavelength photolysis of COS are in the ($^1D_2$) state (reaction [3a]), was first postulated by Lochte-Holtgreven et al. in 1932,[39] and then by Strausz and Gunning in 1962,[3] in consideration of the minimum radiant energy required for photochemical dissociation and because of the spin conservation rule, respectively. Later, however, it was suggested that up to 26% of the S atoms formed in the primary photolytic step were in the (^3P_J) state (reaction [3b]), because not all the sulfur atoms formed could be scavenged by paraffins.[18] Recently, Sivakumar et al.[15] have shown that the quantum yield for the formation of S(^{3}P) atoms in the primary photolytic step is 0.00 ± 0.02 at 222 nm. This is consistent with the conclusion reached by van Veen et al., that in the 210 to 250 nm region only ($^1D_2$) state sulfur atoms are formed.[40] The quantum yield for the overall production of sulfur atoms was determined to be 0.91, and that for CO, 1.81, by Sidhu et al. using the chemical actinometer HBr.[18] Gollnick and Leppin, using uranyl oxalate as an actinometer in the liquid phase and acetone as an actinometer in the gas phase, also determined the quantum yield of CO in the primary photolysis step to be 0.90 ± 0.05.[41] Rudolph and Inn, however, using a calibrated photodiode to measure photon fluxes, obtained a quantum yield value of only 0.72 ± 0.08 over the 200 to 260 nm region.[42] Very recently, Sivakumar et al., using laser-induced fluorescence, claim that the quantum yield for S(^{1}D), i.e. for reaction [3a], is nearly 1.0.[15]

Ground-state sulfur atoms are rapidly formed by the collisional deactivation of ($^1D_2$) sulfur atoms, according to reaction [6].[17,40,43,44] S($^1D_2$) + COS collisions can also result in the formation of S_2 molecules in the ground ($^3\Sigma_g^-$) and the lowest excited ($^1\Delta_g$) states,[40] as shown by reactions [5a] and [5b]. According to van Veen's observations, reactions [5a], [5b] and [6] occur with equal probability.[40] Black recently determined that in the absence of a buffer gas like helium, (45 ± 10)% of the S(^{1}D) + COS collisions result in quenching of the S(^{1}D) to the ground state,[45] whereas in the presence of helium, reaction [6] was four times[43] more probable than reactions [5a] and [5b]. Absolute rate constants reported for the reaction and quenching of S(^{1}D) atoms with COS, i.e. $k_{5a} + k_{5b} + k_6$,

measured by the direct observation of $S(^1D)$ atoms, vary from $1.5 \pm 0.2 \times 10^{-10}$ cm^3 molecule^{-1} s^{-1}, at 300 K in the presence of added helium[45] to $2.98 \pm 0.30 \times 10^{-10}$ cm^3 molecule^{-1} s^{-1}, without any added helium to thermalize the velocity distribution of the $S(^1D)$ atoms.[40] The latter value is similar to that obtained by Addison et al. from a resonance fluorescence study of the $S(^1D)$ atoms, $3.0 \pm 1.0 \times 10^{-10}$ cm^3 molecule^{-1} s^{-1},[20] which was believed to be a better value than the rate constant $1.2 \pm 0.3 \times 10^{-10}$ cm^3 molecule^{-1} s^{-1}, obtained by using time-resolved atomic absorption photometry.[46] Donovan had earlier determined, by following the growth of the S_2 ($g^1\Delta_u \leftarrow a^1\Delta_g$) spectrum, $k_{5a} + k_{5b} \geq 6.6 \times 10^{-11}$ cm^3 molecule^{-1} s^{-1}, using helium as a diluent gas.[44] In the absence of helium the following rate constants are recommended: $k_{5a} + k_{5b} + k_6 \approx 3.0 \times 10^{-10}$ cm^3 molecule^{-1} s^{-1} and $k_6 \approx 1.2 \times 10^{-10}$ cm^3 molecule^{-1} s^{-1}.

The ground state (^3P_J) sulfur atoms formed can also react with COS to give ground state S_2 as shown by reaction [7], which Sidhu et al. estimated to be about 30 times slower than reactions [5a] + [5b].[18] Klemm and Davis, however, calculated a value of only $3.48 \pm 0.39 \times 10^{-15}$ cm^3 molecule^{-1} s^{-1} for k_7[47] which is about four thousand times smaller than $k_{5a} + k_{5b}$. Van Veen et al. recently suggested a value of $3.32 \pm 0.40 \times 10^{-11}$ cm^3 molecule^{-1} s^{-1} for k_7[40] but this estimate probably refers to $k_7 + k_{8a} + k_{8b} + k_{10}$. Van Roodselaar reported a value of 1.7×10^{-13} cm^3 molecule^{-1} s^{-1} for the decay of ground state sulfur atoms, $k_7 + k_8$. According to Fowles et al., at high flash intensities, recombination of the $S(^3P_J)$ atoms through three-body collisions (reaction [8a]) and wall reactions (reaction [8b]) are the main sinks for the ground-state sulfur atoms,[48] whereas at low light intensities reaction [7] predominates.

Reaction [9] accounts for the collisional deactivation of the S_2 molecule, and reaction [10], for the solid sulfur deposited on the face of the cell. Except for S_7, all the polymeric states of the sulfur atom from S_2 to S_8 have been detected in flash photolysis studies.[17]

As indicated previously, the addition of a tenfold excess of CO_2 to the COS system causes more than 90% of the $S(^1D)$ sulfur atoms to be collisionally deactivated to the

ground state.[49] The predominant reactions in this system then become [3a], [4], [7], [8a], [8b] and [10].

Following the sequence of reactions [3a] to [7] which occur in pure COS, it is seen that for every S atom produced, two molecules of CO should be formed. The measured values of $\Phi \geq 0.9$ for $S(^1D)$ atom production and $\Phi = 1.81$ for CO indicate that the recombination processes [8a] and [8b] occur to a minor extent. In the presence of a substrate, such as a hydrocarbon, the CO yield should decrease since the substrate would compete with the COS for the S atom. In fact, it has been found that when 1-butene is added to pure COS, the CO yield drops to almost half its value in COS[16] at high 1-butene pressure, Figure I–1, which means that all the sulfur atoms formed are reacting with the 1-butene and not with COS, i.e. reactions [5a] and [5b] are suppressed. Therefore if $R^o(CO)$ is the rate of CO formation in pure COS, and R(CO) is the rate of CO formation in the presence of a substrate, then the rate of S atoms reacting with a substrate is given by:

$$R(\text{reaction}) = R^o(CO) - R(CO)$$

and the rate of sulfur atoms reacting with COS is given by:

$$R(\text{abstraction}) = R(CO) - \frac{R^o(CO)}{2}$$

Hence,

$$R(\text{reaction}) + R(\text{abstraction}) = \frac{R^o(CO)}{2}$$

is the rate of formation of S atoms in pure COS.[50]

The % recovery of S atoms in the products (not including any polymer) is given by:

$$\frac{R(\sum \text{S-containing products})}{R^o(CO) - R(CO)} \times 100$$

The CO evolved is easy to measure and is therefore useful as an internal actinometer to determine how much reaction has occurred in the COS + substrate system.

D. Reactions of Group VIA Atoms

The reactions of (^{1}D) and (^{3}P) oxygen, sulfur, selenium and tellurium atoms with hydrocarbons and sulfides will now be reviewed. Most of the reported data are for gas-phase reactions; where available, results from liquid- and solid-phase experiments will also be presented.

(a) with alkanes

(i) S(^{1}D) Atom Reactions

The gas-phase reactions of S(^{1}D) atoms with CH_4, C_2H_6, C_3H_8, iso-C_4H_{10}, cyclo-C_3H_6, cyclo-C_4H_8 and cyclo-C_5H_{10}[48,51-53] have been studied by Strausz and coworkers and have been found to yield the corresponding thiol according to the general reaction:

$$S(^1D) + RH \longrightarrow RSH \qquad [11]$$

This proceeds via insertion of the S(^{1}D) atom into a C–H bond. The enthalpy change accompanying the breaking of a C–H bond and formation of a C–S and an S–H bond is ≈ –81 kcal mol^{-1}.

Two mechanisms have been postulated to explain how the insertion occurs. The first mechanism proposed is a three-centred transition state[52,54] analogous to that proposed for

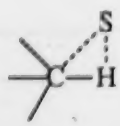

methylene insertion into C–H and H–H bonds. Such a transition state was proposed mainly because S(^{1}D) was found not to discriminate among C–H bond orders in the gas

phase. For instance the distribution of thiols from the S(^{1}D) + propane and isobutane reactions were as follows:[52]

$$\frac{[CH_3CH_2CH_2SH]}{[CH_3CHSHCH_3]} = 2.85 \pm 0.05 \sim 3; \quad \frac{[CH_3CH(CH_3)CH_2SH]}{[CH_3C(SH)(CH_3)CH_3]} = 8.8 \pm 0.1 \sim 9$$

These product ratios correspond exactly to the ratios of primary to secondary C–H bonds in propane (3) and primary to tertiary C–H bonds in isobutane (9).

Recently, using UMNDO calculations, McKee determined the transition states for the S(^{1}D$_2$) + CH_4 and the S(^{1}D$_2$) + C_2H_6 reactions to have the following geometries:[55]

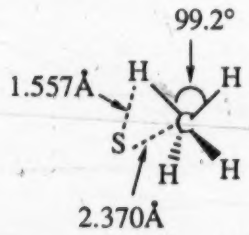

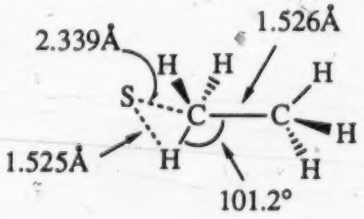

The second mechanism proposed is analogous[17] to the one initially proposed by Benson to account for the insertion of a bulky singlet methylene ($^1CH_2$) group into a C–H bond.[56] In this mechanism, the S(^{1}D) atom attacks the hydrogen atom directly to form a hydrogen bond-like transition state, and this transition state features ionic and radical character:

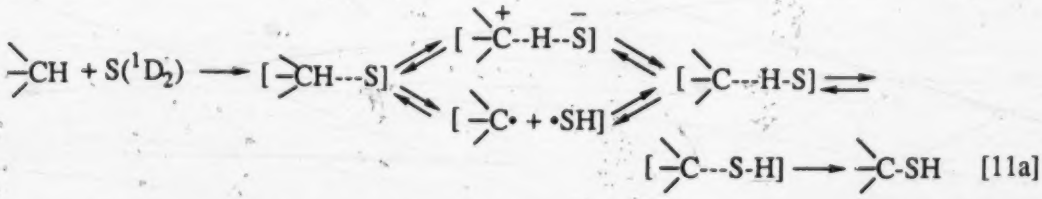

[11a]

It is believed that the partial contributions from the ionic species in the initially-formed transition state aid the abstraction of the hydrogen atom by the sulfur atom[57] to give a weakly coupled alkyl and SH radical pair in which rotation of the SH perpendicular to the CH axis occurs so that the S atom is between the carbon and hydrogen atoms.[57] The

solvent cage is believed to aid this process. This is the preferred mechanism in the liquid phase where the insertion products have been found to follow the order tertiary > secondary > primary, which is the order of increasing C–H bond dissociation energies and decreasing frontier electron densities at the respective H atoms.[58] The reason for the selectivity of the $S(^1D_2)$ atom in the liquid phase would be due to loss of some excess vibrational energy via numerous collisions in the liquid phase. However, in the reaction of $S(^1D)$ atoms with $(CH_3)_3SiH$, the $S(^1D_2)$ atom inserts preferably into the Si–H bond rather than the C–H bond.[17] The H in Si–H has greater hydridic character.[58]

A third, radical mechanism, has been discounted

$$S(^1D) + RH \longrightarrow R\cdot + \cdot SH \qquad [11b]$$

$$R\cdot + \cdot SH \longrightarrow RSH \qquad [12]$$

because no H_2S_2 or R–R products were detected.[52]

In addition to inserting into C–H bonds $S(^1D)$ atoms were postulated to undergo collisional deactivation[50] because the CO yield, even at high alkane pressures, decreased to only about 60% of the CO yield in pure COS,[12] whereas in the presence of alkenes, the CO

$$S(^1D_2) + RH \longrightarrow RH^* + S(^3P_J) \qquad [13]$$

yield is known to decrease to almost 50% of the CO yield in pure COS. Furthermore, it was observed that ground-state sulfur atoms did not insert into C–H bonds at room temperature to form thiols.[52] Recently, Black monitored the evolution profile of $S(^3P_2)$, produced by the interaction of $S(^1D_2)$ atoms with various gases, to determine the branching ratios for insertion and quenching of $S(^1D)$ atoms.[43] Earlier, Black and Jusinski[45] measured the total rate of decay of $S(^1D)$ atoms, i.e. $k_{11a} + k_{13}$, in the presence of helium as a thermalizer, and reported values of $1.70 \pm 0.2 \times 10^{-10}$ and $2.2 \pm 0.2 \times 10^{-10}$ cm^3 molecule^{-1} s^{-1}, for CH_4 and C_2H_6, respectively. The corresponding rate constants for the higher alkanes are believed to be within half an order of magnitude of the CH_4 and C_2H_6 values.[57] The branching ratios obtained by Black[43] for CH_4 and C_2H_6 show about 60%

reaction and 40% quenching in the presence of helium and argon as buffer gases. Hence, k_{11a} = 1.0–1.4 x 10^{-10} cm^3 $molecule^{-1}$ s^{-1} and k_{13} = 6.8–8.8 x 10^{-11} cm^3 $molecule^{-1}$ s^{-1}.

The reaction of $S(^1D)$ with methane has been found to be more complex than the reactions with the higher alkanes because the initially-formed CH_3SH adduct is vibrationally very hot and tends to fragment as shown below:[48]

$$CH_3SH^{*} \longrightarrow CH_3S\cdot + H\cdot \quad [14a]$$

$$\longrightarrow CH_2\cdot + H_2S \quad [14b]$$

$$\longrightarrow CH_3\cdot + HS\cdot \quad [14c]$$

$$\longrightarrow CS\cdot + 2H_2 \quad [14d]$$

The final product distribution obtained is as follows: CH_3SH, 63%; CH_3SSCH_3, 12%; CH_3SCH_3, 6%; C_2H_6, 6%; H_2, 7%; and CS_2, 6%.[52] Prolonged irradiation can cause the secondary photolysis of the thiol products which usually absorb in the photolysis region.

(ii) <u>$O(^1D)$ Atom Reactions</u>

The gas-phase reactions of $O(^1D_2)$ atoms, generated by the 185 or 213.9 nm photolysis of N_2O, with CH_4, C_2H_6, C_3H_8, iso-C_4H_{10}, neo-C_5H_{12}, cy-$(CH_2)_4$ and cy-$(CH_2)_5$ [59,60] were studied in the early 1960's and early 1970's and it has been found that the main reaction that occurs – about 65% of the overall reaction – is insertion of the $O(^1D_2)$ into the C–H bonds as was observed for $S(^1D_2)$ atoms. However, $O(^1D_2)$ atoms have also been found to abstract H atoms from alkanes to give alkyl and hydroxyl radicals.[60] Abstraction occurs to an extent of ~20–30%. Finally, molecular elimination of H_2, accompanied by the formation of the corresponding aldehyde or ketone, is believed to occur to a small extent (less than 10%). The possibility of deactivation of $O(^1D)$ atoms to

the ground state was investigated and it was found that alkanes like methane and neopentane did not deactivate $O(^1D)$.[61] The $O(^1D)$ + alkane reaction sequence is shown below:[60,62]

$$O(^1D_2) + R\text{–}H \longrightarrow ROH^* \quad [15a]$$

$$\longrightarrow R\cdot + \cdot OH \quad [15b]$$

$$\longrightarrow R'HC{=}O \text{ or } R'R''C{=}O + H_2 \quad [15c]$$

$$ROH^* \longrightarrow \text{Fragmentation} \quad [16]$$

$$ROH^* + M \longrightarrow ROH + M^* \quad [17]$$

$$RH + OH \longrightarrow H_2O + R \quad [18]$$

$$R\cdot + R\cdot \longrightarrow R\text{–}R \quad [19a]$$

$$\longrightarrow RH + \text{corresponding alkene} \quad [19b]$$

The insertion reaction, [15a], results in the formation of a vibrationally "hot" alcohol which fragments at low pressures. The fragmentation products vary to some extent with the nature of the R group. The enthalpy change accompanying the breaking of the C–H bond and the formation of C–O and O–H bonds is about ~–141 kcal mol^{-1} which is much higher than that of the corresponding reactions with $S(^1D)$ atoms, hence the formation of "hot" alcohols. At high enough pressure (reaction [17]) the "hot" alcohols may be stabilized. "Hot" propanols formed at room temperature from the 2139 Å photolysis of N_2O in the presence of propane, require more than 2500 Torr pressure for stabilization, whereas the "hot" neopentanol, which has greater degrees of freedom, is stabilized at about 150 Torr.[62] Evidence for the occurrence of the abstraction reaction [15b] is found in the formation of H_2O in reaction [18], of the corresponding alkene in reaction [19b] and the dialkane in reaction [19a]. $O(^1D)$ atoms are able to abstract hydrogen from alkanes because the $O(^1D)$ atom reaction is exothermic by about 66 kcal mol^{-1} whereas the $S(^1D)$ atom

abstraction reaction is exothermic by about only 19 kcal mol^{-1}.[50] Reaction [15c] illustrates the H_2 elimination reaction.

The O(^{1}D) + alkane insertion reaction gives a statistical ratio of products. For the abstraction reaction the O(^{1}D) atom is believed to approach the alkane in a direction colinear to an R–H bond, while for the insertion reaction the O(^{1}D) atom approaches the alkane perpendicular to a C–H bond.[63] Rate constants for the O(^{1}D) + alkane reaction vary between 3.1 x 10^{-10} and 12.4 x 10^{-10} cm^3 molecule^{-1} s^{-1}.[64] As in the S(^{1}D) atom reactions, secondary products may be formed from the photolysis of the primary products upon prolonged irradiation.

(iii) Se(^{1}D) and Te(^{1}D) Atom Reactions

The reactions of Se($^1D_2$) atoms, generated from the photolysis of COSe, were studied by Tyerman et al.,[27] who found that Se($^1D_2$) atoms inserted into the C–H bonds of propane, cyclopropane and cyclobutane to give the corresponding selenomercaptans as the major products. However, Se_2 was also observed to be a product, as a result of the more rapid rate of abstraction of Se from COSe, even at high alkane to COSe ratios. The major reactions that occur when Se(^{1}D) atoms react with alkanes are as follows:

$$Se\ (^1D_2) + R\text{–}H \longrightarrow R\text{–}Se\text{–}H \qquad [20]$$

$$Se\ (^1D_2) + COSe \longrightarrow CO + Se_2 \qquad [21]$$

Se_2 formation was not suppressed even when a 15-fold excess of hydrocarbon was used. Se($^1D_2$) atoms also insert into the C–H bonds of alkanes in a statistical manner, as do O(^{1}D) and S(^{1}D) atoms. Insertion of Se(^{1}D) into C–H bonds would, however, be expected to be less exothermic than the corresponding S(^{1}D) insertion reaction.

Although Te($^1D_2$) atoms have been observed for periods up to 500 μs[31] following the flash photolysis of D_2Te, no data have been reported on the reaction of Te($^1D_2$) atoms with alkanes.

(iv) S(^3P) Atom Reactions

S(^3P) + alkane systems have been studied in the temperature range 20 to 200 °C and no evidence of any reaction with alkanes was found.[17] This is not surprising since insertion of S(^3P) would have to form triplet state thiols which lie at prohibitively high energies, and abstraction of an H atom from an alkane to form an SH radical is thermodynamically unfavorable.

(v) O(^3P) Atom Reactions

O(^3P) atoms, generated by the photolysis of NO_2 at 366 nm, have been found to react with alkanes probably via hydrogen abstraction, with OH and alkyl radicals being the primary products.[65,66] The rate of abstraction is highest from tertiary C–H bonds and lowest from the primary C–H bonds. The C–H bond strengths of alkanes and the associated activation energies and enthalpy change for O(^3P) + RH reactions are given below (in kcal mol^{-1}):[66]

	Primary C–H	Secondary C–H	Tertiary C–H
C–H bond strength	~100	~95	~92
Activation energy	~6.9	~4.5	~3.3
Enthalpy change	–2.3	–7.0	–10.3

From the enthalpy changes it can be seen that the $O(^3P)$ + RH abstractions reactions are thermodynamically allowed but they are quite slow because of the relatively high activation energies. Rate constants may range from 8.3×10^{-16} cm^3 $molecule^{-1}$ s^{-1} for cyclopropane at 298 K to 2.0×10^{-13} cm^3 $molecule^{-1}$ s^{-1} for 2,3-dimethylbutane at 300 K.[67] Reaction takes place when the approaching $O(^3P)$ atom is colinear with a C–H bond.[66] The $O(^3P)$ + RH reaction follows a complicated pathway due to the formation, recombination and regeneration of radicals. The following is a simplified model of the $O(^3P) + CH_4$ reaction.[68]

$$O(^3P) + CH_4 \longrightarrow CH_3\cdot + \cdot OH \quad [22]$$

$$\cdot O + CH_3\cdot \longrightarrow HCHO + H\cdot \quad [23]$$

$$\cdot OH + CH_3\cdot \longrightarrow CH_3OH \quad [24]$$

$$\cdot O + OH\cdot \longrightarrow \cdot H + O_2 \quad [25]$$

$$\cdot O + HCHO \longrightarrow \cdot OH + HCO\cdot \quad [26]$$

$$\cdot H + HCHO \longrightarrow H_2 + HCO\cdot \quad [27]$$

$$\cdot O + HCO\cdot \longrightarrow \cdot OH + CO \quad [28a]$$

$$\cdot O + HCO\cdot \longrightarrow \cdot H + CO_2 \quad [28b]$$

$$\cdot H + HCO\cdot \longrightarrow H_2 + CO \quad [29]$$

$$\cdot H + O_2 + M \longrightarrow \cdot HO_2 + M \quad [30]$$

$$\cdot HO_2 + O\cdot \longrightarrow \cdot OH + O_2 \quad [31]$$

$$\cdot HO_2 + H\cdot \longrightarrow 2HO\cdot \quad [32]$$

$$\cdot OH + CH_4 \longrightarrow CH_3\cdot + H_2O \quad [33]$$

(vi) Se(^{3}P) and Te(^{3}P) Atom Reactions

Unlike $O(^3P)$ atoms, and similarily to $S(^3P)$ atoms, neither $Se(^3P)$ nor $Te(^3P)$ atoms react with alkanes.[30] They are not expected to react with alkanes for the same reasons the $S(^3P)$ atoms do not.

(vii) S-Atom Reactions in the Liquid Phase

When carbonyl sulfide (COS) was photolyzed at 253.7 nm at room temperature in liquid alkanes, the S(^{1}D) atoms generated were found to insert into the C–H bonds of the alkanes to form the corresponding alkanethiols, as was observed in the gas phase.[41]

$$COS\ (^1\Sigma^+) \longrightarrow COS^*\ (^1\Delta, \text{dissociative}) \longrightarrow CO\ (^1\Sigma^+) + S(^1D) \qquad [3a]$$

$$S(^1D) + R\text{–}H \longrightarrow R\text{–}SH \qquad [11a]$$

The S(^{1}D) atoms may also be deactivated to the ground state by the alkanes in a solvent-catalyzed reaction.[41,58]

$$S(^1D) + R\text{–}H \longrightarrow S(^3P) + R\text{–}H^* \qquad [11a]$$

The abstraction reactions [5a] and [5b] which occur in the gas phase are not observed in the liquid phase, because of the relatively low concentration of COS ($\leq$ 0.7M) in the solvent alkane. Hence Φ (CO) = 0.94[1] in the liquid phase compared to 1.8 in the gas phase.[18] Elemental sulfur is also seen as a product, as in the gas phase, due to the following reaction.[41]

$$2S(^3P) \xrightarrow{M} S_2\ (\Sigma_g^-) \qquad [8a]$$

The thiol products obtained show some deviation from a statistical distribution. Insertion into tertiary C–H bonds occurs consistently and significantly more often than the expected statistical amount.[58] The total amount of secondary thiols also appears to be consistently higher than the expected ratio. Therefore insertion seems to favor the weaker C–H bonds in the solution phase. For example:[58]

$$S(^1D) + (CH_3)_2CHCH_2CH_3 \longrightarrow HS(CH_2)(CH_3)CHCH_2CH_3\ (47\%;\ \text{theor.},\ 50\%)$$
$$+ (CH_3)_2CHCH_2CH_2SH\ (16\%;\ \text{theor.},\ 25\%)$$
$$+ (CH_3)_2CHCH(SH)CH_3\ (23\%;\ \text{theor.},\ 16.7\%)$$
$$+ (CH_3)_2C(SH)CH_2CH_3\ (14\%;\ \text{theor.},\ 8.3\%) \qquad [34]$$

The mechanisms proposed for $S(^1D)$ insertion into the C–H bond have been discussed before. Leppin and Gollnick estimate a value of about 8×10^{-14} cm^3 $molecule^{-1}$ s^{-1} as an upper limit for the rate of insertion of $S(^1D)$ atoms into C–H bonds,[58] since the insertion reaction is believed to be slower in the liquid phase due to the loss of excess translational energy in the $S(^1D)$ atom.

(viii) S-Atom Reactions in Low Temperature Matrices

$S(^1D)$ atoms have been generated in a solid methane matrix containing COS at 13–20 K, upon photolysis near 230 nm. The main products obtained were CO, CH_3SH, $H_2C{=}S$ and CS_2[69] as identified by their infrared spectra. The formation of CH_3SH proves the initial generation of $S(^1D)$ atoms.

$$CH_4 + S(^1D) \longrightarrow [CH_3SH]^* \xrightarrow{\text{deactivation}} CH_3SH \qquad [35a]$$

$H_2C{=}S$ is believed to arise from the decomposition of the initial hot adduct:

$$CH_4 + S(^1D) \longrightarrow [CH_4S]^* \longrightarrow H_2C{=}S + H_2, \qquad [35b]$$

and CS_2, from a secondary reaction between $H_2C{=}S$ and $S(^3P)$:

$$H_2C{=}S + S(^3P) \longrightarrow [H_2C(S\cdot)S\cdot] \longrightarrow H_2 + CS_2 \qquad [36]$$

$S(^1D)$ atoms do not survive long enough to migrate to any significant extent in the matrix. This is especially evident when a matrix of the composition $Ar:CH_4:COS$ = 100:20:1 is photolyzed:[69] no CH_3SH or $H_2C{=}S$ products could be detected since the $S(^1D)$ atoms are rapidly quenched by the Ar in the matrix to the ground state, which does not react with methane.

(ix) $S(^1S_0)$ Atom Reactions

The reactions of $S(^1S_0)$ atoms have barely been studied. It is known that $S(^1S_0)$ atoms are much less reactive than the $S(^1D)$ atoms.[70] Dunn et al. obtained the following rate constant values for the deactivation of $S(^1S_0)$ atoms in the presence of COS, CH_4 and C_2H_6 : $4 \pm 2 \times 10^{-13}$, $1.5 \pm 0.2 \times 10^{-15}$ and $4.4 \pm 0.5 \times 10^{-14}$ cm^3 $molecule^{-1}$ s^{-1}, respectively.[71] These values are about three to five orders of magnitude smaller than the corresponding rate constant values for $S(^1D_2)$ atoms. In the case of oxygen atoms the order of reactivity is as follows:[72]

$$O(^1D_2) >> O(^1S_0) \geq O(^3P_J)$$

This order of reactivity of the electronic states is probably true for the sulfur atoms atoms as well, and shows that chemical reactivity does not depend solely on energetics.

(b) with alkenes

(i) $S(^1D)$ Atom Reactions

$S(^1D)$ atoms have been found to react with alkenes in two ways. The first is by insertion into C–H bonds as with alkanes, and the second, by addition across the double bond to form the three-membered ring thiirane or a thiacyclopropane.[16,73] The types and

distributions of products obtained when S(^{1}D) atoms react with propene are shown below:[74]

$$S(^1D) + CH_3CH{=}CH_2 \longrightarrow HSCH_2CH{=}CH_2\ (19\%)$$
$$+ \text{cis- and trans-}CH_3CH{=}CHSH\ (19\%)$$
$$+ \text{cy–}CH_2SCH(CH_3)(62\%) \qquad [37]$$

$CH_3CSH{=}CH_2$ is not a product. To date, only vinylic mercaptans arising from insertion into a terminal methylene group have been detected, and addition reactions predominate,[74] although the enthalpy change accompanying addition is smaller than that for the insertion reaction, i.e. about –86 kcal mol^{-1} for the former as compared to ~ –90 kcal mol^{-1} for the insertion reaction.

In the case of the S(^{1}D) + C_2H_4 reaction, it was found that the vinylthiol (CH_2=CHSH) to thiirane product ratio decreased with increasing ethylene pressure although the sum of the products remained constant.[75] This was shown to be due to the formation of a vibrationally excited thiirane which at low pressures isomerized to the vinylthiol, but at high pressures was stabilized to the ground-state thiirane. The reaction scheme is shown as follows:[75]

$$S(^1D) + C_2H_4 \longrightarrow C_2H_3SH \qquad [38a]$$
$$\longrightarrow C_2H_4S^* \qquad [38b]$$
$$C_2H_4S^* \longrightarrow C_2H_3SH \qquad [39]$$
$$C_2H_4S^* + M \longrightarrow C_2H_4S + M^* \qquad [40]$$

"Hot" methylthiirane from the S(^{1}D) + C_3H_6 reaction undergoes a small amount of isomerization to methylvinylthiol, but this reaction is not expected to occur for more substituted thiiranes since there would be sufficient degrees of freedom within the molecule to dissipate excess energy.[75]

Theoretical calculations show that the $S(^1D_2) + C_2H_4$ system correlates with the $^1A_1$ ground state of thiirane, and the addition reaction proceeds by a concerted least motion, symmetry-allowed process where the S(1D) atom approaches the double bond along its C_{2v} rotational axis, so that only stereospecific products may be expected.[76,77]

S(1D) atom reactions with a variety of alkenes have been studied and it appears that the presence of electron-releasing methyl or alkyl groups adjacent to a double bond increases the reactivity of the double bond,[49] whereas the presence of electronegative fluorine atoms adjacent to a double bond decreases its reactivity.[78] In the case of tetrafluoroethylene, the thiirane formed is very transient and can only be observed by means of flash photolysis-kinetic mass spectrometry.[77] The effects of adjacent chlorine groups on the reactivity of the double bond with respect to S(1D) atoms have only been briefly examined, but there appears to be a tendency towards polymer formation as shown below:[78]

$$S(^1D) + H_2C{=}CHCl \rightarrow [cy\text{–}CH_2SCHCl]^* \longrightarrow \cdot S\text{–}CH_2\text{–}\dot{C}HCl \quad [41]$$

$$\cdot S\text{–}CH_2\text{–}\dot{C}HCl + H_2C{=}CHCl \longrightarrow ClH\dot{C}\text{–}CH_2\text{–}S\text{–}CH_2\text{–}\dot{C}HCl \quad [42]$$

$$ClH\dot{C}\text{–}CH_2\text{–}S\text{–}CH_2\text{–}\dot{C}HCl + nC_2H_3Cl \longrightarrow \text{polymer} \quad [43]$$

The overall rate constant for the $S(^1D) + C_2H_4$ reaction, $k_{37a} + k_{37b}$, was estimated by Sherwood et al. to be 1.3×10^{-10} cm^3 molecule^{-1} s^{-1}.[75] This rate constant does not include possible quenching of the S(1D) atom by C_2H_4. Recently Black and Jusinski reported a total rate constant of 4.1×10^{-10} cm^3 molecule^{-1} s^{-1} for reaction and quenching,[45] where the rate constant for the reaction is about $0.94 \pm 0.21 \times 10^{-10}$ cm^3 molecule^{-1} s^{-1}.[43] The relative reactivities of C_2H_4, C_3H_6 and i–C_4H_8 towards S(1D) atoms are 1:2.5:4.6, respectively,[79] demonstrating the electrophilic character of S(1D) atoms.

(ii) O(¹D) Atom Reactions

The reactions of O(¹D) atoms with alkenes have not been studied in detail, mainly because very high pressures are required to stabilize the hot intermediate products. Kajimoto et al. studied the reactions of O(¹D) with propylene at pressures up to 150 atmospheres,[80] at which pressures products were obtained which were believed to be due to insertion reactions of the O(¹D) atom. The major products obtained were methyloxirane, propionaldehyde, allyl alcohol and acetone. Carbon monoxide, hydrogen, small amounts of acrolein and acetaldehyde, as well as various hydrocarbons were also formed. From the distribution of the products extrapolated to limiting high pressure it is found that insertion of O(¹D) into the various C–H bonds occurs about 55% of the time whereas addition to the double bond occurs about 20% of the time. The remainder of the O(¹D) atoms are believed to abstract hydrogen from the alkene. Up to 2% of the time acrolein may be formed, accompanied by molecular elimination of H_2, as shown below:[80]

$$O(^1D) + CH_3CH{=}CH_2 \xrightarrow{\text{terminal vinyl insertion}} CH_3CH_2CH(O)\ \sim 22\% \quad [44a]$$

$$\xrightarrow{\text{central vinyl insertion}} CH_3C(O)CH_3\ \sim 11\% \quad [44b]$$

$$\xrightarrow{\text{alkyl C–H insertion}} HOCH_2CH{=}CH_2\ \sim 20\% \quad [44c]$$

$$\xrightarrow[-H_2]{\text{alkyl C–H insertion}} (O)CHCH{=}CH_2\ \sim 2\% \quad [44d]$$

$$\xrightarrow{\text{addition to double bond}} \text{cy-}CH_2OCH(CH_3)\ \sim 22\% \quad [44e]$$

$$\xrightarrow{\text{abstraction}} \cdot CH_2CH{=}CH_2 + OH\cdot\ <25\% \quad [44f]$$

From the relative importance of the various pathways, the addition of O(¹D) to the double bond appears to be twice as fast as insertion into a C–H bond. However, compared to S(¹D) atoms, O(¹D) atoms give a larger percent yield of insertion products, which is probably due to the greater excess energy, about 45 kcal mol^{-1}, in the O(¹D) atoms. Kajimoto and Fueno[81] have also determined relative rate constants for the addition of

$O(^1D)$ to a few alkenes at about 200 Torr total pressure. The calculated absolute rate constants vary from 2.2 x 10^{-10} cm^3 $molecule^{-1}$ s^{-1} for ethylene to 10.6 x 10^{-10} cm^3 $molecule^{-1}$ s^{-1} for 2-methyl-2-butene. Theoretical calculations show that the $O(^1D)$ + C_2H_4 addition reaction features the lowest activation energy when it follows a symmetric, concerted addition pathway.[82]

(iii) Se(^{1}D) and Te(^{1}D) Atom Reactions

Only $Se(^1D)$ reactions with a few alkenes have been studied.[10] The adducts formed when $Se(^1D)$ atoms add to C_2D_4, C_2F_4 and CHCl=CHCl, were observed by means of flash photolysis-kinetic mass spectrometry,[27] and were postulated to be the corresponding seleniranes by analogy with the $O(^1D)$ and $S(^1D)$ atom reactions with alkenes and on the basis of the mass spectrometric fragmentation patterns of the adducts.

$$Se(^1D) + R_2C{=}CR_2 \longrightarrow cy\text{–}R_2CSeCR_2 \qquad [45]$$

The seleniranes have very short lifetimes and are believed to decompose via a bimolecular reaction giving Se_2 and two olefin molecules, or by reaction with COSe.[27]

(iv) S(^{3}P) Atom Reactions

As noted before, $S(^3P)$ atoms do not insert into C–H bonds. They have been shown to add across the double bonds of alkenes to form cyclic three-membered thiiranes. An interesting feature of this addition is that it is highly stereoselective.[16]

In the 1950's when the chemistry of the divalent species methylene (CH_2) was being studied, Skell suggested that since the products of the reactions of methylene, generated from the photolysis of diazomethane, with various alkenes were stereospecific, the reacting

methylene must be in the singlet state.[83,84] Later, Herzberg observed the spectrum of the methylene radical, formed from the photolysis of CH_2N_2, and established that it was formed in a singlet state and that it had a triplet ground state.[85] Anet et al. then studied methylene reactions with alkenes in the presence of a large excess of nitrogen and found that the previously observed stereospecificity was lost[86] owing to the formation of triplet methylene by collisional deactivation of the singlet methylene. The experiments were repeated by Frey,[87] and Bader et al.[88] with different pressures of quenchers and similar results were found. These results appeared to be in agreement with Skell's hypothesis that the intermediate complexes for the singlet and triplet methylene addition to alkenes were different. For the singlet methylene additon, a three-centre intermediate was postulated which results in the retention of the original geometry.[84,88]

$$CH_2\ (\uparrow\downarrow) + CH_3CH{=}CHCH_3 \longrightarrow \text{cy–}CH(CH_3)CH_2CH(CH_3) \qquad [46]$$

In the case of triplet methylene addition, a triplet state intermediate is postulated, where rotation about the original C–C bond can give rise to non-stereospecific products.[84,88]

$$CH_2\ (\uparrow\uparrow) + \text{cis–}CH_3CH{=}CHCH_3 \longrightarrow CH_3CH_2(\dot{C}H_2)\dot{C}HCH_3 \longrightarrow$$

$$\text{cis- and trans-cy-}CH(CH_3)CH_2CH(CH_3) \qquad [47]$$

Thus the stereochemistry of the product reflects the spin state or multiplicity of methylene. Cvetanovic found that the $O(^3P)$ + alkene reactions also gave non-stereospecific products,[89] and similar results were obtained with singlet and triplet nitrenes.[90]

DeMore and Benson, however, disagreed with the idea that the reactions of triplet species with alkenes would necessarily give rise to non-stereospecific products.[91] They suggested that both singlet- and triplet-state divalent species would add to a double bond to form a diradical which may undergo ring closure, and the stereospecificity of the final

products depended on the competition between the rates of ring closure and rotation about the C–C bond.

DeMore and Benson's suggestion that stereospecific addition products do not necessarily imply a singlet state divalent species was confirmed by the results of Sidhu et al. who found that triplet sulfur atoms added to cis- and trans-2-butene to give highly stereoselective products as shown:[16]

$$\text{trans-}CH_3CH{=}CHCH_3 + S(^3P) \longrightarrow \underset{>94\%}{\text{trans-cy-}CH(CH_3)SCH(CH_3)} \qquad [48]$$

$$\text{cis-}CH_3CH{=}CHCH_3 + S(^3P) \longrightarrow \underset{>87\%}{\text{cis-cy-}CH(CH_3)SCH(CH_3)} \qquad [49]$$

The steroeselectivity seen was believed to be due to more rapid spin inversion and slower rotation about the C–C bond in the intermediate, coupled with efficient ring closure. Lown et al. suggested the triplet state π-thiacyclopropane structure shown below as an intermediate in the S(3P) atom + ethylene reaction. The sigma–pi hybrid bond between the terminal methylene carbon and the sulfur atom accounts for the barrier to rotation about the C–C bond.[92]

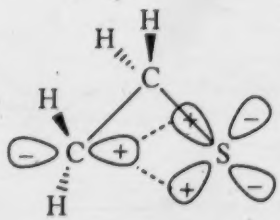

Leppin and Gollnick, however, proposed that a low-lying excited triplet-state thiirane is formed directly with retention of spin and geometry in the $S(^3P) + C_2H_4$ reaction.[93] Hoffmann and coworkers, using extended Hückel calculations, also suggested that the $S(^3P) + C_2H_4$ potential curve correlates with an excited triplet state T_1 of thiirane in which C–C bonding and the original C_2H_4 configuration is retained, but which has a broken C–S

bond.[77] The ring-opened intermediate was predicted to have a planar geometry with a CCS angle of about 110°. The barrier to twisting the methylene group by 90° was calculated to be about 5 kcal mol^{-1}. Strausz et al., however, using a virtual orbital technique, calculated a barrier for rotation of about 23 kcal mol^{-1} in the T_1 state of the thiirane, and this implies a relatively strong binding interaction between sulfur and the terminal methylene carbon.[76] The primary product of the C_2H_4 + $S(^3P)$ reaction was calculated to have only about 20 kcal mol^{-1} excess vibrational energy which is not sufficient for rotation about the C–C bond to occur, so that the reaction proceeds stereoselectively.

Quite recently McKee, using higher level calculations and optimized geometries, computed the rotational barrier about the C–C bond to be only about 3 kcal mol^{-1}.[55] He cited rapid intersystem crossing from the triplet to the ground singlet state as being the reason for the observed stereoselectivity of the products. This claim contradicts the earlier finding by Lown et al. who showed that a single triplet-state thiirane molecule mediates the geometrical isomerization of several alkene molecules through reversible addition to alkenes as shown below. Triplet state thiiranes therefore would have to have a long radiative lifetime and be highly resistant to collisional deactivation.[94]

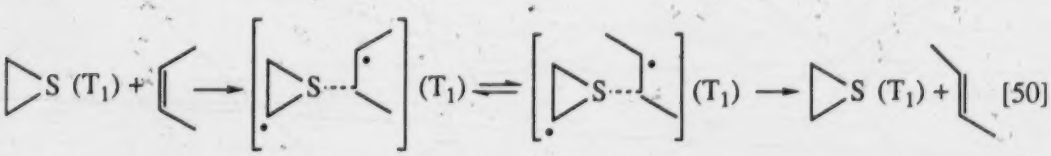

[50]

More recent ab initio calculations[95] on the $S(^3P)$ + C_2H_4 reaction will be discussed in detail in Chapter 5.

The absolute rate constant for the $S(^3P)$ + C_2H_4 reaction was first measured by Donovan et al.[96] and Connor et al.,[97] who obtained values of 1.2 x 10^{-12} and 1.5 x 10^{-12} cm^3 $molecule^{-1}$ s^{-1}, respectively. More recently Davis et al.[98] and Black measured[43] values of 4.96 x 10^{-13} and 5.1 ± 0.5 x 10^{-13} cm^3 $molecule^{-1}$ s^{-1}, respectively. Black also

measured a rate constant of $2.9 \pm 0.3 \times 10^{-12}$ cm^3 molecule^{-1} s^{-1} for the S(^{3}P) + C_3H_6 reaction.[43]

The relative rates of addition of S(^{3}P) atoms with various alkenes have been measured and Table I–3 gives the rate parameters and the corresponding rate constants for selected S(^{3}P) + alkene reactions at 298 K.[99]

The electrophilic nature of S(^{3}P) is evident from the way the rate parameters change with the nature of the substituents on the C=C bond. The activation energy, E_a, decreases with increasing alkyl substitution and increases with increasing number of halogen substituents. This trend in the activation energies has been correlated with the ionization potentials of the alkenes.[57] From Table I–3, it can also be seen that the reactions of S(^{3}P) atoms with some highly-substituted alkenes such as tetramethylethylene (TME) have negative activation energies. This is explained as being due to the intersection of an attractive potential surface with the repulsive part of the S(^{3}P) + alkene potential energy surface below the potential energies of the separated S(^{3}P) atom and alkene.[50,57]

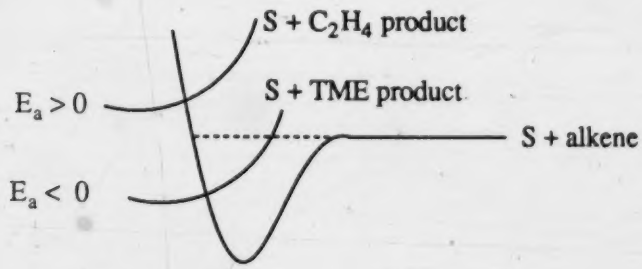

This situation means that an increase in temperature would increase the rate of crossing to the attractive potential surface for the S(^{3}P) + C_2H_4 reaction, but would tend to cause the redissociation of the activated complex for the S(^{3}P) + TME reaction.[57]

Finally, with increasing deuteration of ethylene, the A-factor is seen to increase. This is probably due to the greater mass of the deuterated ethylene and consequently higher momentum and moment of inertia, making the molecule more susceptible to reaction.

(v) O(^{3}P) Atom Reactions

The behavior of O(^{3}P) atoms in the gas phase is similar to that of S(^{3}P) atoms, in that they do not insert into C–H bonds; the major reaction is addition to the double bond to form a triplet biradical intermediate:[101]

$$O(^3P) + R_1R_2C{=}CR_3R_4 \longrightarrow R_1R_2\dot{C}{-}C(\dot{O})R_3R_4 \qquad [51]$$

The O(^{3}P) atom is usually attached to the least substituted carbon in the triplet biradical intermediate and rotation about the C–C bond occurs to some degree. That the intermediate is short-lived even with respect to rotation about the C–C bond is seen from the fact that the products of the O(^{3}P) atom + cis-2-butene reaction and that of the O(^{3}P) atom + trans-2-butene reaction do not give the same ratio of cis- to trans-1,2-dimethyloxirane.[101] The non-stereoselective products obtained and the triplet biradical intermediate structures, which have been confirmed by quantum mechanical calculations, are, however, consistent with Skell's hypothesis.[84]

Thus from the biradical intermediate formed, firstly, ring closure can occur with the formation of "hot" oxiranes. Next, rearrangement within the biradical intermediate, by the internal migration of H atoms or alkyl groups can give rise to "hot" carbonyl compounds. Thirdly, the intermediate can undergo pressure-independent fragmentation (PIF) which generally results in the loss of a vicinal alkyl group or an H atom when the biradical intermediate has rearranged to form a carbonyl bond.[101] The "hot" oxiranes and carbonyl compounds formed may either be collisionally stabilized or may undergo pressure-

dependent fragmentation (PDF), depending on the number of degrees of freedom available in the molecule and the bond strengths of the weak bonds in the molecule. Schematically, for cis-2-butene the reaction proceeds as follows:[101]

$$O(^3P) + \text{cis-}CH_3CH{=}CHCH_3 \longrightarrow \text{cis-}CH_3\dot{C}H\text{-}C(\dot{O})HCH_3 \quad [52]$$

$$\text{cis-}CH_3CH\text{–}C(O)HCH_3 \longrightarrow \text{cis- and trans-cy-}CH(CH_3)OCH(CH_3)^*(OX^*) \quad [53a]$$

$$\longrightarrow (O)CHCH(CH_3)_2^* + CH_3CH_2C(O)CH_3^*(A^*+K^*) \quad [53b]$$

$$\longrightarrow \text{PIF (pressure independent fragmentation)} \quad [53c]$$

$$OX^*, A^*, K^* + M \longrightarrow \text{stabilized products} \quad [54a]$$

$$\longrightarrow \text{PDF (pressure dependent fragmentation)} \quad [54b]$$

In the gas-phase reaction of $O(^3P)$ with ethylene, the final stable products obtained at room temperature were found by Cvetanovic to be CO, H_2, CH_4, C_2H_6, C_3H_8, C_4H_{10}, CH_3CHO, higher aldehydes and small amounts of ethylene oxide.[25]

Hydrogen abstraction from alkenes by $O(^3P)$ atoms occurs to a very small extent at room temperature, but is expected to become more significant at elevated temperatures.[101]

Some of the rate constants which have been measured for the $O(^3P)$ + alkene reaction[100] are presented in Table I–3. As with the $S(^3P)$ atom, the electrophilic nature of the $O(^3P)$ atom is evident from the decrease in the activation energy with increasing alkyl substitution on the double bond. Negative activation energies are also observed for some $O(^3P)$ + alkene reactions. To explain the negative activation energies, Cvetanovic suggested the following mechanism,[101] a variation of which, formulated by Green,[48] is shown below:

$$O(^3P) + \text{alkene} \underset{E_{a(-1)}}{\overset{E_{a(1)}}{\rightleftharpoons}} \text{complex} \xrightarrow{E_{a(2)}} \text{product} \quad [55]$$

Where E_a is negative when $E_{a(-1)} > (E_{a(1)} + E_{a(2)})$. A graphical representation is shown below:

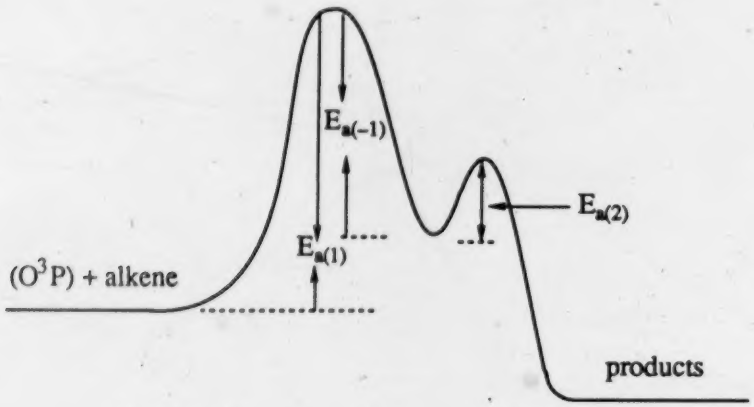

for $E_a > 0$

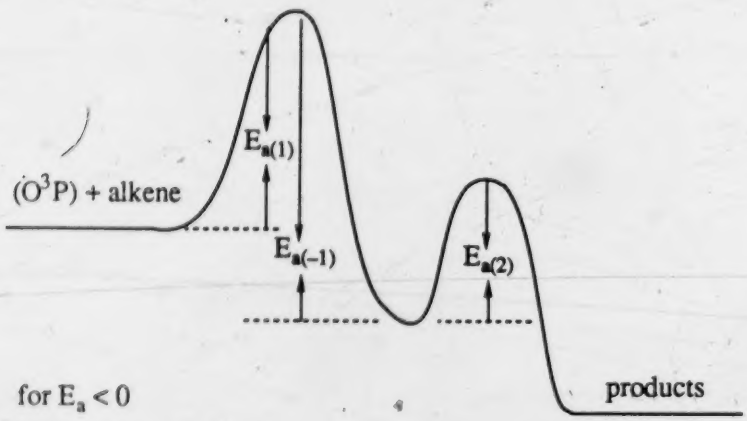

for $E_a < 0$

Thus at higher temperatures the complex would have the energy to overcome $E_{a(-1)}$ and would tend to dissociate back to $O(^3P)$ atoms + alkene, just as in the case of the $S(^3P)$ + alkene reaction. The nature of the complex has been postulated to be one in which there is partial charge transfer from the alkene to the attacking oxygen atom.[25]

(vi) Se(^{3}P) and Te(^{3}P) Atom Reactions

Both Se(^{3}P) and Te(^{3}P) atoms, like O(^{3}P) and S(^{3}P) atoms, add across the double bonds of alkenes to form seleniranes[10,102] and telluriranes,[10,30] respectively. They are short-lived adducts which can be monitored by kinetic absorption spectroscopy[103] and flash photolysis-kinetic mass spectrometry.[30] The selenirane spectra persist several minutes after flashing,[103,104] but the telluriranes have lifetimes of several milliseconds or less.[30]

The addition of Se(^{3}P) atoms to cis- and trans-2-butene has been claimed to be stereoselective,[103] on the basis of the UV spectra of the adducts. Corresponding data for the Te(^{3}P) atoms are not available but they would be expected to add stereoselectively as well, since with the heavier group VIA atoms, ring closure is expected to be faster due to a more rapid triplet-to-singlet inversion, and the barrier to rotation about the C–C bond would be expected to be greater.[103]

Callear and Tyerman have measured the rates of Se(^{3}P) atom reactions with some alkenes and have found that the activation energies of the various reactions correlate with the ionization potentials of the alkenes according to the equation:[102]

$$(0.147 - E_a)^{-1} = 22.06\ (I.P.) - 149.5$$

The reaction of Te(^{3}P) with tetramethylethylene (TME) was found to have a negative activation energy[97] similar to that found in the O(^{3}P) and S(^{3}P) atom reactions (see Table 1–4). E_a for the Se(^{3}P) + TME reaction is predicted to be negative as well, according to the predicted correlation with the ionization potential of TME.[97] Possible explanations for the negative activation energies have been already discussed.

(vii) S-Atom Reactions in the Liquid Phase

Leppin and Gollnick have also studied the reactions of S(^{1}D) and S(^{3}P) atoms with alkenes in the solution phase and found that in both cases thiiranes are formed.[105] It could not be established whether S(^{1}D) atoms inserted into the C–H bond of alkenes since the S(^{1}D) + alkene reactions were studied in a liquid alkane which, being in excess, would scavenge the S(^{1}D) atoms.[105] S(^{3}P) atoms were formed by photolyzing solutions of COS in benzene, toluene or p-xylene, which act as triplet sensitizers.[106] The S(^{3}P) atoms were found to react at a faster rate with trimethylethylene than with cyclohexene, as expected. The rate constant for the S(^{3}P) + cyclohexene reaction was estimated to be about 6.64 x 10^{-19} cm^3 molecule^{-1} s^{-1}, and that for the S(^{3}P) + trimethylethylene reaction $\geq$ 1.66 x 10^{-17} cm^3 molecule^{-1} s^{-1}.[106] These rate constants are about four or five orders of magnitude smaller than the rate constants measured for the corresponding gas-phase reactions.

(viii) S- and O-Atom Reactions in Low Temperature Matrices

The reaction of S(^{3}P) with C_2H_4 in a low-temperature matrix of the composition Ar:COS:C_2H_4 = 100:1:1, was studied by Hawkins et al., who found the thiirane molecule to be the sole product of the reaction.[69] The reaction of oxygen atoms with ethylene in a solid argon matrix at 15 K has also been studied,[107] the primary products of the reaction being acetaldehyde, ethylene oxide, ketene and vinyl alcohol. The ketene may be formed by H_2 elimination from the vinyl alcohol as shown:

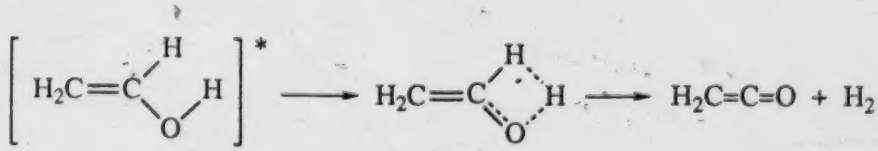

[56]

(ix) S($^1S_0$) Atom Reactions

The rate constants for the deactivation of S($^1S_0$) atoms and O($^1S_0$) atoms by C_2H_4 have been reported by Dunn et al. and the values obtained are $1.3 \pm 0.2 \times 10^{-13}$ and 9.6×10^{-10} cm^3 molecule^{-1} s^{-1}, respectively.[71]

(c) with alkynes

(i) S(^1D) Atom Reactions

The reactions of S(^1D) atoms with C_2H_2, $(CH_3)C_2H$, $(CH_3)C_2(CH_3)$ and $(CF_3)C_2(CF_3)$ have been studied by flash photolysis-kinetic mass spectrometry, where adducts with lifetimes of 2s (C_2H_2S), 5s (C_3H_4S), 7s (C_4H_6S) and >0.1s (C_4F_6S) were observed.[108] The final products, obtained in very low yields, include CS_2 and substituted benzenes and thiophenes, which means that the adducts react further with the alkyne. The only product detected in the reaction of S(^1D) and C_4F_6 at low conversions was perfluorotetramethylthiophene.[109]

For the C_2H_2S adduct, the following structures were proposed:[110]

$H\dot{C}{=}CH\dot{S} \leftrightarrow H\ddot{C}C(S)H$	cy-SCH=CH	$H_2C{=}C{=}S$
I	II	III
HC≡C–SH	cy-$H_2C\ddot{C}S$	HSHC=C:
IV	V	VI

Because of the long lifetime of the adducts, all radical structures may be discounted. Structure IV is possible only for C_2H_2 and monosubstituted alkynes, and therefore cannot represent the general adduct formed. Structure III requires the migration of H or alkyl groups, both for its formation and for the formation of a thiophene. In the case of

perfluoro-2-butyne it is unlikely that the CF_3 group would be so mobile. The thiirene structure II, is the most likely candidate for the intermediate adduct formed. SCF MO CI calculations[109] show that thiirene would be formed by a spin- and orbital symmetry-allowed least-motion pathway; this and the other possible primary steps in the $S(^1D)$ + C_2H_2 reaction are:[109]

$S(^1D_2) + HC{\equiv}CH$	$\longrightarrow$	cy-SCH=CH (S_0)	$\Delta H \sim -60$ kcal mol^{-1}	[57]
$S(^1D_2) + HC{\equiv}CH$	$\longrightarrow$	$H\dot{C}{=}CH{-}\dot{S}$ (S_1)	$\Delta H \sim -46$ kcal mol^{-1}	[58]
$S(^1D_2) + HC{\equiv}CH$	$\longrightarrow$	$HC{\equiv}C{-}S{-}H$	$\Delta H \sim -87$ kcal mol^{-1}	[59]

Insertion of the $S(^1D)$ atom into the C–H bonds of alkynes, reaction [59], requires 125 kcal mol^{-1} to break the C–H bond and no evidence of $S(^1D)$ atom insertion into the C–H bonds of even the methyl groups of propyne and 2-butyne has been observed. It is possible that insertion does occur but that the unsaturated thiol formed is unstable and decomposes or polymerizes.[78]

In the reaction of $S(^1D)$ with acetylene, the products obtained are CS_2, benzene and thiophene in a 4:3:1 ratio at room temperature, and in a 10:3:1 ratio at 160 °C.[109] At the higher temperature CS_2 may be formed according to the following reaction,

$$H\dot{C}{=}CH{-}\dot{S}\ (S_1) + H_2C{=}C{=}S \longrightarrow CS_2 + C_3H_4 \qquad [60]$$

where the thioketene is formed by isomerisation of the biradical:[109]

$$H\dot{C}{=}CH{-}\dot{S}\ (S_1) \longrightarrow H_2C{=}C{=}S \qquad [61]$$

The benzene and thiophene products which are formed from the $S(^1D)$ + alkyne reactions may arise from the following pathways:

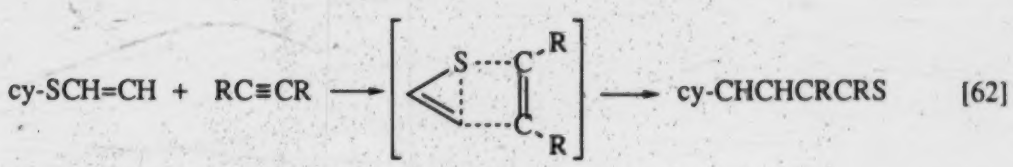

[62]

$$HC{=}CH{-}\dot{S}(S_1) \rightleftharpoons HC{=}CH{-}\dot{S}(T_0) \xrightarrow{C_2H_2} HC{=}CH{-}CH{=}CH{-}\dot{S}(T_1) \quad [63]$$

$$HC{=}CH{-}CH{=}CH{-}\dot{S}(T_1) \xrightarrow{M} \text{cy-CHCHCHCHS} \quad [64a]$$

$$\xrightarrow{C_2H_2} C_6H_6 + S(^3P) \quad [64b]$$

$$\xrightarrow{nC_2H_2} \text{polymer} \quad [64c]$$

Many novel Dewar benzenes, Dewar thiophenes, dimers and trimers may also form at longer photolysis times in the S(1D) + alkyne reactions.[109]

Thiirene, which is a 4π, conjugated, planar, antiaromatic molecule, and therefore highly unstable, has been isolated and identified in low temperature matrices from the photolysis of 1,2,3-thiadiazoles[111] and of vinylene trithiocarbonates.[112]

Little and Donovan determined the ratio of the rate constant for the reaction of S(1D) with acetylene to that for quenching of S(1D) by CO_2, to be 2.5 ± 0.4.[113] Black and Jusinski determined a rate constant of 1.5 x 10^{-10} cm^3 $molecule^{-1}$ s^{-1} for the removal of S(1D)by CO_2.[45] Black, by monitoring the S(3P) signal, determined that 90% of the time the S(1D) atom is quenched by CO_2.[43] Therefore the rate constant for the S(1D) + C_2H_2 reaction can be estimated to be ~ 3.4 ± 0.6 x 10^{-10} cm^3 $molecule^{-1}$ s^{-1}. Verkoczy, from relative rate studies, estimated the rate constant for the S(1D) + C_4F_6 reaction to be ≥ 6 x

10^{-11} cm^3 $molecule^{-1}$ s^{-1}.[114] This smaller value is reasonable since the electron-withdrawing CF_3 groups decrease the electron density of the triple bond.

(ii) O(^{1}D) Atom Reactions

Ogi and Strausz have briefly examined the reaction of O(^{1}D) atoms with 2-butyne and found that CO was the major product of the reaction.[115] Many fragmentation products were obtained but not identified. However, methyl vinyl ketone ($CH_3C(O)CH=CH_2$) was definitely not a product. It was also found that the CO yield was not affected by the addition of large amounts of SF_6, indicating that the lifetime of the initially-formed hot adduct is very short with respect to fragmentation.

More recently, Schaub studied the $O(^1D) + C_2H_2$ reaction, which is highly exothermic ($\Delta H = -86$ kcal mol^{-1}), and he postulated that the major reaction pathway generates a vibronically-excited ketene which decomposes to a vibrationally-excited CO and a vibronically-excited methylene:[116]

$$O(^1D_2) + C_2H_2 \longrightarrow C_2H_2O^{*\dagger} \longrightarrow CO^* + \ddot{C}H_2{}^{*\dagger}(\tilde{a}\,{}^1A_1) \qquad [65a]$$

The CH_2 radical is believed to be scavenged by the NO_2 used to generate $O(^1D_2)$, and by the NO photoproduct.

Csizmadia et al., using extended Hückel MO studies, concluded that the addition of O(^{1}D) atoms to acetylene should give oxirene in a single step, spin- and orbital symmetry-allowed concerted reaction.[117] The oxirene ring can then open via C–O cleavage and the resulting biradical can isomerize to formylmethylene[118] which can further isomerize to the more stable C_2H_2O isomer, ketene,[119] as shown below:

$$O(^1D) + HC{\equiv}CH \longrightarrow [\text{cy-O-CH=CH}]^* \longrightarrow [H\dot{C}C(\dot{O})H] \longrightarrow$$
$$[H_2C{=}C{=}O] \longrightarrow :CH_2 + CO \qquad [65b]$$

This postulated reaction pathway appears to be consistent with the observation that SF_6 does not decrease the CO yield.

No rate constants are available for the $O(^1D)$ + alkyne reactions but Schaub suggested that the rate constant for the $O(^1D) + C_2H_2$ reaction should be similar to that for the $O(^1D) + C_2H_4$ reaction, which is ~ 2–3 x 10^{-10} cm^3 $molecule^{-1}$ s^{-1}.[116]

(iii) Se(^{1}D) and Te(^{1}D) Atom Reactions

No Se(^{1}D) or Te(^{1}D) atom reactions with alkynes have been reported.[10]

(iv) S(^{3}P) Atom Reactions

The products obtained from the reaction of S(^{3}P) atoms with alkynes are essentially the same as those obtained in the S(^{1}D) + alkyne reactions, but only one initial adduct is theoretically possible, having the ring-opened, thioformylmethylene structure, shown below:[109]

$$S(^3P) + HC{\equiv}CH \longrightarrow H\text{–}\dot{C}{=}C(\dot{S})\text{–}H\ (T_0) \quad \Delta H \sim -6\ \text{kcal mol}^{-1} \qquad [66]$$

Product yields for the reaction were poor, less than 4%, and did not improve at higher temperatures. This means that polymerization of the acetylene occurs quite readily:

$$H\dot{C}{=}C(\dot{S})H\ (T_0) + HC{\equiv}CH \longrightarrow H\dot{C}{=}CH\text{–}CH{=}CH\text{–}\dot{S}\ (T_0) \xrightarrow{nC_2H_2} \text{polymer} \qquad [64c]$$

In the $S(^3P) + C_4F_6$ reaction, however, it was found that the yield of the perfluorotetramethylthiophene product increased with increasing temperature, although the product yields were lower than those from the corresponding $S(^1D) + C_4F_6$ reaction below 144 °C.

The rate constant for the $S(^3P) + C_2H_2$ reaction was determined by Kerr and Parsonage to be 2.7×10^{-13} cm^3 molecule^{-1} s^{-1} at 298 K and by Little and Donovan, $5.0 \pm 0.5 \times 10^{-13}$ cm^3 molecule^{-1} s^{-1} at 295 K,[113] in the presence of 150 Torr argon. Strausz et al. had earlier determined the ratios of the Arrhenius parameters for a few $S(^3P)$ + alkyne reactions relative to the $S(^3P) + C_2H_4$ reaction.[99] From these results the rate constants for the $S(^3P)$ atom reactions with C_2H_2, C_3H_4 and C_4H_6 are calculated to be 1.06×10^{-13}, 6.78×10^{-13} and 1.21×10^{-11} cm^3 molecule^{-1} s^{-1}. Although the value for the $S(^3P) + C_2H_2$ reaction is probably too low, the order of reactivity should be correct.

(v) <u>O(^{3}P) Atom Reactions</u>

The reactions of $O(^3P)$ atoms with alkynes have been studied quite extensively, and Shaub et al. suggested that the $O(^3P)$ atom adds,[120] in general, to the less substituted carbon of the alkynyl bond, giving a triplet diradical which isomerizes to a ketenyl intermediate which dissociates to give CO and an alkyl methylene radical:

$$O(^3P) + RC{\equiv}CH \longrightarrow \left[R-\dot{C}=\overset{O\bullet}{\overset{|}{C}}H \right] \rightleftharpoons \left[R-\ddot{C}-\overset{O}{\overset{\|}{C}}H \right] \longrightarrow$$

$$[RHC=C=O] \longrightarrow CO + R\ddot{C}H \quad [67]$$

In the reaction with propyne, the major products obtained included CO, C_2H_2 and C_2H_4. C_2H_4 is believed to be formed from the CH_3CH radical as follows:

$$CH_3\ddot{C}H^* \longrightarrow C_2H_4^{**} \quad [68]$$

$$C_2H_4^{**} \longrightarrow C_2H_2 + H_2 \qquad [69]$$

$$C_2H_4^{**} + M \longrightarrow C_2H_4 + M \qquad [70]$$

As can be expected from the above mechanism, the $[C_2H_2]/[C_2H_4]$ ratio is very pressure dependent. A similar mechanism is believed to be operative for higher homologs, resulting in the formation of alkenes with one less carbon than the original alkyne. The $O(^3P) + C_2H_2$ reaction is believed to proceed via two important primary channels:[121]

$$C_2H_2 + O(^3P) \longrightarrow :CH_2 + CO \qquad \Delta H = -47 \text{ kcal mol}^{-1} \qquad [71a]$$

$$C_2H_2 + O(^3P) \longrightarrow \dot{H}\dot{C}CO + H\cdot \qquad \Delta H = -19 \text{ kcal mol}^{-1} \qquad [71b]$$

There has been much controversy as to the relative importance of the two pathways at room temperature. It is presently accepted that reaction [71a] predominates at room temperature and that reaction [71b] becomes more important at higher temperatures. For the $O(^3P) + C_2H_2$ reaction, Löhr and Rohr also report seeing the radicals CHO and C_3H_3 as well as the molecules CO, CH_2CO and C_3H_4.[122] Williamson and Bayes found H_2 and polymer as well as CO and C_3H_4.[123] Ogi and Strausz, in their study of the $O(^3P)$ + 2-butyne reaction, found that only 40% of the O atoms could be accounted for.[115] The rest of the $O(^3P)$ atoms were believed to be tied up in the polymer which, according to Williamson and Bayes, could originate from a relatively long-lived C_2H_2O complex.[123]

Recommended rate constants for the $O(^3P)$ + alkyne reactions have been compiled by Cvetanovic.[101] The $O(^3P) + C_2H_2$ reaction has the smallest rate constant, 1.5×10^{-13} cm^3 molecule^{-1} s^{-1}, and the $O(^3P)$ + 2-butyne has the highest, 4.8×10^{-12} cm^3 molecule^{-1} s^{-1}. The $O(^3P)$ + propyne, 1-pentyne and 1-hexyne reactions have rate constants in the range 5–8 $\times 10^{-13}$ cm^3 molecule^{-1} s^{-1}.

(vi) Se(^{3}P) and Te(^{3}P) Atom Reactions

Only the reaction of Se(^{3}P) with C_2H_2 has been briefly studied, which yielded an unsaturated selenirane product C_2H_2Se, which is expected to be much less stable than thiirene C_2H_2S.[10,104] The rate constant for the reaction has been estimated to be 1.5 x 10^{-14} cm^3 molecule^{-1} s^{-1}.

(vii) S-Atom Reactions in the Condensed Phases

No reactions of sulfur atoms with alkynes have been reported in the liquid phase but Hawkins et al. have studied the reactions of S(^{3}P) atoms with C_2H_2 in a 20 K argon matrix of composition Ar:COS:C_2H_2 = 100:1:1.[69] The major products observed are CO, ethynethiol, thioketene, thiirene and CS_2 according to the following scheme proposed by Hawkins et al.:

$$S(^3P) + HC{\equiv}CH \longrightarrow HC(S\bullet){=}C\bullet H \longrightarrow cy\text{–}CH{=}CHS \quad [72a]$$

$$\downarrow h\nu$$

$$\longrightarrow HC{\equiv}CSH \quad [72b]$$

$$\uparrow h\nu$$

$$\longrightarrow H_2C{=}C{=}S \quad [72c]$$

$$\downarrow S(^3P)$$

$$\longrightarrow H_2C{:} + CS_2 \quad [73]$$

(viii) S($^1S_0$) Atom Reactions

Dunn et al. have measured the rate constant for the deactivation of S($^1S_0$) by C_2H_2 and found it to be 1.6 ± 0.2 x 10^{-13} cm^3 molecule^{-1} s^{-1},[71] which is comparable to the rate

constant for the deactivation of $S(^1S_0)$ by C_2H_2. The corresponding rate constant for the deactivation of $O(^1S_0)$ by C_2H_2 is ~ 6 x 10^{-11} cm^3 $molecule^{-1}$ s^{-1}.

(d) with dienes

(i) $S(^1D, ^3P)$ Atom Reactions

The reactions of both $S(^1D)$ and $S(^3P)$ atoms with 1,3-butadiene, allene and 1,2-butadiene have been studied and were found to be analogous to the $S(^1D, ^3P)$ atom reactions with alkenes.

Both $S(^1D)$ and $S(^3P)$ atoms add to 1,3-butadiene via a 1,2 addition to give vinylthiacyclopropane as the major product,[16, 79] as shown:

$$S(^1D,^3P) + CH_2{=}CHCH{=}CH_2 \longrightarrow \left[\text{vinylthiacyclopropane}\right]^* \xrightarrow{M} \text{vinylthiacyclopropane} \qquad [74]$$

In the presence of excess CO_2, the yield of vinylthiacyclopropane (VTCP) is higher, due to stabilization of the initially-formed complex. At low pressures or high butadiene pressure, the initially-formed adduct forms a biradical and polymerizes or decomposes to form H_2 and thiophene, according to the following reactions:[79]

$$\left[\text{vinylthiacyclopropane}\right]^* \longrightarrow [CH_2{=}CH\dot{C}HCH_2S\bullet] \xrightarrow{nC_4H_6} \text{polymer} \qquad [75]$$

$$[CH_2{=}CH\dot{C}HCH_2S\bullet] \rightleftharpoons [H_2\dot{C}CH{=}CHCH_2S\bullet] \qquad [76]$$

$$[H_2\dot{C}CH{=}CH\dot{C}H_2S\bullet] \longrightarrow \left[\text{thiophene}\right]^* \qquad [77a]$$

$$\longrightarrow C_4H_5S\bullet + H\bullet \qquad [77b]$$

[78]

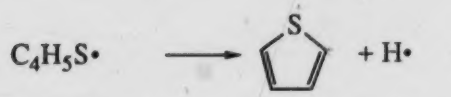

[79]

No insertion products were seen in the S(^{1}D) + 1,3-butadiene reaction, although insertion into the terminal methylene C–H bonds has been seen with alkenes.[79]

In cumulated dienes, the adjacent π bonds are mutually perpendicular and there is little overlap between them,[124] as shown.

Thus their reactions with S(^{1}D) and S(^{3}P) atoms also proceed via addition of the S atom to one of the double bonds. Therefore the major addition product obtained in the S(^{1}D, ^{3}P) + allene reactions is methylenethiirane.[114,125] At high pressures and short

[80]

photolysis times, the product yield is nearly quantitative.[125] Again, no insertion products were detected. Methylenethiirane decomposes slowly at room temperature to give a polymer, but at high temperatures allene, C_2H_4 and CS_2 are formed, possibly via tautomerism through a thioxyallyl ion to cyclopropanethione, as shown below.[114]

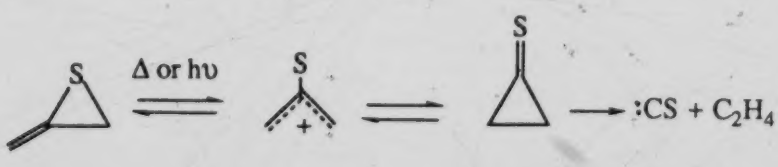

[81]

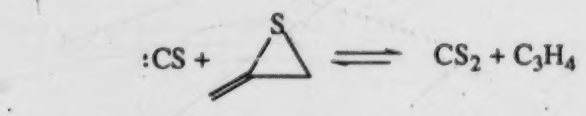

[82]

Evidence for this tautomerism has been reported by Block et al., who conclude that the methylenethiirane tautomer is more stable than the cyclopropanethione.[126]

In the reaction of S(^{1}D, ^{3}P) atoms with 1,2-butadiene, five major products were identified, which arise from addition to a double bond and insertion into a C–H bond.[50]

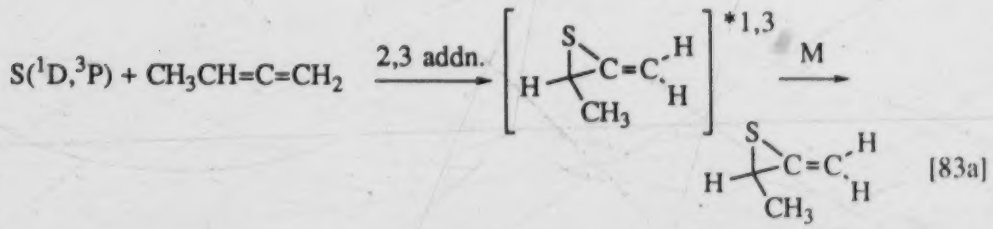

[83a]

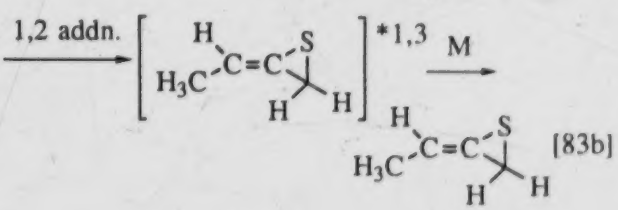

[83b]

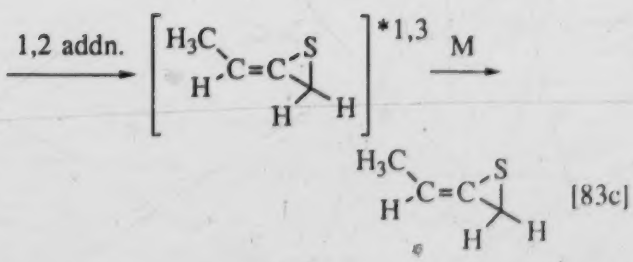

[83c]

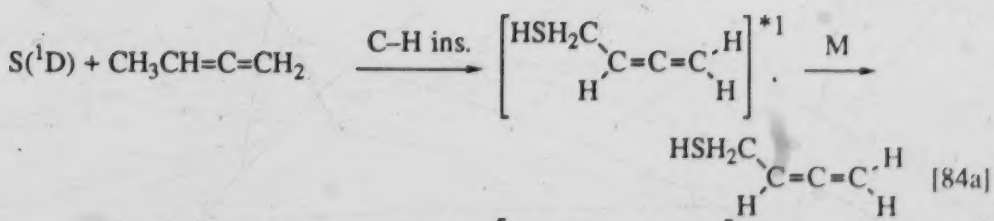

[84a]

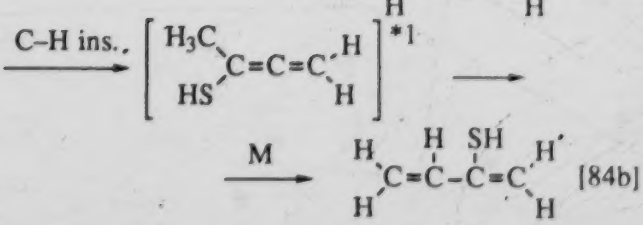

[84b]

The ratio of 2,3 addition to 1,2 addition for the S(^{1}D) atom reaction with C_4H_6 is 1.3, whereas in the S(^{3}P) + C_4H_6 reaction, it is 2.1.[125] This means that the S(^{3}P) atom is more electrophilic and discriminating in its choice of addition to a particular double bond. The presence of the CH_3 group makes the 2,3 double bond more electron-rich. The trans-/cis- product ratio from reactions [83b] and [83c] is nearly 6.[50] The product formed in reaction [84b] was quite unexpected and is believed to arise as follows:

$$S(^1D) + CH_3CH{=}C{=}CH_2 \longrightarrow CH_3(SH)C{=}C{=}CH_2 \rightleftharpoons$$

$$CH_3\overset{\overset{S}{\|}}{C}CH{=}CH_2 \rightleftharpoons CH_2{=}\overset{\overset{SH}{|}}{C}CH{=}CH_2 \qquad [84b]$$

This is the first substituted vinylthiol observed. Again there was no evidence for insertion into the terminal methylene CH bonds. All the products obtained decompose with time, as observed for methylenethiirane.[50]

From the relative rate parameters measured for the addition of S(^{3}P) to 1,3-butadiene and 1,2-butadiene, their rate constants can be calculated to be ~ 3.8 x 10^{-11} and ~ 1.0 x 10^{-11} cm^3 molecule^{-1} s^{-1} , respectively.[125] The rate constant for the S(^{3}P) + allene reaction has not been measured but was estimated by Green to be about 5 x 10^{-12} cm^3 molecule^{-1} s^{-1} at room temperature.[50]

(ii) O(^{1}D, ^{3}P) Atom Reactions

The O(^{3}P)-atom reactions with the conjugated dienes 1,3-butadiene and 1,3-cyclopentadiene have been studied and they are similar to the O(^{3}P)-atom reactions with alkenes. In the O(^{3}P) + 1,3-butadiene reaction, Cvetanovic and Doyle obtained only the 1,2 addition products,[127] vinyl oxirane and 3-butenal, as well as CO and polymer. Using different analytical techniques, Havel and Chan,[128] also obtained vinyloxirane, 3-butenal and CO but in addition they detected small amounts of 3-buten-2-one, vinyl ether and

propene. The initial adduct is again a biradical and the tendency is for the oxygen atom to add to the less substituted carbon, as shown:[128]

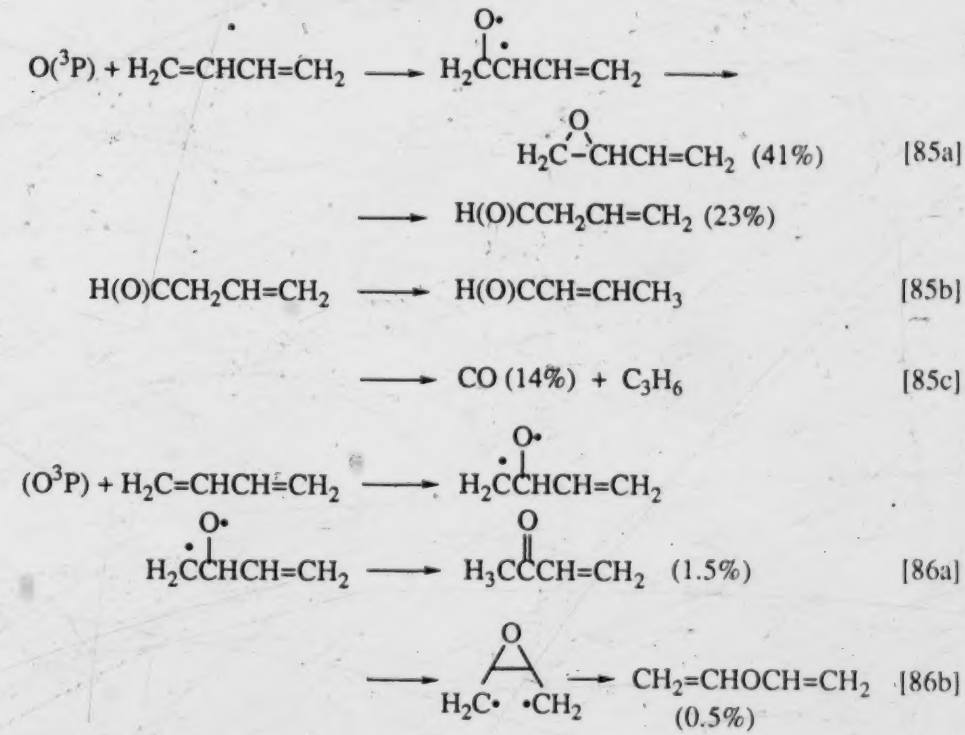

From the $O(^3P)$ + 1,3-cyclopentadiene reaction, Nakamura and Koda[129] obtained CO and the following C_4H_6 isomers: 1,3-butadiene, 1,2-butadiene, 3-methylcyclopropene and 1-butyne. In this reaction, apart from 1,2 addition, 1,4 addition is postulated to occur because of the proximity of the 1,4 carbons in the cyclic structure. A possible reaction scheme is presented below:[129]

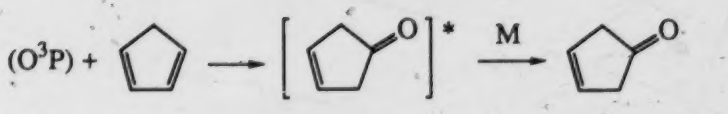

[87a]

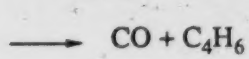

[87b]

or

[88a]

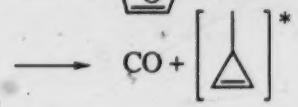

[88b]

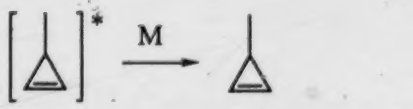

[89a]

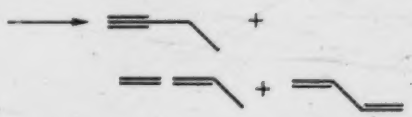

[89b]

The amount of CO generated was equal to the total amount of all the C_4H_6 isomers.

The reactions of $O(^3P)$ atoms with allenes proceed quite differently from the reaction of $O(^3P)$ atoms with alkenes, in that a methyleneoxirane structure is not formed. Instead, the $O(^3P)$ atom appears to add to the central carbon atom of the allene to form a cyclopropanone intermediate from which CO is eliminated, leaving an alkene.[130,131] The cyclopropanone, under certain conditions, could ring open to give conjugated aldehydes and ketones.[130] For example, the reaction of $O(^3P)$ with 1,2-butadiene yields the products shown below:

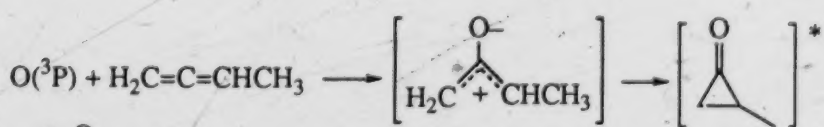

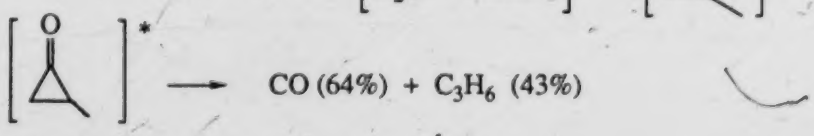

[90]

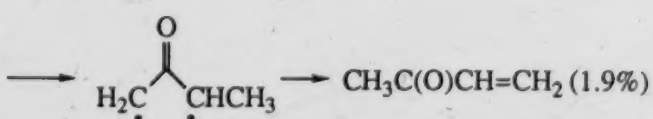

[91a]

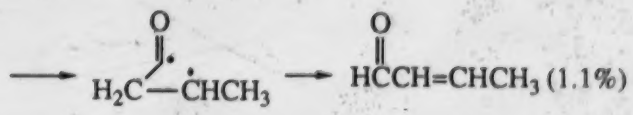

[91b]

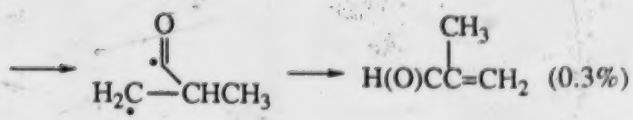

[91c]

Cyclopropanone is believed to exist in a tautomeric relationship with methyleneoxirane and an oxyallyl ion,[132] analogous to the methylenethiirane-cyclopropanethione tautomerism:

[92]

The cyclopropanone structure has been calculated to be more stable than the methyleneoxirane structure.

Rate constants recommended for the $O(^3P)$ + 1,3-butadiene, allene and 1,3-cyclohexadiene reactions are 1.98×10^{-11}, 1.23×10^{-12} and 9.13×10^{-11} cm^3 $molecule^{-1}$ s^{-1},[101] respectively. From relative rate constant measurements, rate constants for the $O(^3P)$ + 1,3-cyclopentadiene,[129] 1,2-butadiene, 3-methyl-1,2-butadiene and 2-methyl-2,3-pentadiene[130] reactions can be calculated to be ~ 4.9×10^{-11}, 6.5×10^{-12}, 4.3×10^{-11} and 6.0×10^{-11} cm^3 $molecule^{-1}$ s^{-1}.

Fluorination alters the chemistry of the $O(^3P)$ + alkene reactions somewhat.[133] For example the $O(^3P)$ + C_3F_6 reaction proceeds as follows:

$$O(^3P) + C_3F_6 \longrightarrow CF_2O + CF_3\ddot{C}F \quad [93a]$$

$$\longrightarrow CF_3CFO + \ddot{C}F_2 \quad [93b]$$

$$\longrightarrow C_3F_6O^* \quad [93c]$$

$$C_3F_6O^* + C_3F_6 \longrightarrow C_5F_{10} + CF_2O \quad [94]$$

or

$$C_3F_6O^* \longrightarrow CF_2O + CF_3\ddot{C}F \quad [95]$$

Similarly, the reaction between $O(^3P)$ atoms and with 1,3-perfluorobutadiene[133] yields CF_2O as the major product, as well as cy-$(CF)_2CF_2$, CF_2CFCFO, (C_3F_4O) and cy-$OCF_2CF(CFCF_2)$, in a mechanism similar to steps [93]–[95]. The rate constant for the $O(^3P)$ + 1,3-C_4F_6 reaction has been determined to be 4.82×10^{-13} cm^3 molecule^{-1} s^{-1}.

(iii) Se and Te Atom Reactions

The rate constant for the $Se(^3P)$ atom reaction with 1,3-butadiene has been reported to be 2.0×10^{-11} cm^3 molecule^{-1} s^{-1}.[10,102] The product formed is probably vinylselenirane, analogous to the vinylthiacyclopropane formed in the $S(^3P)$ + 1,3-butadiene reaction.

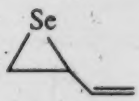

No other studies have been carried out.

(e) with aromatics

(i) S-Atom Reactions

The reactions of $S(^1D, ^3P)$ atoms with benzene were found to give no identifiable volatile products.[50] However, from the study of the $S(^1D, ^3P)$ + $CF_3C{\equiv}CCF_3$ reaction, some products were obtained which may be postulated to arise as follows:

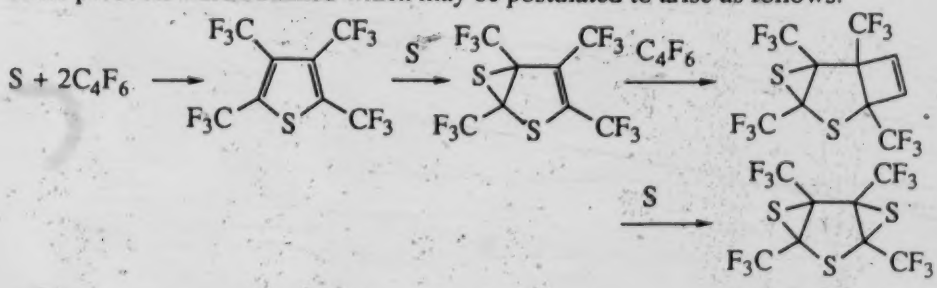

From the nature of these products it would appear that S atoms may add to the double bonds of thiophene, although no direct evidence of S(^{1}D, ^{3}P) atom reactions with aromatic compounds is yet available.

In the solution phase, when COS is photolyzed in benzene, toluene or p-xylene, the major products obtained are CO and elemental sulfur. The latter is formed from the solvent-catalyzed recombination of S(^{3}P) atoms. Traces of thiophenol were also observed[106] in benzene.

(ii) O(^{3}P) Atom Reactions

The reaction of O(^{3}P) atoms with benzene has been extensively studied and the initial rate-determining step has been shown to be addition of the O(^{3}P) atom to the benzene molecule to form a triplet biradical intermediate which may either isomerize to form phenol or eliminate a hydrogen atom, as shown below:[134]

$$O(^3P) + C_6H_6 \xrightarrow{\text{slow}} [C_6H_6O\,\dot{}] \xrightarrow{\text{fast}} C_6H_5OH \qquad [97a]$$

$$[C_6H_6O\,\dot{}] \xrightarrow{\text{fast}} C_6H_5O\cdot + H\cdot \qquad [97b]$$

Some early researchers reported CO elimination,[135] but this has since been determined to be due to secondary reactions.[134] The relative importance of the two reaction pathways [97a] and [97b] was found to be energy- and isotope-dependent,[136] such that the formation of phenol is favored at higher collision energies and with increasing deuterium substitution. Phenol is the major volatile product obtained and most of the reaction products are in the form of non-volatile polymeric tars.[137]

Grovenstein and Mosher studied the reactions of O(^{3}P) with a series of thirteen aromatic compounds, twelve of which gave phenols comprising > 95% of the volatile

products formed.[138] In the $O(^3P)$ + toluene reaction, it was found that ortho substitution was favored over para substitution, probably because the ortho position has a slightly higher electron density, thus favoring attack by the electrophilic $O(^3P)$ atom. An interesting product obtained in the $O(^3P)$ + 1,2,3-trimethylbenzene reaction was 2,6-dimethylphenol. No insertion into the C–C bond to give the 2,6-dimethylanisole was seen; instead the methyl group was displaced as shown:[138]

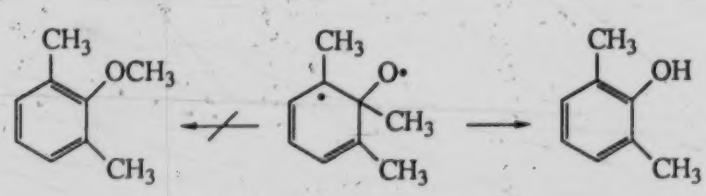

[98]

Grovenstein and Mosher also determined partial rate factors for the different positions on the aromatic ring in order to explain the observed substitution patterns.

Absolute rate constants for a variety of $O(^3P)$ + aromatic hydrocarbon reactions have been measured.[101] The rate constant for the $O(^3P)$ + benzene reaction is 2.03×10^{-14} cm^3 $molecule^{-1}$ s^{-1} and increases with increasing alkyl substitution on the aromatic ring to a value of about 2.66×10^{-12} cm^3 $molecule^{-1}$ s^{-1} for the $O(^3P)$ + 1,3,5-trimethylbenzene reaction. Fluorine substitution decreases the rate constant, e.g. the $O(^3P)$ + trifluoromethylbenzene reaction rate constant is 5.81×10^{-15} cm^3 $molecule^{-1}$ s^{-1}.[101]

The reaction of $O(^3P)$ atoms with thiophene[139] was also studied and it was deduced that the $O(^3P)$ atom could add to the sulfur atom of the thiophene as well as to either of the two double bonds, as shown below, since the overall rate constant for $O(^3P)$-atom addition to thiophene was two orders of magnitude larger than that for $O(^3P)$-atom addition to benzene. However, due to delocalization of electron density from the sulfur atom in thiophene, the rate constant for the $O(^3P)$ + thiophene reaction is less than the rate constants for $O(^3P)$ addition to CH_3SCH_3 and cy-CH_2CH_2S.[139]

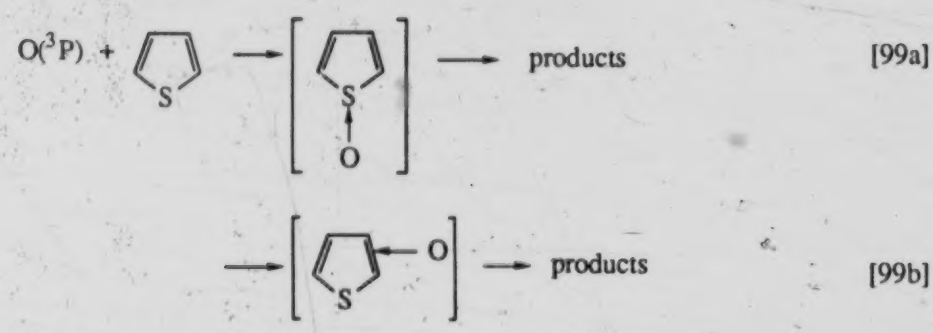

Lee and Tang propose that above 262 K, O(3P) adds to thiophene predominantly via reaction [99a], whereas below 262 K, addition to the double bonds (reaction [99b]) becomes important. They determined the rate constant for the O(3P) + thiophene reaction to be ~ 4.9 x 10^{-12} cm^3 $molecule^{-1}$ s^{-1} at room temperature.[139]

(f) with thioethers

(i) S(1D, 3P) Atom Reactions

The reactions of S atoms with the acyclic thioether, dimethyl sulfide, and the cyclic thioethers, thiirane, methylthiirane, trans-1,2-dimethylthiirane and thietane, have been studied.

In the $S(^1D) + CH_3SCH_3$ reaction the $S(^1D)$ atom is believed to add to the sulfur atom of the dimethylsulfide to form a singlet-state thiosulfoxide which isomerizes to form dimethyldisulfide,[50,140] the only sulfur-containing product. The proposed reaction pathway is shown below:

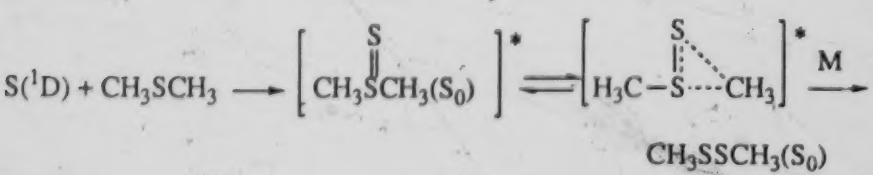

$$\overset{S}{\overset{\|}{CH_3SCH_3}}(S_0) \longrightarrow C_2H_6 + S_2(^1\Delta_g) \qquad [100b]$$

$$\overset{S}{\overset{\|}{CH_3SCH_3}}(S_0) \longrightarrow 2\,CH_3SCH_3 + S_2(^1\Delta_g) \qquad [100c]$$

The other major product formed is elemental sulfur; C_2H_6 was a minor product.[50] No C–H insertion products were observed and the same products were obtained in the $S(^3P) + CH_3SCH_3$ reaction but in much lower yields. The initial adduct formed in the $S(^3P) + CH_3SCH_3$ reaction is postulated to be the triplet thiosulfoxide, shown below:[50]

$$S(^3P) + CH_3SCH_3 \longrightarrow \left[CH_3\overset{S\bullet}{\underset{\bullet}{S}}CH_3(T_1) \right]^* \longrightarrow \left[CH_3\overset{S}{\overset{\|}{S}}CH_3(S_0) \right]^* \longrightarrow CH_3SSCH_3 \qquad [101]$$

In the $S(^3P)$ reaction with the thiirane, desulfurization occurs with the formation of the corresponding alkene, possibly through a thiosulfoxide intermediate:[140,141]

$$S(^3P) + \text{cy-}CH_2CH_2S \rightarrow [CH_2CH_2\text{–}S\text{–}S(T_1)] \rightarrow C_2H_4 + S_2\,(^3\Sigma_g^-) \qquad [102]$$

The $S(^1D,\ ^3P)$ + cy-$CH_2(CH_2)_2S$ reaction was studied by Green and coworkers,[50,140] and the primary adduct in this case is also believed to be the thiosulfoxide, which probably ring-opens to isomerize to 1, 2-dithiolane:[50]

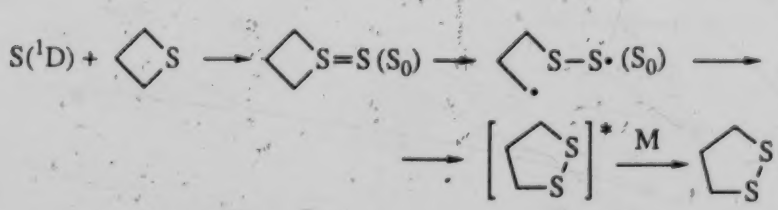

$$\longrightarrow \left[\text{1,2-dithiolane} \right]^* \xrightarrow{M} \text{1,2-dithiolane}\ (S_0) \qquad [103a]$$

$$\longrightarrow C_2H_4 + CH_2S_2 \qquad [103b]$$

$$\longrightarrow C_3H_6 + S_2(^1\Delta_g) \qquad [103c]$$

[103d]

C_2H_4 is the other major product of the reaction. In the $S(^3P)$ + cy-$CH_2(CH_2)_2S$ reaction, the products obtained are the same as for the $S(^1D)$ atom reaction, except that the product yields are lower, especially that of C_2H_4.[140]

From absolute and relative rate measurements, the rate constants for the $S(^3P)$ atom reactions with CH_3SCH_3,[140] cy-CH_2SCH_2,[141] cy-$CH_2SCH(CH_3)$, trans-cy-$CH(CH_3)SCH(CH_3)$[11] and thietane at 298 K are 3.49×10^{-10}, 2.32×10^{-11}, 4.48×10^{-11}, 6.64×10^{-11} and 4.82×10^{-10} cm^3 $molecule^{-1}$ s^{-1}, respectively. They also feature very small or negative activation energies.[140] The reference rate constant taken was the absolute value determined by Klemm and Davis for the $S(^3P)$ + thiirane reaction.[141]

(ii) <u>$O(^3P)$ Atom Reactions</u>

The reactions of $O(^3P)$ atoms with thioethers and thiols have been studied and the general reaction pathway appears to proceed via addition of the $O(^3P)$ atom to the sulfur atom of the thioether or thiol to form a short-lived sulfoxide:[142]

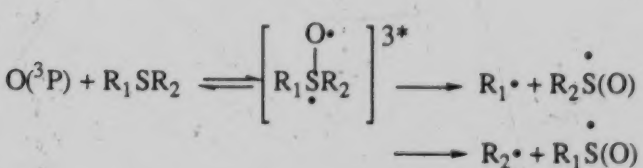

[104a]

[104b]

where R_1 = alkyl and R_2 = alkyl or H·

In the case of CH_3SH, reaction [104a] accounts for 60% of the overall reaction, reaction [104b], 30%, and an additional (10%) decomposition pathway generates hydroxyl and thiyl radicals:[143]

$$O(^3P) + CH_3SH \rightleftharpoons \left[CH_3\overset{\overset{O\bullet}{|}}{S}H \right]^{3*} \longrightarrow CH_3\bullet + \bullet OSH \quad (60\%) \qquad [105a]$$

$$\longrightarrow CH_3SO\bullet + H\bullet \quad (30\%) \qquad [105b]$$

$$\longrightarrow CH_3S\bullet + \bullet OH \quad (10\%) \qquad [105c]$$

Cvetanovic et al.[144] studied the $O(^3P) + CH_3SCH_3$ reaction and determined that reaction [104a] predominates (>95%). The major retrievable products are C_2H_6 and dimethylsulfoxide , believed to be formed not by collisional deactivation of the initial adduct, but by recombination of radicals as shown below:[144]

$$O(^3P) + CH_3SCH_3 \longrightarrow \left[CH_3\overset{\overset{O\bullet}{|}}{S}CH_3 \right]^{3*} \xrightarrow{fast} CH_3SO\bullet + CH_3\bullet \qquad [106]$$

$$2\ CH_3\bullet \longrightarrow C_2H_6 \qquad [107]$$

$$CH_3\bullet + CH_3SO\bullet \longrightarrow (CH_3)_2SO \qquad [108a]$$

$$CH_3\bullet + CH_3SO\bullet \longrightarrow CH_3SOCH_3 \qquad [108b]$$

$$2\ CH_3SO\bullet \longrightarrow CH_3S(O)OSCH_3 + CH_3S(O)_2SCH_3 \qquad [109]$$

Lee et al. also studied the $O(^3P) + CH_3SCH_3$ reaction at lower pressures, and observed the SO_2 afterglow which they postulate arose as follows:[145]

$$CH_3SO\bullet \longrightarrow CH_3\bullet + SO \qquad [110]$$

$$O(^3P) + SO \longrightarrow SO_2^* \longrightarrow SO_2 + h\nu \qquad [111]$$

$$O(^3P) + CH_3SO\bullet \longrightarrow CH_3 + SO_2 + h\nu \qquad [112]$$

Slagle et al.[146] claim to have detected small amounts of the species $CH_3O\cdot$ and $CH_3S\cdot$ which could be produced as follows:

$$O(^3P) + CH_3SCH_3 \rightleftharpoons \left[CH_3\overset{O\cdot}{\underset{\cdot}{S}}CH_3 \right] \longrightarrow \left[CH_3\overset{OCH_3}{\underset{}{S}} \right] \longrightarrow$$

$$\longrightarrow CH_3S\cdot + CH_3O\cdot \quad [113]$$

Tevault et al.[147] studied the reaction in low-temperature argon matrices in which dimethylsulfoxide and also dimethylsulfone were the only products detected. C–S bond cleavage was not observed. The observation of dimethylsulfoxide, which cannot be formed via [108b] under these conditions, supports the intermediacy of triplet-state dimethylsulfoxide in the gas-phase experiments.

The sulfoxide intermediate is also proposed for the $O(^3P)$ + thiirane reaction as well,[145] which generates C_2H_4 and SO:

$$O(^3P) + \text{cy-}CH_2SCH_2 \longrightarrow \left[\text{cy-}CH_2\overset{O\cdot}{\underset{\cdot}{S}}CH_2 \right]^{3*} \longrightarrow C_2H_4 + SO \quad [114]$$

Lee et al. also detected the SO_2 afterglow from reaction [111]. Singleton studied the $O(^3P)$ + cy-$CH_2SCH_2CH_2$ reaction and obtained the products C_2H_4 and cy-$(CH_2)_3$ in about 90% yield.[50] This reaction is also believed to proceed via a triplet-state sulfoxide intermediate.

The $O(^3P)$ + dimethyldisulfide reaction has been studied recently by Singleton et al. and the primary reaction pathway is believed to be:[143]

$$O(^3P) + CH_3SSCH_3 \longrightarrow \left[CH_3\overset{O\cdot}{\underset{\cdot}{S}}SCH_3 \right]^{3*} \longrightarrow CH_3SO\cdot + CH_3S\cdot \quad [115]$$

One of the products of the reaction, identified as methylmethanethiosulfonate, is postulated to be formed as follows:[143]

$$CH_3SO\cdot + CH_3SO\cdot \longrightarrow CH_3S(O)OSCH_3 \longrightarrow CH_3S(O)_2SCH_3 \qquad [116]$$

The rate constant values for the $O(^3P)$ + thiol reactions increase from a value of 1.99 x 10^{-12} cm^3 $molecule^{-1}$ s^{-1} for CH_3SH to 3.49 x 10^{-12} cm^3 $molecule^{-1}$ s^{-1} for 1-pentanethiol.[148] Rate constants measured for the $O(^3P)$ + CH_3SCH_3, cy-CH_2SCH_2 and CH_3SSCH_3 reactions are 5.15 x 10^{-11}, 1.26 x 10^{-11} and 9.96 x 10^{-11} cm^3 $molecule^{-1}$ s^{-1}, respectively. Slagle et al.[142] have correlated the activation energies of a few $O(^3P)$ + R_1SR_2 reactions to the ionization potentials of the R_1SR_2 (thioethers and thiols), and postulate that the $[O\cdot R_1\text{–}S\text{–}R_2]$ complex has charge transfer characteristics similar to those in complexes formed in $O(^3P)$ + substituted ethylene reactions.

E. Other Gas-Phase Reactions and Quenching Interactions of S Atoms

(a) with hydrogen

The stable products obtained in the reaction of $S(^1D)$ with hydrogen are H_2S, H_2S_2 and elemental sulfur.[48,149] The transient species, $HS(^2\Pi)$, $S_2(^3\Sigma_g^-)$ and HS_2 were also detected by de Sorgo.[149] The $S(^1D)$ atom is believed to insert into the H_2 molecule to give a vibrationally excited H_2S molecule, which may be collisionally stabilized or decompose:[149]

$$S(^1D) + H_2 \longrightarrow H_2S^* \qquad [117]$$

$$H_2S + M \longrightarrow H_2S + M^* \qquad [118]$$

$$H_2S^* \longrightarrow H\cdot + HS\cdot \qquad [119]$$

$$COS + H\cdot \longrightarrow CO + HS\cdot \qquad [120]$$

$$2HS\cdot \longrightarrow H_2S + S(^3P) \qquad [121]$$

$$2HS\cdot + M \longrightarrow H_2S_2 \qquad [122]$$

$$HS\cdot + S(^3P) \longrightarrow HS_2 \qquad [123]$$

$$S(^1D) + COS \longrightarrow CO + S_2(^1\Delta, {}^3\Sigma_g^-) \qquad [5]$$

The $S(^3P)$ atom is not expected to insert into the H_2 molecule and the abstraction reaction,[48] is

$$S(^3P) + H_2 \longrightarrow \cdot H + HS \qquad \Delta H = 21 \text{ kcal mol}^{-1} \qquad [124]$$

endothermic. Experimental results show that when CO_2 is added to the COS + H_2 system to quench the $S(^1D)$ atom, the HS· yields decrease sharply and the S_2 production is unaffected.[149] The rate constant for the $S(^1D_2) + H_2$ reaction and quenching was determined by Black and Jusinski to be $2.1 \pm 0.2 \times 10^{-10}$ cm^3 molecule^{-1} s^{-1} [45] of which 57% accounts for quenching.[43] Total quenching of the $S(^1S_0)$ atom to both the $(^1D_2)$ and (^3P_J) states by H_2 is comparatively slow, having a rate constant of only about $7.7 \pm 1.5 \times 10^{-16}$ cm^3 molecule^{-1} s^{-1}.[71]

(b) <u>with oxygen</u>

$S(^1D)$ atoms may react with O_2 as shown[45]

$$S(^1D) + O_2(X^3\Sigma_g^-) \longrightarrow SO\ (b^1\Sigma^+) + O(^3P) \qquad \Delta H = -2 \text{ kcal mol}^{-1} \qquad [125]$$

but from Black's experiments,[43] it appears that only quenching to the $S(^3P)$ state occurs with a rate constant of 5.3×10^{-11} cm^3 molecule^{-1} s^{-1} at 298 K.[45]

$S(^3P)$ atoms, however, have been found to react chemically with O_2:[11]

$$S(^3P) + O_2(X^3\Sigma_g^-) \longrightarrow [S\cdots O\text{–}O]^* \rightarrow SO(X^3\Sigma^-) + O(^3P) \qquad [126]$$

SO_2 was not a product.[11] The rate constant for this reaction has been determined to be $2.2 \pm 0.2 \times 10^{-12}$ cm^3 molecule^{-1} s^{-1} at 300 °K.[43] The S($^1S_0$) atom is quenched by O_2 to the ($^1D_2$) and (^3P_J) states, with a rate constant of $6.0 \pm 0.6 \times 10^{-13}$ cm^3 molecule^{-1} s^{-1} 298 K.[71]

(c) <u>with NO_2</u>

The S(^{1}D) + NO_2 reaction has not been studied, but the S(^{1}D) atom is expected to be efficiently deactivated by NO_2.[150] The S(^{3}P) + NO_2 reaction was studied by Clyne and Whitefield,[151] and generates the following products.

$$S(^3P) + NO_2\ (X^2A_1) \longrightarrow SO + NO \qquad [127]$$

$$SO + NO_2\ (X^2A_1) \longrightarrow SO_2 + NO \qquad [128]$$

$$O + NO_2 \longrightarrow O_2 + NO \qquad [129]$$

The rate constants for reactions [127] to [129] are $6.7 \pm 0.9 \times 10^{-11}$, 1.4×10^{-11} and 0.93×10^{-11} cm^3 molecule^{-1} s^{-1}, respectively.[151] NO_2 is found to deactivate S($^1S_0$) very efficiently with a rate constant of $6.1 \pm 0.6 \times 10^{-10}$ cm^3 molecule^{-1} s^{-1}.[71] Apart from the deactivation of S($^1S_0$) to the S($^1D_2$) and S(^3P_J) states, the following reaction pathway is suggested for the interaction of S($^1S_0$) atoms with NO_2:[71]

$$S(^1S_0) + NO_2\ (X^2A_1) \longrightarrow NO\ (X^2\Pi) + SO\ (a^1\Delta, b^1\Sigma^+) \qquad [130]$$

$$\longrightarrow NS\ (X^2\Pi) + O_2\ (a^1\Delta_g, b^1\Sigma_g^+) \qquad [131]$$

(d) with N_2O

$S(^1D)$ can react with N_2O in one of two ways:[45]

$$S(^1S_0) + N_2O \longrightarrow NS\ (X^2\Pi) + NO\ (X^2\Pi) \qquad \Delta H = -28 \text{ kcal mol}^{-1} \quad [132]$$

$$\longrightarrow SO\ (^1\Delta \text{ or } ^1\Sigma) + N_2 \qquad \Delta H = (-93 \text{ or } -81) \text{ kcal mol}^{-1} \quad [133]$$

Although these two pathways are equally important, physical quenching of the $S(^1D)$ is dominant, occurring about 69% of the time.[43] The rate constant for the deactivation of $S(^1D)$ by N_2O was measured by Black and Jusinski to be 1.6×10^{-10} cm^3 molecule^{-1} s^{-1}.[45] For the deactivation of $S(^1S_0)$ by N_2O, Dunn reports a rate constant of $< 3 \times 10^{-15}$ cm^3 molecule^{-1} s^{-1}.[71]

(e) with CO_2

A thermodynamically possible reaction pathway between $S(^1D)$ and CO_2 is:[45]

$$S(^1D) + CO_2\ (^1\Sigma^+) \longrightarrow SO\ (^1\Delta) + CO\ (^1\Sigma^+) \qquad \Delta H = -6 \text{ kcal mol}^{-1} \quad [134]$$

The rate constant for the deactivation of $S(^1D)$ by CO_2 is 1.5×10^{-10} cm^3 molecule^{-1} s^{-1}.[45] According to Black, quenching of $S(^1D)$ to $S(^3P)$ by CO_2 occurs about 90% of the time.[43] $S(^3P)$ would not be expected to have any significant interaction with CO_2. The rate constant for the deactivation of $S(^1S_0)$ by CO_2 is reported by Dunn et al. to be $< 6 \times 10^{-17}$ cm^3 molecule^{-1} s^{-1}.[71]

(f) with NO

In the presence of NO, photolysis of CS_2 + Ar and COS + Ar systems results in an enhancement in the formation of S_2.[11] The mechanism believed to bring about this catalytic behavior is:

$$S(^3P) + NO + M \longrightarrow SNO + M \qquad [135]$$

$$S(^3P) + SNO \longrightarrow S_2 + NO \qquad [136]$$

where $k_{[135]} << k_{[136]}$ at low total pressures. From the relative rate constant reported by Little,[150,152] and using the $S(^1D) + C_2H_4$ reaction rate constant value of 4.1×10^{-10} cm^3 $molecule^{-1}$ s^{-1} obtained by Black and Jusinski,[45] the rate constant for reaction with NO can be calculated to be 2.8×10^{-10} cm^3 $molecule^{-1}$ s^{-1}. The $S(^1S_0)$ interaction with NO could follow the reactive pathway[71]

$$S(^1S_0) + NO(X^2\Pi) \longrightarrow SO(^1\Delta) + N(^2D_J) \qquad [137]$$

NO, however, deactivates $S(^1S_0)$ efficiently with a rate constant of $3.2 \pm 0.4 \times 10^{-10}$ cm^3 $molecule^{-1}$ s^{-1}.[71]

(g) with CS_2, SO_2 and H_2S

The reaction of $S(^1D)$ with CS_2 could proceed as follows:[150,153]

$$S(^1D) + CS_2 \rightleftharpoons :CS + S_2(^1\Delta_g) \qquad \Delta H = -5.2 \text{ kcal mol}^{-1} \qquad [138a]$$

or

$$S(^1D) + CS_2 \rightleftharpoons CS_3 \rightleftharpoons CS_2 + S(^3P) \qquad [138b]$$

or

$$S(^1D) + CS_2 \rightleftharpoons CS_3 \qquad [139]$$

followed by

$$S + CS_3 \rightleftharpoons CS_2 + S_2 \qquad [140]$$

$$2\,CS_3 \rightleftharpoons 2\,CS_2 + S_2 \qquad [141]$$

Breckenridge and Taube[153] estimated that the rate constant for the deactivation of $S(^1D)$ by CS_2 is 1.9 times the rate constant for deactivation by OCS.

The deactivation of $S(^1D)$ by SO_2 and H_2S could proceed via the following reactive pathways:[150]

$$S(^1D) + SO_2 \rightleftharpoons 2\,SO \quad \Delta H = -19.7 \text{ kcal mol}^{-1} \qquad [142]$$

$$S(^1D) + H_2S \rightleftharpoons 2\,SH\bullet \quad \Delta H = -21.2 \text{ kcal mol}^{-1} \qquad [143]$$

These reactions have not been studied yet. Dunn et al. have reported the rate constants for the deactivation of $S(^1S_0)$ by COS, CS_2, SO_2 and H_2S to be $4 \pm 2 \times 10^{-13}$, $8.1 \pm 0.8 \times 10^{-10}$, $1.0 \pm 0.2 \times 10^{-10}$ and $4.9 \pm 0.5 \times 10^{-10}$ cm^3 $molecule^{-1}$ s^{-1}, respectively.[71]

(h) <u>with CO, N_2, Xe, Kr, Ar, Ne, He and SF_6</u>

Only physical quenching of the $S(^1D)$ and $S(^1S_0)$ atoms is possible with CO, N_2, Xe, Kr, Ar, Ne, He and SF_6.[45,150] These molecules are postulated to form collision complexes such as SCO or SNN with S atoms, which then fall apart after several collisions. The heavier noble gases and CO are more efficient quenchers.[154] The rate constants for the deactivation of $S(^1D)$ and $S(^1S_0)$ atoms by these molecules are listed in Table I–5.

constants for the deactivation of $S(^1D)$ and $S(^1S_0)$ atoms by these molecules are listed in Table I–5.

(i) with silanes, boranes and carboranes

$S(^1D)$ atoms have been found to insert into the Si–H bonds of silanes[17] and into the B–H bonds of boranes[17] and carboranes.[155] Examples are given below.

$$S(^1D) + (CH_3)_3\,SiH \longrightarrow (CH_3)_3\,SiSH + (CH_3)_2\,SiHCH_2SH \qquad [144]$$

$$S(^1D) + B_2H_6 \longrightarrow \begin{matrix} & H & & H \\ H_2B & & B & \\ & H & & SH \end{matrix} \qquad [145]$$

$$S(^1D) + 1,5\text{–}C_2B_3H_5 \longrightarrow 2\text{–}SH\text{–}1,5\text{–}C_2B_3H_4 \qquad [146]$$

Insertion of $S(^1D)$ atoms into Si–H and B–H bonds is much faster than insertion into C–H bonds.[17,155]

F. Aim of the Present Investigation

The first project undertaken was a study of the reaction of $S(^1D)$ atoms with the cyclic thioether tetrahydrothiophene. Since the reaction of $S(^1D, ^3P)$ atoms with thietane had been shown to lead to ring expansion to give 1,2-dithiolane,[50] it was of interest to see whether $S(^1D, ^3P)$ atoms would add to tetrahydrothiophene and whether ring expansion of the adduct would form six-membered 1,2-dithiane.

The next project was to characterize the novel compounds obtained from the reactions of $S(^1D)$ atoms with 2-fluoropropene. Some kinetic studies on this reaction were also carried out in order to observe, with the better detection system and analytical techniques

presently available, possible new features in the S(^{1}D) + fluoroalkene systems which may have been overlooked ten or twenty years ago.[156]

Finally, the stereoselective behavior of S(^{3}P) atoms had only been investigated in detail with cis- and trans-2-butene,[16] and two outstanding questions remained unresolved; first, the extent of stereoselectivity at low conversions and secondly, the cause of the observed loss of stereoselectivity with increasing conversion. The S(^{3}P) + cis– and trans-2-butene reaction was therefore re-examined and this time the isomeric purity of the starting alkene was checked before and after photolysis of the reaction mixture to verify the earlier claim by Lown et al.[94] that triplet state thiiranes could facilitate the geometrical isomerization of an alkene. The reactions of S(^{1}D, ^{3}P) atoms with cis- and trans-1,2-difluoroethylene and with cis- and trans-1,2-dichloroethylene were also studied to determine whether fluorine and chlorine substituents would affect the stereoselectivity of the reaction. A minor project was carried out to determine whether triplet state thiiranes could cause geometrical isomerization of cis-1,2-difluoroethylene.

Table I–1: Atomic Energy Levels of Ground and Lower Excited States of the Group VIA Atoms[a]

State/Atom	O	S	Se	Te[b]	Po[b]
$^3P_2$	0.0	0.0	0.0	0	0
$^3P_1$	158.5	396.8	1989.5	4751	16831
	(0.453)	(1.134)	(5.688)	(13.584)	(48.122)
$^3P_0$	226.5	573.6	2534.4	4707	7514
	(0.648)	(1.640)	(7.246)	(13.458)	(21.483)
$^1D_2$	15867.7	9239.0	9576.1	10559	21679
	(45.368)	(26.415)	(27.379)	(30.189)	(61.983)
$^1S_0$	33792.4	22181.4	22446.0	23199	39081
	(96.616)	(63.419)	(64.176)	(66.329)	(111.737)

a In cm^{-1} ($kcal\ mol^{-1}$). From Reference 8.

b Note that the energies of the $^3P_1$ and $^3P_0$ states in tellurium and polonium are inverted.

Table I–2: Some Photochemical Sources of the Group VIA Atoms in the Gase Phase

	Wavelength (nm)	Φ
1. S Atoms		
$COS\ (^1\Sigma^+) + h\upsilon \rightarrow CO\ (^1\Sigma^+) + S(^1S_0)$[13,14]	147 – 157.5	>0.80
$COS\ (^1\Sigma^+) + h\upsilon \rightarrow CO\ (^1\Sigma^+) + S(^1D_2)$[15]	222 – 248	1.0±0.02
$COS\ (^1\Sigma^+) + h\upsilon \rightarrow CO\ (^1\Sigma^+) + S(^1D_2)$	229 – 255	
$S(^1D_2) + CO_2 \rightarrow CO_2^* + S(^3P_J)$[16]		~0.9
$Hg(^3P_1) + COS(^1\Sigma^+) \rightarrow Hg(^1S_0) + CO(^1\Sigma^+) + S(^3P_J)$[17,18]	253.7	~0.9
Other S Atoms sources are: CS_2 (193 nm)[9,19,20]		
C_2H_4S(193.3 nm)[21] and H_2S (2-photon; 285–316 nm)[22]		
2. O Atom		
$N_2O + h\upsilon \rightarrow N_2 + O(^1S_0)$[23]	128 – 138	≥0.90
$N_2O + h\upsilon \rightarrow N_2 + O(^1D_2)$[24]	213.9	
$N_2O + Hg(^3P_1) \rightarrow N_2 + Hg(^1S_0) + O(^3P_J)$[25]	253.7	
3. Se Atoms		
$COSe(^1\Sigma^+) + h\upsilon \rightarrow CO(^1\Sigma^+) + Se(^1S_0)$[26]	173	~1.0
$COSe(^1\Sigma^+) + h\upsilon \rightarrow CO(^1\Sigma^+) + Se(^1D_2)$[10,27,28]	~200 – 260	
$CSe_2 + h\upsilon \rightarrow CSe(X^1\Sigma) + Se(^3P_J)$[29]	230	
4. Te Atoms		
$(CH_3)_2Te + CO_2 + h\upsilon \rightarrow CO_2 + 2CH_3\cdot + Te(^3P_{2,1,0})$[30]	200 – 250	
$D_2Te + h\upsilon \rightarrow D_2 + Te(^1D_2)$[31]	200 – 250	

Table I–3: Rate Constants at 298 K and Rate Parameters for $S(^3P_J)$ and $O(^3P_J)$ Reactions with Selected Alkenes

	$S(^3P)$			$O(^3P)$	
Alkene	$10^{14}k^{a,c}$	$E_a^{b,c}$	$10^{12}A^{a,c}$	$10^{14}k^{a,d}$	$E_a^{b,d}$
C_2H_4	49.6	1.58	7.13	73.1	1.59
C_2D_4	56.4	1.58	8.13	73.1	1.59
CD_2CH_2	52.9	1.58	7.63		
C_3H_6	318*	0.44	7.13	399	0.556
1-C_4H_8	396*	–0.14	5.35	415	0.695
Cis-2-C_4H_8	1044	–0.51	3.78	1760	–0.278
$(CH_3)_2C=CH_2$	2583	–0.78	6.92	1690	–0.026
$(CH_3)_2C=CH(CH_3)$	4073	–1.43	3.64	5650	–0.397
$(CH_3)_2C=C(CH_3)_2$	7193	–1.78	3.56	7640	–0.656
$CH_2=CHF$	20.2	2.31	9.98	32.5	2.05
Cis-CHF=CHF	0.865	4.29	12.12	27.6	2.32
C_2F_4	6.51	2.98	9.98	97.6	0.616
$CH_2=CHCl$	69.8	2.10	24.2	63.9	1.33

a Units for A and k are cm^3 $molecule^{-1}$ s^{-1}.
b Units for E_a are kcal mol^{-1}.
c Calculated from relative rate data in Reference 99 and the absolute rate constant for the $S(^3P) + C_2H_4$ reaction in Reference 98(a), except for * values which are based on absolute rate constants reported in Reference 98(b).
d From Reference 100.

Table I–4: Rate Constants at 298 K and Rate Parameters for Se(^3P_J) and Te(^3P_J) Reactions with Selected Alkenes

	Se(^3P)		Te(^3P)	
Alkene	$10^{14}k^{a,c}$	$E_a^{b,c}$	$10^{14}k^{a,d}$	$E_a^{b,d}$
C_2H_4	15	2.82	2.2	2.5
C_2D_4				
CD_2CH_2				
C_3H_6	40.7	2.35	20	0.6
1-C_4H_8	115	2.25		
Cis-2-C_4H_8	430	1.21		
$(CH_3)_2C=CH_2$	716	1.01		
$(CH_3)_2C=CH(CH_3)$				
$(CH_3)_2C=C(CH_3)_2$			648	–1.6
$CH_2=CHF$				
Cis-CHF=CHF				
C_2F_4				
$CH_2=CHCl$	21	2.44		

a Units for A and k are cm^3 $molecule^{-1}$ s^{-1}.
b Units for E_a are kcal mol^{-1}.
c From Reference 10.
d From Reference 97.

Table I–5: Rate Constants for the Deactivation of $S(^1D_2)$ and $S(^1S_0)$ Atoms by Various Molecules

	k(cm^3 $molecule^{-1}$ s^{-1})	
Molecules	$S(^1D_2)$	$S(^1S_0)$[c]
CO	7.8×10^{-11} [a]	$< 3.5 \pm 0.7 \times 10^{-16}$ *
N_2	2.5×10^{-11} [a]	$< 1 \times 10^{-17}$
Xe	6.6×10^{-11} [a]	$\leq 1.6 \times 10^{-16}$
Kr	1.1×10^{-11} [a]	$\leq 6 \times 10^{-17}$
Ar	1.4×10^{-11} [b]	$< 3.5 \pm 1.5 \times 10^{-17}$ *
Ne	$\leq 5 \times 10^{-14}$ [b]	
He	$\leq 5 \times 10^{-14}$ [b]	$\leq 6 \times 10^{-18}$
SF_6	$< 7 \times 10^{-14}$ [b]	$\leq 3.5 \times 10^{-16}$

a Calculated from relative rate data in Reference 150 and absolute rate constant for the $S(D) + C_2H_4$ reaction in Reference 45;
b From Reference 45;
c From Reference 150, * values are also reported in Reference 71.

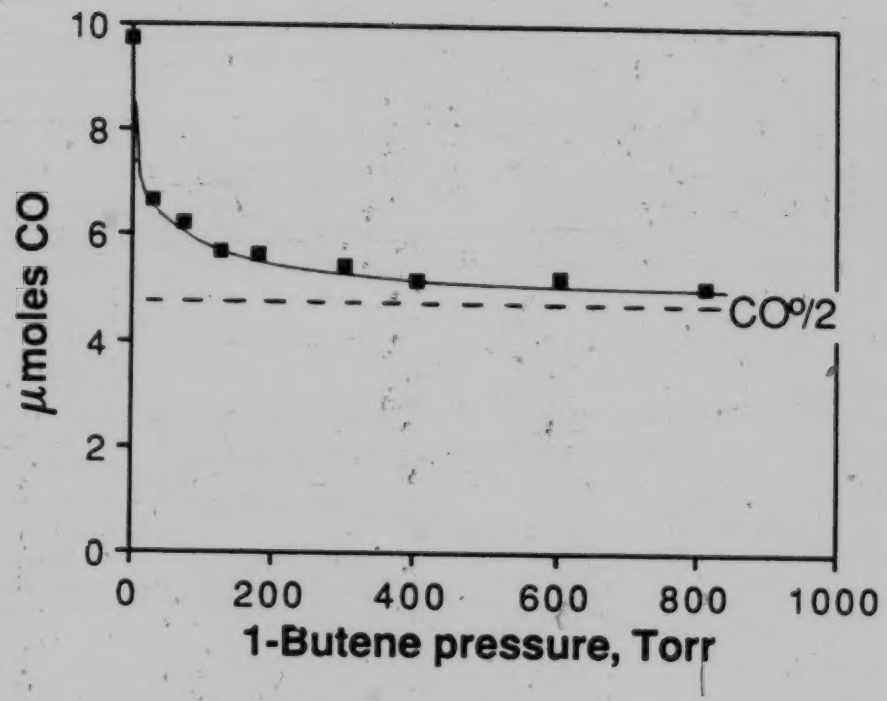

Figure I–1 : CO Yield as a Function of Increasing 1-Butene Pressure in the COS + 1-C_4H_8 Reaction[16]

CHAPTER II

EXPERIMENTAL

A. High-Vacuum System

The reactions investigated were gas-phase reactions and thus required a closed high vacuum system for the transfer and manipulation of the gases, typically less than two atmospheres in total pressure. The system, constructed of Pyrex tubing clamped onto a framework of aluminum rods on iron brackets, consisted of a mercury-free section where the photolysis, storage and distillation of reactants and products were carried out, and an adjoining non-mercury-free system where analyses of products were done.

The mercury-free system comprised three 3-L storage bulbs, two distillation trains containing two U-traps in each train for the purification of reactants and for the separation of the reaction mixture into fractions for easier analysis, two reaction cells and a circulating system which was used for storage, all of which were separated from each other by means of Springham and Hoke valves, and interspersed with pressure gauges. This section was separately evacuated by a three-stage oil diffusion pump, backed by a Welch Duo Seal oil mechanical pump, to achieve high vacuum. A one-stage oil diffusion pump linked the mercury-free and non-mercury-free sections. Products were transferred from the mercury-free to the non-mercury-free section either via the single-stage oil diffusion pump or by means of transfer tubes with Springham valves and ground glass joints for temporary attachment to the vacuum system. All diffusion pumps were cooled by cold water from the taps using Tygon tubing clamped with ring clamps.

The non-mercury-free section consisted of two U-traps to store or trap products before sending them into the gas chromotograph (GC), a Toepler pump-gas buret system with five calibrated volumes for measuring gases, a one-stage mercury diffusion pump to speed the transfer of gases into the Toepler pump-gas buret, pressure gauges, and another

Toepler pump which collected or trapped the gases for analyses in a 30-mL injection loop for introduction into the GC. Springham valves, Hoke valves, mercury float valves, and Rotaflo TF2/18 and Ace Glass Incorporated teflon stopcocks were used to separate sections of this part of the vacuum system, which was evacuated by a two-stage mercury diffusion pump connected to another Welch Duo Seal vacuum pump. Hoke injection valves were used to send the gaseous sample into the GC.

There was also a low-vacuum line pumped by a Conco Hyvac 2 rotary pump which was used to rough-pump sections of the vacuum apparatus and to open the mercury float valves. From the GC outlet there was a set of three coil traps to trap products of interest. This section could be pumped by the low vacuum line and had a line connecting it to the high vacuum line of the non-mercury-free section.

Pirani vacuum gauges (Consolidated Vacuum Corporation), which measured residual gas pressures during distillation, toeplering and transfer of gases, were used throughout the whole vacuum system. In the mercury-free section there were two mechanical gauges to read absolute gas pressures. The Speedivac type C.G.3. read up to 760 Torr while the Wallace and Tiernan (ser. no. FA 160–MMI 3270) read only up to 50 Torr. There was also a Barocel Electronic manometer Model 1174 (Datametrics) in the mercury-free section which was used to measure small pressures of gases (less than 20 Torr) for UV analysis. All electrical equipment were plugged into five plug-in bars with five sockets each and these were connected to 115 V, A.C. outlets by means of extension cords.

There was a cold trap kept at –196 °C, using liquid nitrogen in a taped silvered dewar, between the two-stage mercury diffusion pump and the non-mercury-free section and one between the three-stage oil diffusion pump and the mercury-free section. The cold trap was used to remove unwanted condensable gases such as water vapour. Greased Pyrex stopcocks were used in the region between the mechanical pumps and the cold traps only, to minimize losses of products which may be soluble in the stopcock grease. Apiezon T grease was used for these stopcocks. For temporary male-female ground glass joints either

Apiezon N or Dow Corning high vacuum silicone grease was used. Figures II–1a and II–1b show schematic diagrams of the high-vacuum system.

B. Photolytic Assembly

The four reaction cells used were cylindrical quartz tubes with high-quality quartz faces of about 5-cm o.d. and 10-cm long, equipped with a cold finger to freeze reactants into the cell. The cell volumes ranged from 205 to 250 mL. They were removable cells having graded quartz-to-Pyrex connections and sealed to the mercury-free section of the system by black wax affixed to ground glass joints. This allowed the cells to be removed and washed with a 10% HF solution and chloroform after every run.

Photolysis was effected by a Hanovia model 3062 medium-pressure mercury arc, equipped with several 2-mm thick Vycor #7910 glass filters, clamped about 7–8 cm from the face of the cell. For the tetrahydrothiophene and 2-fluoropropene experiments three Vycor filters were used, while for the other reactions only two Vycors were used. The short-wavelength limit of the radiation was about 225 nm when two filters were used and 230 nm, with three filters. The net absorbance of 80 and 100 Torr COS in the presence of two and three filters and the measured lamp profile, are shown in Figure II–2. Of the organic substrate molecules employed, only tetrahydrothiophene has appreciable absorption in this photolysis region (see Appendix A).

C. Materials Used and Their Purification

1. Carbonyl sulfide (Matheson) was passed through two bottles of saturated sodium hydroxide solution followed by two bottles of saturated lead acetate solution, and then passed through anhydrous $CaSO_4$ (Drierite) to remove CO_2, H_2S and H_2O impurities.

Once introduced into the vacuum line, it was degassed at –196 °C (liquid nitrogen) and distilled at –130 °C (n-pentane slush) into the storage bulb. The COS thus obtained is ~99% pure.

2. Tetrahydrothiophene (Eastman Organic Chemicals) had to be purified by preparative GC using a Varian Aerograph model 90-P, with a steel S.E. 30 column. By this method, the tetrahydrothiophene obtained is almost 100.00% pure.

3. 2-Fluoropropene (PCR Research Chemicals Inc.) was degassed at –196 °C and distilled at –130 °C. Its purity was determined to be better than 98.5%.

4. Carbon dioxide (Airco) was degassed at –196 °C and used as such. Carbon dioxide (Linde, Union Carbide) was degassed at –196 °C and distilled at –130 °C before use.

5. Cis- and trans-2-butene (Aldrich) were degassed at –130 °C and distilled at –78 °C (dry ice/acetone) at different vapour pressures. The resulting cis-2-butene was ~98% pure while the trans-2-butene obtained was ~99% pure.

6. Cis- and trans-1,2-difluoroethylene (PCR) were degassed at –161 °C (isopentane slush) and distilled at –130 °C. Cis-1,2-difluoroethylene had to be partially degassed at –130 °C. The distillations were carried out until a purity of about 99% was achieved for both isomers.

7. Cis- and trans-1,2-dichloroethylene (Aldrich) were both purified by GC using a 16-foot 10% tricresyl phosphate column at about 40 °C (see Tables II–1 and II–2), and purities of ~98% and 96%, respectively, were achieved for the isomers.

D. Operating Procedures

Each reagent was expanded into the photolysis cell until the desired pressure was reached, then stored temporarily in an adjacent U-trap. The large pressures of CO_2 required for the triplet sulfur studies meant that two aliquots of this reagent had to be measured. After the reaction mixture was condensed into the cell, it was allowed to equilibrate at room temperature for one hour, or overnight when carbon dioxide was present.

After photolysis the mixture was transferred to a trap at –196 °C and the non-condensable gases were transferred into the gas buret by means of the single-stage oil and mercury diffusion pumps as well as the Toepler pump to which the gas buret was connected. The remaining frozen mixture was thawed and refrozen to ensure that no gases were trapped in the mixture. The non-condensable gases were measured in the gas buret and then transferred to the injection loop for GC analysis.

The remaining products and reactants, condensed at –196 °C, were generally separated into two fractions. Distillation at –123 °C (1-chlorobutane slush) released most of the carbon dioxide, unreacted carbonyl sulfide and the substrate, and this mixture was collected at –196 °C. After equilibration at room temperature, aliquots were analyzed by GC. The heavier fraction, containing the sulfur products as well as varying amounts of substrate, was transferred directly to the GC system for analysis.

E. Analytical Techniques

1. Quantitative analysis of the products obtained was achieved by using the GC in conjunction with the gas buret. The detector response was calibrated with authentic compounds, when possible, by measuring peak areas with an Ott planimeter Type

314. In some cases the detector response had to be calibrated using isomeric compounds, in which case the detector response was assumed to be the same.

Calibrating cis- and trans-1,2-dimethyl thirane (C_4H_8S; m.w.~88 g mol^{-1}) proved to be difficult and therefore the detector response to aliquots of a solution of 13.53 g 1-butanethiol ($C_4H_{10}S$; m.w.~90 g mol^{-1}) in 50-mL diethyl ether was measured and the correction for molecular weight was done as follows. Messner et al. [157] have investigated the correlation between the relative thermal detector responses and the molecular weights of structurally similar compounds and of homologous series of compounds and have found a straight-line relation of the form:

Relative Molar Response (RMR) = A + (B x molecular weight)

where A is the intercept and B is the slope of the line.

Hence,

RMR(n-butane, n-C_4H_{10}) = 6.7 + (1.35 x 58.123) = 85.2

and

RMR(1-butene, 1-C_4H_8) = 13.0 + (1.20 x 56.107) = 80.3

Since

RMR (n-C_4H_{10}) / RMR (1-C_4H_8) = 85.2 ÷ 80.3 = 1.06,

it can be assumed that

RMR ($C_4H_{10}S$) / RMR (C_4H_8S) ~ 1.06

If the GC sensitivity of $C_4H_{10}S$ was 329 area units/umole, then the GC sensitivity of C_4H_8S is about 310 a.u./umole.

The calibration factor for C_3H_5FS and $C_2H_2F_2S$ was determined experimentally to be 274 a.u./umole.

The gas buret was calibrated by drawing up mercury into each volume and weighing it.

The GC unit used consisted of a Gow Mac Instrument Co. model 9999 D1 power supply with a home-made two-chamber thermistor block for the detector,

housed in a temperature-regulated cell assembly kept at 100°C by a Gow Mac Model no. 24–500 temperature controller. The filament current was maintained at 9 mA. A Sargent strip chart recorder was used to record the chromatograms for the sulfur atom plus tetrahydrothiophene reaction. For all the other reactions carried out, an Omniscribe recorder model B5 237–5I (Houston instrument) was used to chart the detector signals.

The carrier gas was Helium (Linde-Union Carbide) purified by passage through a 5 Å molecular sieve column. A bubble flowmeter was used to determine the flow rate and an oil manometer was connected to the GC outlet to monitor changes in the flow rate.

Packed columns made of Pyrex were used and the temperatures of the columns were regulated using home-made cylindrical tumbler-shaped aluminum ovens connected to an "Adjust-A-Volt" variac except for 0 °C, where an ice-bath was used. The Pyrex columns were removable and were attached to the rest of the system by means of two 1/4 inch diameter through-hole rubber septa and two Type–'A' connectors by Burrel. Tables II–1 and II–2 list the GC conditions, the types of columns used and the retention times of the compounds examined.

2. Identification of the products was accomplished mainly by means of gas chromatographic – mass spectrometric (GC-MS) and nuclear magnetic resonance spectroscopic (NMR) analyses. For some of the products which had not been reported in the literature, their ultraviolet (UV) and infrared (IR) absorption spectra were obtained as well.

(a) GC-MS was used to determine the molecular weights of the products obtained. First the products were separated on the appropriate column, then trapped from the GC effluent. The mixture was then frozen into the bottom of a thin Pyrex tube about 5 mm

in diameter which was then sealed and stored at –196 °C. The ampule was put into a crusher in the AEI MS–12 instrument, brought to room temperature and passed through the same packed column under the same conditions as used before. All the mass spectra were obtained with the ion source at 70 eV.

(b) NMR spectra of the major products were obtained on the Bruker WH-200 or the Bruker WH-400 spectrometer. To obtain the NMR spectrum, the product was collected from several runs, isolated in a post-GC trap and frozen into a medium-wall Pyrex NMR tube containing about 0.5-mL degassed $CDCl_3$. The NMR tube was then sealed and stored at about –18 °C until the spectrum could be run. Coupled with the mass spectral data, the structure of a product may be assigned from the NMR spectrum.

(c) The UV spectra of most of the products and reactants were examined to determine whether they absorb in the COS photolysis region. The gaseous products or reactants were expanded into a cylindrical quartz cell 10 cm long and 2 cm in diameter, the pressure of the gas being measured by the Barocel Electronic Manometer. A Hewlet Packard 8450 A Diode Array spectrophotometer was used to obtain the spectra.

(d) The infrared spectra of the products of the S+ 2- fluoropropene reaction were also obtained in the gas phase by expanding the product into the 10 cm x 2 cm quartz cell which was then placed in the sample chamber of a Nicolet T199 FTIR Spectrometer.

Table II–1: Columns and Conditions Used

Column No.	Size and packing of column	Temp (°C)	He Flow mL/min
I	8 ft. x 6 mm I.D. glass column, 13 X molecular sieve 30–60 mesh.	~25°	60
II	7 ft. x 4 mm I.D. glass column, silica gel	~65°	60
III	5 ft. x 5 mm I.D. glass column, 80–100 mesh Porapak QS.	55°	54
IV	20 ft. x 6 mm I.D. glass column, 30–60 mesh Firebrick coated with 30% Glutaronitrile – Propylene Carbonate.	0°	49
V	28 ft. x 5 mm I.D. glass column, 60–80 mesh Ultrasorb AW coated with diisodecylphthalate	0°	53
VI	8 ft. x 4 mm I.D. glass column, 10% tricresyl phosphate (TCP) on chromosorb WAW–DHCS, HP 100–200 mesh	25°, heated after 10 min	60
VII	6 ft. x 5 mm I.D. glass column, 10% tricresyl phosphate (TCP) on chromosorb WAW–DHCS, HP 60–80 mesh	25°, heated after 45 min	53
VIII	6 ft. x 5.5 mm I.D. glass column, 10% TCP on on chromosorb WAW 60–80 mesh	55°, heated after 30 min	59
IX	16 ft. x 4 mm I.D. glass column, 10% TCP on on chromosorb WAW DMCS 80–100 mesh	30°	49
X	Same column as IX	25°, heated after 20 min	49
XI	Same column as IX	~44°	44

Table II–2: Retention Times of Reactants and Products under Given Conditions on Given Columns

Compound	Column No.	Retention time (min.)
Hydrogen	I	1.7
Nitrogen	I	2.5
Oxygen	I	4.3
Methane	I	6.8
Carbon Monoxide	I	11.0
Carbon Dioxide	II	5.4
Carbonyl Sulfide	II	12.1
Ethane	II	4.1
Ethylene	II	6.7
Hydrogen Sulfide	II	22
2-Fluoropropene	III	24.1
Trans-2-butene	IV	15.0
Cis-2-butene	IV	17.7
Trans-1, 2-difluoroethylene	V	6.9
Cis-1, 2-difluoroethylene	V	11.5
Methanethiol	VI	2.7
Carbon disulfide	VI	4.5
Thiirane (thiacyclopropane)	VI	8.3
8-C compound m.w. = 112	VI	14.8
n-Butanethiol	VI	16.3
Tetrahydrothiophene (THT)	VI	26 → 30
1-Fluoro-1-methylthiirane	VII	21.6

Table II-2 Cont'd

Compound	Column No.	Retention time (min.)
2-Fluoro-2-propenethiol	VII	27.5
E-2-Fluoro-1-propenethiol	VII	36.7
Isomer of difluorodimethyl THT	VII	70.6
Trans-1,2-dimethylthiirane	IX	~42
Cis-1, 2-dimethylthiirane	IX	~70
Z-2-buten-2-thiol	IX	~47
E-2-buten-2-thiol	IX	~61.8
Trans-1,2-difluorothiirane	X	~14
Cis-1,2-difluorothiirane	X	~48
Cis-1,2-dichlorothylene	XI	~20.3
Trans-1,2-dichlorothylene	XI	~10.5
Trans-1,2-dichlorothiirane	VIII	~30
Cis-1,2-dichlorothiirane	VIII	~75
Isomer of 1,4-dichloro-1,3-butadiene	VIII	~38
Isomer of 1,4-dichloro-1,3-butadiene	VIII	~41

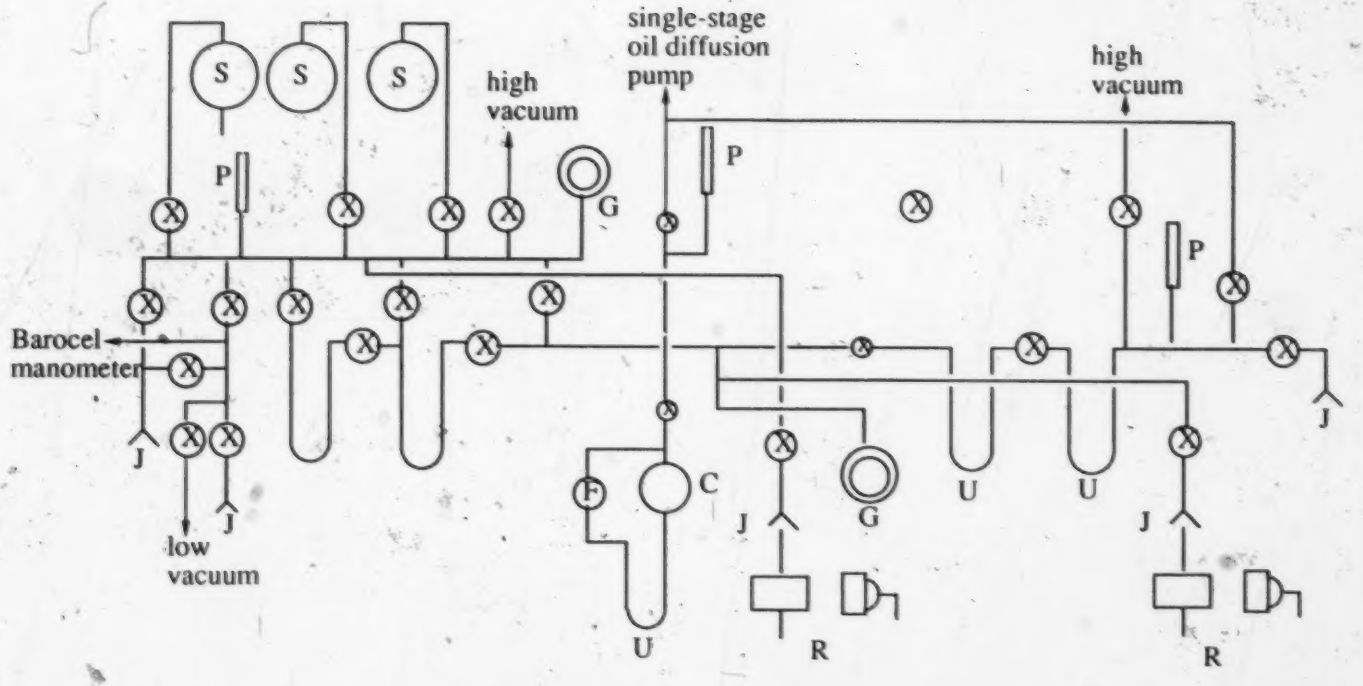

C = circulating system; G = mechanical gauge; J = female ground glass joint; P = Pirani gauge; R = reaction cell and lamp; S = storage bulb; U = U-trap; (X) = Springham valve; (⊗) = Hoke valve; (F) = fan

Figure II–1a : The Mercury-free Section of the High Vacuum System

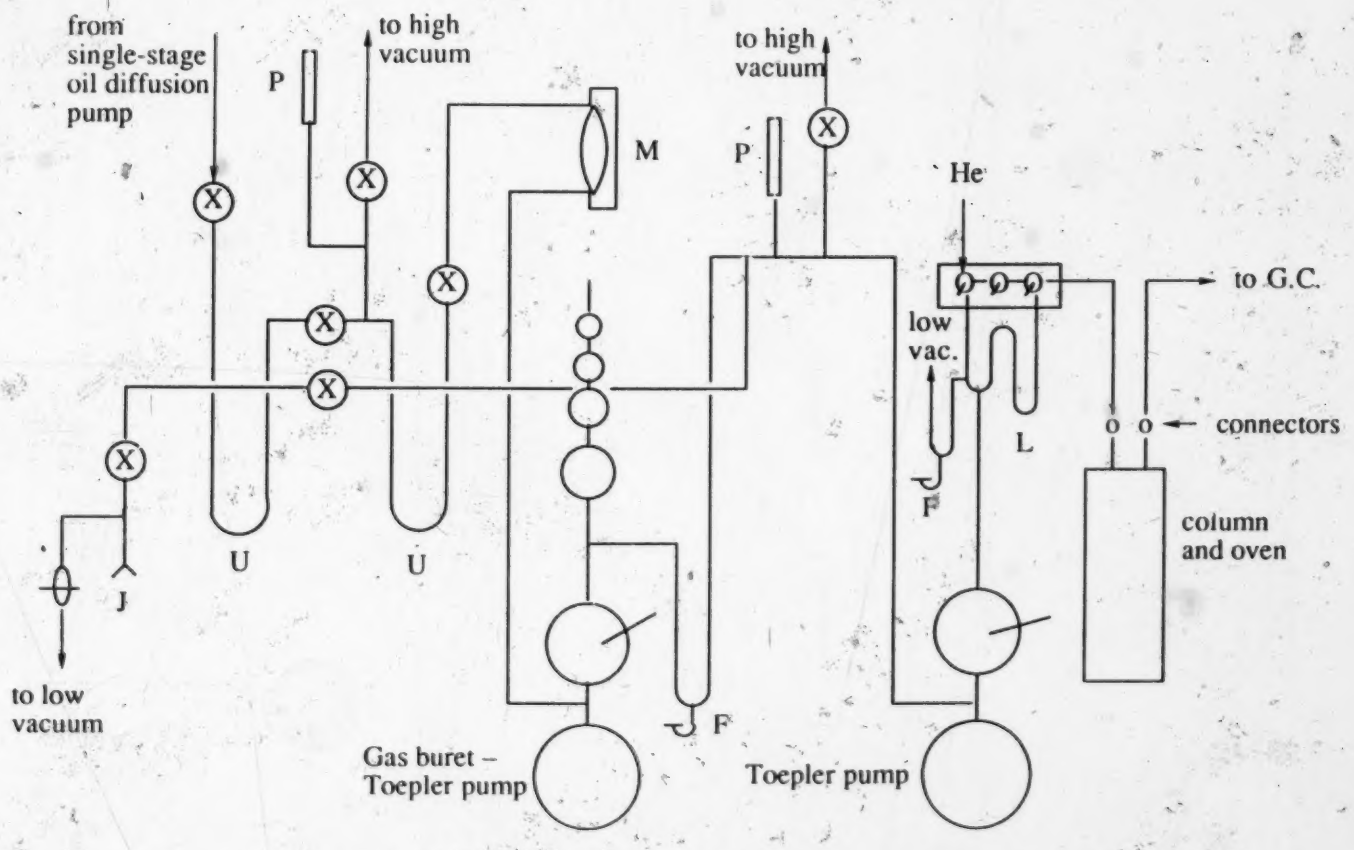

F = mercury float valve; J = female ground glass joint; L = injection loop; M = single-stage mercury diffusion pump; P = Pirani gauge; U = U-trap; (X) = Springham valve; ⊖ = glass stopcock; ℘ = injection Hoke valve

Figure II–1b : The Non-mercury-free Part of the High Vacuum System

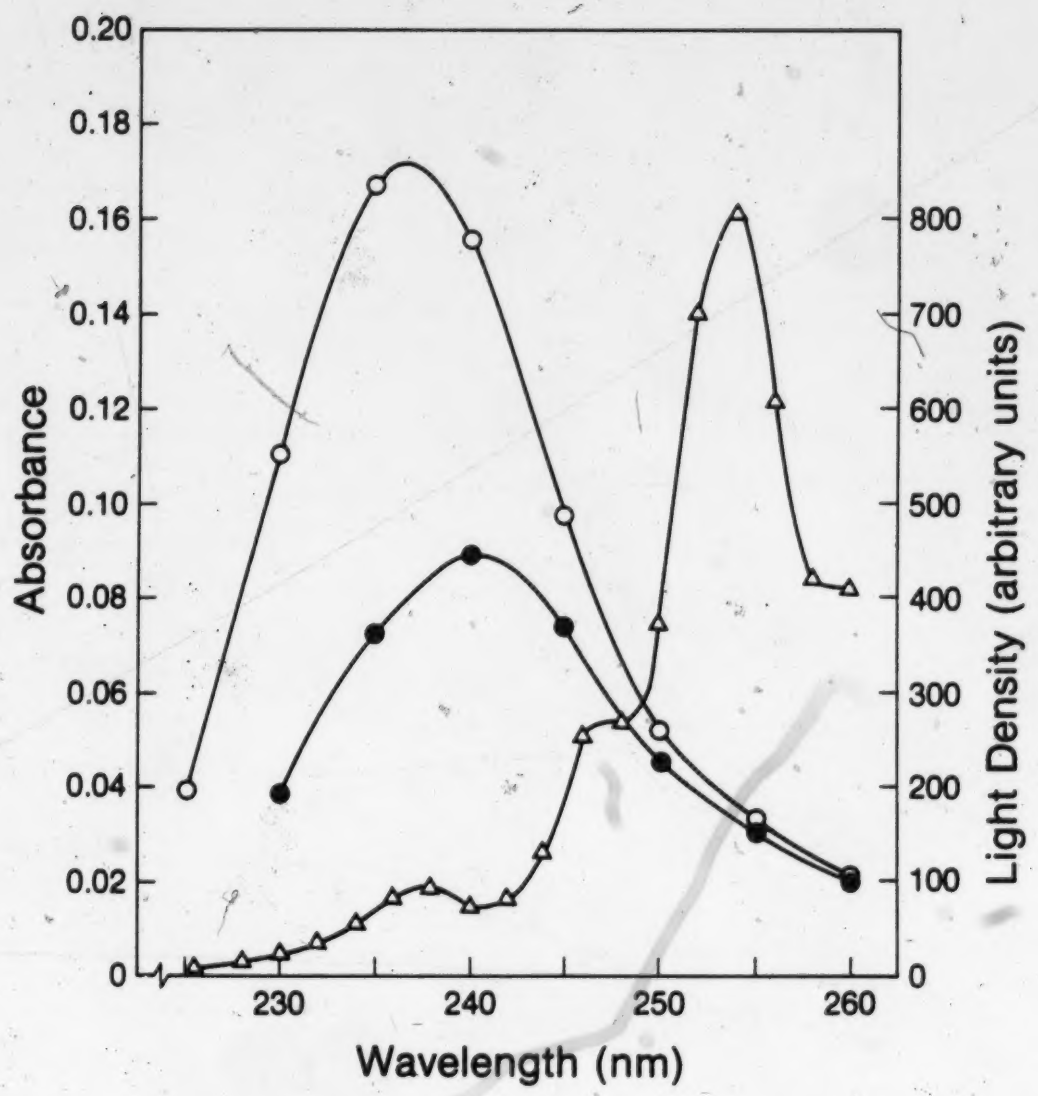

Figure II–2 : Lamp Profile (Δ) and Absorbance Profile of: 80 Torr COS, 2 Vycor Filters (○) and 100 Torr COS, 3 Vycor Filters (●).

CHAPTER III

REACTIONS OF SULFUR ATOMS WITH TETRAHYDROTHIOPHENE

A. Results

(a) UV absorption of tetrahydrothiophene

The UV spectrum of tetrahydrothiophene (C_4H_8S) vapor shows a strong absorption in the photolysis region, with an extinction coefficient 3.7 times that of COS at 240 nm (see Appendix A). Therefore a large ratio of COS to C_4H_8S must be used to ensure that COS absorbs most of the radiation. The photolysis of 3.9 Torr C_4H_8S afforded small amounts of C_2H_4S, C_2H_6, C_3H_6, H_2S, C_2H_4, n-C_4H_9SH, CH_4,CH_3SH and polymer. This identification of products is based solely on mass spectral data.

(b) Reaction Products

When a mixture of 100 Torr COS and 3.9 Torr C_4H_8S was photolyzed, COS absorbed more than 87% of the incident radiation. Under this condition no sulfur addition products were found. The major products observed by GC–MS were CS_2, 1-butanethiol and H_2S as well as some C_2H_4. At long photolysis times, the products become similar to those generated in the photolysis of tetrahydrothiophene. Since no disulfides were found, this reaction was not studied further.

B. Discussion

Sulfur atoms are believed to react with thioethers mainly by attacking the sulfur atom to form a thiosulfoxide intermediate which, in the case of the thiirane, decomposes to form ethylene and elemental sulfur.[140]

$$S(^3P) + cy\text{-}CH_2CH_2S \rightarrow [\dot{C}H_2CH_2S\text{–}\dot{S}(T_1)] \rightarrow C_2H_4 + S_2 \qquad [102]$$

With thietane, both $S(^1D)$ and $S(^3P)$ atoms react to give 1,2-dithiolane and ethylene.[50]

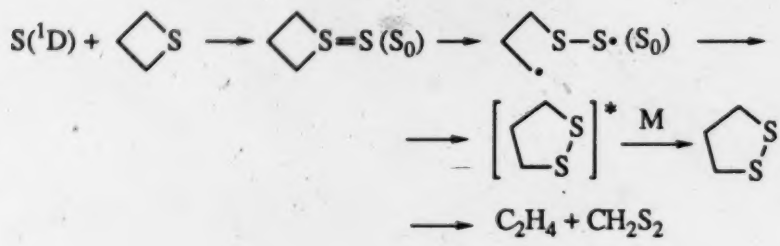

[103a]

$$\longrightarrow C_2H_4 + CH_2S_2 \qquad [103b]$$

It was therefore anticipated that $S(^1D, ^3P)$ atoms would react with tetrahydrothiophene (THT) to form a thiosulfoxide which would rearrange to give the ring-expanded 1,2-dithiane.

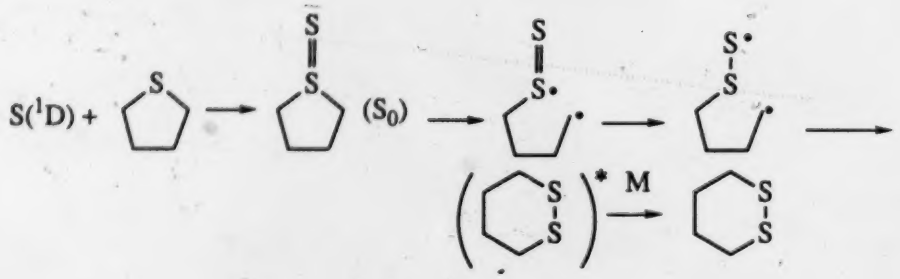

[147]

The dithiane product, however, was not observed. Since the total pressure in the cell was only about 104 Torr, it is possible that any vibrationally excited dithiane formed would fragment to give the observed products CS_2, 1-butanethiol, H_2S and C_2H_4.

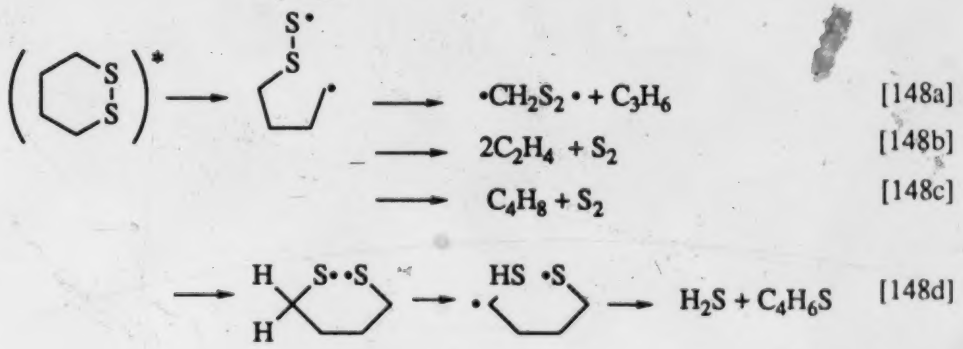

[148a] [148b] [148c] [148d]

The $\cdot CH_2S\text{–}S\cdot$ diradical may isomerize and form CS_2, via a dithioformic acid intermediate:

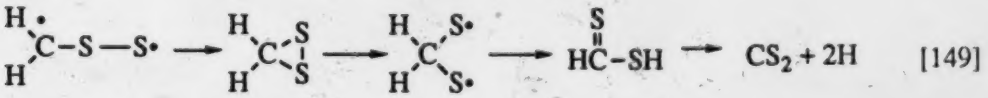

[149]

Hydrogen atoms thus formed may react with THT to give 1-butanethiol:[158]

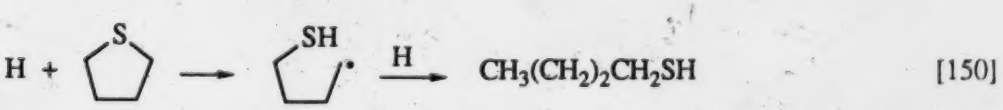

[150]

Reaction [148d] shows one possible pathway for the formation of H_2S. The overall product yield is low (in terms of S-atoms consumed), therefore polymerization is probably the major overall reaction.

The total strain energies in cyclopropane, cyclobutane, cyclopentane and cyclohexane are 27.6, 26.3, 6.5 and 0.0 kcal mol^{-1}, respectively.[159] The greatest reduction in strain occurs in going from cyclobutane to cyclopentane. The ring strain energy in thietane would

probably be less than 26 kcal mol^{-1} since the sulfur atom is larger than the carbon atoms and the ring could be slightly expanded. The five-membered 1,2-dithiolane, having two sulfur atoms, would probably have less than 6.0 kcal mol^{-1} strain so there is a great increase in thermodynamic stability in the reaction of S atoms with thietane to give 1,2-dithiolane. To go from the three to the four-membered ring in paraffins means only a gain of about 1 kcal mol^{-1} in strain energy, so the reaction of $S(^3P)$ atoms with thiirane results in the more exothermic ($\Delta H_{rxn[102]} \approx -43$ kcal mol^{-1}) abstraction of the S atom of the thiirane, rather than ring expansion. Cyclohexane in the chair configuration does not have any ring strain at all since all carbons have tetrahedral symmetry in that configuration. The six-membered 1,2-dithiane might, however,be expected to have $\sim\leq 1$ kcal mol^{-1} ring strain since the two large sulfur atoms would cause some expansion of the ring. Since the five-membered THT would have less than 6.5 kcal mol^{-1}, there is not much, about 5 kcal mol^{-1} or less, loss of ring strain in forming 1,2-dithiane from THT. However, since the reaction was not carried out at high total pressure, it is not possible to say that vibrationally excited 1,2-dithiane does not form.

According to Davis,[160] the electron donor abilities of the sulfur atoms of cyclic sulfides have been observed to be in the order: 4>5>6>acyclic>3, although from the UV study of cyclic sulfides, the order of the position of the weak band of the cyclic sulfides is 4>3>5>6. The rate of the S-atom reaction with thietane would therefore be expected to be faster than with THT and thiirane. The rate constant for the $S(^3P)$ atom reaction with thietane has been determined from relative rate studies to be 4.82×10^{-10} cm^3 $molecule^{-1}$ s^{-1}, while the absolute rate constant for the $S(^3P)$ atom reaction with thiirane has been measured to be 2.32×10^{-11} cm^3 $molecule^{-1}$ s^{-1}.

Since $S(^1D)$ atoms are known to insert into C–H bonds of many hydrocarbons, the α and β thiol derivatives of THT may be expected. They were, however, not observed. This may be due either to a much faster rate of attack at the sulfur site of the substrate, which is

electron-rich compared to a C–H bond, or to the instability of vibrationally excited α or β thiols of THT, which may decompose as shown.

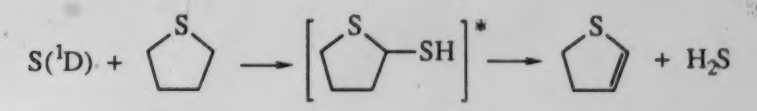

[151]

The dihydrothiophene product is very reactive and may photolyze or react with S atoms to form polymer.

The reactions of the other group VIA atoms with THT have not been reported. Singlet carbon atoms, however, have been found to desulfurize THT,[161]

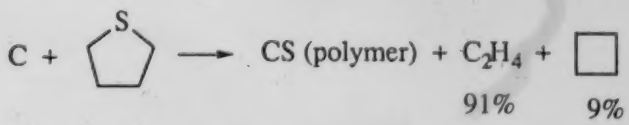

[152]

and cis-1,2-dimethylthiirane.[161]

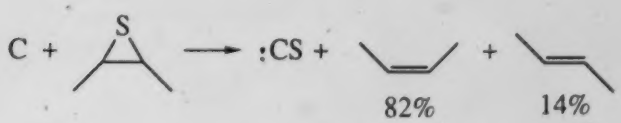

[153]

Hydrogen atoms have been found to react with THT to give 1-butanethiol, and n-butane as the main products, which arise from H-atom attack on the S atom of THT followed by C–S bond dissociation,[158] as shown in reaction [150].

SO_2 reacts with THT in the solution phase to give the following sulfone.[162]

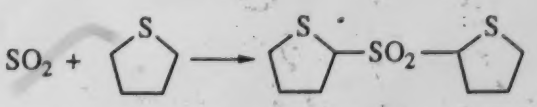

[154]

It was noted before that at much longer photolysis times, > 15 hours, the products of the COS + THT photolysis are virtually identical to those of the photolysis of THT, namely C_2H_4S, CH_3SH, n-C_4H_9SH, C_2H_4, C_2H_6, H_2S, CH_4 and polymer. Sidhu obtained 1-C_4H_9SH, 1-butene, propene and cyclopropane in a 3.6:1 ratio, and C_2H_4, C_2H_4S, hydrogen and polymer, when he photolyzed 10 Torr THT at 254 nm.[163] At 214 nm, Braslavsky and Heicklen obtained C_2H_4 as the major product as well as 1-butene, propene and ethane.[164] They also observed CH_4, c-$(CH_2)_3$,1,3-butadiene, CH_2CHSH, C_2H_4S, 1-C_4H_9SH, H_2, C_3H_8, n-C_4H_{10}, c-$(CH_2)_4$ and polymer.[164] From the 147-nm photolysis of THT Scala et al. also reported C_2H_4 as the major product.[165] Other products were C_3H_6, 1,3-C_4H_6, C_2H_2, CH_4, c-$(CH_2)_3$,C_3H_4, C_2H_6, C_3H_8 and H_2S. There is quite a variation in the products reported obtained from the photolysis of THT, but according to Scala et al., the major dissociation pathways are as follows:[165]

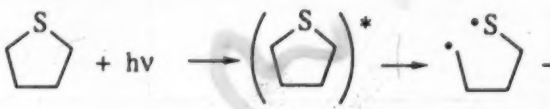

$$\longrightarrow C_2H_4 + C_2H_4S \qquad [155a]$$

$$\longrightarrow [CH_2{=}S] + C_3H_6 \qquad [155b]$$

$$\longrightarrow H_2S + C_4H_6 \qquad [155c]$$

Since the photolysis of THT in the 230 to 260 nm region is complex and gives rise to numerous products due to extensive fragmentation, the study of the S + THT reaction is not easy because most of the products generated in the latter reaction are the same ones obtained in the photolysis of THT. It is possible that other products may be obtained at higher total pressure, if vibrationally excited species are formed in the reaction which may be collisionally deactivated.

CHAPTER IV

REACTIONS OF SULFUR ATOMS WITH 2-FLUOROPROPENE

A. Results

(a) Reaction Products

On photolysis of 100 Torr COS in the presence of 2-fluoropropene, three major sulfur addition products with molecular mass of 92 g mol^{-1} (C_3H_5FS) were observed using GC-MS. These were novel compounds which had not been reported in the literature and so were collected and characterized by means of NMR and IR. Their mass spectral data are tabulated in Appendix B-1. Some secondary products having molecular weights of 118, 150 and 152 g mol^{-1} were also found, which could correspond to a diene $C_6H_8F_2$, a dialkenyl sulfide $C_6H_8F_2S$ and a thiolane $C_4H_4S(CH_3)_2(F_2)$, but since their yields were low they could not be conclusively identified.

(i) Identifications

Product 1

This C_3H_5FS product was obtained in the highest yield and its proton and fluorine NMR spectra are shown in Figure IV–1. The proton NMR spectrum shows a doublet and two doublets of doublets in a 3:1:1 ratio, respectively. This means that there are at least three different types of protons, and three equivalent protons, which suggests the presence of a methyl group. The doublets of doublets suggest that each of the two remaining protons is coupled to the other and to the fluorine. The coupling constants are not as large as they would be across a double bond and no vinylic protons (4.5 – 5.0 ppm) are present,

so there is probably no C=C double bond. The 2-fluoro-2-methylthiirane structure appears to be consistent with the NMR data where the large doublet is due to the resonance of the methyl group protons (H_C) being split by the fluorine only, since a four-sigma bond coupling to the other hydrogens is very weak. The two other resonances are due to the protons H_a and H_b which have a coupling constant of 2.4 Hz between them. It is not easy to determine which doublet of doublet is due to which proton. Miller and Neuzil give the following coupling constants for an oxirene structure:[166]

cis $J_{AB} = 0 - 5$ Hz

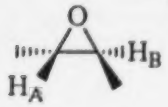

trans $J_{AB} = 1 - 3$ Hz

If the cis- and trans- coupling follow a similar trend in the thiirane, then the coupling between the fluorine and H_a, the proton cis to the fluorine, should be larger than the coupling between the fluorine and H_b, the proton trans to the fluorine. Furthermore, H_a, being spatially closer to the fluorine, may be expected to be more deshielded and so shifted farther downfield than H_b. Thus the assignment.

The ^{19}F NMR shows a quartet which is split into doublets. The quartet confirms the presence and proximity of the methyl group relative to the fluorine. The splitting of the quartet into doublets occurs due to the coupling between H_a and the fluorine. The coupling constants measured are the same as those obtained in the proton NMR. The coupling between H_b and the fluorine is small and can only be seen as a broadening of the lines.

Since sufficient product **1** was collected, a ^{13}C NMR was also obtained (Figure IV–2). The methyl carbon $C_{(3)}$ split, by the three equivalent hydrogen, into a quartet, which is further split into doublets by the fluorine. The central carbon $C_{(2)}$, to which the fluorine is

attached, is split into a doublet only by the fluorine. The $C_{(1)}$ carbon resonance is split, by the two equivalent hydrogens attached to it, into a triplet, which is further split into doublets by the fluorine. The one-bond $C_{(2)}$-F coupling is very large. The one-bond $C_{(1)}$-H coupling is significantly larger than the one-bond $C_{(3)}$-H coupling, because $C_{(1)}$ is a ring carbon. The $C_{(3)}$-F coupling is almost twice the $C_{(1)}$-F coupling, probably because the $C_{(3)}$ is closer to the fluorine than the $C_{(1)}$.

The infrared spectrum of product 1 (Figure IV–3) shows no C=C bond stretch in the 1600–1700 cm^{-1} region, which confirms that product 1 is not an alkene. The 2-fluoro-2-methylthiirane structure is therefore consistent with all the spectroscopic data obtained for product 1.

The central carbon of 2-fluoro-2-methylthiirane, to which the fluorine is attached, is a chiral carbon, so there exist both an S-2-fluoro-2-methylthiirane and an R-2-fluoro-2-methylthiirane structure. It is not possible to separate or distinguish between the enantiomers by conventional analytical methods.

S-2-fluoro-2-methylthiirane

R-2-fluoro-2-methylthiirane

Product 2

This was the second major C_3H_5FS product. Both the proton and fluorine NMR spectra were also obtained for this product (Figure IV–4). There are four proton resonances observed in the proton NMR, a triplet and three doublets of doublets, two of which seem to be further split. Hence there are four different types of protons. From integrating the resonances, one of the doublets of doublets at 3.23 ppm was found to be twice the area of the other resonances, suggesting a methylene group. The triplet at 1.82

ppm, which corresponds to one proton, must be close to the methylene group and sufficiently far from the fluorine and the other two protons, which appear to be vinylic in nature from their chemical shifts. Since an aliphatic R–SH group has a proton shift between 1.2 and 1.8 ppm, the triplet resonance H_d could be a thiol proton, which would be adjacent to a methylene group if the ^1D sulfur atom inserted into the methyl group of the 2-fluoropropene.

Since trans couplings are larger than cis couplings, the vinylic proton, H_b, must be trans to the fluorine and the other vinylic proton, H_a, must be cis to the fluorine. H_a and H_b split each other with a much smaller coupling constant than the proton-fluorine coupling constants. H_c, which is the resonance due to the methylene group, is split into two by the fluorine and then into two again by the thiol proton H_d. Since the H_c–H_d coupling is about half the H_c–F coupling, the splitting pattern looks like a quartet except that the peaks are all the same height. There is a very small coupling between H_b and H_c. The proton NMR therefore suggests that product **2** is 2-fluoro-2-propene-1-thiol.

The fluorine NMR spectrum substantiates the results of the proton NMR spectrum. At first glance, the reason for the splitting pattern of the fluorine NMR is not obvious. The 1:3:3:2:3:3:1 pattern arises due to the fact that many of the coupling constants are almost multiples of each other. To simplify the explanation, if we approximate the coupling constants as follows:

$$^3J(H_b, F) = 48 \text{ Hz}; \; ^3J(H_c, F) = 16 \text{ Hz}; \; ^3J(H_a, F) = 16 \text{ Hz}$$

then if the fluorine is first split by H into a doublet in a 1:1 ratio, which is next split by H_c into a triplet in a 1:2:1 ratio, and the resulting lines split further by H_a into doublets, the following pattern is obtained:

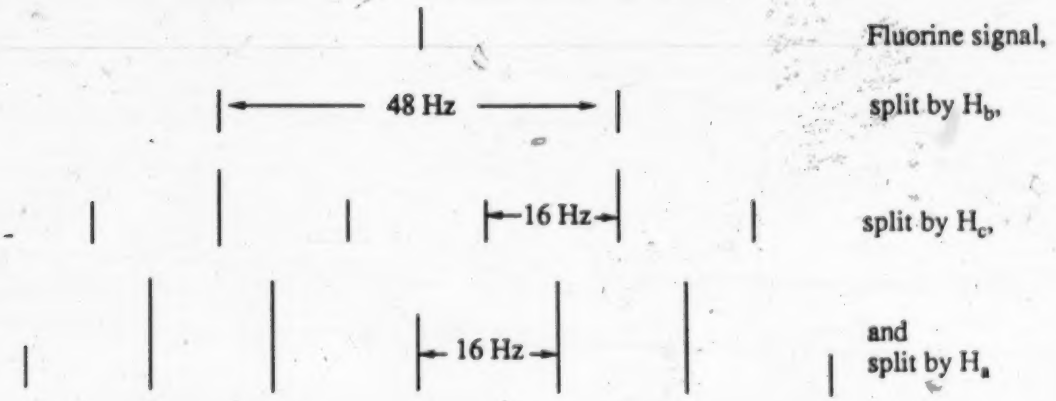

This is the pattern seen.

The infrared spectrum (Figure IV–3) of product **2** shows the presence of a C=C absorption at about 1650 cm^{-1} which proves that product **2** is an alkene. Therefore, the spectroscopic data obtained for product **2** are consistent with the 2-fluoro-2-propene-1-thiol assignment.

Product **3**

The yield of the third isomeric mw 192 product, was quite small and several experiments had to be carried out in order to obtain sufficient quantities for proton and fluorine NMR spectra (Figure IV–5). The proton NMR shows three resonances, two of which are doublets, and the third a doublet of a doublet. The integrated areas under the peaks show that the doublet at 1.96 ppm is due to three equivalent protons, which could suggest a methyl group. There is at least one vinyl proton at 4.99 ppm which is coupled to the proton at 2.81 ppm. The latter is not coupled to anything else. Product 3 therefore could have one of the following two structures:

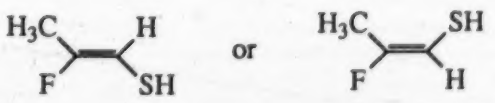

(i) (ii)

In the case of product **2**, the trans H_b–F coupling is 47.6 Hz while the cis H_a–F coupling is 15.6 Hz. The coupling between the vinyl proton and the fluorine in product **3** is 32.2 Hz which is greater than the cis coupling constant in product **2** but less than the trans coupling constant. If the electron-withdrawing nature of the sulfur atom removes some of the electron density from the double bond, then the trans H–F coupling may be expected to be smaller but the cis coupling between the fluorine and a vinyl proton would not become larger. Therefore product **3** must have structure (i), which is Z-2-fluoro-1-propenethiol. It is interesting to note that the 3-bond coupling between H_a and H_b is 9.2 Hz as compared to the 2-bond coupling between H_a and H_b in product 2, which was only 3 Hz. The geminal coupling in CH_2=CHF is reported to be –3.2 Hz,[167] which is very similar to the geminal coupling in product 2. Two-bond couplings are frequently negative. The 3-bond coupling in product **3** would possibly follow the Karplus curve where coupling is greatest when the dihedral angle between the two protons is 0° or 180° giving coupling constants of 8.5–9 Hz. The anti-conformation shown below would lead to hydrogen bonding between the fluorine atom and H_a, and is more likely than the eclipsed conformation which would lead to a weak interaction between H_a and H_b.

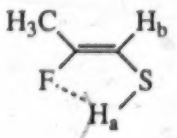

The coupling between the fluorine and the protons in the methyl group is similar to the coupling between H_c and the fluorine in product **2**.

The fluorine NMR of product **3** shows a sextet having intensities in the ratio 1:3:4:4:3:1. Again, this pattern is due to the coupling constants being approximate multiples of each other. If the approximations $J(H_b, F) \sim 32$ Hz and $J(H_c, F) \sim 16$ Hz are

made, and the fluorine signal is split into a quartet by the methyl protons and then into doublets by the vinyl proton, the resulting pattern of lines is shown below:

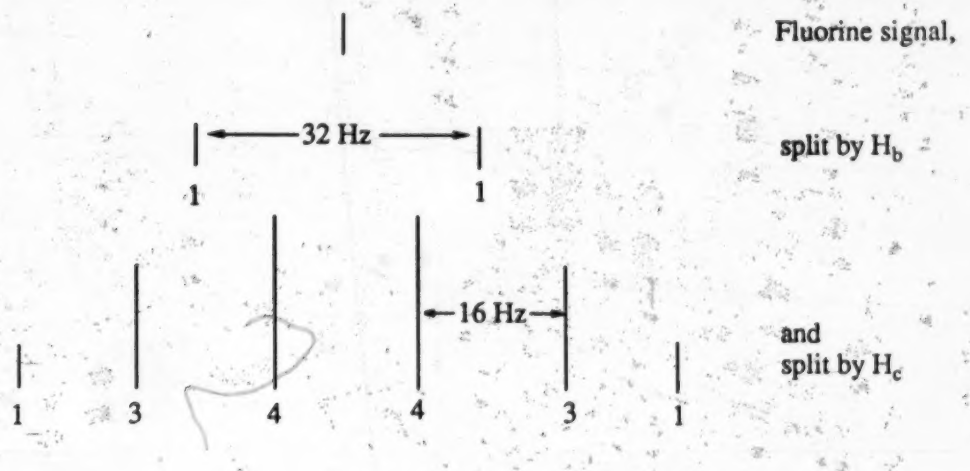

This is the approximate pattern of the intensities observed in the fluorine NMR spectra. The small splitting in the sextet peaks is due to the coupling with the thiol proton H_a.

The infrared spectrum obtained for product **3** (Figure IV–3) shows C=C stretch at about 1700 cm^{-1} and vinyl C–H stretch at about 3050 cm^{-1}, so product **3** is definitely an alkene. The very weak absorption at about 2600 cm^{-1} could be due to S–H stretch.

(ii) Properties of products **1**, **2** and **3**

The gas-phase UV spectra of products **1**, **2** and **3** show appreciable absorption of radiation in the photolysis region. Product **2** has the strongest absorption and its extinction coefficients of absorption are larger than that for COS in the photolysis region (see Appendix A). Products **1**, **2** and **3** were generally stored in the dark at ≤ -18 °C.

The products obtained in low yields are believed to be due to secondary photolysis of the primary products **1**, **2** and **3**, since they do not extrapolate to zero time.

(b) Variation in Product Yields as a Function of Irradiation Time and Pressure

Under the conditions given in Table IV–1, the amounts of products **1**, **2** and **3** were measured as a function of photolysis time. Table IV–1 lists the product yields and their rates of formation as a function of CO yield and Figure IV–6 shows how the rate of product formation decreases with increasing CO yield, i.e. with increasing conversion. After about three hours of photolysis, the ratio of product **2** to product **3** seems to be constant at ~8:3 and both products appear to have reached steady state concentration, according to Table IV–1. The formation of product **1**, however, has not reached a photostationary state even after 9 hours of photolysis.

The amounts of **1**, **2** and **3** formed as a function of increasing 2-fluoropropene pressure, and the rates of formation of the products are recorded in Table IV–2. If shorter conversions had been used, the rates of product formation would be about 1.5 times greater. Figure IV–7 shows how the product yields increase with increasing 2-fluoropropene pressure and the corresponding decrease in the CO yield. At about 400 Torr the yields of both products **2** and **3** are almost equal. This shows that some pressure stabilization of product **3** probably occurs. The rate of formation of product **1** increases slowly above about 100 Torr 2-fluoropropene pressure due to competition between COS and the 2-fluoropropene for $S(^1D)$ atoms.

B Discussion

On the basis of the known reactivity of $S(^1D)$ atoms, the products expected from the $S(^1D, ^3P)$ atom reaction with 2-fluoropropene (2FP) are 2-fluoro-2-methylthiirane (FMT), 2-fluoro-2-propene-1-thiol (2,2FPT) and the Z and E isomers of 2-fluoro-1-propenethiol (2,1FPT).

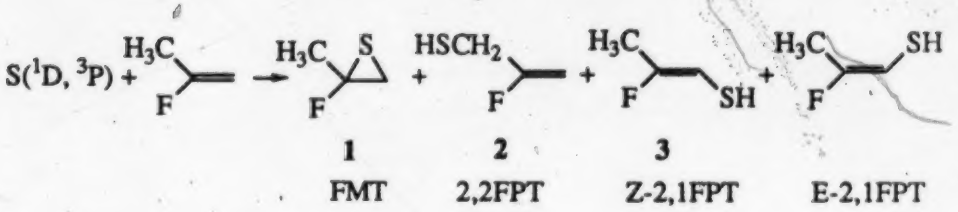

[156]

1 FMT **2** 2,2FPT **3** Z-2,1FPT E-2,1FPT

The only product not detected was E-2-fluoro-1-propenethiol.

The site in 2FP for the greatest probability of attack by the S(^{1}D) atom is the double bond since it is the most electron-rich, and sulfur atoms are known to be electrophilic in nature. Furthermore, any S(^{3}P) atoms generated by the collisional deactivation of the S(^{1}D) atoms can only add across the double bonds of 2FP to give FMT, so the latter is the most predominant product of the reaction. There are five C–H bonds available for S(^{1}D) atom insertion, insertion into three of which would give the same product, 2,2FPT, which is the second major product obtained. Insertion into vinyl C–H bonds generally occurs only if the alkene has a terminal methylene group.

From the results obtained by Wiebe[74] in the reaction of S(^{1}D) atoms with propene, vinylthiol comprised 19% of the S-addition products, with yield of the cis-1-propene-1-thiol being about 1.5 times the yield of the trans isomer at high alkene pressures. In the S(^{1}D) + 1-C_4H_8 reaction as well, the yield of cis-1-butene-1-thiol was twice that of trans-1-butene-1-thiol at high 1-C_4H_8 pressure. Therefore, sulfur atoms appear to favor inserting into the vinyl C–H bond cis to an alkyl group. The vinylthiol formed by insertion of the S atom into the C–H bond trans to an alkyl group appears to require more collisional stabilization. In the S(^{1}D) + vinyl fluoride reaction, investigated by Wiebe, the yield of cis-2-fluoroethene-1-thiol was only 1.1 times greater than that of its trans isomer at high vinyl fluoride pressures.[74] In the S(^{1}D) + 2-methylpropene reaction only about 12% of the products consited of vinylthiol since alkenyl type C–H bonds were also available for insertion. With 1,1-difluoroethene, 31% of the products obtained on reaction with S atoms was 2,2-difluoroethenethiol.

In the present study both the E and Z isomers of 2-fluoro-1-propenethiol (2,1FPT) were expected but only the Z isomer due to insertion into the C–H bond cis to the fluorine was detected. This could be due to a stronger directing effect by the fluorine atom than by the methyl group. It is also possible that E-2,1FPT is formed but is very unstable either thermodynamically or due to excess vibrational energy which would result in its rapid decomposition. If E-2,1FPT has a strong absorption in the photolysis region, it could undergo photodecomposition or photopolymerization. It is also likely that the C–H bond trans to the fluorine was the least efficient in competing with other sites for S atom attack, meaning that the rate of formation of E-2,1FPT is very low.

Some time ago, O'Callaghan studied the relative rate of $S(^3P)$ atom addition to 2FP with respect to ethylene,[156] and found that $S(^3P)$ atoms add to 2FP 2.6 times faster than to ethylene. Since $k(S(^3P) + C_2H_4) = 5.0 \times 10^{-13}$ cm^3 molecule^{-1} s^{-1}, the rate constant for the $S(^3P)$ + 2FP reaction is 1.3×10^{-12} cm^3 molecule^{-1} s^{-1}. The $S(^1D)$ atom reaction with 2FP should have a rate constant very similar to that for the $S(^1D) + C_2H_4$ reaction, ~1×10^{-10} cm^3 molecule^{-1} s^{-1}.

From Figure IV–7 it can be seen that the rates of formation of FMT and 2,2FPT decrease with increasing photolysis time. The UV spectra of the products show some absorption in the photolysis region (see Appendix A). Above 240 nm, FMT has larger extinction coefficient values than COS and above 260 nm, where COS has negligible absorption, FMT may absorb radiation and undergo secondary photolysis leading to photodecomposition and polymerization, as shown below:

$$\text{cy-}(CH_3)CFSCH_2 + h\upsilon \longrightarrow \text{cy-}(CH_3)CFSCH_2\ (S_0) \longrightarrow \text{cy-}(CH_3)CFSCH_2\ (T_1) \quad [157]$$

$$\text{cy-}(CH_3)CFSCH_2\ (S_0) \longrightarrow \text{polymerization/decomposition} \quad [158]$$

Another possible mechanism for the disappearance of FMT is desulfurization by S atoms. The rate constant for the $S(^3P)$ + FMT reaction is probably close to the value for the

$S(^3P)$ + thiirane reaction which is 2.32×10^{-11} cm^3 $molecule^{-1}$ s^{-1}. The $S(^1D)$ atom + FMT reaction would be expected to have a rate constant $\geq 0.94 \times 10^{-10}$ cm^3 $molecule^{-1}$ s^{-1}, which is the rate constant for the $S(^1D) + C_2H_4$ reaction, since $S(^1D)$ atoms should react with FMT with a rate constant larger than that for the $S(^1D)$ + 2FP reaction. Therefore the extent of desulfurization of FMT by S atoms is dependent on the concentration of FMT. However, the rates of destruction of FMT must be small relative to its rate of formation since even after nine hours of photolysis, the production of FMT has not reached a photostationary state. Desulfurization of FMT would occur as follows:

$$S + \text{cy-}(CH_3)CFSCH_2 \longrightarrow S_2 + CH_3CF{=}CH_2 \qquad [159]$$

The rates of production of the two thiol products 2,2FPT and Z-2,1FPT reach a photostationary state quite quickly. From its UV spectrum, the extinction coefficient values for absorption by 2,2FPT in the region 225 – 260 nm are greater than those for COS. The concentration of 2,2FPT in the system, however, is quite small but some of it should undergo photodecomposition and polymerization. Recently, Lam[168] studied the photolysis of simple thiols at 254 nm and found the primary products to be H_2 and RSSR, with a quantum yield ≥ 0.90. Minor products obtained were RH, R(-H) and H_2S. The mechanism and relative rates of S atom reactions with thiols are not known. If the $S(^1D)$ atom attacks the sulfur atom of the thiol to form a thiosulfoxide, the following reactions could occur.

$$S(^1D) + \begin{matrix} HSCH_2 \\ \diagdown \\ = \\ \diagup \\ F \end{matrix} \longrightarrow HS(=S)CH_2CF{=}CH_2 \ (S_0) \longrightarrow$$

$$HS(\cdot)(S\cdot)CH_2CF{=}CH_2 \ (S_0) \longrightarrow S_2 + CH_3CF{=}CH_2 \qquad [160a]$$

$$\longrightarrow HS\cdot + \cdot SCH_2CF{=}CH_2 \qquad [160b]$$

$$\cdot SCH_2CF{=}CH_2 + CH_3CF{=}CH_2 \longrightarrow \text{polymerization} \qquad [161]$$

Since the rate of formation of 2,2FPT is small, a photostationary state is reached quickly.

The rate of formation of Z-2,1FPT is much lower than those of FMT and 2,2FPT. It has, however, smaller extinction coefficient values than FMT and 2,2FPT above 238 nm. With increasing 2FP pressure, it can be seen from Figure IV–7 that the yield of Z-2,1FPT increases relative to the 2,2FPT yield, so that above ~350 Torr the yield of Z-2,1FPT is almost the same as that of 2,2FPT. This probably means that the Z-2,1FPT formed at lower pressures has excess vibrational energy. At higher pressures it is collisionally stabilized.

Several secondary products can be observed with increasing photolysis time, probably due to the photolysis of 2,2FPT and FMT which have relatively strong absorption in the photolysis region. The photolysis of 2,2FPT would give the following radicals, by analogy with the mechanism suggested by Lam.[168]

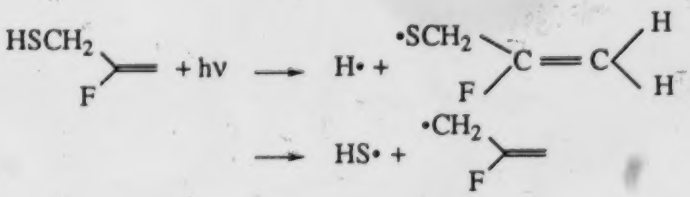

[162a]

[162b]

One of the secondary products observed in the reaction is a diene having the molecular formula $C_6H_8F_2$, which may be formed from the alkyl radical generated in reaction [162b].

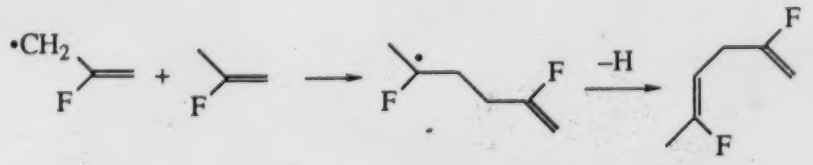

[163]

Another secondary product, a dialkenyl sulfide with molecular formula $C_6H_8F_2S$ may be formed from the thiyl radical obtained in reaction [162a].

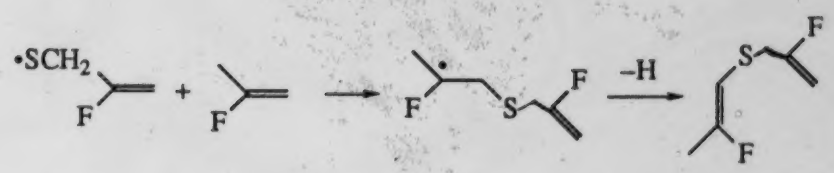

[164]

The photolysis of FMT would give rise to a triplet state FMT which could possibly add to a 2FP molecule to give rise to a third secondary product, $C_4H_4S(CH_3)_2F_2$ which, from the cracking pattern in its mass spectrum, appears to be a tetrahydrothiophene.

$$\text{cy-}(CH_3)CFSCH_2 + h\upsilon \longrightarrow \text{cy-}(CH_3)CFSCH_2\ (S_0)$$
$$\longrightarrow \text{cy-}(CH_3)CFSCH_2\ (T_1) \qquad [165]$$

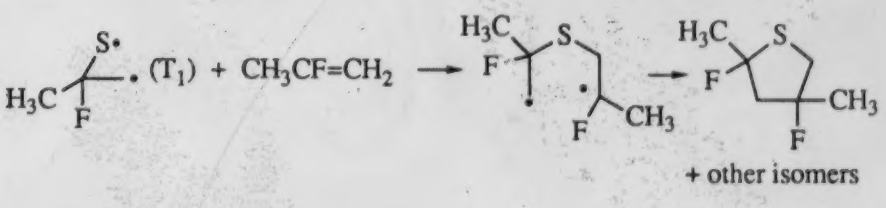

[166]

+ other isomers

A theoretical study of the $O(^3P)$ atom reaction with 2FP has been carried out and the reaction pathway predicted is:[169]

$$(O^3P) + CH_3CFCH_2 \longrightarrow {}^3CH_2 + FCCH_3 \qquad [167]$$

Since C=C bond cleavage requires ~ 150 kcal/mol, the intial adduct formed in the above reaction must have a considerable amount of vibrational energy. The relative rate of the addition has been determined to be 2.66 times faster than the $O(^3P) + C_2H_4$ reaction,[170] of the same order of magnitude as the $S(^3P)$ atom reactions.

Table IV–1 : Variation in Product Yields from the S(^{1}D, ^{3}P) + 2-Fluoropropene Reaction as a Function of Irradiation Time[a]

Photolysis Time (min.)	Products, μmoles				% Product Recovery[b]
	CO	1	2	3	
15	2.69	1.61 (0.599)[c]	0.281 (0.104)	0.110 (0.041)	111[d]
32	5.72	3.26 (0.570)	0.562 (0.098)	0.266 (0.047)	106[d]
45	7.13	3.98 (0.558)	0.738 (0.104)	0.314 (0.044)	79.3
60	11.11	4.89 (0.440)	0.854 (0.077)	0.350 (0.032)	88.9
102	19.37	7.56 (0.390)	1.23 (0.064)	0.693 (0.036)	84.9
170	28.03	10.60 (0.378)	1.62 (0.058)	0.569 (0.020)	55.9
300	40.73	11.97 (0.294)	1.61 (0.040)	0.606 (0.015)	28.9
540	49.06	12.67 (0.258)	1.64 (0.033)	0.547 (0.011)	13.2

a P(COS) = 100 Torr, P(C_3H_5F) = 100 Torr

b % Recovery = [R(1 + 2 + 3)/R(CO^0 – CO)] x 100 where R (CO^0) = 0.2995 μmoles/min

c Numbers in brackets are rates, μmoles/μmole CO

d Indicates error in either the R(CO^0) value or in the GC calibration or both

Table IV–2 : Variation in Product Yields from the $S(^1D, ^3P) + C_3H_5F$ Reaction as a Function of C_3H_5F Pressure[a]

C_3H_5F Pressure (Torr)	Products, μmoles				% Product Recovery[b]
	CO	1	2	3	
20	33.45	4.19 (0.125)[c]	0.456 (0.014)	0.223 (0.007)	94.3
40	30.58	5.64 (0.184)	0.704 (0.023)	0.405 (0.013)	83.6
60	29.31	6.35 (0.217)	0.876 (0.030)	0.522 (0.018)	83.3
90	27.83	7.70 (0.277)	1.08 (0.039)	0.759 (0.027)	88.4
160	26.76	8.79 (0.328)	1.39 (0.052)	0.993 (0.037)	94.0
240	25.68	9.55 (0.372)	1.53 (0.060)	1.25 (0.049)	95.4
320	26.36	10.31 (0.391)	1.61 (0.061)	1.50 (0.057)	109[d]
380	26.58	10.91 (0.410)	1.76 (0.066)	1.72 (0.065)	119[d]

a P(COS) = 100 Torr, Photolysis time = 100 min.
b % Recovery = $[R(1 + 2 + 3)/R(CO^0 - CO)] \times 100$ where $R(CO^0) = 0.3863$ μmoles/min
c Numbers in brackets are rates, in units μmoles/μmole CO
d Indicates error in either the $R(CO^0)$ value or in the GC calibration or both

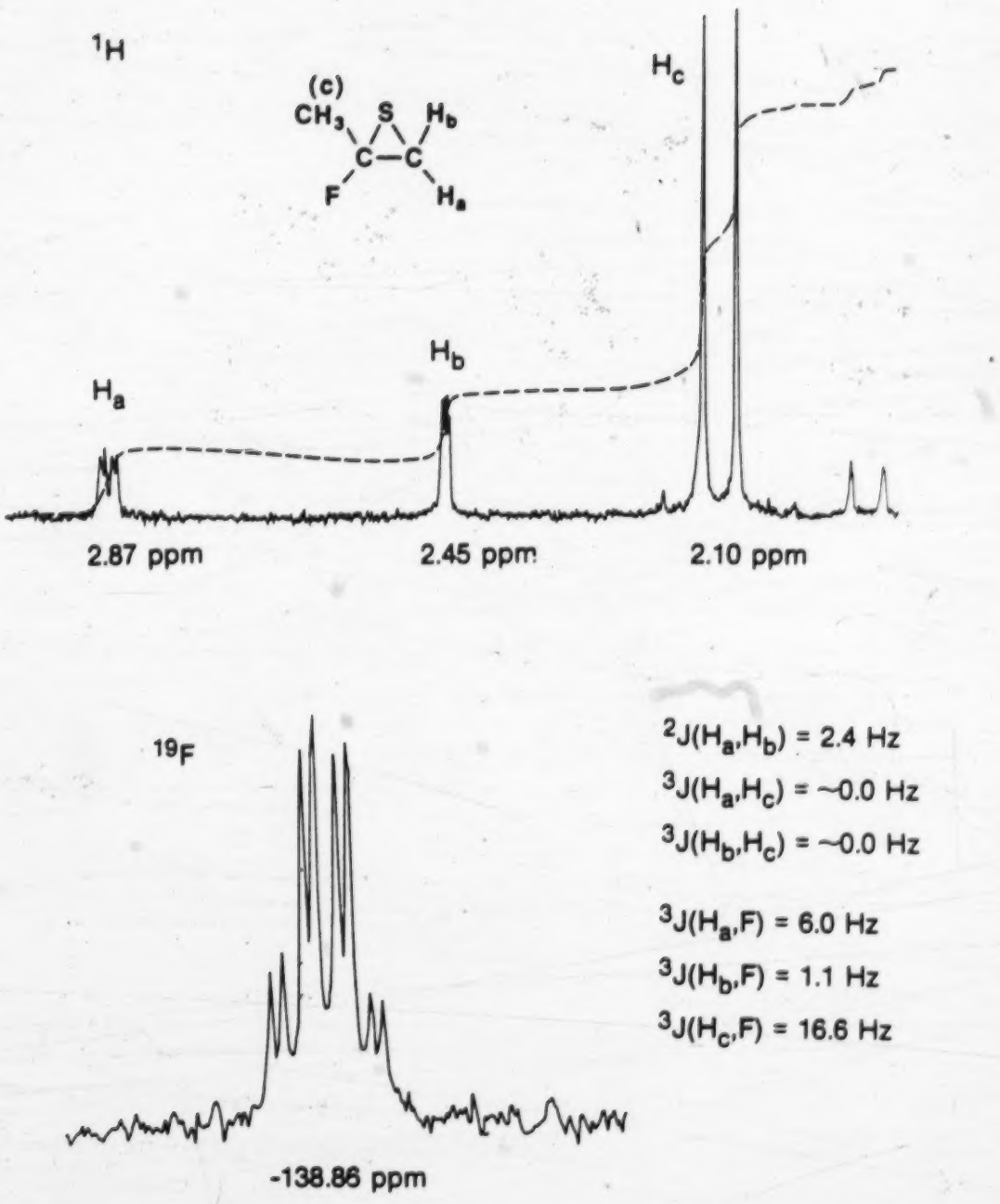

Figure IV–1: ^{1}H and ^{19}F NMR Spectra of Product 1

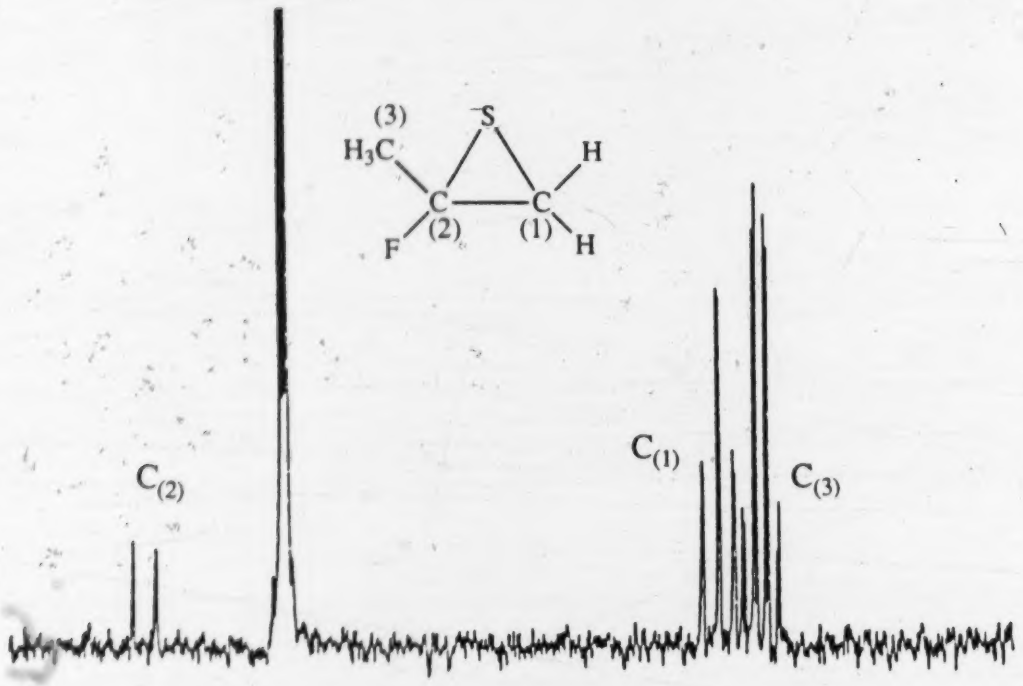

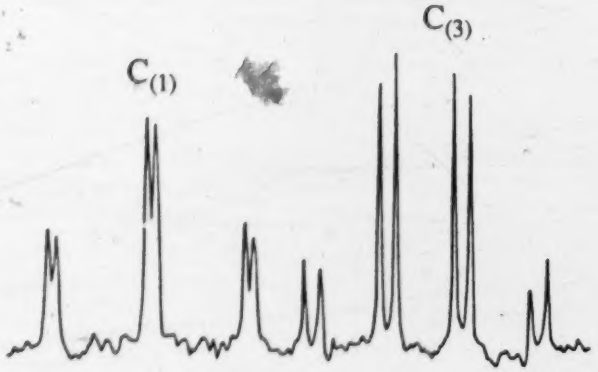

$^2J(C_1, F) = 14.2$ Hz
$^1J(C_1, H) = 170.3$ Hz
$^1J(C_2, F) = 256.8$ Hz
$^2J(C_3, F) = 28.0$ Hz
$^1J(C_3, H) = 129.7$ Hz

Figure IV–2 : ^{13}C NMR Spectrum of Product 1

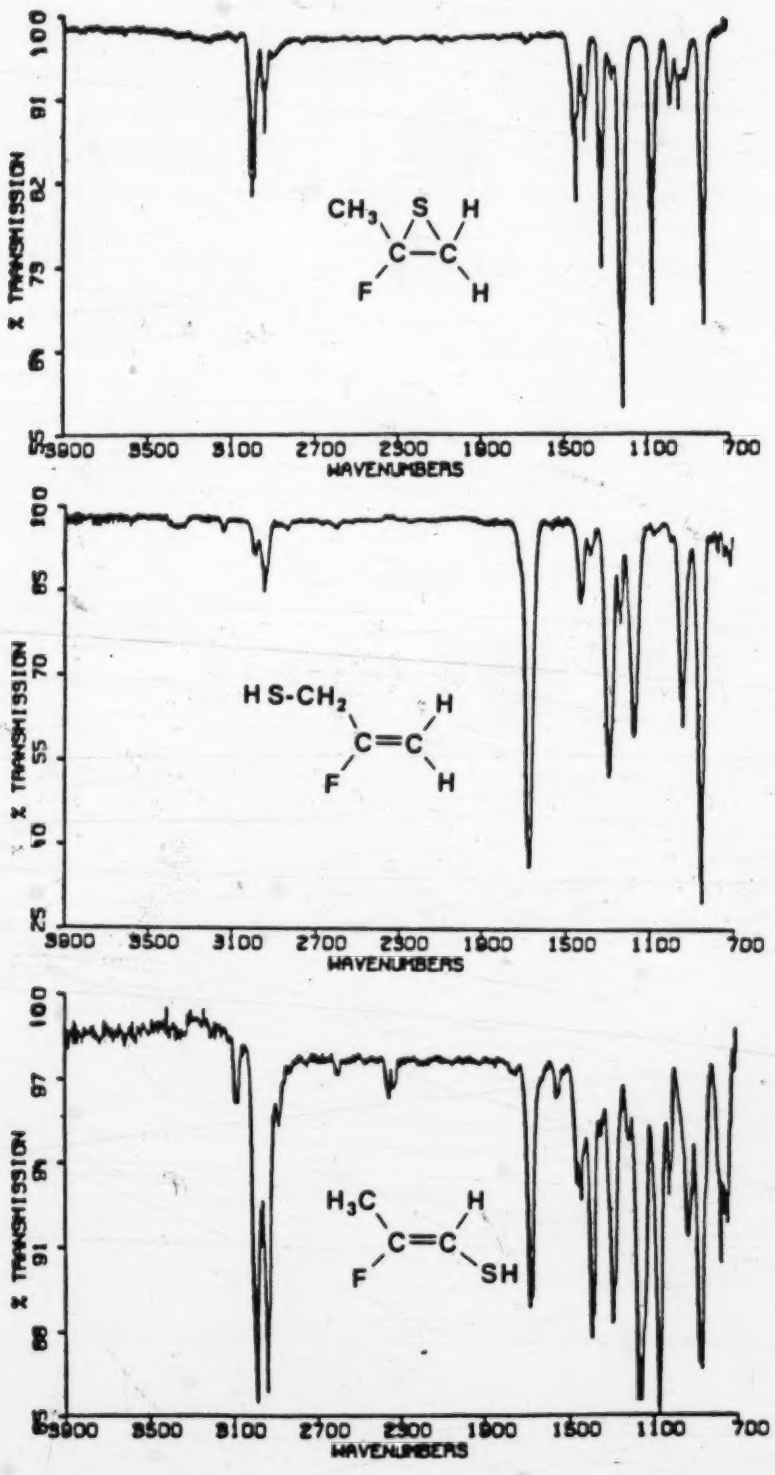

Figure IV–3 : Infared Spectra of Products **1**, **2** and **3**

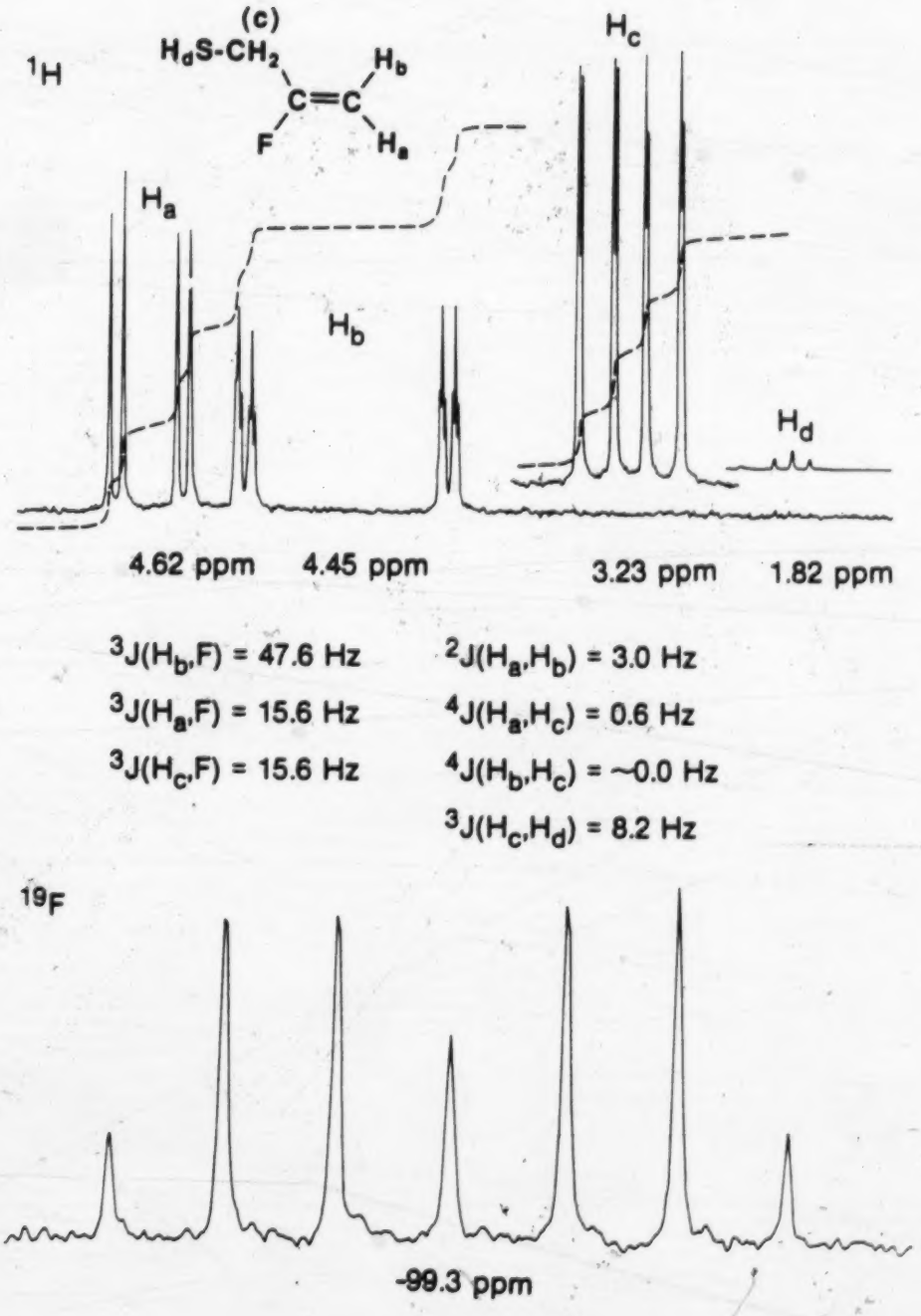

Figure IV–4 : ^1H and ^{19}F NMR Spectra of Product 2

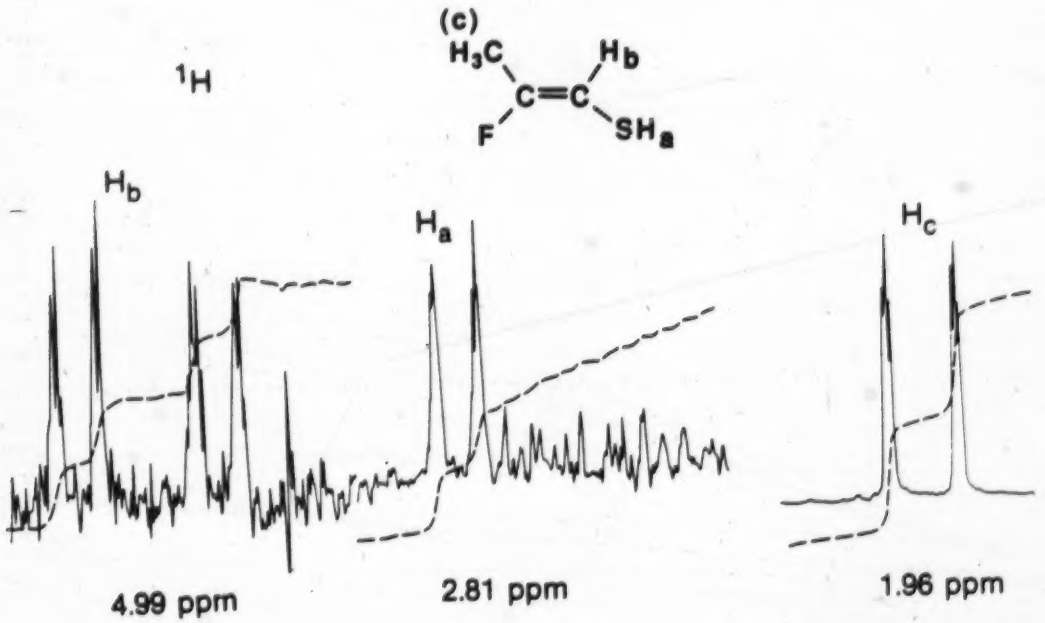

$^3J(H_b,F)$ = 32.2 Hz* $^3J(H_a,H_b)$ = 9.2 Hz

$^4J(H_a,F)$ = 1.0 Hz $^4J(H_b,H_c)$ = 0.6 Hz

$^3J(H_c,F)$ = 15.4 Hz

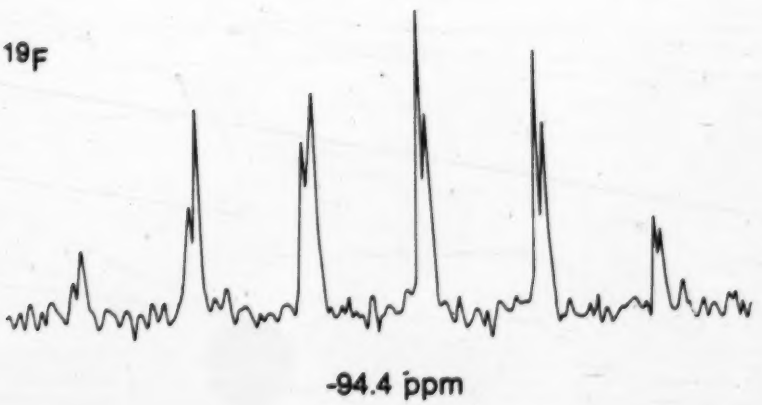

Figure IV–5 : ^1H and ^{19}F NMR Spectra of Product 3

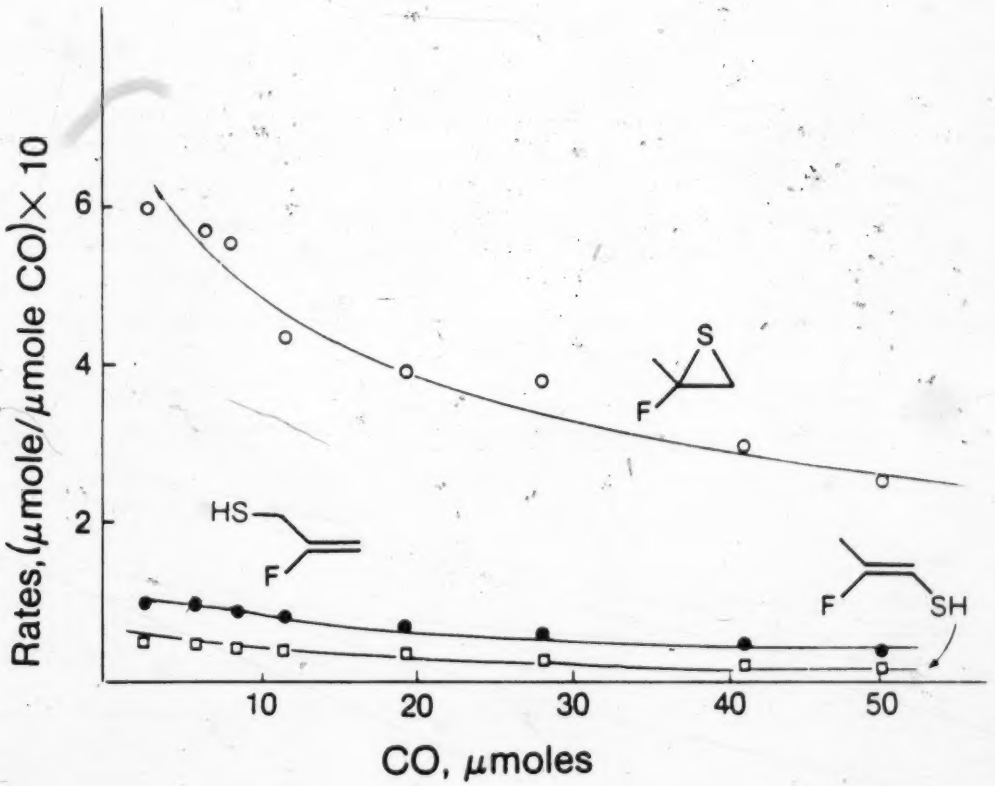

Figure IV–6 : Rates of Formation of Products **1**, **2** and **3** as a Function of CO yield

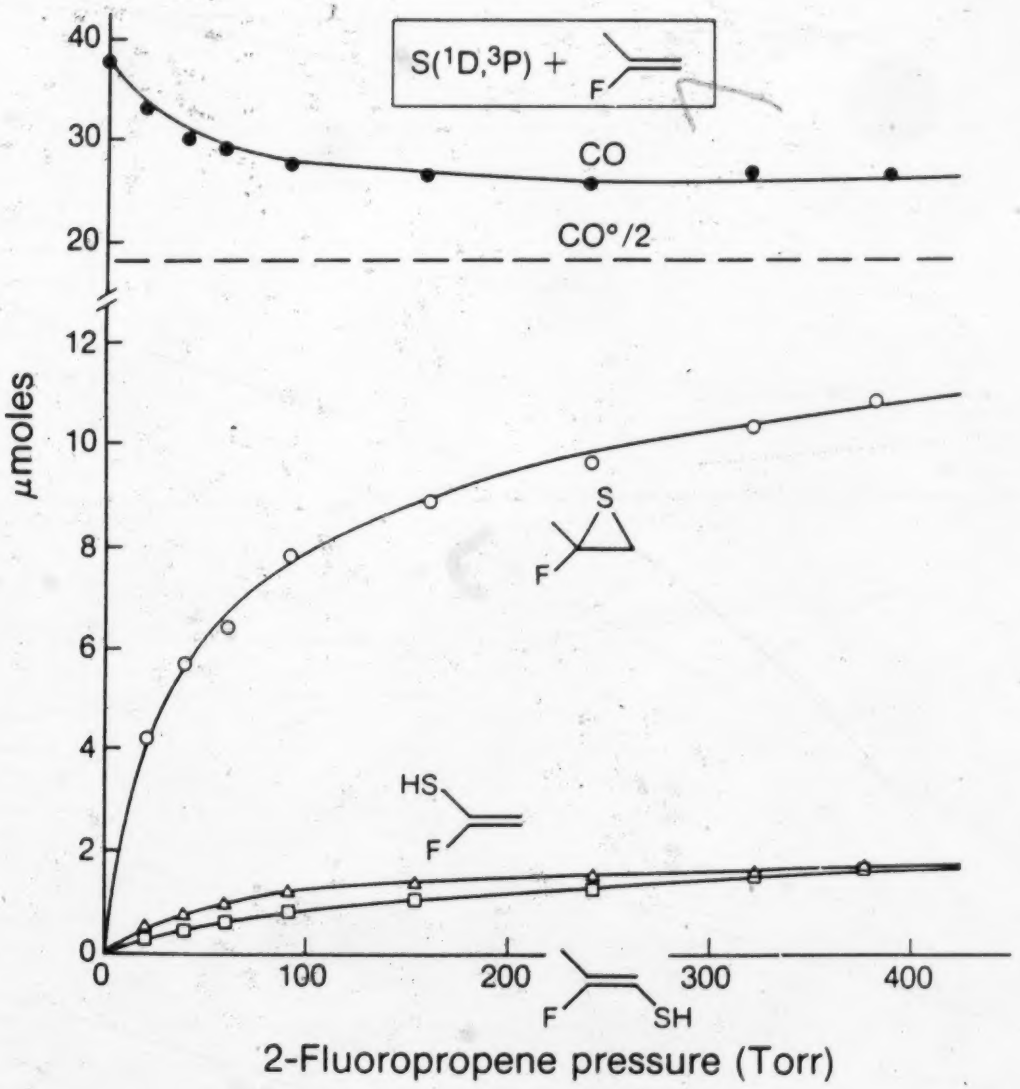

Figure IV–7 : Variations in the Yields of CO and Products **1**, **2** and **3** as a Function of 2-Fluoropropene Pressure

CHAPTER V

REACTIONS OF SULFUR ATOMS WITH CIS- AND TRANS-ALKENES

A. Results

1. $S(^3P)$ + Cis- and Trans-2-butene

(a) Reaction Products

When 80 Torr COS was photolyzed in the presence of 38.5 Torr cis- or trans-2-butene and 1200 Torr carbon dioxide, in each case one major and one minor sulfur addition product, both having a mass of 88 g mol^{-1} (C_4H_8S), were seen by GC–MS. The mass spectral data for these products are given in Appendix B–2 and are quite similar to those obtained by Sidhu et al.[16] and assigned to cis- and trans-2,3-dimethylthiirane. In the present study more exact product assignments were achieved with the aid of high resolution ^1H NMR spectroscopy and computer simulation calculations.

(i) Identification

The C_4H_8S formula suggests the presence of a double bond (an alkene) or a cyclic structure which has either a thiol or sulfide functional group. Thiocarbonyls are generally not stable at room temperature. The NMR spectra obtained for each of the two C_4H_8S products look quite similar, as seen in Figure V–1, and comprise two sets of multiplets, corresponding to two types of protons.

The NMR spectrum of the product which elutes first on the GC shows that the more complex multiplet at 2.65 ppm has about 12 lines while the simpler multiplet at 1.50 ppm has 8 lines. On integration of the peak areas, the peak area of the latter multiplet is three

times that of the former, meaning that since there are eight available protons in C_4H_8S, six of them are in one type of environment and two of them are in another. If all the former six protons were equivalent and the latter two protons were equivalent, then a triplet and septet in a 3:1 ratio should arise. The more complex multiplets obtained suggest that the latter two protons are magnetically non-equivalent and the remaining six protons probably belong to two methyl groups which are also in similar but magnetically non-equivalent environments. The resulting spectrum is therefore of the type $AA'X_3X_3'$. This rules out the possibility of the product being a thiol, since only one thiol functional group is possible. The product could therefore be a sulfide.

Since the product which elutes first on the GC is the major product of the $S(^3P)$ + trans-2-butene reaction, the product is most likely trans-2,3-dimethylthiirane as shown below:

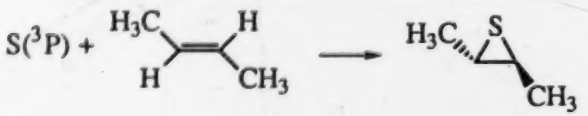

[168]

The trans-2,3-dimethylthiirane (trans-DMT) structure is consistent with the molecular formula C_4H_8S and has two similar but magnetically non-equivalent methyl groups and two similar but magnetically non-equivalent protons.

The NMR spectrum of the other C_4H_8S product shows a multiplet with 10 lines at 1.49 ppm and another multiplet with 24 lines at 3.04 ppm. On integration of the peak areas, it is seen that the former multiplet arises from three times as many protons as the latter. Again since there are eight available protons, and the spectrum is not a first-order type spectrum, the multiplet at 3.04 ppm must be due to two protons which are in similar but magnetically non-equivalent environments and the other six protons probably belong to two similar but magnetically non-equivalent methyl groups which give rise to the multiplet at 1.49 ppm. Since this product is the major one obtained in the $S(^3P)$ + cis-2-butene

reaction at short conversions, it is probably cis-2,3-dimethylthiirane as shown below, since the NMR spectrum of a thiol would give rise to one proton which has a different chemical shift from the other protons.

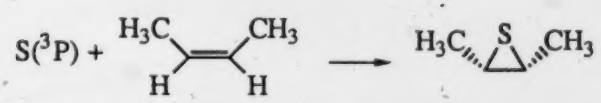

[169]

The cis-2,3-dimethylthiirane (cis-DMT) structure is again consistent with the NMR data obtained. For both products the chemical shift of the protons of the methyl group is shifted downfield due to their proximity to the S atom, and that of the tertiary CH group is shifted even more since the sulfur atom is attached to that carbon. The latter shift is more pronounced in cis-DMT because each H is flanked only by the other H and one methyl group, whereas in trans-DMT, each H atom on the tertiary carbon is flanked by two methyl groups so it is more shielded.

That trans-DMT elutes before cis-DMT is in agreement with the observations of Neureiter and Bordwell,[171] who found that trans-DMT has a slightly lower boiling point and hence a slightly higher vapor pressure at room temperature than cis-DMT. To further confirm the structures, computer simulations of the NMR spectra were carried out using a 1985 version of Bruker's PANIC (Parameter Adjustment in NMR by Iteration Calculation) program on an Aspect 3000 computer equipped with an Array Processor.[95] Starting values for the coupling constants were estimated from literature data[172] and previous experience with spin simulation.[173,174] These values were then increased or decreased until a good fit was obtained following which the iteration routine was carried out on the values to optimize the parameters further. Using the coupling constants thus obtained, and a linewidth of 0.15 Hz, the resulting simulated spectra matched the original spectra quite well, confirming the assignments. The coupling constants and the chemical shifts for the two C_4H_8S isomers are listed below:

	trans-DMT	cis-DMT
δ_H	2.65	3.04
δ_{CH_3}	1.50	1.49
$^3J_{H-H'}$	+5.32	+7.04
$^3J_{H-CH_3}$	+5.80	+6.07
$^4J_{H-CH_3}$	–0.36	–0.26
$^5J_{CH_3-CH_3}$	0	+0.05

It was noticed that the ^4J coupling constants had to be negative otherwise the spectra would look quite different. The five-bond coupling between the two methyl groups is zero for trans-DMT, despite the trans configuration, owing to the system being a saturated system. There is, however, a small coupling between the two methyl groups of cis-DMT, despite the lack of a π-bond connecting them. This is due to "through-space" coupling, an effect seen more prominently among fluorine nuclei, due to spatial proximity of the nuclei.

For the same reason H–H coupling is also larger in cis-DMT, whereas the H–CH_3 coupling is larger in trans-DMT.

(ii) Properties of the C_4H_8S isomers

The UV spectra of the cis- and trans-C_4H_8S isomers show no appreciable absorption between 225 and 260 nm. However, Clark and Simpson,[175] while studying the UV spectrum of methylthiirane, observed some absorption in that wavelength region. Assuming similar absorption patterns for the cis- and trans-DMT's, extinction coefficients are estimated for DMT's based on the spectrum of methylthiirane reported by Clark and Simpson and are listed in Appendix A.

Many problems were encountered in trying to determine the GC molar response of the DMT products by direct calibration in the gas buret, therefore it had to be estimated relative to that of n-butanethiol as described in the Experimental section.

(b) Retention of Stereospecificity in the Products and Extent of Isomerization of the Reactants

The effects of increasing conversion on the product yields and distributions, and on the extent of isomerization of the butene following photolysis of COS + CO_2 + trans- and cis-2-butene mixtures, are listed in Table V–1 and V–2, respectively, and the data are illustrated in Figures V–2 to V–4. Note that the rates of C_4H_8S formation are quoted in terms of CO production in order to correct for possible variations in light intensity. From Figures V–2 and V–3 it can be seen that the zero-time extrapolated mole fractions of trans- and cis-DMT are ~0.99 and 0.98, respectively. With increasing conversion, however, the isomeric purities of both the products and the reactants decrease, and these effects are more pronounced for the case of the cis-2-butene. Figure V–4 shows that cis-DMT is much more photolabile than trans-DMT. Due to problems in the calibration of the DMT products, their % yields were not always determined. Table V–3 shows that reasonably good product recoveries were achieved at short conversions.

2. S + Cis- and Trans-1,2-difluoroethylene

(a) Reaction Products

When 80 Torr COS was photolyzed with cis- or trans-1,2-difluoroethylene (DFE) in the presence or absence of carbon dioxide, only CS_2 and one major and one minor sulfur addition product, each having MW 96 ($C_2H_2F_2S$) were found by GC–MS. The mass

spectra of the isomeric products are recorded in Appendix B–3. Proton and fluorine NMR spectra of the two isomers were also obtained.

(i) Identifications

The molecular formula $C_2H_2F_2S$ shows only two hydrogen and two fluorine atoms. The ^1H and ^{19}F NMR spectra of both products, shown in Figures V–5 and V–6, show just one multiplet in each case, meaning that the two hydrogens and the two fluorines are in similar environments.

In the case of the $C_2H_2F_2S$ product which elutes first on the GC, the multiplet in the proton NMR is centred about 6.11 ppm and comprises eight lines. The product cannot be a thiol since the latter would give rise to two distinct proton resonances of equal intensity, and in this case only one resonance is seen. The two fluorines also give rise to one resonance centred at –176.7 ppm which is a multiplet of about ten lines, as seen from the fluorine NMR. Since this $C_2H_2F_2S$ product is the major one obtained in the S + trans-DFE reaction, it is probably trans-2,3-difluorothiirane (trans-DFT):

[170]

The trans-DFT structure has the right molecular formula and the two fluorines and the two protons are in similar environments, respectively, but are magnetically non-equivalent.

The other $C_2H_2F_2S$ product has its proton resonance centred further upfield at 5.92 ppm and is split into about ten lines as seen in Figure V–6. Its ^{19}F NMR spectrum is virtually identical to the ^1H NMR spectrum, and has its fluorine resonance centred at –187.3 ppm. As with the other isomer, this $C_2H_2F_2S$ is also not a thiol since the two hydrogens

and the two fluorines are similar enough to give one resonance each. Since this isomer is the major one obtained in the S(^{3}P) + cis-DFE reaction, it must be the cis-2,3-difluorothiirane (DFT).

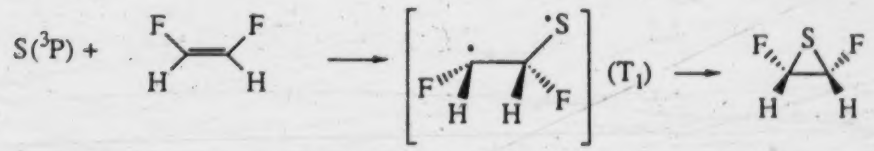

[171]

The cis-DFT structure is consistent with the proton resonance being shifted further upfield since it is flanked by only one fluorine nucleus and one proton, whereas the protons in the trans-DFT molecule are flanked by two fluorine nuclei and hence are more deshielded.

If the hydrogen nuclei and the fluorine nuclei were equivalent, then only a triplet would be seen in each of the ^{1}H and ^{19}F NMR spectra. The more complex spectra arise from the magnetic non-equivalence of the protons and the fluorines and the spin system is described as AA'XX'. The similarities between the ^{1}H and ^{19}F multiplets are due to a first-order relationship between the two kinds of nuclei.[176]

Computer simulations of the ^{1}H and ^{19}F NMR spectra were also carried out for cis- and trans-DFT in a manner similar to the simulation carried out for the DMT products. Starting values for the coupling constants were estimated from those of similar compounds reported in the literature.[176,177] Initial adjustment of the parameters for a good fit, followed by the iteration procedure for optimized values, were applied separately to the ^{1}H and ^{19}F NMR spectra. The resulting simulated spectra matched well with the experimental spectra.

The proton chemical shifts relative to internal TMS and the ^{19}F chemical shifts relative to external $CFCl_3$ as well as the coupling constants are listed below:

	trans-DMT	cis-DMT
δ_H	6.11	5.92
δ_F	–176.7	–187.3
$^2J_{H-F}$	71.43	73.00
$^3J_{H-H}$	0.83	2.77
$^3J_{F-F}$	47.18	57.29
$^3J_{H-F}$	1.44	6.60

It is interesting to note that all of the cis-DFT couplings are larger than those for the trans isomer. While "through-space" coupling may be cited for the larger F–F and H–H constants in cis-DFT, it is not immediately obvious why $^3J_{H-F}$ is larger for cis-DFT although the proton and fluorine are further apart in a trans configuration. One possible reason is that the electron density in the C–C bond of trans-DFT is much reduced, due to the presence of electronegative fluorines in a trans configuration, resulting in very little "through-bond" coupling in trans-DFT as compared to cis-DFT. The slightly larger geminal H–F coupling in cis-DFT may be due to the greater proximity of the H and F nuclei in the cis isomer as compared to the trans, which would occur if a greater repulsion between the vicinal fluorine nuclei in the cis-DFT pushed them closer to the hydrogen nuclei. From molecular modeling using the Alchemy program, the distance between the two fluorine nuclei in cis-DFT is found to be 2.7 Å compared to 3.68 Å in trans-DFT, which accounts for the larger $^3J_{F-F}$ value for cis-DFT. All the coupling constants given are absolute values.

(ii) Properties of the reaction products

The $C_2H_2F_2S$ isomers both absorb slightly in the photolysis region. Their calculated extinction coefficients are given in Appendix A.

(b) Effect of Photolysis Time and Increasing $C_2H_2F_2$ Pressure on Product Yields and Distributions in the $S(^3P) + C_2H_2F_2$ Reaction

When a mixture consisting of 80 Torr cis- or trans-1,2-difluoroethylene, 80 Torr COS and 1200 Torr CO_2 is photolyzed, the product yields vary with photolysis time as shown in Tables V–4 and V–5, respectively. There is no observable isomerization of the difluoroethylenes (DFE's) with increasing conversion. The variations in the mole fractions of the products are shown in Figure V–7 and the rates of product formation from the two reactions are plotted in Figure V–8, as a function of the CO yield.

Unlike the case of the $S(^3P)$ + 2-butene reactions, the extrapolated zero-time mole fractions of trans- and cis-$C_2H_2F_2S$ (Figure V–7) indicate ~87% and 97% stereoselectivity, respectively, for the addition reaction. Also, the difluorothiiranes are more stable (Figure V–8) with respect to secondary reactions than their dimethyl analogs (Figure V–4). The product recoveries are markedly lower than those from the 2-butene reactions.

Next, the effects of varying the $C_2H_2F_2$ pressure between 10 and 400 Torr were examined. Tables V–6 and V–7 list the product yields for the $S(^3P)$ + cis- and trans-1,2-DFE reactions, respectively, and the variations in the mole fractions of the $C_2H_2F_2S$ products are plotted in Figure V–9. The mole fractions and rates of formation of the products attain constant values only at very high (>300 Torr) pressures of DFE (Figure V–10).

(c) Effect of Photolysis Time and Increasing $C_2H_2F_2$ Pressure on Product Yields and Distributions in the $S(^1D, ^3P) + C_2H_2F_2$ Reaction

In the absence of carbon dioxide, when most of the sulfur atoms are in the (^1D) state, the product yields and distributions might be expected to be different from those observed in the $S(^3P)$ atom reactions. Product yields as a function of exposure time at a constant (80

Torr) pressure of $C_2H_2F_2$ are listed in Table V–8 for the $S(^1D, ^3P)$ + cis-$C_2H_2F_2$ reaction. The rates of product formation as a function of CO yield are plotted in Figure V–11 for the $S(^1D, ^3P)$ + cis-$C_2H_2F_2$ reactions, and variations in the mole fractions of the products for the $S(^1D, ^3P)$ + cis-$C_2H_2F_2$ reaction are shown in Figure V–12.

The rates of formation of both isomeric products decrease with increasing conversion owing to the destruction of the initially formed products in secondary reactions. However, the mole fraction as a function of conversion appears to be little affected (see Figure V–12) and shows a very slight increase in the value of the mole fraction with decreasing conversion, from 0.88 at 30.5 μmoles CO to ~0.91 at zero conversion.

Variations in the yields and distribution of the $C_2H_2F_2S$ products on increasing the $C_2H_2F_2$ pressure from 10 Torr to 400 Torr were also studied, and are tabulated in Tables V–9 and V–10 for the $S(^1D, ^3P)$ + trans- and cis-$C_2H_2F_2$ reactions, respectively. The mole fractions of the trans- and cis-$C_2H_2F_2S$ products at high $C_2H_2F_2$ pressures were found to attain constant values of ~0.8 and ~1.0, respectively, as can be seen from Figure V–13. This high pressure behavior is similar to that seen in the corresponding $S(^3P)$ atom reactions. In the $S(^1D, ^3P)$ + trans-$C_2H_2F_2$ reaction, the rate of formation of cis-$C_2H_2F_2S$ increases proportionally with the rate of formation of trans-$C_2H_2F_2S$ as shown in Figure V–14. The overall product recoveries are lower for the $S(^1D, ^3P)$ reactions as compared to those for the corresponding $S(^3P)$ atom reactions (see Figure V–10).

3. S + Cis- and Trans-1,2-dichloroethylene

(a) Reaction Products

When 80 Torr COS was photolyzed in the presence of cis- and trans-1,2-dichloroethylene with or without added carbon dioxide, two sulfur addition products were detected.

The product yields were very small and if they were not analyzed within twelve hours of photolysis the last-eluting product would not be seen at all. The latter peak and the other one, by GC–MS, show molecular weights of 128, 130 and 132 g mol^{-1} ($C_2H_2Cl_2S$) in approximately 9:6:1 ratio because of the natural abundance of the ^{35}Cl(75.77%) and ^{37}Cl(24.23%) isotopes. The major peak obtained from the trans-$C_2H_2Cl_2$ reaction is the one that elutes first and it is assumed to be trans-2,3-dichlorothiirane. The product which elutes last is the major product obtained from the cis-$C_2H_2Cl_2$ reaction and is assumed to be cis-2,3-dichlorothiirane.

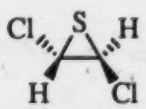

trans-2,3-dichlorothiirane

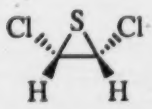

cis-2,3-dichlorothiirane

Unlike the mass spectra of other thiiranes where the isomers had very similar cracking patterns, the cracking patterns of these two $C_2H_2Cl_2S$ isomers seem to be quite different (see Appendix B–4). For the trans isomer the $(S{=}C{-}H)^+$ ion seems to be the predominant one, and the molecular ion is also quite strong and tends to lose chlorine, whereas the cis compound has a small molecular ion signal with the sulfur atom being the first to be lost, followed by a chlorine atom to give a large signal at 61 which probably is due to the ion $(ClHC{=}CH)^+$.

There are also two other small products which appear in the S + trans-$C_2H_2Cl_2$ reaction, having molecular masses of 122, 124 and 126 g mol^{-1} because of the chlorine isotopes. These appear to be formed from the recombination of two ClCH=CH· radicals to give $C_4H_4Cl_2$ isomers. The ultraviolet spectrum of trans-$C_2H_2Cl_2S$ showed appreciable absorption in the photolysis region (see Appendix A). Cis-$C_2H_2Cl_2S$ was found to decompose readily and it was not possible to collect sufficient quantities for UV analysis.

(b) Effect of Photolysis Time on the Yields and Mole Fractions of the $C_2H_2Cl_2S$ Products from the S + $C_2H_2Cl_2$ Reactions

Since the product yields of these reactions were very small, no calibrations could be made and the product yields are reported as peak areas. The variations in the product yields as a function of time are listed in Tables V–11 and V–12 for the $S(^3P)$ + trans- and cis-$C_2H_2Cl_2$ reactions, respectively. The mole fractions of the stereoselective products are shown as a function of time in Figure V–15. Figure V–16 shows how the product rates vary with the CO yield. The rate of formation of trans–$C_2H_2Cl_2S$ decreases with increasing photolysis time until a steady state is reached after which the rate of formation drops sharply for the $S(^3P)$ + trans-$C_2H_2Cl_2$ reaction. Cis-$C_2H_2Cl_2S$ was only observed at very long exposure times in the latter reaction. The rate of cis-$C_2H_2Cl_2S$ formation in the $S(^3P)$ + cis-$C_2H_2Cl_2$ reaction decreases very rapidly with increasing photolysis time, and the product recoveries are lower for the cis-$C_2H_2Cl_2$ reaction. The mole fraction of trans-$C_2H_2Cl_2S$ extrapolates to almost 1.0 at zero exposure time whereas the mole fraction of cis-$C_2H_2Cl_2S$ in Figure V–14 extrapolates to about 0.91 at zero exposure time.

The results obtained for the $S(^1D, ^3P)$ reactions are also given in Tables V–11 and V–12 and shown graphically in Figures V–15 and V–16. From Figure V–16, it can be seen that the rates of formation of $C_2H_2Cl_2S$ products are lower for the $S(^1D, ^3P)$ reactions. There is no sharp decrease in the rate of trans-$C_2H_2Cl_2S$ formation after 90 minutes of

photolysis as was seen in the $S(^3P)$ + trans-$C_2H_2Cl_2$ reaction. The mole fraction of trans-$C_2H_2Cl_2$ in the $S(^1D, ^3P)$ + trans-$C_2H_2Cl_2$ reaction remains approximately constant at about 0.89, while the mole fraction of cis-$C_2H_2Cl_2S$ for the corresponding cis-$C_2H_2Cl_2$ reaction extrapolates to almost 1.0 at zero time.

B. Discussion

The reactions of $S(^3P)$ atoms with cis- and trans-2-butene, cis- and trans-1,2-difluoroethylene and cis- and trans-1,2-dichloroethylene were all found to be highly stereoselective as summarized below. There are, however, different features in all three reactions and so they will be discussed separately.

Reaction	Maximum value from	Mole Fraction of Stereoselective Product	
		trans-	cis-
$S(^3P)$ + $(CH_3)HC=CH(CH_3)$	time study*	0.99	0.98
$S(^3P)$ + HFC=CHF	time study*	0.87	0.97
	pressure study	0.87	0.99
$S(^1D, ^3P)$ + HFC=CHF	time study*		0.91
	pressure study	0.85	0.99
$S(^3P)$ + HClC=CHCl	time study*	~1.0	0.91
$S(^1D, ^3P)$ + HClC=CHCl	time study*	0.87	~1.0

* zero time extrapolated value

1. S(^{3}P) + Trans- and Cis-2-butene

S(^{3}P) atoms can only add to the double bonds of alkenes,[57] so the products expected from the reaction of S(^{3}P) with trans- and cis-2-butene are trans- and cis-2,3-dimethylthiirane as shown in reactions [168] and [169].

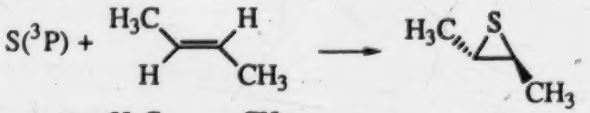

[168]

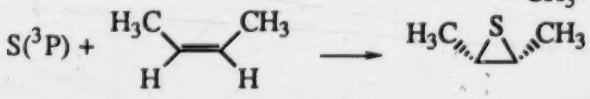

[169]

For both reactions, the expected products were indeed obtained as the major products at short conversions, although with increasing photolysis time, increasing amounts of the stereoisomeric product were obtained in each case. On extrapolation to zero photolysis time, the mole fraction of trans-2,3-dimethylthiirane (trans-DMT) was found to be 0.99, which was approximately the isomeric purity of the trans-2-butene before photolysis (see Figure V–2), while for the S(^{3}P) + cis-2-butene reaction, the mole fraction of cis-DMT was found to be 0.98, which is about the same as the starting purity of cis-2-butene (see Figure V–3). This means that within experimental error, both reactions are 100% stereospecific.

This is a surprising result for a triplet divalent atom addition, and S(^{3}P) atoms are the only triplet divalent species known to show stereospecific behavior. Generally, it was believed that, according to Skell's hypothesis, only singlet divalent species would add to alkenes to give stereospecific products whereas triplet divalent species would add to alkenes to give non-stereoselective products, since in the latter reaction a triplet-state intermediate is formed which, since it has to undergo intersystem crossing, would have time for rotation about the original C=C bond to occur.[83,84] The results obtained here are therefore contradictory to Skell's postulate but they are in agreement with arguments presented by DeMore and Benson who suggested that other factors such as competing rates

of ring closure and rotation about the C–C bond can affect the stereochemistry of the products rather than spin state alone.[91]

That S(^{3}P) atoms added to cis- and trans-2-butene to give highly stereoselective products had been determined earlier by Sidhu et al.[16] and was attributed to more rapid spin inversion and slower rotation about the central C–C bond in the intermediate, as well as efficient ring closure. To account for the slow rotation about the C–C bond, a π-thiacyclopropane structure with a sigma-pi hybrid bond between the terminal methylene carbon and the sulfur atom was postulated by Lown et al.[92] to be the intermediate in the S(^{3}P) + C_2H_4 reaction, as discussed in the Introduction.

Leppin and Gollnick then studied the molecular orbital correlation for the S(^{3}P) + C_2H_4 reaction and found that the orbitals of the reactants do transform continuously into orbitals of two intermediate triplet states of thiirane, if the S(^{3}P) atom approaches the ethylene molecule symmetrically along its C_{2v} axis.[93] Only the lower-lying triplet state thiirane would lead to a ground-state thiirane in which the geometry of the starting ethylene is retained. Hoffmann et al. using extended Hückel calculations to determine the minima in the S(^{3}P) + C_2H_4 potential surface, obtained results similar to those of Leppin and Gollnick.[77] They also determined that the triplet-state thiirane intermediate formed had a broken C–S bond and a CCS angle of 110°, and that the terminal methylene group lies in a plane perpendicular to the CCS plane. The energy required to rotate the methylene group by 90° was calculated to be only 5 kcal mol^{-1}.[77]

Strausz et al., using the virtual orbital technique, repeated the calculations and obtained a value of 23.0 kcal mol^{-1} for the barrier to rotation of the methylene group in the T_1 state of thiirane.[76] It was further determined that the excited triplet-state thiirane formed had only 20 kcal mol^{-1} excess vibrational energy, which is not sufficient to allow rotation about the central C–C bond. The latter result was cited by Strausz and his co-workers as the reason for the observed stereoelectivity of the S(^{3}P) atom reactions.[76]

In 1986, McKee, using MNDO calculations, recalculated the barrier to rotation about the C–C bond in the triplet state thiirane molecule and found it to be only 3.3 kcal mol^{-1}.[55] He therefore cited rapid intersystem crossing from the triplet to the singlet state as being the reason for the observed stereoselectivity of the products. This postulate, however, is contradictory to earlier experimental results obtained by Lown et al. which suggest that triplet-state thiirane has a relatively long radiative lifetime.[95]

The $S(^3P) + C_2H_4$ reaction has therefore been reinvestigated using ab initio SCF MO and CI methods[95] with the hope that the study of this simple system will help to explain the reactions of $S(^3P)$ atoms with higher alkenes. The initial adduct is predicted to be $^3A''$ state thiirane which has an open-ring biradical structure with one of the C–S bonds broken. The SCF-level optimized geometry is shown below.

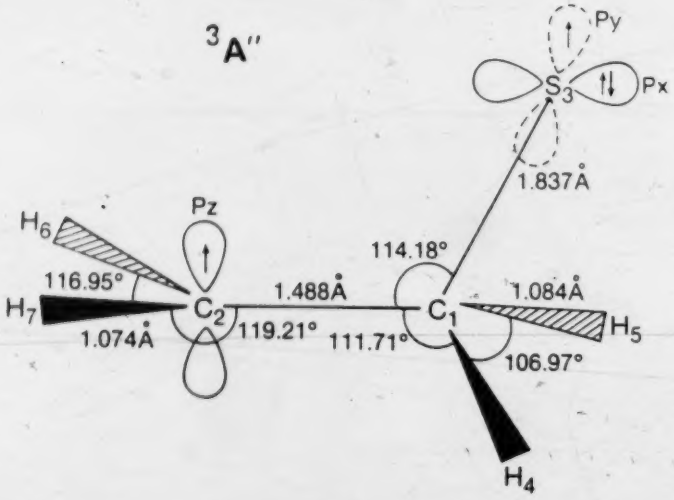

$^3A''$ state thiirane was computed to lie 54.05 kcal mol^{-1} above ground state ($^1A_1$) thiirane and the barrier to rotation about the C–C bond was determined by calculating the energy required to rotate the terminal methylene group by 90° so that H_6 and H_7 lie in the $C_1C_2S_3$ plane. In this rotational transition state the electron in the orbital on C_2 has moved into the orbital which is perpendicular to the $C_1C_2S_3$ plane. The C–C bond length is slightly longer and the C–S bond length, slightly smaller than in the ground state. The rotational energy barrier calculated at the CI level is 5.38 kcal mol^{-1}.[95]

The exothermicity of the $S(^3P) + C_2H_4$ reaction is the sum of the activation energy E_a, (measured by flash photolysis-resonance fluorescence)[98a] and the enthalpy change, ΔH, of the reaction,[95] i.e. (1.6 + 58.9) kcal mol^{-1} = 60.5 kcal mol^{-1}. According to M.O. calculations, the minimum energy that the triplet state thiirane requires for rotation about the C–C bond is the sum of the excitation energy of the $^3A''$ state, 54.05 kcal mol^{-1}, plus the energy required to overcome the rotational barrier, 5.38 kcal mol^{-1}, which is 59.43 kcal mol^{-1}.

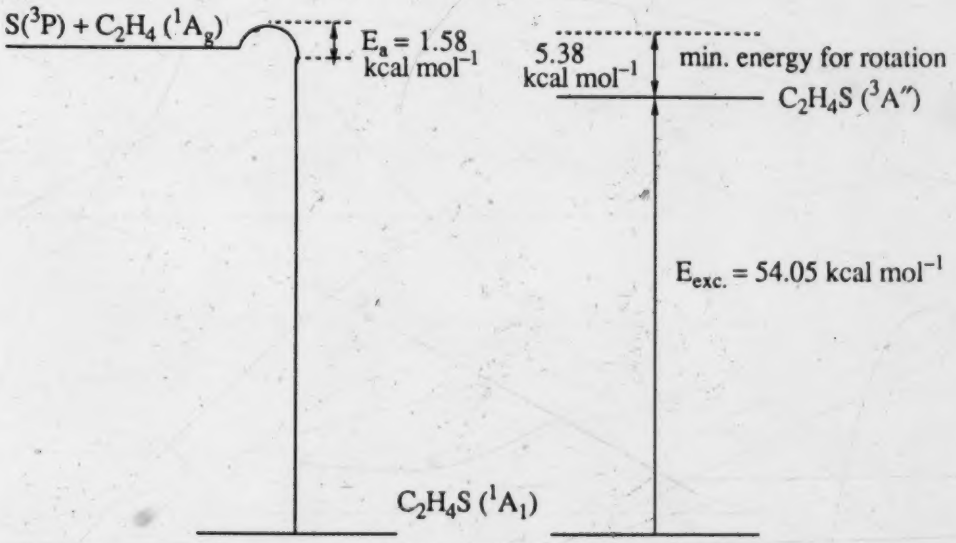

Although the available internal energy, 60.5 kcal mol^{-1}, is about 1 kcal mol^{-1} greater than the minimum calculated energy required for rotation, it is not sufficient to effect rapid rotation about the C–C bond in the initially formed $^3A''$ state. Therefore collisional removal of excess energy will be more important and once the adduct undergoes collisions, its geometry is fixed and remains so when deactivated to the ground vibrational state. This is a more plausible reason for the observed stereospecificity than rapid intersystem crossing since the latter suggests a shallow potential well but the potential energy surface calculated

for the $S(^3P) + C_2H_4$ reaction leading to the $^3A"$ state, shown in Figure V–17, shows a relatively deep well, suggesting a relatively long lifetime for the $^3A"$ state of thiirane.

For the $S(^3P) + C_2H_4$ reaction, at the CI level, if the $S(^3P)$ approached the C=C bond along an asymmetric path it would reach one of two weakly bonding surfaces, $^3A'$ and $^3A"$, whereas a symmetric C_{2v} approach would lead to three fully repulsive surfaces, $^3A_2$, $^3B_2$, $^3B_1$.[95] It is postulated that for the $S(^3P) + C_2H_4$ reaction, the addition initially proceeds along the lowest fully repulsive $^3B_1$ curve from where it undergoes internal conversion to the $^3A"$ surface. The crossover occurs at 1.91 kcal mol^{-1} energy which is designated as the activation energy for the reaction. The $^3A"$ thiirane molecule then undergoes deactivating collisions until it reaches the vibrational level at which the $^3A"$ potential surface crosses the $^1A_1$ potential energy surface of the $S(^1D) + C_2H_4(^1A_g)$ reaction, at which point intersystem crossing may occur to form a vibrationally-excited ground state thiirane molecule, which may be collisionally deactivated further. Alternatively, the intersystem crossing is probably pressure induced:

$$C_2H_4S(T_1) + C_2H_4S(S_0) \longrightarrow 2C_2H_4S(S_0) \qquad [172]$$

Extrapolating from the $S(^3P) + C_2H_4$ reaction to the $S(^3P)$ + cis- and trans-2-butene reactions, it is known that cis- and trans-2-butene are 13.9 and 14.9 kcal mol^{-1}, respectively, more stable than ethylene.[32] Cis- and trans-DMT would be expected to be more stable than thiirane by at least 9–12 kcal mol^{-1} since cis- and trans-1,2-dimethylcyclopentanes are about 12.5 and 14.2 kcal mol^{-1}, respectively, more stable than cyclopentane, and ethylcyclopropane is 8.9 kcal mol^{-1} more stable than cyclopropane.[32] Therefore the enthalpy change for the $S(^3P)$ + cis- and trans-2-butene will be similar to that for the $S(^3P) + C_2H_4$ reaction. The barrier to rotation about the central C–C bond in the inital triplet dimethylthiirane adduct would be expected to be greater than that for the $^3A"$ thiirane adduct by about 3 kcal mol^{-1},[95] since the methyl groups would increase the

electron density of the central C–C bond leading to stronger interaction between the S atom and the central β carbon in the triplet C_2H_4S adduct and also because rotation of the bulkier methyl groups would be sterically unfavourable. The excitation energy required to raise the ground state dimethylthiirane (DMT) to the triplet excited state is possibly about the same or slightly lower than the excitation energy for thiirane.

From the observed stereospecificity, therefore, the possibly similar or slightly lower exothermicity of the $S(^3P)$ + 2-butene probably does not provide sufficient energy to induce rotation about the central C–C bond in the triplet DMT adduct. To estimate the rate of rotation about the C–C bond in the triplet DMT molecule, the Rice-Rampsberger-Kassel (RRK) relation, $k_r = A[(E-E_a)/E]^{s-1}$ may be used, where E_a, the rotational barrier in the triplet DMT is about 8.4 kcal mol^{-1}, A = 10^{11} s^{-1}, s~(3N–6)/2 ~ 17 and E = sRT = 10.1 kcal mol^{-1}. k_r is therefore only about 4 x 10^{-2} s^{-1}, which is very slow.

In this system in the presence of 1200 Torr CO_2, the number of collisions per second each triplet DMT molecule experiences may be calculated by the expression:[178]

$$z_{AB} = \pi(r_A + r_B)^2[8RT(M_A + M_B)/\pi M_A M_B]^{0.5} N_B/V$$

where z_{AB} is the number of collisions each molecule A experiences at a given pressure P_B of B molecules. r_A and r_B are the radii of molecules A and B, respectively. M_A and M_B are molar massess of A and B, and N_B is the number of molecules of B in a volume V.

If A is a triplet DMT molecule and B is CO_2, then

r_A ~ 1.87 x 10^{-10} m if the geometry of triplet DMT is similar to that of $^3A''$ state thiirane,

r_B ~ 1.21 x 10^{-10} m,

M_A = 88.17 x 10^{-3} kg mol^{-1},

M_B = 44.01 x 10^{-3} kg mol^{-1} and

$N_B/V = P_B \times N_0/RT$, where N_0 is Avogadro's number.

For P_B = 1200 Torr,

N_B/V = (1200 x 6.022 x 10^{23} x 1000/0.08206 x 298 x 760) = 3.89 x 10^{25} .

Thus

$$z_{AB} = \pi(3.08 \times 10^{-10})^2 [8 \times 8.314 \times 298 (0.1322)/\pi(3.880 \times 10^{-3})]^{0.5} 3.89 \times 10^{25}$$

$$= 5.38 \times 10^9 \text{ collisions } s^{-1}.$$

Therefore the triplet state DMT formed would lose excess vibrational energy much faster than rotation about the C–C bond could occur and therefore only stereospecific products are formed.

However, as noted before, the stereoselectivity of the $S(^3P)$ + trans- and cis-2-butene reactions appears to decrease with increasing photolysis time. For instance the mole fraction of trans-DMT from the former reaction decreases from ~0.98 after ten minutes of photolysis to ~0.91 after sixty minutes, thereafter remaining constant. In the $S(^3P)$ + cis-2-butene reaction the mole fraction of cis-DMT decreases from ~0.91 after ten minutes of photolysis to about 0.72 after sixty minutes.

When the 2-butene composition was checked before and after photolysis, it was found that the trans-2-butene, which was about 99% pure isomerically before photolysis, was less than 89% pure after ninety minutes of photolysis. Similarly, the mole fraction of cis-2-butene decreased from 0.98 before photolysis to 0.59 after sixty minutes (see Figures V–2 and V–3).

The change in the isomeric composition of the 2-butene during irradiation indicates the occurrence of isomerization. The mercury-photosensitized and benzene-photosensitized cis-trans isomerization of 2-butene have been reported in 1959 and 1960 by Cvetanovic et al.[179] and by Cundall and Palmer,[180] respectively. In both cases the quantum yield of the cis-trans isomerization was found to be less than 1.0, i.e. 0.95 and 0.36, respectively. In 1969 Schmidt and Lee reported that when COS was photolyzed in the presence of low pressures (≤5 Torr) of cis-2-butene, extensive isomerization of the 2-butene occurred, with a quantum yield of ~230, which suggests a chain reaction.[181] They postulated the "catalytic chain initiator" to be the $S(^3P)$ atom and suggested the following mechanism to account for the large quantum yield.[181]

Initiation:

$$COS + h\upsilon(254\ nm) \longrightarrow CO + S(^1D) \quad [3a]$$

$$S(^1D) + M \longrightarrow S(^3P) + M^* \quad [6]$$

Chain Propagation:

$$S(^3P) + cis\text{-}(CH_3)CH{=}CH(CH_3) \rightleftharpoons cy\text{-}cis\text{-}(CH_3)CHSCH(CH_3)\ (T_1) \quad [172]$$

$$\Updownarrow$$

$$S(^3P) + trans\text{-}(CH_3)CH{=}CH(CH_3) \rightleftharpoons cy\text{-}trans\text{-}(CH_3)CHSCH(CH_3)\ (T_1) \quad [173]$$

Chain Termination:

$$S(^3P) + COS \longrightarrow CO + S_2 \quad [7]$$

$$S(^1D) + cis\text{-}(CH_3)CH{=}CH(CH_3) \longrightarrow cy\text{–}cis\text{-}(CH_3)CHSCH(CH_3)\ (S_0) \quad [175]$$

$$S(^1D) + trans\text{-}(CH_3)CH{=}CH(CH_3) \longrightarrow cy\text{–}trans\text{-}(CH_3)CHSCH(CH_3)\ (S_0) \quad [176]$$

$$S(^3P) + wall \longrightarrow (S)\ inactive \quad [177]$$

This mechanism features both labile and non-labile addition of S to 2-butene. The authors also suggested, however, that chain propagation could occur via a bimolecular step involving the S-butene adduct and 2-butene.[181] The S atom however, could not be the species to induce the isomerization of the 2-butene in the system studied here since at extrapolated zero time the mole fraction of the dimethylthiirane obtained is the same as the starting purity of the 2-butene, i.e. the reaction is stereospecific. Furthermore, theoretical calculations show that the $S(^3P) + C_2H_4$ reaction is a non-reversible one step concerted reaction and therefore it is not likely that $S(^3P)$ atoms would add to 2-butene in a labile fashion.

In 1978, Clark et al. reported a quantum yield of 180 for the cis-2-butene isomerization initiated by the 248 nm photolysis of 1 Torr COS,[182] but discounted the

$S(^3P)$ atom as the chain propagator on the basis that the efficiencies of added gases, such as C_2H_4, CO_2, C_3H_6 in quenching the cis-trans isomerization, did not correlate with their rates of reaction with $S(^3P)$ atoms. They suggested instead that the $S_2(^3\Sigma_g)$ molecule was the chain propagator since neither COS nor CO catalyzed the isomerization, and the catalytic species therefore had to be the product of the S atom reaction with 2-butene. However, except for the reaction of S_2 molecules with other S atoms to form S_8 molecules, such reactivity on the part of S_2 is not known.[57]

In 1981, Lown et al.[94] reported that triplet state thiirane generated by the photolysis (λ>240 nm) of thiirane could effect the isomerization of cis-2-butene with a quantum yield of 50 for the formation of trans-2-butene at 400 Torr cis-2-butene pressure. A search for $S(^3P)$ atoms in the system showed that none were present and therefore $S(^3P)$ atoms were not the radical chain propogators. The major processes postulated to occur on photolysis (λ>240 nm) of thiirane are as follows:[94]

$$C_2H_4S(S_0) + h\upsilon \longrightarrow C_2H_4S(S_1) \qquad [178]$$

$$C_2H_4S(S_1) \longrightarrow C_2H_2, H_2S, H_2, CH_4 \qquad \Phi\sim0.14 \qquad [179]$$

$$C_2H_4S(S_1) \longrightarrow C_2H_4S(T_1) \qquad \Phi\sim0.86 \qquad [178]$$

$$C_2H_4S(T_1) + C_2H_4S(S_0) \longrightarrow S_2 + 2C_2H_4 \qquad \Phi\sim0.65 \qquad [181]$$

$$C_2H_4S(T_1) + C_2H_4S(S_0) \longrightarrow 2C_2H_4S(S_0) \qquad \Phi\sim0.21 \qquad [172]$$

To account for the isomerization of cis-2-butene, the S atom of the triplet state thiirane is postulated to attack the double bond of a butene molecules to give an excited triplet state adduct, in which the double bond character of the butene is weakened enough to allow rotation about the central C–C bond. When the adduct decomposes, the resulting butene has at least a 50% chance of being the trans isomer.[94]

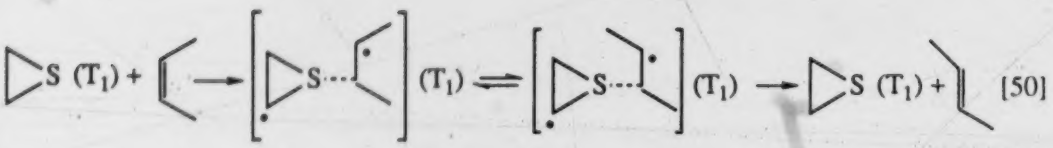

[50]

Such a scheme requires that the triplet-state thiirane have a long radiative lifetime, be relatively resistant to collisional deactivation, and should be able to add reversibly to alkenes to induce their geometrical isomerization.[94]

Further support for the mechanism proposed by Lown et al. comes from the results obtained earlier by Graham et al. who found that thiyl radicals also catalyze the isomerization of 2-butene,[183] presumably by the reversible addition of thiyl radicals to 2-butene:

$$RS\bullet + cis\text{-}C_4H_8 \rightleftharpoons [RS\text{---}C_4H_8] \rightleftharpoons RS\bullet + trans\text{-}C_4H_8 \qquad [182]$$

Since, from the recent ab initio SCF MO calculations, the barrier to rotation about the C–C bond in the $^3A''$ adduct of the $S(^3P) + C_2H_4$ reaction was determined to be about 5.4 kcal mol^{-1}, this means that there is a weak bonding or interaction between the C and S atoms. The normal C–S bond dissociation energy is ~65 kcal mol^{-1}, hence in $^3A''$ thiirane the C–S bond is only about 8% as strong as it could be. The atomic spin densities on C and S are 0.950 and 1.022, respectively in the $^3A''$ state.[95]

This lends support to the postulate that the S atom of the $^3A''$ thiirane adduct, by analogy with the S atoms in thiyl radicals, may attack the double bond of 2-butene and form a bond strong enough to weaken the double bond in the butene and allow rotation about the central C–C bond to occur. Therefore, in the present study of the reaction of $S(^3P)$ with trans- and cis-2-butene, the triplet state DMT formed is proposed to be the agent responsible for the isomerization of the starting butene by analogy with the mechanism proposed by Lown et al.[94] for the case of triplet thiirane. The rate of isomerization of the

two isomeric butenes are not the same; the cis isomerizes faster than the trans because the trans isomer is the thermodynamically more stable. The isomerization occurs as illustrated below.

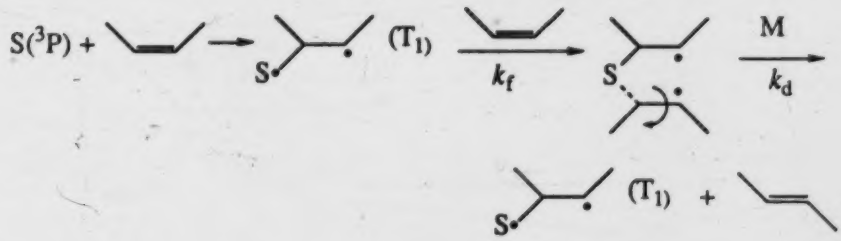

[183]

The number of 2-butene molecules isomerized by each triplet DMT may be estimated from the data in Table V–3 and Figure V–3. Since there is 38.5 Torr 2-butene in a 246-mL cell, this is equivalent to (3.85 x 0.246)/(0.08206 x 298 x 760) = 510 μmoles 2-butene. In the S(^{3}P) + trans-2-butene reaction after 10 minutes of photolysis the amount of triplet DMT produced is 1.325 μmoles which on zero-time extrapolation corresponds to 1.61 μmoles. This causes the isomerization of (0.04 x 510) = 20 μmoles of trans-2-butene to cis-2-butene. Since the chance of forming a cis-2-butene molecule during isomerization is about 50%, approximately 40 μmoles trans-2-butene must have added to 1.61 μmoles triplet trans-DMT, meaning that each DMT molecule formed adds to 25 trans-2-butene molecules on the average before it is deactivated to the ground state or destroyed via polymerization and decomposition. However, since some triplet DMT may be formed from secondary photolysis of ground state DMT, the triplet DMT formed from the S(^{3}P) + 2-butene may add to about 20 or 22 butene molecules during its lifetime.

The rate of collision between each triplet DMT molecule and the 2-butene is given by

$$z_{AB} = \pi(r_A + r_B)^2[8RT(M_A + M_B)/\pi M_A M_B]^{0.5}\, N_B/V$$

Where A is a triplet DMT molecule and B is 2-butene,

$r_A \sim 1.87 \times 10^{-10}$ m if the geometry of triplet DMT is similar to that of $^3A''$ state thiirane,

$r_B \sim 1.21 \times 10^{-10}$ m,

$M_A = 88.17 \times 10^{-3}$ kg mol^{-1},

$M_B = 56.11 \times 10^{-3}$ kg mol^{-1} and

$P_B = 38.5$ Torr

$N_B/V = P_B \times N_0/RT = (38.5 \times 6.022 \times 10^{23} \times 1000/0.08206 \times 298 \times 760) = 1.25 \times 10^{24}$ m^{-3}

Then

$z_{AB} = \pi(1.55 \times 10^{-19})\,[8 \times 8.314 \times 298\,(0.1443)/\pi(4.947 \times 10^{-3})]^{0.5}\,1.25 \times 10^{24}$

$= 2.61 \times 10^8$ collisions s^{-1}.

Therefore, each triplet DMT-2-butene collision occurs in 3.83×10^{-9} s. Assuming that the 23rd collision with 2-butene results in deactivation of the triplet DMT, the lifetime of the triplet DMT is about $(23 \times 3.83 \times 10^{-9})$ s. From the rate of rotation about the central C–C bond in the triplet DMT determined earlier, only one rotation occurs every 25 seconds. This means that the triplet DMT molecule is deactivated much faster than it can undergo geometrical isomerization.

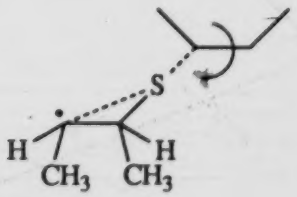

In their study of the S(^{3}P) + trans-2-butene reaction, Sidhu et al. had postulated that the decrease in stereoselectivity of the products with increasing conversion was due to photolysis of the solid polymer which had accumulated on the cell walls.[16] From the data

shown in Figures V–2 and V–3, it is now clear that the apparent decrease in stereoselectivity of the $S(^3P)$ + 2-butene reaction is rather due to the increase in concentration of the isomerized 2-butene.

The rates of formation of both cis- and trans-DMT can be seen from Figure V–4 to decrease with increasing photolysis time to less than one-third of the value at very short photolysis times. At this point only about 2% of the COS and 4% of the 2-butene are consumed and therefore this small depletion should not affect the rate of DMT formation to a great extent. The DMT's absorb appreciably from about 243 nm with a maximum around 270 nm where COS is transparent. Therefore, above 260 nm, even at concentrations of only 0.01 μmoles cm^{-3}, attained after ten minutes of photolysis, the DMT's can absorb radiation, and thereby photodissociate and polymerize by the following mechanism.

$$\text{cis-(trans-)}C_4H_8S(S_0) + h\upsilon \longrightarrow \text{cis-(trans-)}C_4H_8S(S_1) \qquad [184]$$

$$\text{cis-(trans-)}C_4H_8S(S_1) \longrightarrow CH_4, \text{ other decomposition products} \qquad [185a]$$

$$\longrightarrow \text{cis-(trans-)}C_4H_8S(T_1) \qquad [185b]$$

$$\longrightarrow \text{trans-(cis-)}C_4H_8S(T_1) \qquad [185c]$$

The decomposition products were not specifically analyzed and only small amounts of methane and CS_2 were seen.

Since the rate of formation of the major isomeric DMT decreases faster than that of the minor isomeric DMT until the rates of formation of both isomers reach a photostationary state, photopolymerization and decomposition must be the major sinks for the DMT's. From the observation that the photostationary state for trans-DMT is reached at higher concentrations than for cis-DMT, the latter may be expected to be more susceptible to photopolymerization and decomposition. Trans-DMT, therefore, appears to be the more stable isomer.

A second reason for the decreasing rate of DMT formation could be the decomposition of DMT's by $S(^3P)$ atoms according to the following equation:

$$\text{cis-(trans-)}C_4H_8S(S_0) + S(^3P) \longrightarrow \text{cis-(trans-)2-butene} + S_2 \qquad [186]$$

Rate constants relevant to the kinetics of the system are as follows:

$S(^3P) + COS \longrightarrow CO + S_2$	$k = 3.5 \times 10^{-15}$ cm^3 molecule^{-1} s^{-1}	47
$S(^3P) + \text{trans-}C_4H_8 \longrightarrow C_4H_8S$	$k = 9.7 \times 10^{-12}$ cm^3 molecule^{-1} s^{-1}	43,57
$S(^3P) + \text{cis-}C_4H_8 \longrightarrow C_4H_8S$	$k = 9.0 \times 10^{-12}$ cm^3 molecule^{-1} s^{-1}	43,57
$S(^3P) + \text{trans-}C_4H_8S \longrightarrow C_4H_8 + S_2$	$k = 6.64 \times 10^{-11}$ cm^3 molecule^{-1} s^{-1}	11

In the present system after ten minutes of photolysis, $S(^3P)$ atoms react with the 2-butene only about 35 times faster than with the DMT's, with which $S(^3P)$ atoms react at least 37 times faster than with COS. Desulfurization of the DMT's by $S(^3P)$ atoms therefore becomes important with increasing concentration of DMT.

Thus the decrease in the observed stereospecificity of the $S(^3P)$ + 2-butene reaction can be attributed to photopolymerization/decomposition of the major isomeric DMT as well as to the DMT-catalyzed isomerization of 2-butene. Desulfurization of the DMT's by $S(^3P)$ atoms also contributes, but to a much lesser extent, to the decrease in product yields.

Comparing the $S(^3P)$ + 2-butene reaction to the $O(^3P)$ + cis- or trans-2-butene reaction we find that in contrast both of the latter afford cis- and trans-2,3-dimethyloxirane in similar yields, that is, the addition is not stereospecific. MO calculations[95] predict a similarly low rotational barrier in T_1 oxirane, >0.5 kcal mol^{-1} but a low value of 38.5 kcal mol^{-1} for the energy of the T_1 state. Since the internal energy content of T_1 oxirane is 84 kcal mol^{-1}, there is more than enough excess energy to allow rotation about the C–C bond. It has been claimed[103] that the $Se(^3P)$ atom reactions with 2-butene are stereoselective, but

since product identification was based only on UV spectroscopy and time studies were not reported, this conclusion should be viewed with caution.

The rate constants for the O(^{3}P) atom reaction with cis- and trans-2-butene[100] are about twice the rate constants for the S(^{3}P) + cis- and trans-2-butene reactions,[43,57] while those for the corresponding Se(^{3}P) atom reactions are slightly smaller.[103]

2. S + Trans- and Cis-difluoroethylene

(a) S(^{3}P) + trans- and cis-difluoroethylene

The major products obtained from the S(^{3}P) + trans- and cis-1,2-difluoroethylene (DFE) reactions are trans- and cis-2,3-difluorothiiranes (DFT), respectively:

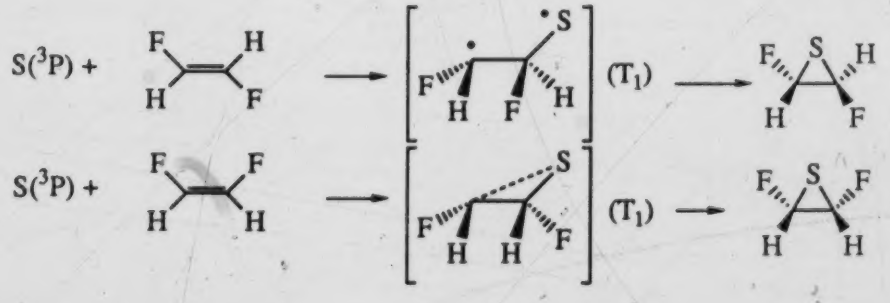

[170]

[171]

As with the S(^{3}P) + 2-butene reactions, small amounts of the isomeric DFT are formed in reactions [170] and [171]. From Figure V–7 it is seen that at zero time the extrapolated mole fractions of cis-DFT from the S(^{3}P) + cis-DFE reaction and of trans-DFT from the S(^{3}P) + trans-DFE reaction are ~0.97 and ~0.87, respectively. Hence the S(^{3}P) + cis-DFE reaction is, within experimental error, stereospecific whereas the S(^{3}P) + trans-DFE reaction is not.

Unlike the S(^{3}P) + 2-butene reactions, the isomeric composition of the trans-DFE was unchanged after photolysis (see Table V–5). (The yield of the trans-DFE could not be measured since CO_2 and trans-DFE could not be resolved on the GC column.)

The formation of cis-DFT from the trans reaction must then be due to rotation about the C–C bond in the initial adduct since the starting purity of the trans-DFE was 98.3%. In the S(^{3}P) + trans-DFE reaction, the mole fraction of the trans-DFT was virtually constant at 0.87 with increasing photolysis time (see Figure V–7). From Figure V–8, it can be seen that the rates of formation of both trans- and cis-DFT decrease slightly with photolysis time until a photostationary state is reached. The UV spectrum of trans-DFT shows a small absorbance in the photolysis region (see Appendix A). However, the extinction coefficients are smaller than those of COS so photodecomposition and polymerization are probably not important avenues for the destruction of trans-DFT. Another reaction which would decrease the concentration of the latter is desulfurization by reaction with S(^{3}P) atoms.

$$\text{trans-DFT} + S(^3P) \longrightarrow S_2 + \text{trans-DFE} \qquad [187]$$

$S(^3P) + COS \longrightarrow CO + S_2$	$k = 3.5 \times 10^{-15}$ cm^3 molecule^{-1} s^{-1}	47
$S(^3P) + \text{trans-DFE} \longrightarrow C_2H_2F_2S$	$k = 2.2 \times 10^{-14}$ cm^3 molecule^{-1} s^{-1}	43,57
$S(^3P) + \text{cis-DFE} \longrightarrow \text{cis-DFT}$	$k = 9.2 \times 10^{-15}$ cm^3 molecule^{-1} s^{-1}	43,57
$S(^3P) + \text{trans-(cis-)DFT} \longrightarrow S_2 + \text{DFE}$	$k \sim 2 \times 10^{-11}$ cm^3 molecule^{-1} s^{-1}	11

Reaction [187] therefore becomes significant with increasing photolysis time, as the concentration of trans-DFT increases, until a photostationary state is reached.

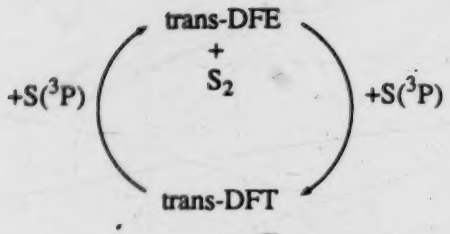

[188]

The rate of formation of cis-DFT, due to rotation about the C–C bond in the $S(^3P)$ + trans DFE adduct, also decreases with increasing photolysis time until it reaches a photostationary state, Figure V–8. The UV spectrum of cis-DFT shows a much stronger absorption in the photolysis region than trans-DFT and it has much larger extinction coefficients than COS at wavelengths greater than 260 nm (see Appendix A). Therefore, cis-DFT may undergo photodecomposition, polymerization and desulfurization as follows:

$$\text{cis-DFT } (S_0) + h\upsilon \longrightarrow \text{cis-DFT } (S_1) \longrightarrow \text{cis-DFT } (T_1) \qquad [189]$$

$$\text{cis-DFT } (S_1) \longrightarrow \text{decomposition} \qquad [190]$$

$$S(^3P) + \text{cis-DFT } (S_0) \longrightarrow S_2 + \text{cis-DFE} \qquad [191]$$

In the $S(^3P)$ + cis-DFE reaction, the decrease in the rate of formation of cis-DFT is much more pronounced (Figure V–8) because of its relatively strong absorption in the photolysis region. Also, after about sixty minutes of photolysis, the cis-DFT formed competes effectively with cis-DFE for $S(^3P)$ atoms.

The rate of formation of trans-DFT in the $S(^3P)$ + cis-DFE reaction remains approximately constant since it is more stable with regard to photodecomposition. The mole fraction of cis-DFT (Figure V–7) decreases at higher photolysis times, mainly because the rate of disappearance of cis-DFT is much greater than that of trans-DFT.

In contrast to the cis-DFE reaction the mole fraction of trans-DFT from the $S(^3P)$ + trans-DFE reaction is constant at about 0.87 and therefore a small amount of rotation about the C–C bond in the initial triplet trans-DFT adduct occurs. The cause of this difference in

the behavior of the isomeric reactions is not clear, but it must be related to the relative stabilities of the isomeric excited triplet and ground state singlet DFT's and the value of the rotational barrier in the triplet state. There are neither experimental nor theoretical reports available on DFT. However, it is known that DFE is more stable in the cis geometry than in the trans geometry by 1.08 kcal mol^{-1}.[184] This has been interpreted in terms of the resonance structures shown below, where greater stabilization is expected in the cis isomer due to the greater proximity of any induced opposite electrostatic charges:

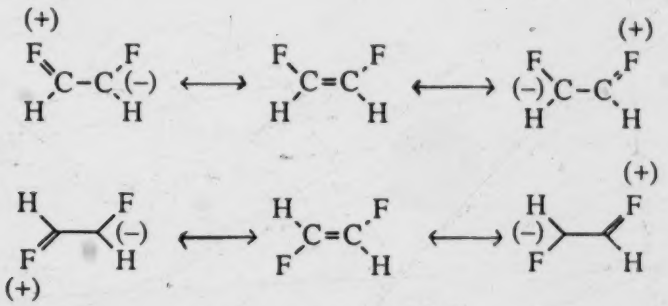

Such structures, however, cannot be drawn for either the triplet or the singlet DFT's.

The results obtained here are similar to those of Wiebe,[74] who found up to 18% isomerization in the products of the S(^{3}P) + trans-DFE reaction, and less than 0.1% isomerization for the S(^{3}P) + cis-DFE reaction. The present reactions were carried out under a total pressure of 1360 Torr, so there should be ample pressure stabilization. The major reason for repeating this experiment was to determine if the minor stereoisomeric DFT was produced as a result of isomerization of the DFE or if rotation about the C–C bond occured in the S + DFE adducts to give the isomeric DFT. The latter appears to be the case for the S(^{3}P) + trans-DFE reaction but in the S(^{3}P) + cis-DFE reaction the trans-DFT formed arises only from the trans-DFE present in the substrate.

With increasing DFE pressure, in the S(^{3}P) + trans-DFE reaction, the production of trans- and cis-DFT increases proportionally up to about 200 Torr trans-DFE and thereafter

remains constant, but the mole fraction of trans-DFT is approximately constant at about 0.8 (see Figures V–9 and V–10). This observation supports the previous conclusion regarding restricted rotation about the C–C bond in the triplet trans-DFT. Product recovery in the trans-DFE increases to about 62% at 400 Torr DFE pressure.

In the $S(^3P)$ + cis-DFE reaction, increasing cis-DFE pressure causes a much larger increase in the rate of production of cis-DFT compared to that of trans-DFT which is very small (see Figure V–10). The mole fraction of cis-DFT appears to be relatively low at low DFE pressure owing to experimental error, but reaches values >0.97 at high DFE pressure. If we correct for the effect of photolysis time or conversion using the plot in Figure V–7, then the mole fraction of cis-DFT would be 1.0 within experimental error. Product recovery is only ~30% even at 400 Torr cis-DFE owing to the relatively long photolysis time (60 minutes), to which the cis-DFT yield is particularly sensitive (see Table V–4).

The reactions which describe the above system and the corresponding rate constants are as follows:

$$COS + h\upsilon \longrightarrow S(^1D) + CO \qquad [3a]$$

$$S(^1D) + CO_2 \longrightarrow S(^3P) + CO_2 \qquad (k_4 = 1.5 \times 10^{-10}\ cm^3\ molecule^{-1}\ s^{-1})^{45} \qquad [4]$$

$$S(^3P) + COS \longrightarrow S_2 + CO \qquad (k_7 = 3.5 \times 10^{-15}\ cm^3\ molecule^{-1}\ s^{-1})^{47} \qquad [7]$$

$$S(^3P) + \text{trans-(cis-)DFE} \longrightarrow \text{trans-(cis-)DFT} + \text{cis-DFT}$$

$$(k_{192} = 2.15 \times 10^{-14}\ (9.2 \times 10^{-15}\ cm^3\ molecule^{-1}\ s^{-1})^{43,57} \qquad [192]$$

$$S(^3P) + \text{trans-(cis-)DFT} \longrightarrow \text{products} \quad (k_{193} \sim 2 \times 10^{-11}\ cm^3\ molecule^{-1}\ s^{-1})^{11} \qquad [193]$$

$$S(^1D) + DFE \longrightarrow \text{products} \qquad (k_* \sim 9.4 \times 10^{-11}\ cm^3\ molecule^{-1}\ s^{-1})^{43,45} \qquad [*]$$

$$S(^1D) + COS \longrightarrow S_2 + CO \qquad (k_5 = 1.8 \times 10^{-10}\ cm^3\ molecule^{-1}\ s^{-1})^{43,45} \qquad [57]$$

$$\longrightarrow S(^3P) + CO_2 \qquad (k_6 = 1.2 \times 10^{-10}\ cm^3\ molecule^{-1}\ s^{-1})^{43,45} \qquad [6]$$

The rate constant for reaction [*] is not known but should be approximately the same as that for the $S(^1D) + C_2H_4$ reaction. From the following expression, it can be determined that under the experimental conditions used, about 90% of the $S(^1D)$ atoms are deactivated.

$$(k_4 [CO_2] + k_6 [COS]/(k_4 [CO_2] + k_6 [COS] + k_5 [COS] + k_\bullet [DFE])$$

The fraction of S(^{1}D) atoms which may react with DFE is given by

$$k_\bullet [DFE]/(k_4 [CO_2] + (k_5 + k_6) [COS] + k_\bullet [DFE])$$

At [COS] = [DFE] = 80 Torr and [CO_2] = 1200 Torr, less than 4% of the S(^{1}D) atoms react with DFE. The fraction of S(^{3}P) atoms scavenged by the DFE molecules is given by k_{192} [DFE]/(k_{192} [DFE] + k_7 [COS]). Hence at [COS] = [DFE] = 80 Torr, trans-DFE scavenges 86% of the S(^{3}P) atoms and cis-DFE, 72%. The rate constant for the S(^{3}P) + DFT reaction is estimated to be similar to that for the S(^{3}P) + thiirane reaction and is almost three orders of magnitude larger than the rate constant for the S(^{3}P) + DFE reactions. At lower DFE pressures, therefore, the DFT products can compete more effectively for the S(^{3}P) atoms. From Figure V–10 it is seen that much higher pressures of cis-DFE are required to scavenge the S(^{3}P) atoms as compared to trans-DFE, due to competition with COS and the DFT's.

(b) <u>S(^{1}D, ^{3}P) + trans- and cis-DFE</u>

In the absence of CO_2, most of the S atoms formed will be in the ($^1D_2$) state but there will be some ground state sulfur atoms, formed by collisional deactivation by COS and presumably by DFE as well. In addition to the DFT products, vinylthiol products due to insertion of S(^{1}D) atoms into C–H bonds, may be expected, as illustrated below, but were not observed.

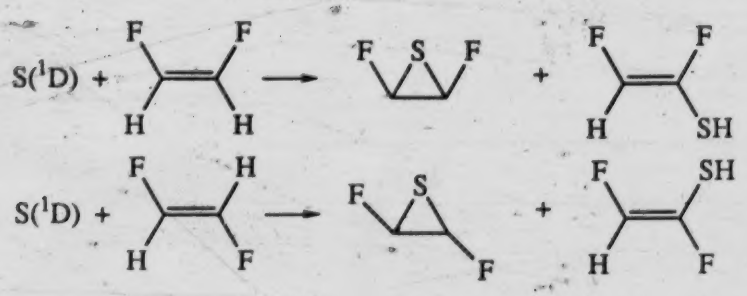

To date vinylthiols have been formed mainly from $S(^1D_2)$ insertion into terminal methylene C–H bonds. An exception is the compound detected by Green, shown in reaction [84b].

As with the $S(^3P)$ atom reactions with cis- and trans-DFE, there was no evidence for the isomerization of trans-DFE to cis-DFE (see Table V–9). Comparing the $S(^1D, ^3P)$ + trans-DFE and $S(^3P)$ + trans-DFE reactions, Tables V–9 and V–5, one obvious difference is the much lower yield of trans-DFT from the former system. This suggests that trans-DFT formed from $S(^1D)$ atoms is vibrationally hot and decomposes readily without pressure stabilization (Figure V–11).

The processes occurring in this system are as follows:

$$COS + h\upsilon \longrightarrow CO + S(^1D) \qquad [3a]$$

$$S(^1D) + COS \longrightarrow COS + S(^3P) \qquad [6]$$

$$S(^1D) + COS \longrightarrow CO + S_2 \qquad [5]$$

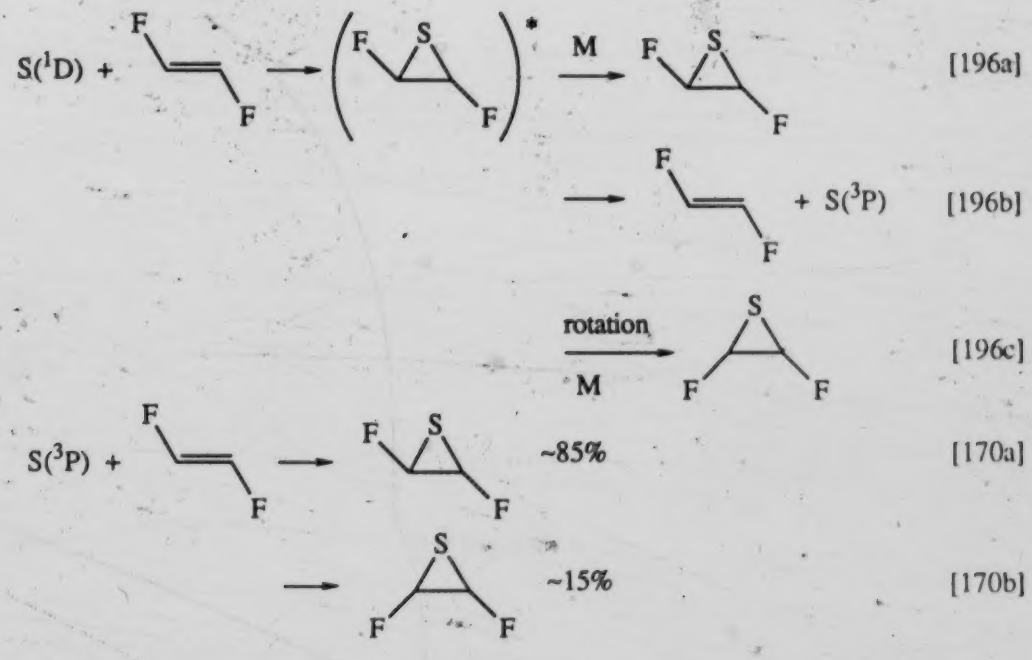

The rate constants for the above reactions are:

$k_6 = 1.2 \times 10^{-10}$ cm^3 molecule^{-1} s^{-1} [43,45]

$k_5 = 1.8 \times 10^{-10}$ cm^3 molecule^{-1} s^{-1} [43,45]

$k_{196} \sim 9.2 \times 10^{-11}$ cm^3 molecule^{-1} s^{-1} [43,45]

$k_{170} = 2.15 \times 10^{-14}$ cm^3 molecule^{-1} s^{-1} [43,57]

The rate constant for reaction [196] is not known but may be estimated to be similar to that of the $S(^1D) + C_2H_4$ reaction. Unlike $S(^3P)$ atoms, $S(^1D)$ atoms react faster with COS than with trans-DFE. Therefore at [COS] = [trans-DFE] = 80 Torr, trans-DFE scavenges $(k_{196}/k_5 + k_6 + k_{196}) = 24\%$ of the $S(^1D)$ atoms. 40% of the reamining 76% of the $S(^1D)$ atoms which react with COS are deactivated to the ground state in which state ~86% of them react with trans-DFE. Therefore, trans-DFE scavenges about 50% of all the sulfur atoms. The observed yield of DFT is therefore only about half the expected amount.

In the $S(^1D) + C_2H_4$ reaction, it was found that some of the vibrationally-excited thiirane formed isomerized to vinylthiol.[185] The latter has been found to polymerize on standing at room temperature. Although no fluorovinylthiol compounds have been found they could be formed transiently and polymerize rapidly.

The yield of cis-DFT formed in the $S(^1D, ^3P)$ + cis-DFE reaction is about 75% of that obtained from the corresponding $S(^3P)$ atom reaction.

[197a]

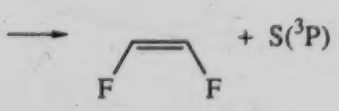

[197b]

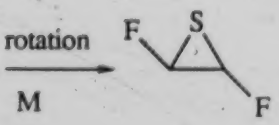

[197c]

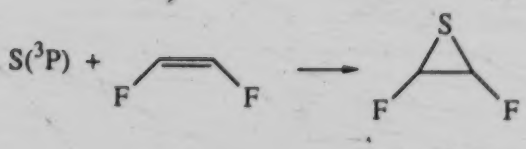

[171]

In this case the extrapolated zero-time mole fraction of cis-DFT is ~0.91, Figure V–12, somewhat less than the value ~0.98 for the $S(^3P)$ reaction. Therefore, in addition to the

~2% trans-DFT formed from the trans-DFE present in the substrate, ~7% trans-DFT must be formed via rotation in the initially formed adduct which contains ~86% kcal mol^{-1} excess energy. At the low total pressure of 160 Torr, rotation can compete with collisional deactivation to a small extent, but at high pressures (see Figure V–13), collisional deactivation predominates.

As with the S(^{1}D, ^{3}P) + trans-DFE reaction, the S(^{1}D) atoms react with COS three times faster than with cis-DFE. Only cis-DFT is formed from the reaction of S(^{3}P) atoms in the system with cis-DFE. The mole fraction of cis-DFT, however, decreases with increasing photolysis time as in the S(^{3}P) + cis-DFE reaction, and this is almost entirely due to the destruction of DFT via photodecomposition and photopolymerization as well as desulfurization by S atoms, as shown by reactions [189] to [191]. Only a slight decrease in the rate of formation of trans-DFT with increasing conversion takes place because this isomer is more stable towards photodecomposition. Cis-DFE has also been found not to isomerize on photolysis.

Although S(^{1}D) atoms react faster with DFE than do S(^{3}P) atoms, even at 400 Torr DFE pressure (see Tables V–10 and V–11), the overall yields of trans- and cis-DFE are lower in the S(^{1}D, ^{3}P) + DFE reaction than in the corresponding S(^{3}P) atom reaction. This is because S(^{1}D) atoms react faster with COS than with the DFE's, whereas S(^{3}P) atoms react preferentially with the DFE's as can be seen from the following rate constants.

$$k(S(^1D) + COS) = 1.8 \times 10^{-10} \text{ cm}^3 \text{ molecule}^{-1} \text{ s}^{-1}$$ [43]

$$k(S(^3P) + COS) = 3.5 \times 10^{-15} \text{ cm}^3 \text{ molecule}^{-1} \text{ s}^{-1}$$ [47]

$$k(S(^1D) + DFE) \leq 0.94 \times 10^{-10} \text{ cm}^3 \text{ molecule}^{-1} \text{ s}^{-1}$$ [43,45]

$$k(S(^3P) + \text{trans-(cis-)DFE}) = 2.15\ (0.92) \times 10^{-14} \text{ cm}^3 \text{ molecule}^{-1} \text{ s}^{-1}$$ [43,47]

The S(^{1}D, ^{3}P) + trans-DFE reaction does not show significant pressure dependence (see Figure V–13). In the cis-DFE reaction, however, at lower DFE pressures more trans-DFT is formed from the isomerization of vibrationally-excited cis-DFT molecules which become collisionally stabilized at total pressure > 200 Torr (see Figures V–13 and V–14).

The analogous reactions of $O(^3P)$ with cis- and trans-DFE have been described in the literature and involve C=C bond cleavage:[186,187]

$$O(^3P) + HFC{=}CHF \longrightarrow [HFC(\cdot)\text{–}CHF(O\cdot)]^* \longrightarrow :CHF + CHFO\ (CO + HF) \quad [198a]$$

$$\longrightarrow \cdot CH_2F + \cdot CFO\ (CO + \cdot F) \quad [198b]$$

$$\longrightarrow C_2HFO + HF \quad [198c]$$

with [198a] predominating. The CHF radical reacts further with the substrates to form cis- and trans-trifluorocyclopropanes which, if not collisionally stabilized, can isomerize to cis- and trans-1,2,3-trifluoropropenes.[186] C=C bond cleavage occurs readily because of the presence of fluorine substituents which decrease the electron density, and therefore the strength, of the π-bond. The C=C bond energy in C_2H_4 is 171 kcal mol^{-1}, whereas in CF_4, it is only 74 kcal mol^{-1}.[187] The C=C bond energy of the DFE's would therefore be expected to have some intermediate value.

The rate constants for the $O(^3P)$ atom reactions with trans- and cis-DFE[100] are about 20 and 30 times greater than those for the $S(^3P)$ + trans- and cis-DFE reactions, respectively.[57,45] It is of interest to note that both $O(^3P)$ and $S(^3P)$ atoms react faster with C_2F_4 than with the DFE's.[100,57]

3. S + Cis- and Trans-1,2-dichloroethylene

(a) S(^{3}P) + trans- and cis-dichloroethylene

The major products obtained,[78] as expected, from the S(^{3}P) + trans- and cis-DClE reaction are the trans- and cis-2,3-dichlorothiiranes (DClT) respectively.

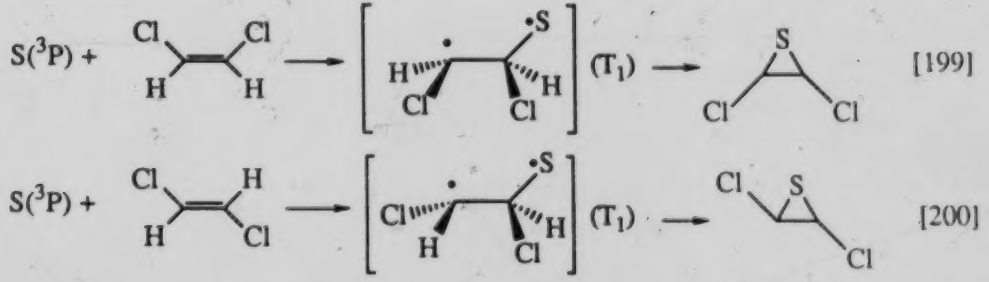

From separate experiments it was determined that the isomeric composition of the DClE's remains constant with increasing photolysis time. In the S(^{3}P) + trans-DClE reaction, only at higher photolysis times was any cis-DClE observed (see Figure V–16), and the mole fraction of trans-DClT was greater than 0.94. The rate constants for the S(^{3}P) + trans- and cis-DClE reactions have not been determined but they should be close to the value for the S(^{3}P) atom reaction with vinyl chloride which is 1.3 x 10^{-10} cm^3 molecule^{-1} s^{-1}.[43,57] Although S(^{3}P) atoms react faster with the DClE's than with the DFE's under similar conditions, the overall yields of the DClT's are less than half the yields of DFT obtained. Neither cis- nor trans-DClE absorbs in the photolysis region, but the UV spectrum of trans-DClT shows significant absorption in the photolysis region. Sufficient cis-DClT could not be collected for UV analysis but it is expected that the latter would have even higher extinction coefficients than the trans isomer in the 225 to 260 nm region (see Appendix A). The rate constants for the S(^{3}P) + DClT reactions should be larger than

those for the $S(^3P)$ + DClE reactions. Therefore with increasing DClT concentrations, desulfurization by $S(^3P)$ atoms becomes more important.

From Figure V–16, the rate of formation of trans-DClT is seen to decrease initially and then reach a photostationary state which declines after about ninety minutes. Although desulfurization of DClT probably occurs, photodecomposition and polymerization are more important sinks for trans-DClT. The sharp decrease in the rate of trans-DClT formation after a short photostationary state could be due to a rapid decrease in the DClE concentration owing to polymer formation:

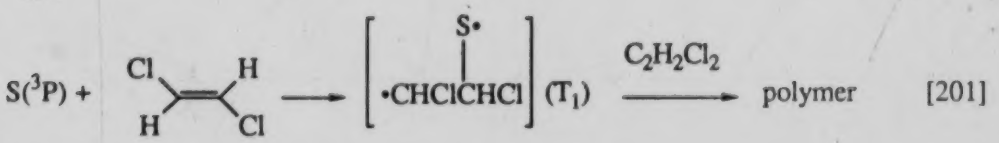

[201]

After the experiments, the cell was observed to be slightly cloudy. Dedio[78] suggested that cracking of the polymer could occur as shown below.

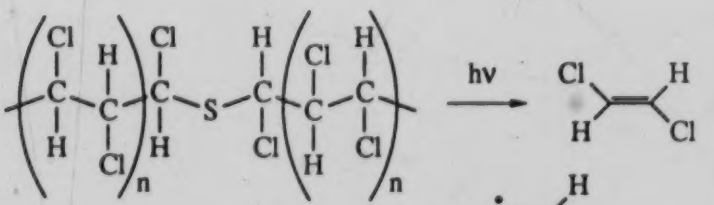

[202]

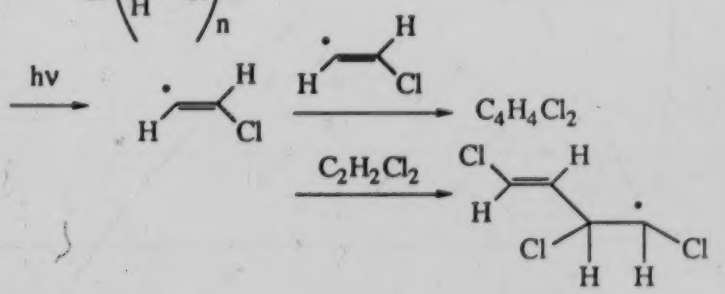

[203]

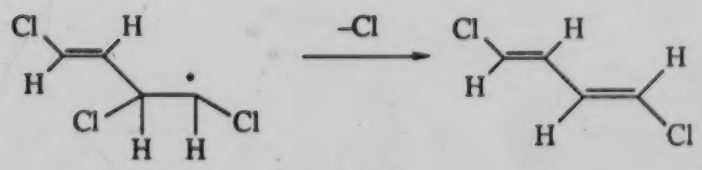

[204a]

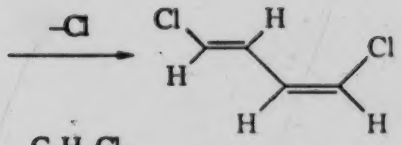

[204b]

$C_2H_2Cl_2$ → polymer [205]

In the S(^{3}P) + trans-DClE reaction at long photolysis times, two other products having molecular formula $C_4H_4Cl_2$ were formed, possibly via reactions [204a] and [204b]. From the mass spectrum of the $C_2H_4Cl_2$ compounds the $C_4H_4Cl^+$ ion is quite prominent.

In the S(^{3}P) + cis-DClE reaction, the apparent rate of formation of cis-DClT decreases even more rapidly with increasing photolysis time. The recoveries of cis-DClT are very low, in agreement with Dedio's yields of 10–20%.[78] The zero-time extrapolated value of the mole fraction of cis-DClT is about 0.9 (Figure V–15), decreasing rapidly with time because cis-DClT is destroyed more quickly than trans-DClT. Photodecomposition is expected to be the major sink for cis-DClT via a mechanism analogous to that for cis-DFT shown in reactions [189] to [191].

(b) S(^{1}D, ^{3}P) + trans- and cis-DClE

S(^{1}D) atoms should add across the double bond of the DClE's to give DClT's, and possibly insert into the C–H bonds to give 1,2-dichloroethylenethiols:

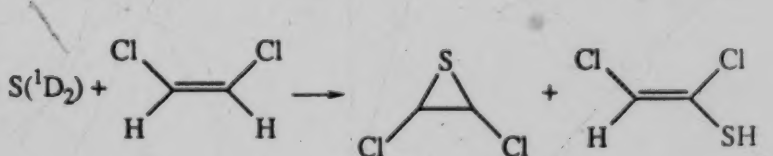

[206]

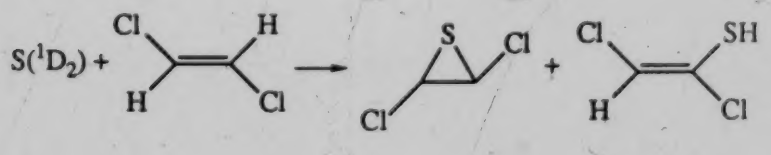

[207]

Thiol products were not observed. Whereas Dedio[78] was not able to detect any sulfur addition in this system, both cis- and trans-DClT products were obtained in the present work, although in very small yields, and both isomers are extremely photolabile, ending up as polymer. Another reason for the lower yields would be formation of vibrationally-excited adducts which, in the absence of sufficient pressure for collisional stabilization, may form biradicals which can polymerize by reacting with DClE or isomerize to the vinylthiol or thioaldehyde and hence form polymer.[185] In the S(^{1}D) + trans-DClE reaction, the mole fraction of trans-DClT extrapolated to zero time is only 0.87, meaning that a small amount of rotation also takes place in the hot trans adduct, since the S(^{3}P) + trans-DClE reaction appears to afford a higher degree of stereoselectivity.

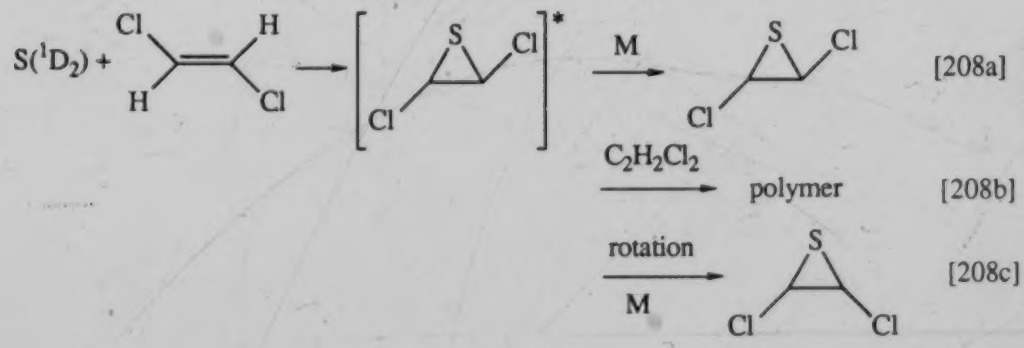

Dedio,[78] using flash-photolysis kinetic mass spectrometry, studied the S(^{1}D) atom reaction with trans-DClE and observed that the $C_2H_2Cl_2S$ signal decays very rapidly at first, followed by the onset of a broader signal which decays very slowly. He attributed the initial sharp decrease to polymerization of the $C_2H_2Cl_2S$ adduct. The broad secondary signal could be due to a longer-lived vinylthiol or thioaldehyde isomer.

In the S(^{1}D, ^{3}P) + cis-DClE reaction, cis-DClT is formed in even lower yields (see Table V–12 and Figure V–16) and the mole fraction of cis-DClT when extrapolated to zero time is ~1.0.

The $O(^3P)$ + DClE reactions have not been studied. The $O(^3P)$ + C_2HCl_3 and $O(^3P)$ + $C_2Cl_2H_2$ reactions proceed as follows:[188,189]

$$O(^3P) + ClCH{=}CCl_2 \longrightarrow (\Phi = 0.23) + HCl + CCl_2 \quad [209a]$$

$$\longrightarrow C_2HCl_3O^* \longrightarrow \text{polymer} \quad [209b]$$

$$O(^3P) + Cl_2C{=}CH_2 \longrightarrow CO(\Phi = 0.35) + (CH_2Cl_2) \quad [210a]$$

$$\longrightarrow Cl_2CCH_2Cl\ (\Phi = 0.06) \quad [210b]$$

$$\longrightarrow \text{polymer} \quad [210c]$$

As seen with the $S(^3P)$ + DClE reaction, there is a strong tendency towards polymerization. Some cleavage of the C=C bond also occurs in the $O(^3P)$ + chloroethylene systems.

Table V–1: Effect of Increasing Photolysis Time on the Product Yields from the $S(^3P)$ + Trans-2-butene Reaction[a]

Photolysis	Products, μmoles			Mole Fractions	
Time (min.)	CO	trans-C_4H_8S	cis-C_4H_8S	trans-C_4H_8S	trans-C_4H_8
0					0.993
11	3.74	2.64 (0.706)[b]	0.061 (0.016)	0.977	0.953
30	11.22	5.63 (0.502)	0.413 (0.037)	0.932	0.930
60	21.74	7.20 (0.331)	0.681 (0.031)	0.914	
90	29.88	8.32 (0.278)	1.026 (0.034)	0.890	0.885
120	31.70	9.67 (0.305)	0.884 (0.028)	0.916	
140	44.74	18.09 (0.404)	1.71 (0.038)	0.914	0.870
160					0.798

a P(COS) = 80 Torr, $P(CO_2)$ = 1200 Torr, P(trans-C_4H_8) = 38.5 Torr;
b Numbers in brackets are rates, in units μmoles/μmole CO.

Table V–2: Effect of Increasing Photolysis Time on the Product Yields from the $S(^3P)$ + Cis-2-butene Reaction[a]

Photolysis	Products, μmoles			Mole Fractions	
Time (min.)	CO	cis-C_4H_8S	trans-C_4H_8S	cis-C_4H_8S	cis-C_4H_8
0					0.982
10	3.38	1.89 (0.559)[b]	0.18 (0.052)	0.914	0.978
20	5.91	3.47 (0.587)	0.426 (0.072)	0.891	0.906
30	10.10	4.39 (0.435)	0.748 (0.074)	0.854	0.679
40	13.00	5.57 (0.428)	1.09 (0.084)	0.837	0.859
50	17.14	5.59 (0.326)	1.50 (0.088)	0.788	0.706
60	22.12	4.80 (0.217)	1.85 (0.084)	0.721	0.590
80	29.43	6.07 (0.206)	3.54 (0.120)	0.632	0.381
100	31.57	6.22 (0.197)	4.16 (0.132)	0.599	0.398
120	31.00	5.34 (0.172)	3.59 (0.116)	0.598	0.368
160	46.54	4.63 (0.099)	6.32 (0.136)	0.423	0.332

a P(COS) = 80 Torr, $P(CO_2)$ = 1200 Torr, P(cis-C_4H_8) = 38.5 Torr,
b Numbers in brackets are rates, in units μmoles/μmole CO.

Table V–3: Product Recoveries in the S(^{3}P) + Trans-2-butene Reaction[a]

Photolysis Time (min.)	μmoles CO°[b]	CO	trans-C_4H_8S	CO°–CO	% Yield[c]
6	2.28	1.24	0.839	1.04	80.7
10	3.81	2.20	1.325	1.61	82.3
17	6.61	3.76	2.003	2.85	70.3
20	7.53	4.12	2.029	3.41	59.5
30	17.44	9.44	4.563[d]	8.00	57.0
41	16.83	8.44	4.113	8.39	49.0

a P(COS) = 80 Torr, P(CO_2) = 1200 Torr, P(trans-C_4H_8S) = 38.5 Torr;
b CO yields in the absence of C_4H_8;
c % Yield = [R(C_4H_8S)/R(CO° – CO)] x 100;
d 4.389 μmoles trans- + 0.174 μmoles cis-2-C_4H_8S. This was the only experiment where some cis-sulfide could be detected.

Table V–4: Effect of Increasing Photolysis Time on the Product Yields from the $S(^3P)$ + Cis-1,2-difluoroethylene Reaction[a]

Photolysis	Products, μmoles			Mole Fraction	% Product
Time (min.)	CO	cis-$C_2H_2F_2S$	trans-$C_2H_2F_2S$	cis-$C_2H_2F_2S$	Recovery[b]
10	3.95	0.558 (0.141)[c]	0.029 (0.007)	0.950	38
30	12.16	1.26 (0.104)	0.080 (0.007)	0.940	31
60	20.20	1.81 (0.090)	0.175 (0.009)	0.912	16
90	32.00	1.85 (0.058)	0.190 (0.006)	0.907	12
120	40.26	2.02 (0.050)	0.325 (0.008)	0.862	9
160	53.52	1.88 (0.035)	0.573 (0.011)	0.766	7

a P(COS) = 80 Torr, $P(CO_2)$ = 1200 Torr, P(cis-$C_2H_2F_2$) = 80 Torr;
b % Product Recovery = [R(cis- + trans-$C_2H_2F_2S$)/R(CO° − CO)] x 100, where R(CO°) = 0.549 μmoles/min.;
c Numbers in brackets are rates, in units μmoles/μmole CO

Table V–5: Effect of Increasing Photolysis Time on the Product Yields from the $S(^3P)$ + Trans-1,2-difluoroethylene Reaction[a]

Photolysis	Products, μmoles			Mole Fraction		
		$C_2H_2F_2S$		$C_2H_2F_2S$	$C_2H_2F_2$	% Product
Time (min.)	CO	trans-	cis-	trans-	trans-	Recovery[b]
10	3.30	0.726 (0.220)[c]	0.099 (0.030)	0.881	0.9992	38
30	10.88	1.66 (0.153)	0.460 (0.042)	0.784	0.9972	38
60	21.96	4.23 (0.193)	0.730 (0.033)	0.853	0.9987	45
90	30.37	5.55 (0.183)	0.697 (0.023)	0.888	0.9961	33
120	41.04	7.79 (0.190)	0.832 (0.020)	0.902	0.9925	35
160	48.92	9.17 (0.187)	0.883 (0.180)	0.912	0.9934	26

a P(COS) = 80 Torr, $P(CO_2)$ = 1200 Torr, P(trans-$C_2H_2F_2$) = 80 Torr;

b % Product Recovery = [R(cis- + trans-$C_2H_2F_2S$)/R(CO° – CO)] x 100, where R(CO°) = 0.549 μmoles/min.;

c Numbers in brackets are rates, in units μmoles/μmole CO

Table V–6: Effect of Increasing Trans-1,2-difluoroethylene Pressure on the Product Yields from the S(^{3}P) + Trans-1,2-difluoroethylene Reaction[a]

Trans-$C_2H_2F_2$ Pressure (Torr)	Products, µmoles			Mole Fraction		% Product Recovery[b]
	CO	$C_2H_2F_2S$ trans-	$C_2H_2F_2S$ cis-	trans-$C_2H_2F_2S$	trans-$C_2H_2F_2$	
10[c]	21.87	0.354 (0.016)[e]	0.091 (0.004)	0.795	0.9392	5
38.5[d]	22.94	2.76 (0.120)	0.420 (0.018)	0.868	0.9883	32
80[c]	21.96	4.23 (0.193)	0.730 (0.033)	0.853	0.9987	45
120[c]	20.28	5.10 (0.251)	0.967 (0.048)	0.841	0.9964	54
200[c]	19.10	4.98 (0.261)	1.51 (0.079)	0.767	0.9967	53
300[c]	18.03	6.00 (0.333)	1.62 (0.090)	0.788	0.9787	57
400[c]	18.56	6.25 (0.337)	1.72 (0.093)	0.785	0.9951	62

a P(COS) = 80 Torr, P(CO_2) = 1200 Torr, Photolysis time = 60 minutes;
b % Product Recovery = [R(cis- + trans-$C_2H_2F_2S$)/R(CO° – CO)] x 100;
c CO° = 32.94 µmoles;
d CO° = 31.44 µmoles;
e Numbers in brackets are rates, in units µmoles/µmole CO.

Table V–7: Effect of Increasing Cis-1,2-difluoroethylene Pressure on the Product Yields from the $S(^3P)$ + Cis-1,2-difluoroethylene Reaction[a]

	Products, μmoles			Mole Fraction	
Cis-$C_2H_2F_2$		$C_2H_2F_2S$		cis-	% Product
Pressure (Torr)	CO	cis-	trans-	$C_2H_2F_2S$	Recovery[b]
10[c]	21.22	0.077	0.011	0.875	0.8
		(0.0036)[e]	(0.0004)		
38.5[d]	23.70	0.783	0.109	0.879	10
		(0.0330)	(0.0046)		
80[c]	20.20	1.81	0.175	0.912	16
		(0.0896)	(0.0087)		
120[c]		1.90	0.102	0.949	
200[c]	19.25	3.11	0.128	0.961	27
		(0.162)	(0.0066)		
300[c]	21.41	4.32	0.128	0.971	39
		(0.202)	(0.0060)		
400[c]	18.79	4.03	0.056	0.986	29
		(0.214)	(0.0030)		

a P(COS) = 80 Torr, $P(CO_2)$ = 1200 Torr, Photolysis time = 60 minutes;
b % Product Recovery = [R(cis- + trans-$C_2H_2F_2S$)/R(CO° – CO)] x 100;
c CO° = 32.94 μmoles;
d CO° = 31.44 μmoles;
e Numbers in brackets are rates, in units μmoles/μmole CO.

Table V–8: Effect of Increasing Photolysis Time on the Product Yields from the S(^{1}D, ^{3}P) + Cis-1,2-difluoroethylene Reaction[a]

Photolysis	Products, μmoles			Mole Fraction		
		$C_2H_2F_2S$		cis-	cis-	% Product
Time (min.)	CO	cis-	trans-	$C_2H_2F_2S$	$C_2H_2F_2$	Recovery[b]
10	5.02	0.566	0.062	0.901		
		(0.113)[c]	(0.012)			
30	11.71	0.960	0.109	0.898	0.9954	22
		(0.082)	(0.009)			
60	23.50	1.38	0.168	0.892	0.9910	16
		(0.059)	(0.007)			
90	30.37	1.55	0.204	0.883	0.9908	9
		(0.0510	(0.007)			
120	33.60	1.64	0.212	0.885	0.9928	9
		(0.046)	(0.006)			
160	40.66	1.57	0.259	0.858	0.9956	2
		(0.039)	(0.006)			

a P(COS) = 80 Torr, P(cis-$C_2H_2F_2$) = 80 Torr;
b % Product Recovery = [R(cis- + trans-$C_2H_2F_2S$)/R(CO° – CO)] x 100, where R(CO°) = 0.549 μmoles/min.;
c Numbers in brackets are rates, in units μmoles/μmole CO.

Table V–9: Effect of Increasing Trans-1,2-difluoroethylene Pressure on the Product Yields from the S(^{1}D, ^{3}P) + Trans-1,2-difluoroethylene Reaction[a]

	Products, µmoles			Mole Fraction		
Trans-$C_2H_2F_2$		$C_2H_2F_2S$		trans-	trans-	% Product
Pressure (Torr)	CO	trans-	cis-	$C_2H_2F_2S$	$C_2H_2F_2$	Recovery[b]
10[c]	27.56	0.814	0.139	0.854	0.983	25
		(0.030)[e]	(0.005)			
38.5[c]	23.10	1.49	0.464	0.762	0.9889	23
		(0.065)	(0.020)			
80[d]	18.34	1.96	0.595	0.767	0.9889	23
		(0.107)	(0.032)			
120[c]	19.89	2.32	0.807	0.742	0.9893	27
		(0.117)	(0.041)			
200[c]	18.80	2.83	0.985	0.742	0.9760	30
		(0.151)	(0.052)			
300[c]	18.33	2.76	0.891	0.756	0.9858	28
		(0.151)	(0.049)			
400[c]	18.41	2.95	0.620	0.826	0.9896	27
		(0.160)	(0.034)			

a P(COS) = 80 Torr, Photolysis time = 60 minutes;
b % Product Recovery = [R(cis- + trans-$C_2H_2F_2S$)/R(CO° – CO)] x 100;
c CO° = 31.44 µmoles;
d CO° = 32.94 µmoles;
e Numbers in brackets are rates, in units µmoles/µmole CO.

Table V–10: Effect of Increasing Cis-1,2-difluoroethylene Pressure on the Product Yields from the S(^{1}D, ^{3}P) + Cis-1,2-difluoroethylene Reaction[a]

	Products, µmoles			Mole Fraction		
Trans-$C_2H_2F_2$		$C_2H_2F_2S$		cis-	cis-	% Product
Pressure (Torr)	CO	cis-	trans-	$C_2H_2F_2S$	$C_2H_2F_2$	Recovery[b]
10[c]	27.64	0.215 (0.008)[e]	0.095 (0.003)	0.694	0.9919	6
38.5[c]	24.70	0.843 (0.034)	0.212 (0.009)	0.799	0.9936	13
80[d]	23.50	1.38 (0.059)	0.168 (0.007)	0.892	0.9910	16
120[c]	18.87	1.67 (0.089)	0.091 (0.005)	0.948	0.989	14
200[c]	19.60	1.71 (0.087)	0.065 (0.003)	0.964	0.9852	15
300[c]	18.24	1.64 (0.090)	0.018 (0.001)	0.989	0.9823	13
400[c]	18.56	1.16 (0.063)	0.022 (0.001)	0.981	0.9783	9

a P(COS) = 80 Torr, Photolysis time = 60 minutes;
b % Product Recovery = [R(cis- + trans-$C_2H_2F_2S$)/R(CO° – CO)] x 100;
c CO° = 32.94 µmoles;
d CO° = 31.44 µmoles;
e Numbers in brackets are rates, in units µmoles/µmole CO.

Table V–11: Effect of Increasing Photolysis Time on the $C_2H_2Cl_2S$ Yields from the S + Trans-1,2-dichloroethylene Reaction[a]

Photolysis time (min.)	CO_2 Pressure (Torr)	CO µmoles	Peak Area, area units		Mole Fraction
			cis-$C_2H_2Cl_2S$	trans-$C_2H_2Cl_2S$	cis-$C_2H_2Cl_2S$
10.0	1200	2.89[b]	113 (39.10)[c]		
30.0	1200	8.67	164 (18.92)		
60.0	1200	20.69[b]	401 (19.38)		
92.5	1200	27.24[b]	478 (17.55)	12 (0.44)	0.973
120	1200	31.90[b]	269 (8.43)	16 (0.50)	0.950
20.5	0	5.27	103 (19.54)	18 (3.42)	0.866
39.0	0	12.39	188 (15.17)	20 (1.61)	0.887
62.5	0	20.01	191 (9.55)	26 (1.30)	0.882
90.0	0	27.21	201 (7.39)	11 (0.40)	0.901

a P(COS) = 80 Torr, P(trans-$C_2H_2Cl_2$) = 80 Torr;
b These values were determined from peak area measurements;
c Numbers in brackets are rates, in units µmoles/µmole CO.

Table V–12: Effect of Increasing Photolysis Time on the $C_2H_2Cl_2S$ Yields from the S + Cis-1,2-dichloroethylene Reaction[a]

Photolysis time (min.)	CO_2 Pressure (Torr)	CO µmoles	Peak Area, area units trans-$C_2H_2Cl_2S$	Peak Area, area units cis-$C_2H_2Cl_2S$	Mole Fraction trans-$C_2H_2Cl_2S$
10.0	1200	3.93	43 (10.94)[b]	9 (2.29)	0.828
40	1200	19.77	48 (2.43)	24 (1.21)	0.667
60	1200	21.86	44 (2.01)	24 (1.10)	0.647
100	1200	40.0	34 (0.85)	24 (0.60)	0.586
60	0	27.12	27 (1.00)	1 (0.04)	0.964
90	0	39.07	28 (0.72)	5 (0.13)	0.849

a P(COS) = 80 Torr, P(trans-$C_2H_2Cl_2$) = 80 Torr;

b Numbers in brackets are rates, in units µmoles/µmole CO.

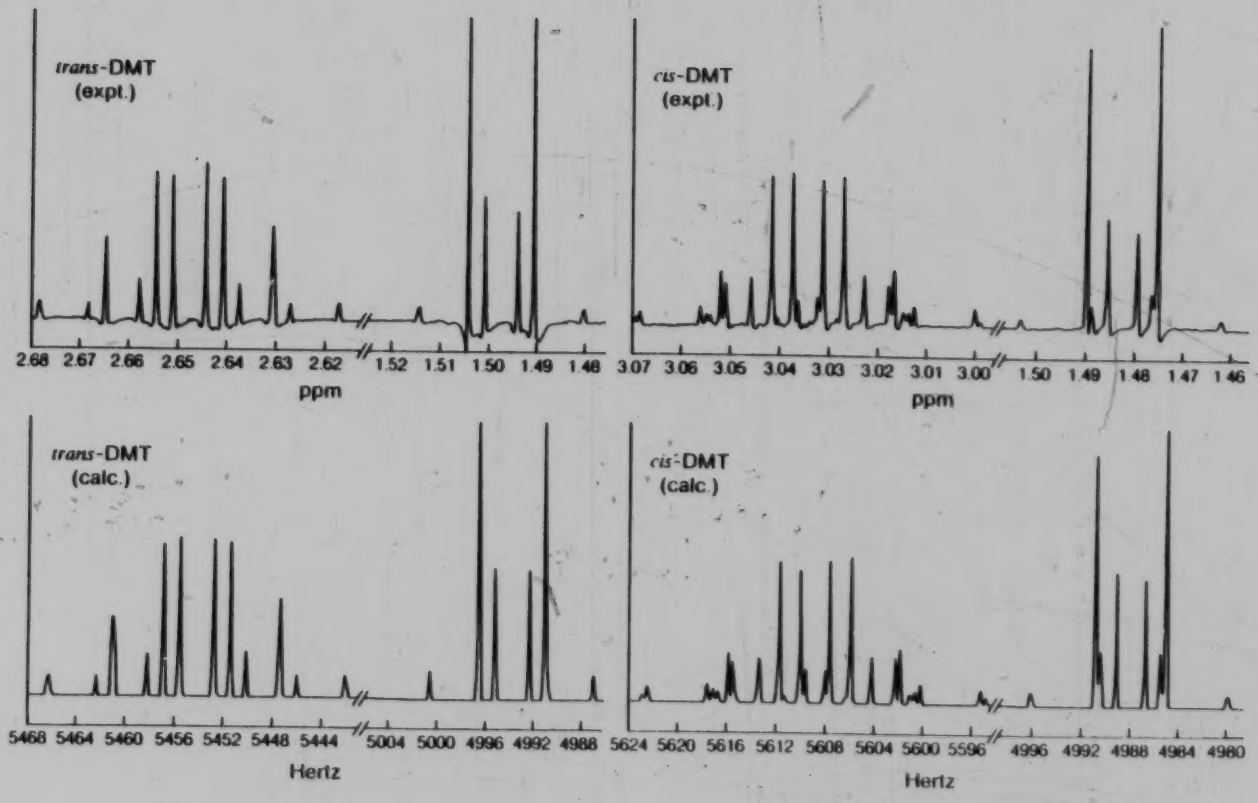

Figure V–1: ^{1}H NMR Spectra of Trans- and Cis-2,3-dimethylthiirane

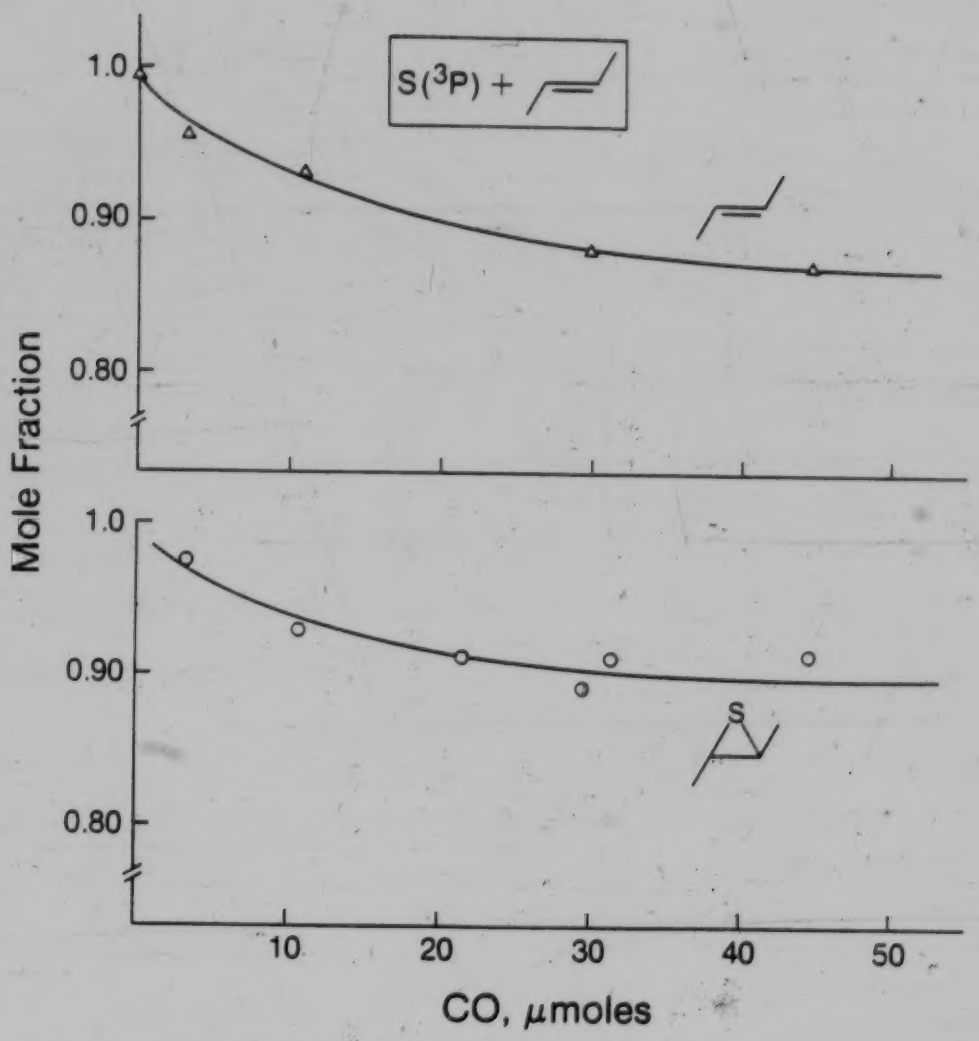

Figure V–2: Mole Fractions of Trans-C_4H_8 and Trans-C_4H_8S as a Function of CO in the $S(^3P)$ + Trans-C_4H_8 Reaction

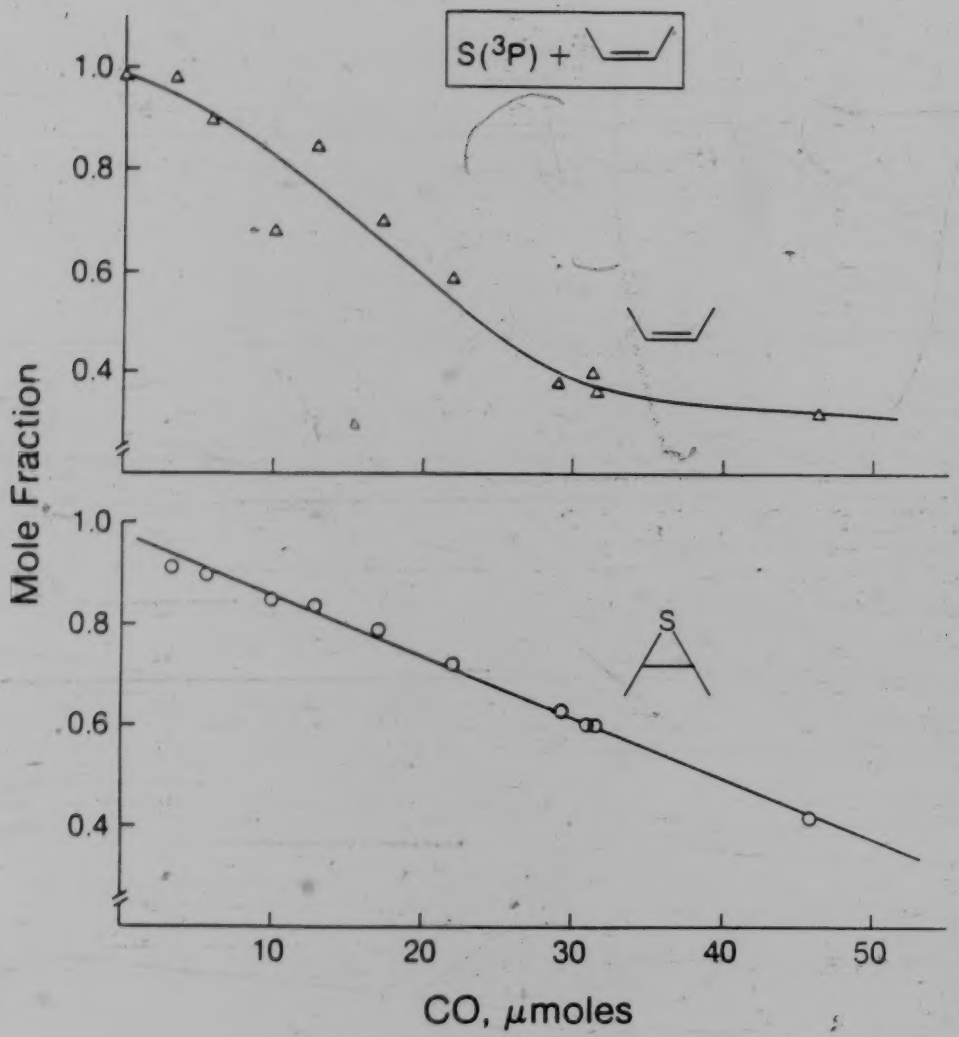

Figure V–3: Mole Fractions of Cis-C_4H_8 and Cis-C_4H_8S as a Function of CO in the $S(^3P)$ + Cis-C_4H_8 Reaction

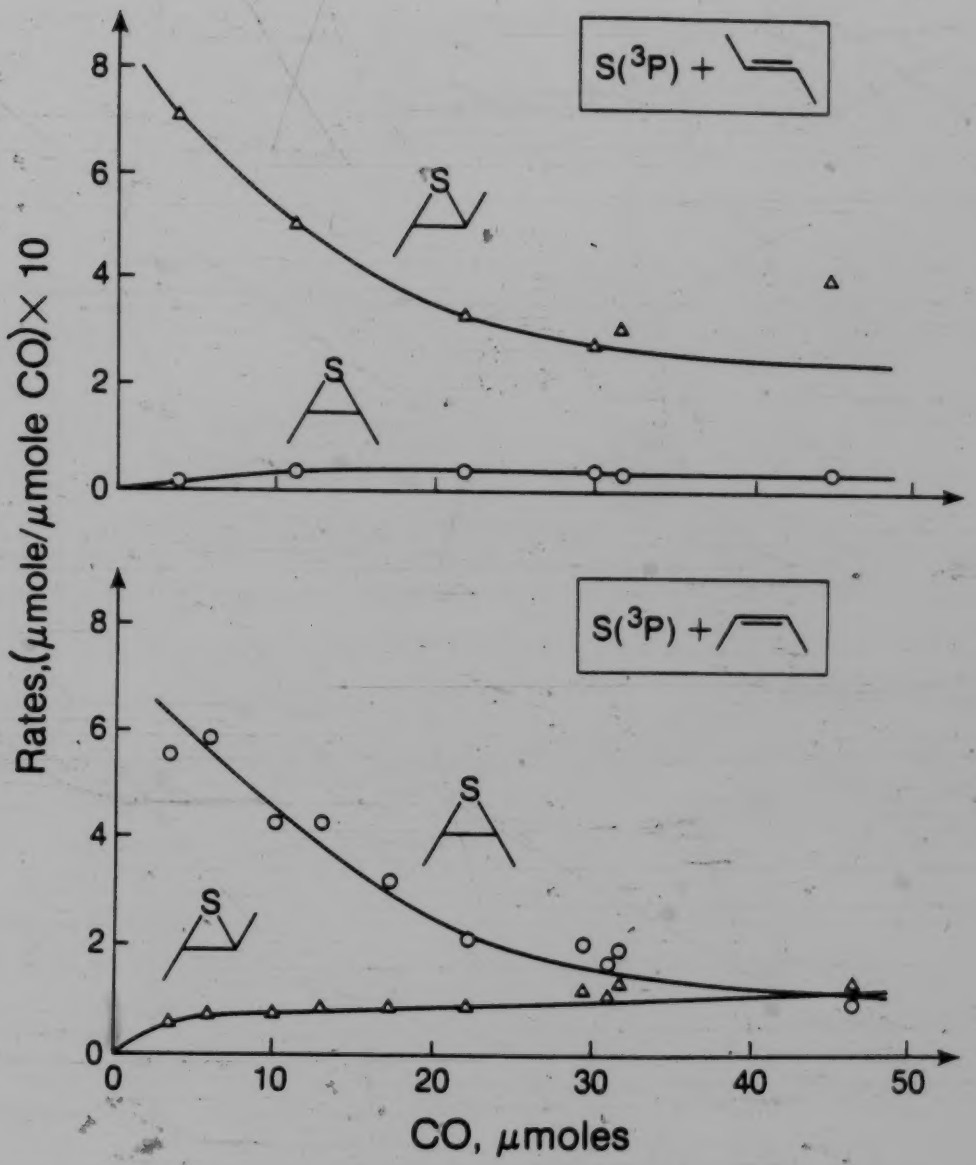

Figure V–4: Rates of C_4H_8S Formation as a Function of CO Yield for the $S(^3P)$ + Trans- and Cis-C_4H_8 Reactions

Figure V–5: ^{1}H and ^{19}F NMR Spectra of Trans-2,3-difluorothiirane

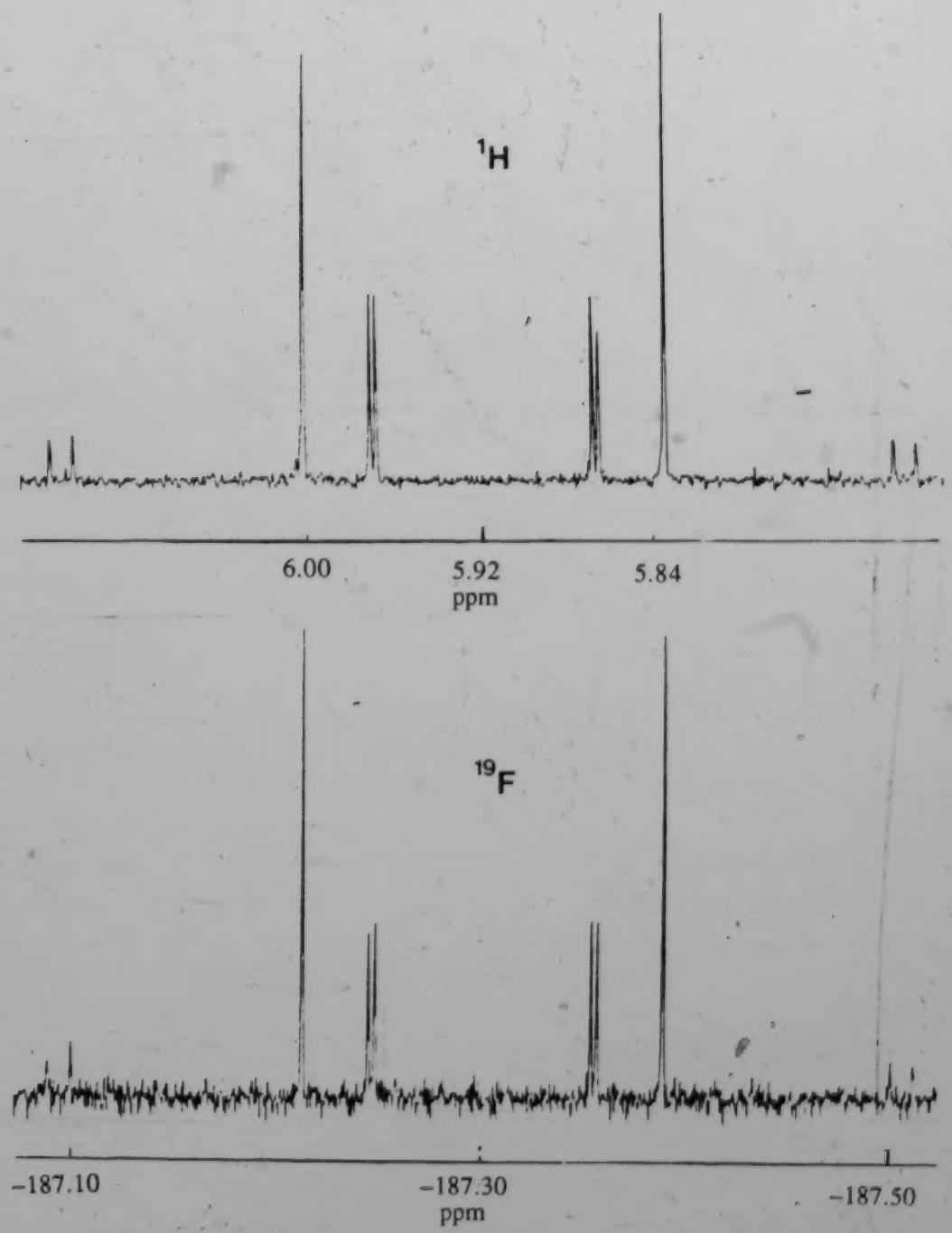

Figure V–6: ^{1}H and ^{19}F NMR Spectra of Cis-2,3-difluorothiirane

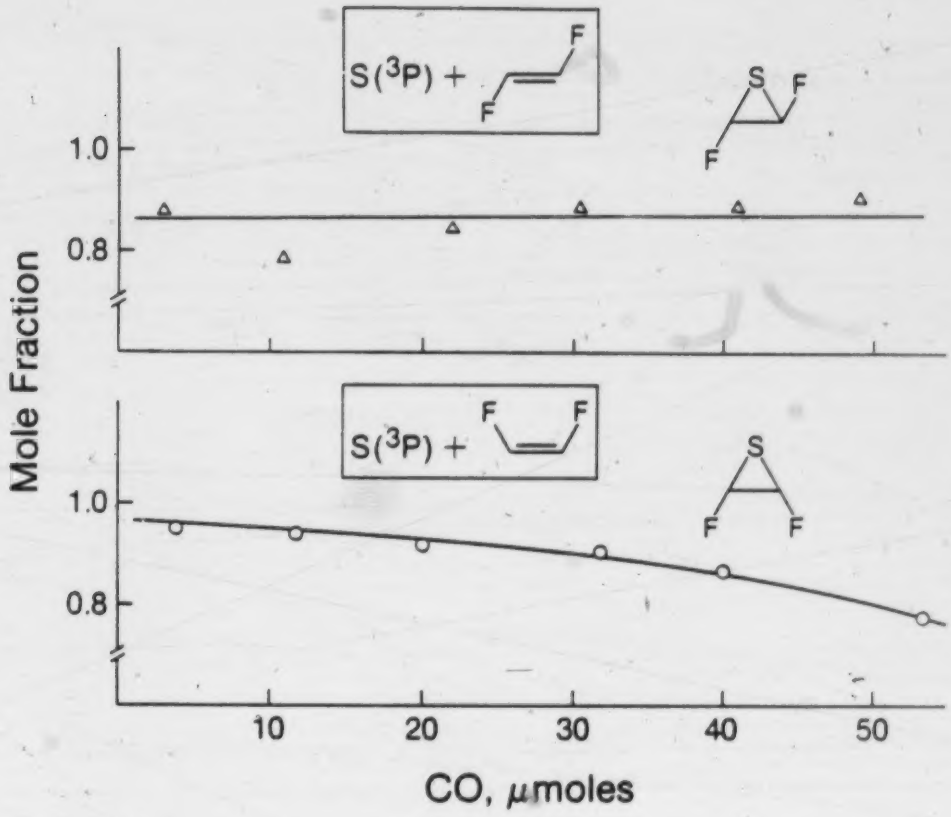

Figure V–7: Mole Fractions of the Stereoselective Product in the $S(^3P)$ + Trans- and Cis-$C_2H_2F_2$ Reactions as a Function of CO Yield

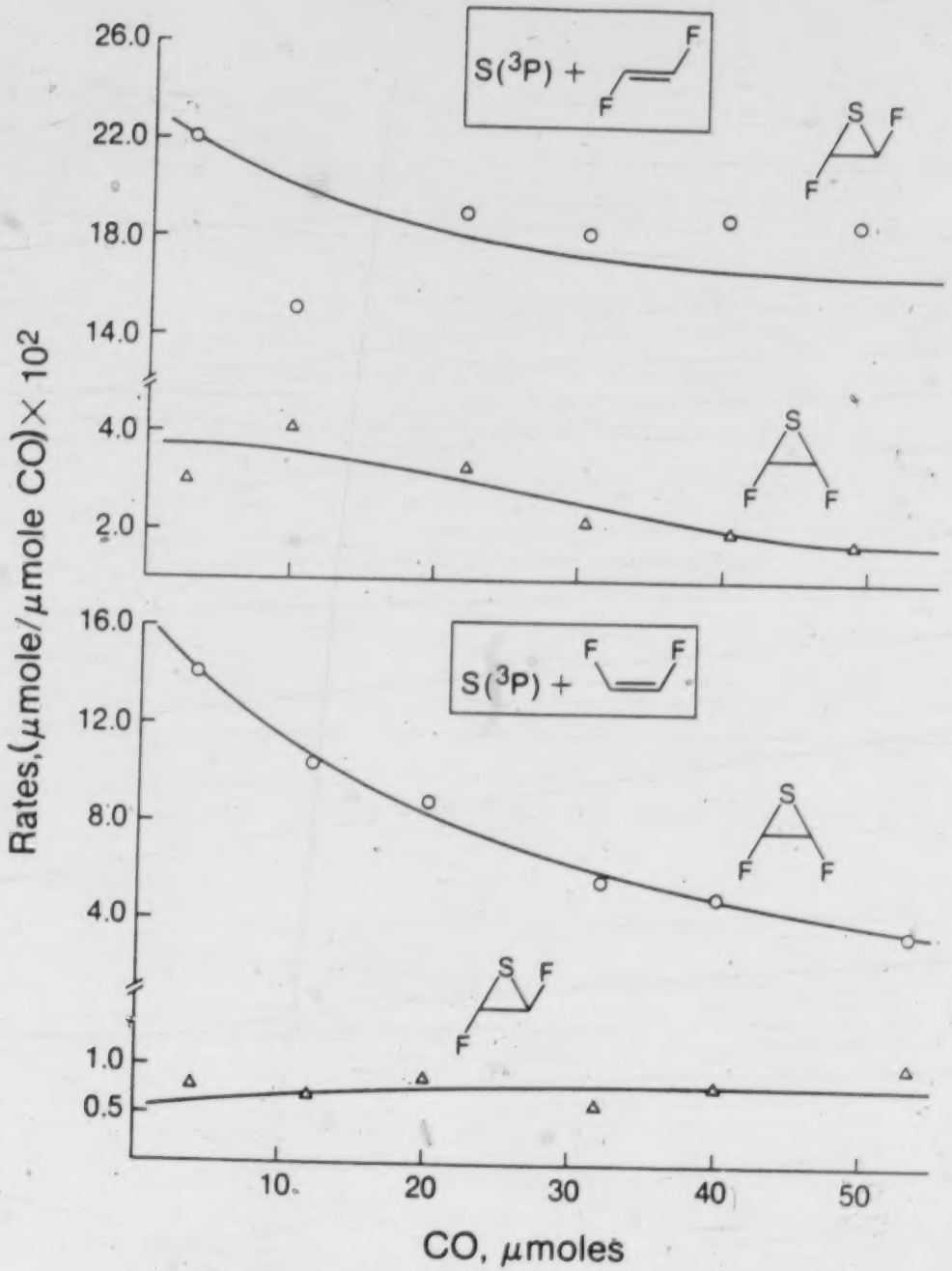

Figure V–8: Rates of Product Formation as a Function of CO Yield in the $S(^3P)$ + Trans- and Cis-$C_2H_2F_2$ Reactions

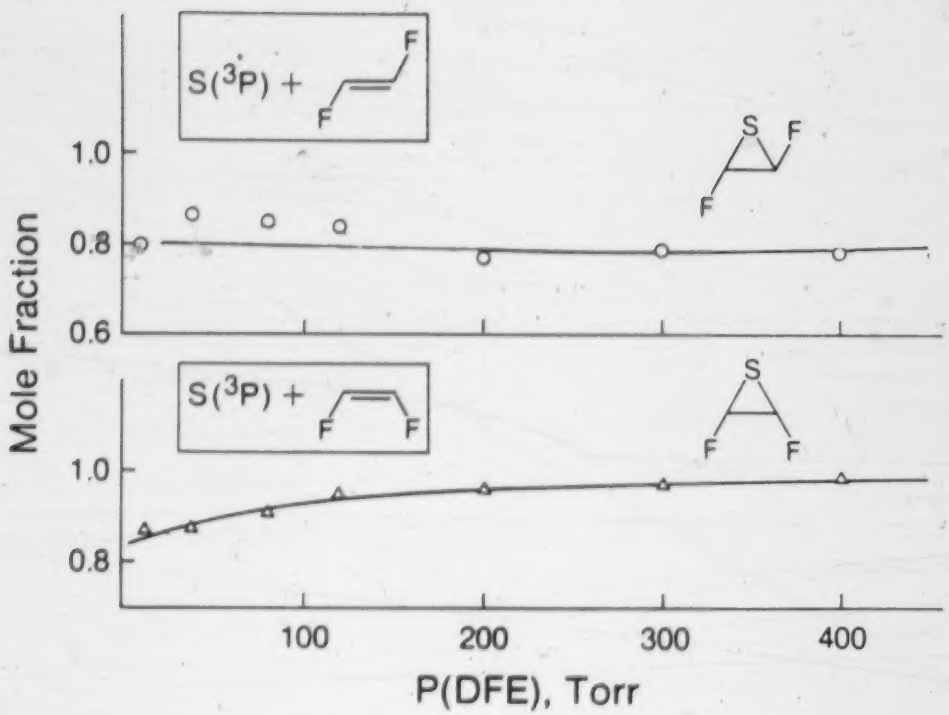

Figure V–9: Mole Fractions of Trans- and Cis-$C_2H_2F_2S$ as a Function of $C_2H_2F_2$ Pressure

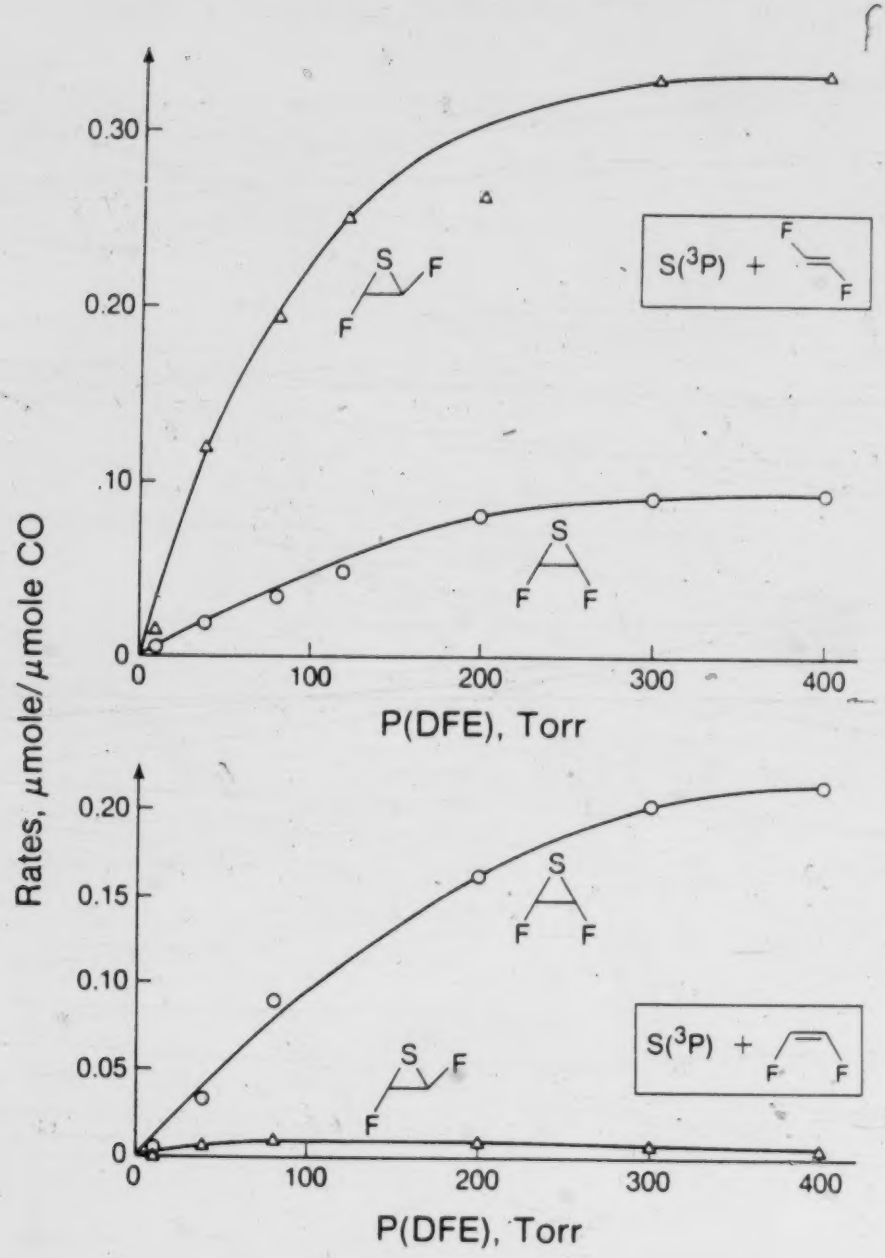

Figure V–10: Rates of Product Formation as Function of $C_2H_2F_2$ Pressure in the — $S(^3P)$ + Trans and Cis-$C_2H_2F_2$ Reactions

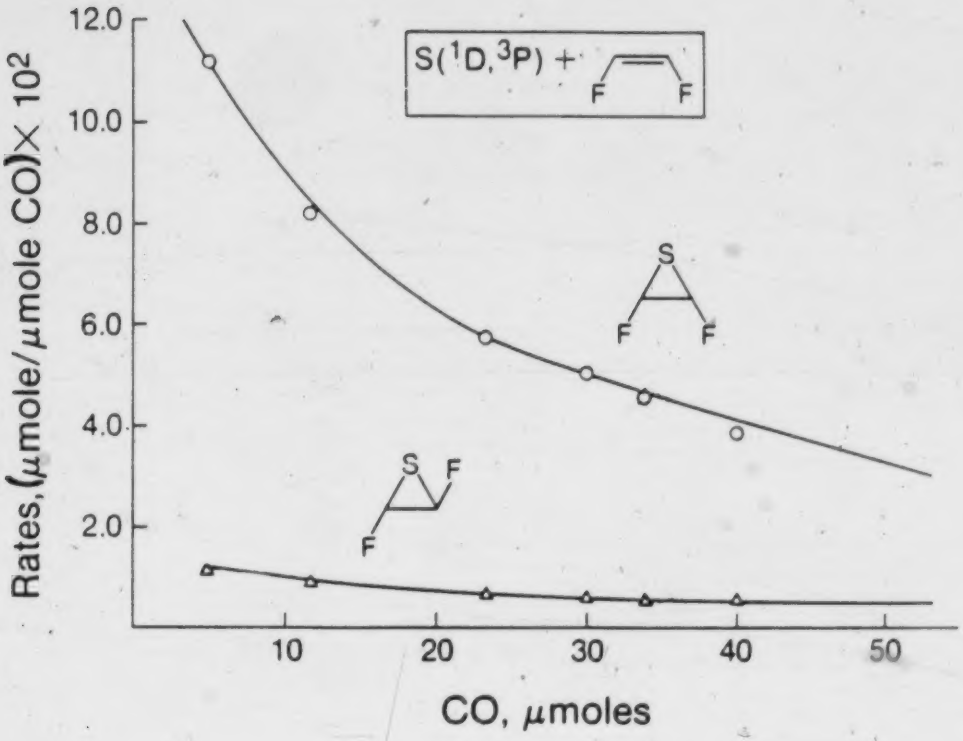

Figure V–11: Rates of Product Formation as a Function of CO Yield for the $S(^1D, ^3P)$ + Cis-$C_2H_2F_2$ Reaction

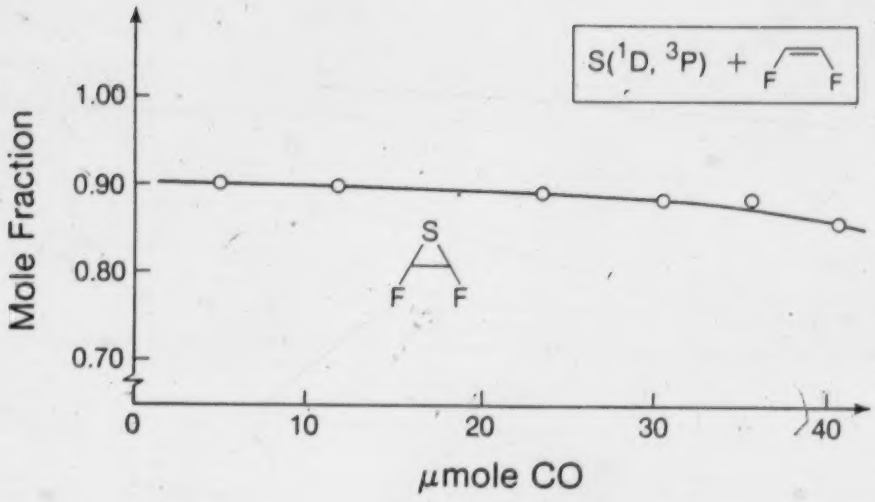

Figure V–12: Mole Fraction of Cis-$C_2H_2F_2S$ as a Function of CO Yield for the $S(^1D, ^3P)$ + Cis-$C_2H_2F_2$ Reaction

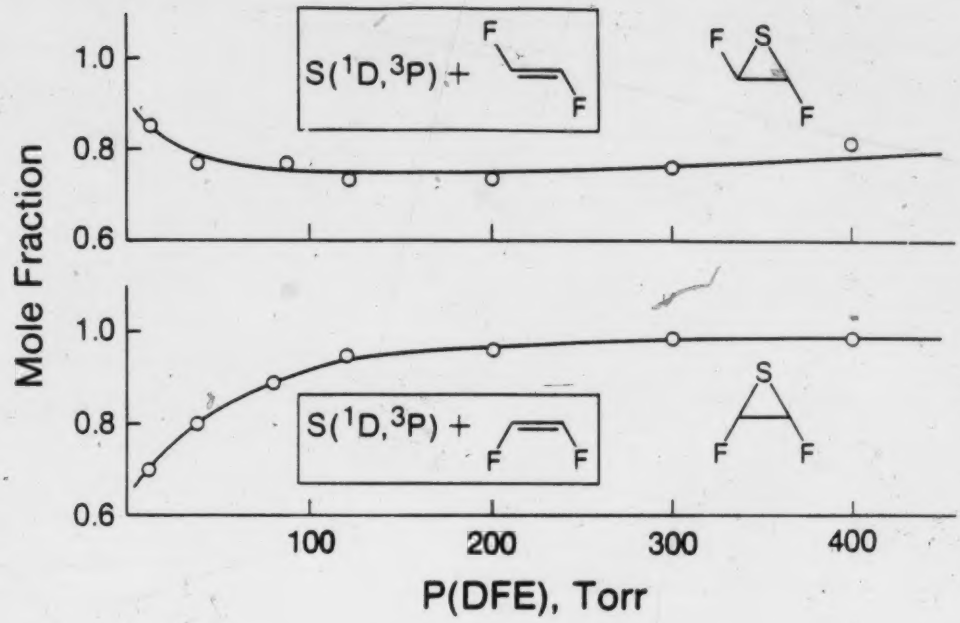

Figure V–13: Mole Fractions of $C_2H_2F_2S$ Products from the $S(^1D, ^3P)$ + Trans- and Cis-$C_2H_2F_2$ Reactions as a Function of $C_2H_2F_2$ Pressure

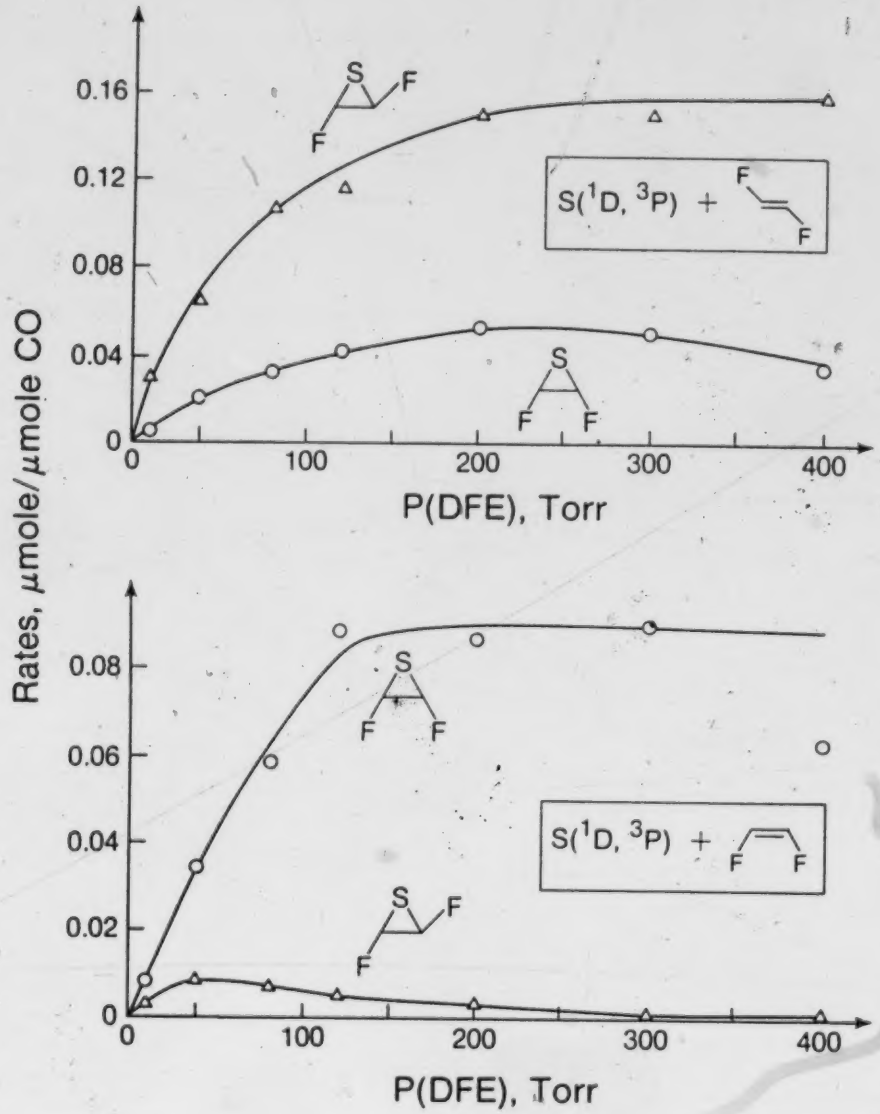

Figure V–14: Variation in Product Yields as a Function of $C_2H_2F_2$ Pressure in the $S(^1D, ^3P)$ + Trans- and Cis-$C_2H_2F_2$ Reactions

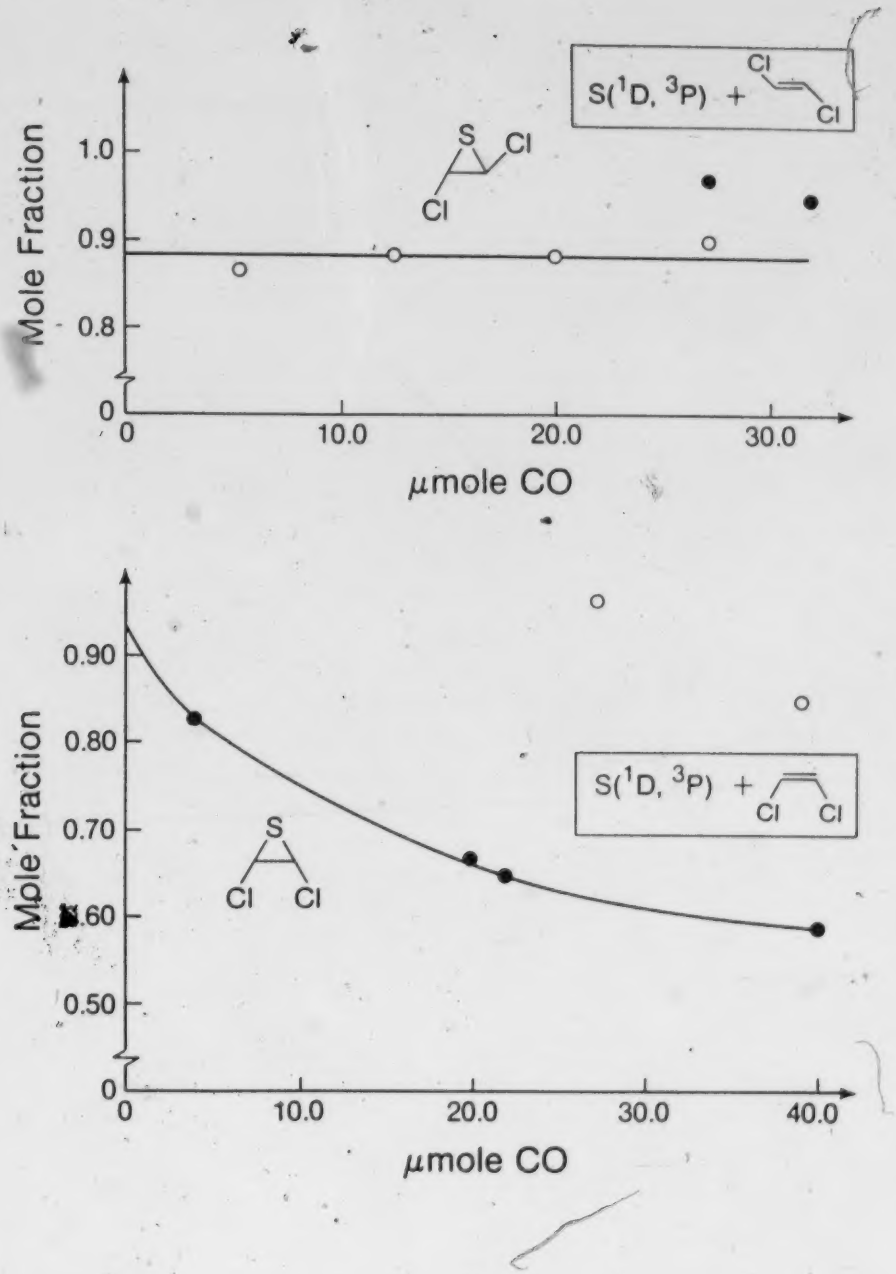

Figure V–15: Mole Fractions of the Stereoselective $C_2H_2Cl_2S$ Products from the S + Trans- and Cis-$C_2H_2Cl_2$ Reactions as a Function of CO Yield in the Presence (•), and in the Absence (○) of 1200 Torr CO_2

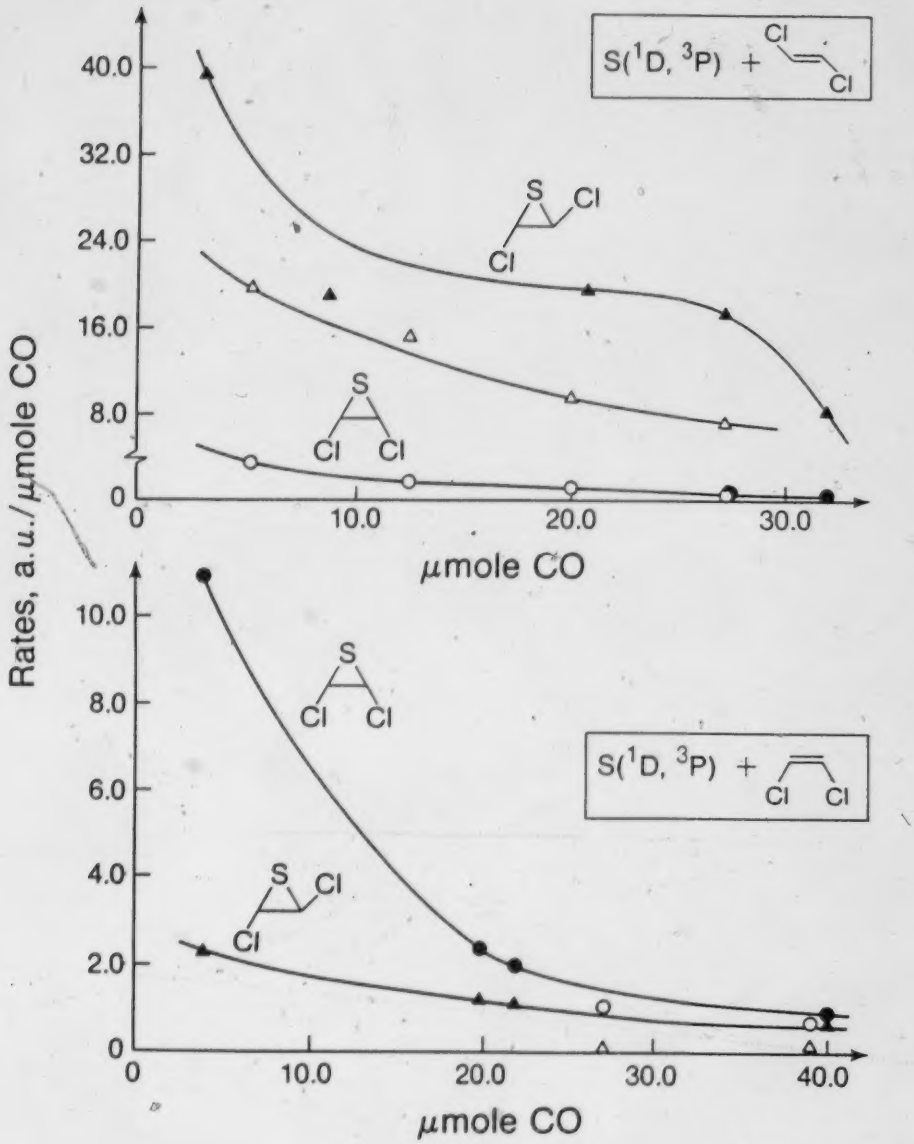

Figure V–16: Rates of Product Formation as a Function of CO Yield for the S + Trans- and Cis-$C_2H_2Cl_2$ Reactions in the Presence (●, ▲), and in the Absence (○, Δ) of 1200 Torr CO_2

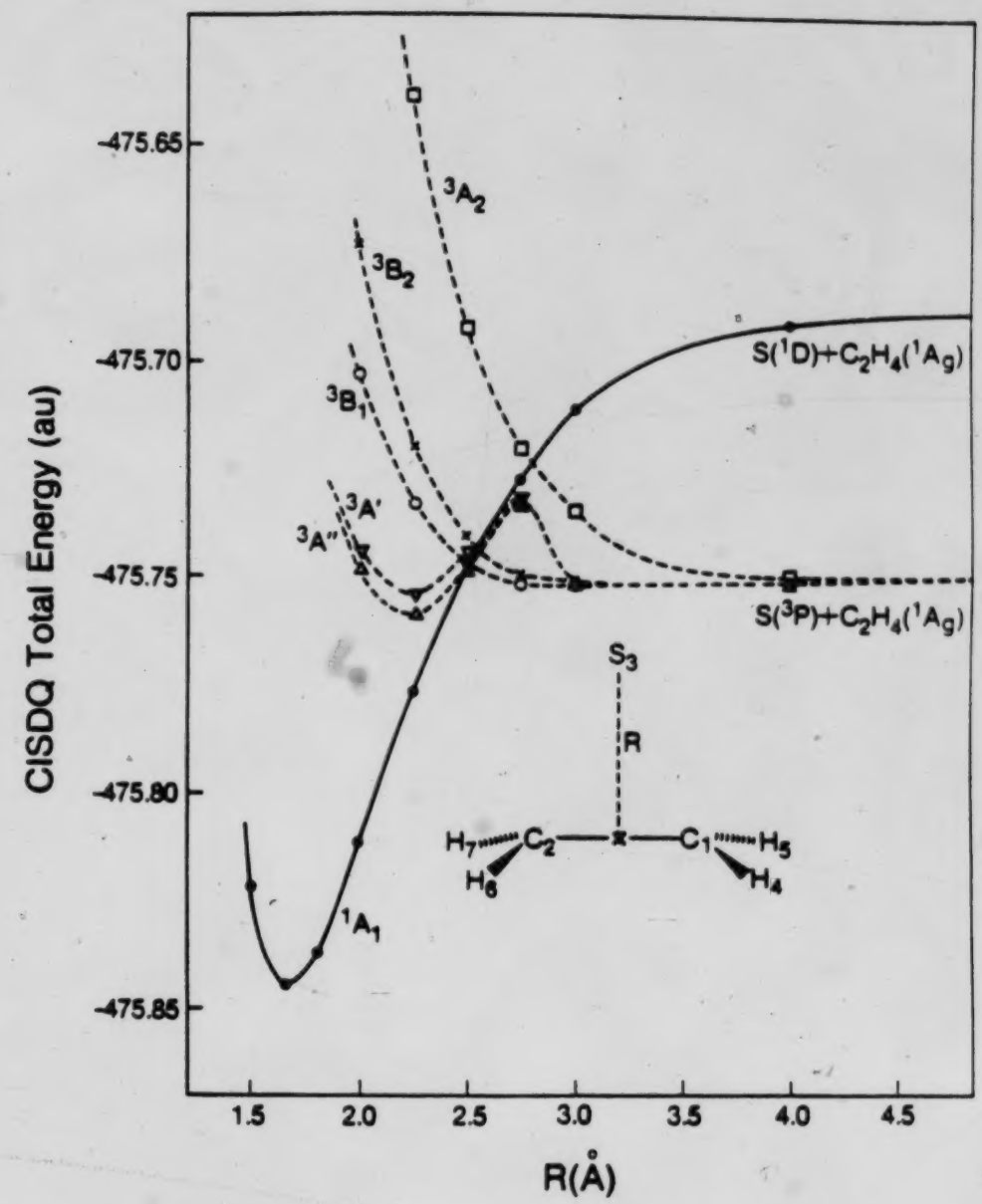

Figure V–17: Reaction Surface for $S(^3P)$ and $S(^1D)$ Addition to $C_2H_4(^1A_g)$

CHAPTER VI

ISOMERIZATION OF ALKENES BY THIIRANE DERIVATIVES

A. Results

The following mixtures were photolyzed in the gas phase and the mole fractions of the reactants and some products are tabulated in Table VI–1.

(a) 1.5 Torr trans-2,3-dimethylthiirane (trans-DMT) + 80 Torr cis-1,2-difluoroethylene (cis-DFE)

(b) <1 Torr cis-2,3-dimethylthiirane (cis-DMT) + 80 Torr cis-DFE

(c) <1 Torr cis-DMT + 80 Torr trans-1,2-difluoroethylene (trans-DFE)

(d) <1 Torr trans-2,3-difluorothiirane (trans-DFT) + 80 Torr cis-2-butene (CB)

(e) 80 Torr COS + 1200 Torr CO_2 + 22 Torr CB + 80 Torr cis-DFE

(f) 80 Torr COS + 1200 Torr CO_2 + 22 Torr CB + 80 Torr trans-DFE

After photolysis the alkene fractions were equilibrated for about one hour and an aliquot was then taken for G.C. analysis. The entire thiirane fraction was transferred to the GC column. In runs (e) and (f) the COS + CO_2 fraction containing the alkenes was first distilled from the mixture.

B. Discussion

In reaction mixtures (a) — (d), the absorbing species are thiiranes. Lown et al. have shown that the photolytic decomposition of thiiranes proceeds via the following elementary steps:

$C_2H_4S(S_0) + h\upsilon$	⟶	$C_2H_4S(S_1)$		[178]
$C_2H_4S(S_1)$	⟶	C_2H_2, H_2S, H_2, CH_4	Φ~0.14	[179]
$C_2H_4S(S_1)$	⟶	$C_2H_4S(T_1)$	Φ~0.86	[180]

$$C_2H_4S(T_1) + C_2H_4S(S_0) \longrightarrow S_2 + 2C_2H_4 \qquad \Phi\sim0.65 \qquad [181]$$

$$C_2H_4S(T_1) + C_2H_4S(S_0) \longrightarrow 2C_2H_4S(S_0) \qquad \Phi\sim0.21 \qquad [173]$$

They also showed that triplet state thiirane from the photolysis of thiirane in the presence of 2-butenes adds reversibly to the double bond of 2-butenes, thereby effecting the isomerization of several 2-butene molecules before the T_1 thiirane is deactivated.

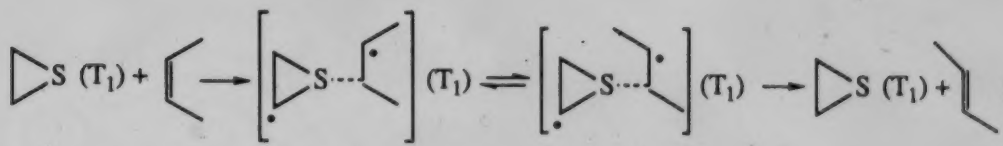

[50]

Photolysis of thiirane in the presence of 1-butene led to the formation of some additional products in small yields, indicating the occurrence of non-reversible addition of T_1 thiirane to the alkene:

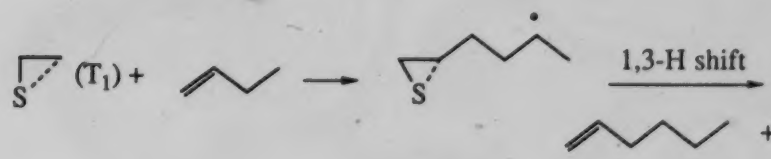

[211]

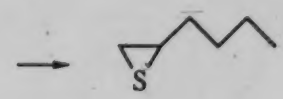

[212]

[213]

It has been shown (Chapter V) that in the reactions of S(^{3}P) atoms with the cis- and trans- isomers of 2-butene, 1,2-difluoro- and 1,2-dichloroethylene, none of the haloalkenes were isomerized, whereas the 2-butenes were extensively isomerized. Only the S(^{3}P) + trans-DFE reaction which afforded ~87% trans-DFT, and the S(^{3}P) + cis-dichloroethylene reaction which yielded 91% cis-2,3-dichlorothiirane were found to be non-stereospecific.

The present experiments were carried out in order to examine whether the nature of the substituents in the thiirane and alkene molecules had any effect on the isomerization of alkenes, reaction [50].

The first system to be examined was the DMT(T_1) + cis- and trans-DFE reactions. From the results listed in Table VI–1, i.e. reactions (a) — (c), it is seen that no isomerization of the DFE's occurred. The non-occurrence of the addition reaction of DMT(T_1) to DFE may be a consequence of the electron-withdrawing F substituents which decrease the electron density of the double bond, thereby making it less reactive with regard to attack by the sulfur radical moiety of DMT(T_1).

The composition of the cis- and trans-DMT appears to be unchanged after 30 minutes of photolysis and no cis- or trans-difluorothiirane (DFT) products were detected. However, some cis- and trans-2-butene are formed, probably from the decomposition of the DMT's, in a reaction analogous to reaction [181].

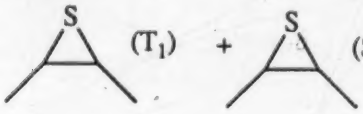

$$(T_1) + (S_0) \longrightarrow S_2 + 2\,C_4H_8 \qquad [214]$$

Conversely, trans-DFT (T_1) does not mediate the isomerization of cis-2-butene, reaction (d). However, the formation of trace amounts of DMT in this system suggests that trans-DFT (T_1) can add to cis-2-butene and that sulfur-atom transfer occurs (analogous to reaction [213]).

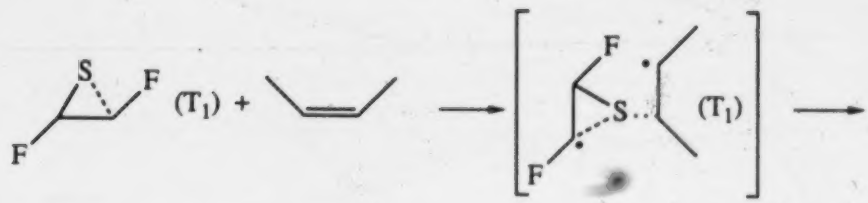

$C_2F_2H_2$ + DMT (T_1) [215]

Some of the DFE produced in this system would arise from this reaction, and the rest from the bimolecular reactions between (T_1) and (S_0) DFT, analogous to reaction [181]. Although the DMT formed in reaction [215] appears to be predominantly trans, the yields were extremely small (<0.1 μmole) and only a single experiment was carried out, hence this result should be viewed with caution. It is difficult to accept the occurrence of step [215] in view of the fact that cis-2-butene is not isomerized. A perhaps more logical explanation would be that the small amounts of DMT are formed from S-atoms generated in the primary process. No S(^{3}P) atoms could be detected in flash photolysis experiments on thiirane using λ>240 nm but in the present work the cutoff was around λ = 225 nm.

In runs (a) to (d) the thiiranes used were prepared from S-atom addition to the appropriate olefins and collected from several experiments. This was very time consuming and it was decided that it would be simpler to photolyze COS in the presence of an excess of CO_2 and a mixture of alkenes and examine the mole ratios of the thiiranes and alkenes in the photolyzates. In these experiments the T_1 thiiranes would be generated in situ by the addition of S(^{3}P) atoms and the results should corroborate those obtained from photochemically-generated T_1 thiiranes. The mole fractions of cis-DMT and of cis-2-butene from reaction (e) are, within experimental error, the same as those reported for the pure cis-2-butene system, (see Table V–2). The mole fraction of cis-DFT after 120 minutes photolysis is similarly unaffected by the presence of DMT (T_1) and cis-2-butene (compare with Table V-4). For reaction (f) the mole fractions of cis-DMT and cis-2-butene

appear to be somewhat low but since the reproducibility of these results is not known, they may well be within experimental error of those reported in Table V–2.

To summarize, fluorine substituents completely suppress the T_1 thiirane-mediated isomerization of alkenes:

- fluorinated alkenes are inert with respect to reversible addition of thiiranes and
- fluorinated thiiranes do not add to alkenes.

In all likelihood chlorine substituents in either the thiirane or the alkene will also inhibit isomerization of the alkene.

Table VI–1 : Mole Fractions of Reactants and Some Products from the Reactions between Substituted Ethylenes and Triplet State Thiirane Derivatives

Reaction[c]	Photolysis time (min.)	Mole Fractions			
		cis-DFE	cis-DFT	cis-2-butene	cis-DMT
(a)	30	0.995		0.150[a]	0.012
(b)	30	0.996		0.33[a]	0.980
(c)	32	0.048			0.997
(d)	30	<0.2[a]	<0.02	>0.99	0.273[a]
(e)	60	>0.99	0.836	0.612	0.723
			(0.223)[b]		(6.21)
	121	>0.99	0.856	0.437	0.510
			(0.354)		(7.27)
(f)	121	0.026	0.118	0.349	0.398
			(0.745)		(1.49)

a Large uncertainties in these mole fractions owing to very small yields (0.1 — 0.01 μmoles) of one or both isomers.

b Numbers in brackets are sums of both isomers in μmoles.

c Reaction (a) = trans-DMT + cis-DFE

" (b) = cis-DMT + cis-DFE

" (c) = cis-DMT + trans-DFE

" (d) = trans-DFT + CB

" (e) = $S(^3P)$ + CB + cis-DFE

" (f) = $S(^3P)$ + CB + trans-DFE

CHAPTER VII

SUMMARY AND CONCLUSIONS

The products obtained in the reactions of excited ($^1D_2$) and ground state (^3P) sulfur atoms with tetrahydrothiophene and 2-fluoropropene were examined and the product yields of the latter reaction were studied as a function of conversion time and pressure. Detailed studies of the S(^3P) atom reactions with the cis- and trans- isomers of 2-butene, 1,2-difluoroethylene (DFE) and 1,2-dichloroethylene (DClE) as well as S(^1D) atom reactions with cis- and trans-DFE and cis- and trans-DClE have been carried out.

Since S(^1D, ^3P) atoms have been found to react with thioethers by attacking the sulfur atom to form a thiosulfoxide which in the S(^1D, ^3P) + thietane (C_3H_6S) reaction ring-expands to form 1,2-dithiolane,[50] the ring-expanded disulfide product, 1,2-dithiane was anticipated from the S(^1D, ^3P) + tetrahydrothiophene (THT) reaction, but was not found. At a total pressure of <104 Torr (100 Torr COS, 3.9 Torr THT), the products obtained at low conversions are CS_2, 1-butanethiol, H_2S and C_2H_4, which are postulated to be due to fragmentation of the vibrationally-excited tetrahydrothiophene thiosulfoxide adduct or of the rearranged product, a vibrationally-excited 1,2-dithiane. To prevent fragmentation of the initially-formed hot adduct, evidently much higher pressures of substrate would be required which, however, could not be used because of its low vapor pressure and high absorption coefficient.

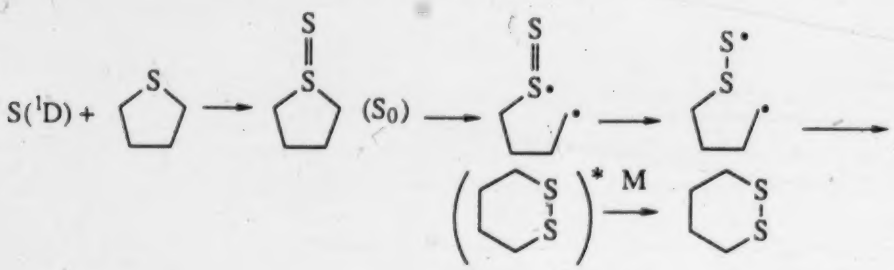

[147]

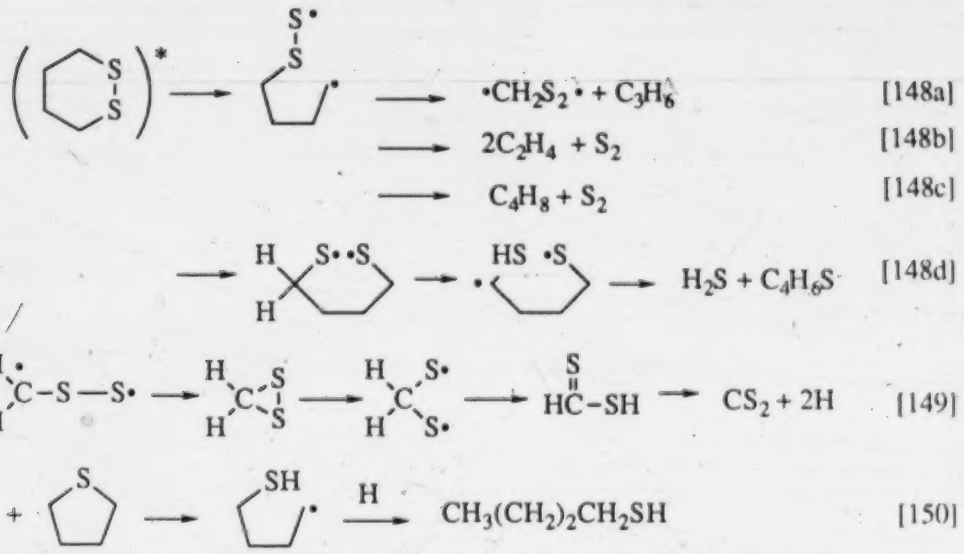

At photolysis times > 15 hours, the products obtained and their distributions are virtually identical to those from the photolysis of THT, which has a significant absorption in the 230 – 260 nm region.

$S(^1D)$ atoms are known to add to the double bonds of alkenes and insert into the various C–H bonds, whereas $S(^3P)$ atoms only add across double bonds. Therefore, in the $S(^1D, ^3P)$ + 2-fluoropropene reaction the expected products are: 2-fluoro-2-methylthiirane (FMT), 2-fluoro-2-propene-1-thiol (2,2FPT), Z- and E-2-fluoro-1-propenethiol (2,1FPT).

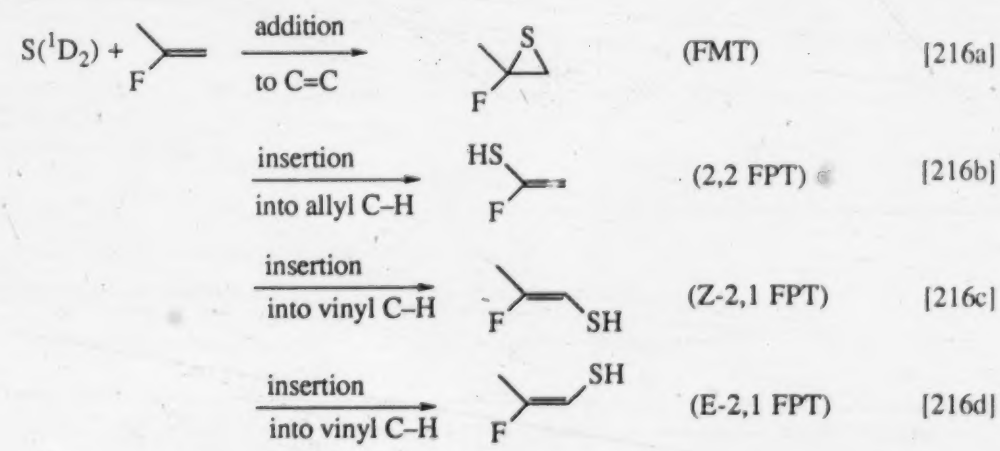

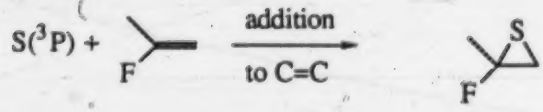

(FMT) [217]

From the mass spectrometric, NMR and IR data obtained, all the expected products were found except for E-2,1FPT, and were identified. FMT was the major product obtained in >80% yield. With increasing 2-fluoropropene pressure, the yields of Z-2,1FPT increase, indicating collisional stabilization requirements in the initially-formed adduct. From their UV spectra, FMT and 2,2FPT show significant absorption in the photolysis region and thus give rise to secondary products at longer photolysis times. From relative rate studies, and knowing the absolute rate constant for the $S(^3P) + C_2H_4$ reaction, the rate constant for the $S(^3P)$ + 2-fluoropropene reaction was calculated to be ~ 1.3×10^{-11} cm^3 $molecule^{-1}$ s^{-1}. None of the products have been reported before in the literature.

Divalent species such as methylene, oxygen atoms and nitrenes[93] in their triplet state have been found to add to the double bonds of alkenes to give both the cis- and trans-isomers of the cyclic addition product. Therefore, the reaction of $S(^3P)$ atoms with cis-and trans-2-butene would be expected to yield both cis- and trans-2,3-dimethylthiirane (DMT) in each case. The products obtained were characterized by means of mass spectrometry and NMR. Since first-order NMR spectra were not obtained, computer simulations of the spectra using the PANIC (Parameter Adjustment in NMR by Iteration Calculation) program were carried out in order to determine coupling constants and the calculated spectra agreed well with the experimental spectra, thus confirming the assignments.[95] From extrapolation of the mole fractions of cis- and trans-DMT obtained in the $S(^3P)$ + cis- and trans-2-butene reactions, respectively to zero time, both reactions were found to be 100% stereospecific. To date this is the only known example of stereospecific addition by a divalent triplet state reagent.

MO calculations were carried out on the $S(^3P) + C_2H_4$ reaction to explore the cause of the stereospecificity of the addition of $S(^3P)$ atoms. The calculations predict that the $S(^3P)$ atom initially approaches the C_2H_4 molecule along its C_{2v} symmetry axis leading to

the lowest fully repulsive $^3B_1$ surface from which it undergoes internal conversion to the lowest weakly-bonding triplet surface of the thiirane molecule, the $^3A''$ state, which lies ~54.3 kcal mol^{-1} above the ground state. In this state, the thiirane molecule has a barrier to rotation of only ~5.4 kcal mol^{-1}. Since the exothermicity of the $S(^3P) + C_2H_4$ reaction is ~60 kcal mol^{-1}, there is insufficient energy released in the reaction to drive rotation about the C–C bond in the $^3A''$ or T_1 thiirane, and collisional deactivation of the T_1 thiirane occurs faster than rotation about the C–C bond.

With increasing photolysis time, the stereoselectivity of the $S(^3P)$ + 2-butene reaction appears to decrease. Analysis of the 2-butene mixture after photolysis showed that the isomeric purity of the 2-butene decreases with increasing photolysis time. It has been shown that triplet state thiirane mediates the cis-trans isomerization of cis-2-butene via the complex

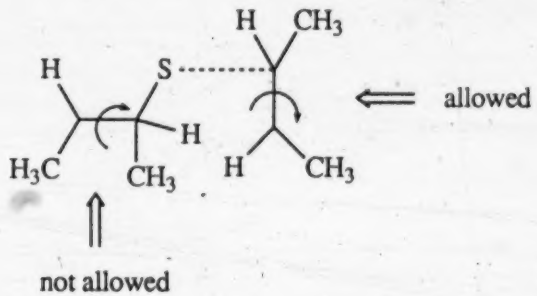

Hence this is one of the reasons for the loss of stereospecificity of the $S(^3P)$ + 2-butene reactions observed in earlier work.

Since extrapolation of the mole fraction of the DMT's to zero time suggests stereospecific products, it appears that rotation about the central C–C bond in T_1 DMT does not occur. From RRK theory the rate of rotation about the central C–C bond in T_1 DMT was estimated to be only 4×10^{-2} s^{-1}.[95] Since, on average, in the present system, each triplet state DMT molecule adds to about 23 butene molecules, therefore the lifetime of triplet DMT can be estimated to be about 8.8×10^{-8} s^{-1}, which means that T_1 DMT is deactivated almost 3×10^8 times faster than it can undergo geometrical isomerization.

Secondary photolysis and desulfurization by S(^{3}P) atoms of the major DMT isomer also resulted in the decrease of the mole fraction of the major DMT isomer, in addition to decreasing the rate of formation of the DMT products. These reactions also contribute to the increasing loss of stereospecificity with increasing conversion.

In the S(^{3}P) atom reaction with cis- and trans-1,2-difluoroethylene (DFE) extrapolation to zero time of the mole fractions of the cis- and trans-2,3-difluorothiiranes (DFT), shows that the S(^{3}P) + cis-DFE reaction is stereospecific, while the S(^{3}P) + trans-DFE reaction is only 87% stereoselective. The DFT products were also identified by means of mass spectrometry and NMR, and computer simulations of the NMR spectra were carried out to determine coupling constants. The compositions of the DFE's before and after photolysis were unchanged. Since the S(^{3}P) + trans-DFE reaction affords only 87% trans-DFE, restricted rotation about the C–C bond occurs in T_1 triplet-state trans-DFT, probably due to sufficient exothermicity of the reaction to allow rotation about the C–C bond at least 13% of the time before being deactivated. Cis-DFT has a much stronger absorption than trans-DFT in the photolysis region and thus undergoes significant photodecomposition and photopolymerization, hence the mole fraction of the cis-DFT decreases much faster with increasing photolysis time.

In the S(^{3}P) + cis- and trans-1,2-dichloroethylene (DClE) reactions, the S(^{3}P) + trans-DClE reaction appears to be stereospecific, whereas the S(^{3}P) + cis-DClE reaction is ~ 91% stereoselective. The overall product yields are low and the dichlorothiirane (DCIT) products absorb strongly in the photolysis region. Photopolymerization and decomposition are believed to be the major sinks for the dichlorothiiranes. No evidence of isomerization of the dichloroethylenes on photolysis was seen.

S(^{1}D) atoms were found to react with cis- and trans-DFE and cis- and trans-DClE to give only the thiirane products. The product yields were lower than those of the corresponding S(^{3}P) atom reactions probably due to the formation of vibrationally highly excited thiiranes which may undergo decomposition even at high alkene pressures.

Since no DFT-mediated isomerization of the DFE's or DCIT-mediated isomerization of the DCLE's were observed, it was desirable to determine if the DMT's, which facilitate the isomerization of the 2-butenes, could cause the isomerization of the DFE's, cis- and trans-DMT were photolyzed in the presence of cis- and trans-DFE. No isomerization of the DFE's was observed. Similarly, when trans-DFT was photolyzed in the presence of cis-2-butene the latter was not isomerized. Halogen substituents, therefore, appear to suppress the addition of T_1 thiiranes to alkenes. Further experimental and theoretical studies in this area would be very informative.

In contrast to $S(^3P)$ atom reactions, $O(^3P)$ atoms add to cis- and trans-2-butene to give non-stereospecific products. Addition of $O(^3P)$ atoms to fluorinated alkenes results in the cleavage of the double bond. Alkenes with chlorine substituents tend to undergo polymerization on reaction with both $S(^3P)$ and $O(^3P)$ atoms.

BIBLIOGRAPHY

1. a) Taylor, H.S. and Marshall, A.L., J. Phys. Chem., 29, 1140 (1925).
   b) Kablunde, K.J., React. Intermed. (Plenum), 1, 37 (1980).

2. Langmuir, I., J. Am. Chem. Soc., 34, 1310 (1912).

3. Strausz, O.P. and Gunning, H.E., J. Am. Chem. Soc., 84, 4080 (1962).

4. Khalil, M.A. and Rasmussen, R.A., Atmos. Environ., 18, 1805 (1984).

5. Servant, J., Atoms. Res., 23, 105 (1989).

6. Hyde, K.E., J. Chem. Educ., 52, 87 (1975).

7. Karplus, M. and Porter, R.N., Atoms and Molecules: An Introduction for Students of Physical Chemistry, The Benjamin/Cummings Publishing Co., Reading, Mass. (1970).

8. Moore, C.E., Atomic Energy Levels, (I-III), Nat. Stand. Ref. Data Ser. -NBS (US), 35 (1971).

9. Black, G., Jusinski, L.E. and Taherian, M.R., Chem. Phys. Lett., 122, 93 (1985).

10. Marquart, J.R., Belford, R.L. and Graziano, L.C., React. Intermed. (Plenum),3, 1 (1983) and references therein.

11. Van Roodselaar, A., Ph.D. Thesis, University of Alberta, 1976.

12. Meyer, B., Elemental Sulfur: Chemistry and Physics, Interscience Publishers, N.Y. (1965).

13. Strauss, C.E., McBane, G.C., Houston, P.L., Burak, I. and Hepburn, J.W., J. Chem. Phys., 90, 5364 (1989).

14. Black, G., Sharpless, R.L., Slanger, T.G. and Lorents, D.C., J. Chem. Phys., 62, 4274 (1975).

15. Sivakumar, N., Hall, G.E., Houston, P.L., Hepburn, J.W. and Burak, I., J. Chem. Phys., 88, 3692 (1988).

16. Sidhu, K.S., Lown, E.M., Strausz, O.P. and Gunning, H.E., J. Am. Chem. Soc., 88, 254 (1966).

17. Gunning, H.E. and Strausz, O.P., Adv. Photochem., 4, 143 (1966).

18. Sidhu, K.S., Csizmadia, I.G., Strausz, O.P. and Gunning, H.E., J. Am. Chem. Soc., 88, 2412 (1966).

19. Waller, I.M. and Hepburn, J.W., J. Chem. Phys., 87, 3261 (1987).

20. Addison, M.C., Donovan, R.J. and Fotakis, C., Chem. Phys. Lett., 74, 58 (1980).

21. Kim, H.L., Satyapal, S., Brewer, P. and Bersohn, R., J. Chem. Phys., 91, 1047 (1989).

22. Steadman, J. and Baer, T., J. Chem. Phys., 89, 5507 (1988).

23. Black, G., Sharpless, R.L., Slanger, T.G. and Lorents, D.C., J. Chem. Phys., 62, 4266 (1975).

24. Preston, K.F. and Barr, R.F., J. Chem. Phys., 62, 4266 (1975).

25. Cvetanovic, R.J., Adv. Photochem., 1, 115 (1963).

26. Black, G., Sharpless, R.L. and Slanger, T.G., J. Chem. Phys., 64, 3985 (1976).

27. Tyerman, W.J.R., O'Callaghan, W.B., Kebarle, P., Strausz, O.P. and Gunning, H.E., J. Am. Chem. Soc., 88, 4277 (1966).

28. Bavia, M., Di Lonardo, G., Galloni, G. and Trombetti, A., J. Chem. Soc., Faraday Trans. 2, 68, 615 (1972).

29. Callear, A.B. and Tyerman, W.J.R., Trans. Faraday Soc., 61, 2395 (1965).

30. Connor, J., Greig, G. and Strausz, O.P., J. Am. Chem. Soc., 91, 5695 (1969).

31. Donovan, R.J., Little, D.J. and Konstantatos, J., J. Photochem., 1, 86, (1972/73).

32. CRC Handbook of Chemistry and Physics, 66th Ed., 1985 - 1986.

33. Rabalais, J.W., McDonald, J.M., Scherr, V. and McGlynn, S.P., Chem. Rev., 71, 73 (1971).

34. McCarthy, M.I. and Vaida, V., J. Phys. Chem., 92, 5875 (1988).

35. Joens, J.A., J. Phys. Chem., 89, 5366 (1985).

36. Gadanken, A. and Burak, I., Chem. Phys. Lett., 137, 587 (1987).

37. Molina, L.T., Lamb, J.J. and Molina, M.J., Geophys., Res. Lett., 8, 1008 (1981).

38. Locker, J.R., Burkholder, J.B., Bair, E.J. and Webster, III, H.A., J. Phys. Chem., 87, 1864 (1983).

39. Lochte-Holtgreven, W., Bawn, C.E.H. and Eastwood, E., Nature, 129, 869 (1932).

40. Van Veen, N., Brewer, P., Das, P. and Bersohn, R., J. Chem. Phys., 79, 4295 (1983).

41. Gollnick, K. and Leppin, E., J. Am. Chem. Soc., 92, 2217 (1970).

42. Rudolph, R.N. and Inn, E.C.Y., J. Geophys. Res., 86, 9891 (1981).

43. Black, G., J. Chem. Phys., 84, 1345 (1986).

44. Donovan, R.J., Kirsch, L.J. and Husain, D., Nature, 222, 1164 (1969).

45. Black, G. and Jusinski, L.E., J. Chem. Phys., 82, 789 (1985).

46. Addison, M.C., Byrne, C.D. and Donovan, R.J., Chem. Phys. Lett., 64, 57 (1979).

47. Klemm, R.B. and Davis, D.D., J. Phys. Chem., 78, 1137 (1974).

48. Fowles, P., de Sorgo, M., Yarwood, A.J., Strausz, O.P., and Gunning, H.E., J. Am. Chem. Soc., 89, 1352 (1967).

49. Lown, E.M., Dedio, E.L., Strausz, O.P. and Gunning, H.E., J. Am. Chem. Soc, 89, 1056 (1967).

50. Green, M., Ph.D. Thesis, University of Alberta, 1983.

51. Knight, A.R., Strausz, O.P. and Gunning, H.E., J. Am. Chem. Soc., 85, 1207 (1963).

52. Knight, A.R., Strausz, O.P. and Gunning, H.E., J. Am. Chem. Soc., 85, 2349 (1963).

53. Knight, A.R., Strausz, O.P., Malm, S.M. and Gunning, H.E., J. Am. Chem. Soc., 86, 4243 (1964).

54. Doering, W. von E. and Prinzbach, H., Tetrahedron, 6, 24 (1959) and references therein.

55. McKee, M.L., J. Am. Chem. Soc., 108, 5059 (1986).

56. Benson, S.W., Adv. Photochem., 2, 1 (1964).

57. Strausz, O.P., Pure Appl. Chem., 4, 165 (1971).

58. Leppin, E. and Gollnick, K., J. Am. Chem. Soc., 92, 2221 (1970).

59. Lin., C.-L. and De More, W.B., J. Phys. Chem., 77, 863 (1973) and references therein.

60. Colussi, A.J. and Cvetanovic, R.J., J. Phys. Chem., 79, 1891 (1975).

61. Paraskevopoulos, G. and Cvetanovic, R.J., J. Am. Chem. Soc., 91, 7572 (1969).

62. Paraskevopoulos, G. and Cvetanovic, R.J., J. Phys. Chem. , 52, 5821 (1970).

63. Luntz, A.C., J. Chem. Phys., 73, 1143 (1980).

64. Michaud, P., Paraskevopoulos, G. and Cvetanovic, R.J., J. Phys. Chem., 78, 1457 (1974).

65. Herron, J.T. and Huie, R.E., J. Phys. Chem. Ref. Data, 2, 467 (1973).

66. Andresen, P. and Luntz, A.C., J. Chem. Phys., 72, 5842 (1980).

67. Herron, J.T., J. Phys. Chem. Ref. Data, 17, 1967 (1988).

68. Cohen, N., Int. J. Chem. Kinet., 18, 59 (1986).

69. Hawkins, M., Almond, M.J. and Downs, A.J., J. Phys. Chem., 89, 3326 (1985).

70. Donovan, R.J., Trans. Faraday Soc., 65, 1419 (1969).

71. Dunn, O.J., Filseth, S.V. and Young, R.A., J. Chem. Phys., 59, 2892 (1973).

72. Lin, M.C., Adv. Chem. Phys., 42, 113 (1980).

73. Wiebe, H.A., Knight, A.R., Strausz, O.P. and Gunning, H.E., J. Am. Chem. Soc., 87, 1443 (1965).

74. Wiebe, H.A., Ph.D. Thesis, University of Alberta, 1967.

75. Sherwood, A.G., Safarik, I., Verkoczy, B., Almadi, G., Wiebe, H.A. and Strausz, O.P., J. Am. Chem. Soc., 101, 3000 (1979).

76. Strausz, O.P., Gunning, H.E., Denes, A.S. and Csizmadia, I.G., J. Am. Chem. Soc., 94, 8317 (1972).

77. Hoffmann, R., Wan, C.C. and Neagu, V., Mol. Phys., 19, 113 (1970).

78. Dedio, E.L., Ph.D. Thesis, University of Alberta, 1967.

79. Lown, E.M., Ph.D. Thesis, University of Alberta 1966.

80. Kajimoto, O., Yamasaki, H. and Fueno, T., Chem. Phys. Lett., 68, 127 (1979).

81. Kajimoto, O., Fueno, T., Chem. Phys. Lett., 64, 445 (1979).

82. Bader, R.F.W., Stephens, M.E. and Gangi, R.A., Can. J. Chem., 55, 2755 (1977).

83. Woodworth, R.C. and Skell, P.S., J. Am. Chem. Soc., 81, 3383 (1959).

84. Skell, P.S. and Woodworth, R.C., J. Am. Chem. Soc., 78, 4496 (1956).

85. a) Herzberg, G. and Shoosmith, J., Nature, 183, 1801 (1959).
b) Herzberg, G., Proc. Roy. Soc. London, Ser. A, 262, 291 (1961).

86. Anet, F.A.L., Bader, R.F.W. and Van der Auwera, A., J. Am. Chem. Soc., 82, 3217 (1960).

87. Frey, H.M., J. Am. Chem. Soc., 82, 5947 (1960).

88. Bader, R.F.W. and Generosa, J.I., Can. J. Chem., 43, 1631 (1965).

89. Cvetanovic, R.J., Can. J. Chem., 36, 623 (1958).

90. McConaghy, J.S., Jr. and Lwowski, W., J. Am. Chem. Soc., 89, 2357 (1967).

91. De More, W.B. and Benson, S.W., Adv. Photochem., 2, 219 (1964).

92. Lown, E.M., Sandhu, H.S., Gunning, H.E. and Strausz, O.P., J. Am Chem. Soc., 90, 7164 (1968).

93. Leppin, E. and Gollnick, K., Tetrahedron Lett., 43, 3819 (1969).

94. Lown, E.M., Sidhu, K.S., Jackson, A.W., Jodhan, A., Green, M. and Strausz, O.P., J. Phys. Chem., 85, 1089 (1981).

95. Joseph, J., Gosavi, R.K., Otter, A., Kotovych, G., Lown, E.M. and Strausz, O.P., J. Am. Chem. Soc., 112, 8670 (1990).

96. Donovan, R.J., Husain, D., Fair, R.W., Strausz, O.P. and Gunning, H.E., Trans. Faraday Soc., 66, 1635 (1970).

97. Connor, J., Van Roodselaar, A., Fair, R.W. and Strausz, O.P., J. Am. Chem. Soc., 93, 560 (1971).

98. a) Davis, D.D., Klemm, R.B., Braun, W. and Pilling, M., Int. J. Chem. Kinet., 4, 383 (1972).
b) Klemm, R.B. and Davis, D.D., Int. J. Chem. Kinet., 5, 375 (1973).

99. Strausz, O.P., O'Callaghan, W.B., Lown, E.M. and Gunning, H.E., J. Am. Chem. Soc., 93, 559 (1971).

100. Cvetanovic, R.J., J. Phys. Chem. Ref. Data, 16, 261 (1987).

101. Cvetanovic, R.J. and Singleton, D.L., Rev. Chem. Intermed., 5, 183 (1984).

102. Callear, A.B. and Tyerman, W.J.R., Trans. Faraday Soc., 62, 2760 (1966).

103. Callear, A.B. and Tyerman, W.J.R., Trans. Faraday Soc., 62, 371 (1966).

104. Callear, A.B. and Tyerman, W.J.R., Proc. Chem. Soc., 296 (1964).

105. Leppin, E. and Gollnick, K., Chem. Ber., 103, 2571 (1970).

106. Leppin, E. and Gollnick, K., J. Am. Chem. Soc., 93, 2847 (1971).

107. Hawkins, M. and Andrews, L., J. Am. Chem. Soc., 105, 2523 (1983).

108. Strausz, O.P., Font, J. Dedio, E.L., Kerbarle, P. and Gunning, H.E., J. Am. Chem. Soc., 89, 4805 (1967).

109. Verkoczy, B., Sherwood, A.G., Safarik, I. and Strausz, O.P., Can. J. Chem., 61, 2268 (1983).

110. Torres, M., Lown, E.M. and Strausz, O.P., Heterocycles, 11, 697 (1978).

111.a) Krantz, A. and Laureni, J., J. Am. Chem. Soc., 96, 6768 (1974).
b) Torres, M., Clement, A., Bertie, J.E., Gunning, H.E. and Strausz, O.P., J. Org. Chem., 43, 2490 (1978).

112. Torres, M., Clement, A., Gunning, H.E. and Strausz, O.P., Nouv. J. Chim., 3, 149 (1979).

113. Little, D.J. and Donovan, R.J., J. Photochem., 1, 371 (1972).

114. Verkoczy, B., Ph.D. Thesis, University of Alberta, 1981.

115. Ogi, K. and Strausz, O.P., unpublished results.

116. Schaub, W.M., Burks, T.L. and Lin, M.C., J. Phys. Chem., 86, 757 (1982).

117. Csizmadia, I.G., Gunning, H.E., Gosavi, R.K. and Strausz, O.P., J. Am. Chem. Soc., 95, 133 (1973).

118. Strausz, O.P., Gosavi, R.K., Denes, A.S. and Csizmadia, I.G., J. Am. Chem. Soc., 98, 4764 (1976).

119. Strausz, O.P., Gosavi, R.K. and Gunning, H.E., Chem. Phys. Lett., 54, 510 (1978).

120. Shaub, W.M., Burks, T.L. and Lin, M.C., Chem. Phys., 45 455 (1980).

121. Peters, J., Schaekers, M. and Vinckier, C., J. Phys. Chem., 90, 6552 (1986).

122. Löhr, R. and Roth, P., Ber. Bunsenges., Phys. Chem., 85, 569 (1981).

123. Williamson, D.G. and Bayes, K.D., J. Phys. Chem., 73, 1232 (1969).

124. Taylor, D.R., Chem. Rev., 67, 317 (1967).

125. Green, M., Verkoczy, B., Lown, E.M. and Strausz, O.P., Can. J. Chem., 63, 667 (1985).

126. Block, E., Penn, R.E., Ennis, M.D., Owens, T.A., Yu, S.L., J. Am. Chem. Soc., 100, 7436 (1978).

127. Cvetanovic, R.J. and Doyle, L.C., Can. J. Chem., 38, 2187 (1960).

128. Havel, J.J. and Chan, K.H., J. Org. Chem., 39, 2439 (1974).

129. Nakamura, K. and Koda, S., Int. J. Chem. Kinet., 9, 67 (1977).

130. Havel, J.J., J. Am. Chem. Soc., 96, 530 (1974).

131. Lin, M.C., Shortridge, R.G. and Umstead, M.E., Chem. Phys. Lett., 37, 279 (1976).

132. Chan, T.H. and Ong. B.S., J. Org. Chem., 43, 2994 (1978).

133. Stockburger, L. III, and Heicklen, J., J. Am. Chem. Soc., 93, 3331 (1971).

134. Nicovich, J.M., Gump, C.A. and Ravishankara, A.R., J. Phys. Chem., 86, 1684 (1982).

135. Boocock, G. and Cvetanovic, R.J., Can. J. Chem., 39, 2436 (1961).

136. Sibener, S.T., Buss, R.J., Casavecchia, P., Hirooka, T., Lee, Y. T., J. Chem. Phys., 72, 4341 (1980).

137. Gaffney, J.S., Atkinson, R. and Pitts, J.N., Jr., J. Am. Chem. Soc., 98, 182 (1976).

138. Grovenstein, E. Jr. and Mosher, A.J., J. Am. Chem. Soc., 92, 3810 (1970).

139. Lee, J.H. and Tang, I.N., J. Chem. Phys., 75, 137 (1981).

140. Green, M., Lown, E.M. and Strausz, O.P., J. Am. Chem. Soc., 106, 6938 (1984).

141. Klemm, R.B. and Davis, D.D., Int. J. Chem, Kinet., 5, 149 (1973).

142. Slagle, I.R., Baiocchi, F. and Gutman, D., J. Phys. Chem., 82, 1333 (1978).

143. Singleton, D.L., Irwin, R.S. and Cvetanovic, R.J., Can. J. Chem., 61, 968 (1983).

144. Cvetanovic, R.J., Singleton, D.L. and Irwin, R.S., J. Am. Chem. Soc., 103, 3530 (1981).

145. Lee, J.H., Timmons, R.B. and Stief, L.J., J. Chem. Phys., 64, 300 (1976).

146. Slagle, I.R., Graham, R.E. and Gutman, D., Int. J. Chem. Kinet., 8, 451 (1976).

147. Tevault, D.E., Mowery, R.L. and Smardzewski, R.R., J. Chem. Phys., 74, 4480 (1981).

148. Singleton, D.L. and Cvetanovic, R.J., J. Phys. Chem. Ref. Data, 17, 1377 (1988).

149. De Sorgo, M. Ph.D. Thesis, University of Alberta, 1968.

150. Schofield, K., J. Phys. Chem Ref. Data, 8, 723 (1979).

151. Clyne, M.A.A. and Whitefield, P.D., J. Chem. Soc., Faraday Trans. 2, 75, 1327 (1979).

152. Little, D.J., Dalgleish, A. and Donovan, R.J., Faraday Discuss. Chem. Soc., 53, 211 (1972).

153. Breckenridge, W.H. and Taube, H., J. Chem. Phys., 53, 1750 (1970).

154. Donovan, R.J. and Husain, D., Chem Rev., 70, 489 (1970).

155. Plotkin, J.S. and Sneddon, L.G., J. Am. Chem. Soc., 99, 3011 (1977).

156. O'Callaghan, W.B., Ph.D. Thesis, University of Alberta, 1970.

157. Messner, A.E., Rosie, D.M. and Argabright, P.A., Anal. Chem., 31, 230 (1959).

158. Horie, O., Kawamata, K., Onuki, K. and Amono, A., Chem. Lett., 753 (1976).

159. Allinger, N.L., Cava, M.P., de Jongh, D.C., Johnson, C.R., Lebel, N.A. and Stevens, C.L., Organic Chemistry, 2nd Ed., Worth Publishers, Inc., 1976

160. Davis, R.E., J. Org. Chem., 23, 1380 (1958).

161. Kablunde, K.J. and Skell, P.S., J. Am. Chem. Soc., 93, 3807 (1971).

162. Takeguchi, H., Nagai, T. and Tokura, N., Bull. Chem. Soc. Jpn., 46, 695 (1973).

163. Sidhu, K.S., Ph.D Thesis, University of Alberta, 1965.

164. Braslavsky, S. and Heicklen, J., Can. J. Chem., 49, 1316 (1971).

165. Scala, A.A., Colon, I. and Rourke, W., J. Phys. Chem., 85, 3603 (1981).

166. Miller, J.A. and Neuzil, E.F., Modern Experimental Organic Chemistry, D.C. Heath and Company, 1980.

167. Jackman, L.M. and Sternhell, S., International Series of Monographs in Organic Chemistry, Vol 5: Applications of Nuclear Magnetic Resonance Spectroscopy in Organic Chemistry. 2nd Ed., 1969.

168. Lam, W.W., Ph.D. Thesis, University of Alberta, 1988.

169. Goldstein, E., Hammond, B.L., Sadri, B. and Hsia, Y., J. Mol. Struct., 105, 315 (1983).

170. Moss, S.J. and Jennings, K.R., Trans. Faraday Soc., 65, 415 (1969).

171. Neureiter, N.P. and Bordwell, F.G., J. Am. Chem. Soc., 81, 578 (1959).

172. Günther, H., NMR - Spektroskopie, Thieme, Stuttgart (1973).

173. Otter, A., Neuenschwander, M. Kellerhals, H.P., Magn. Reson. Chem., 24, 353 (1986).

174. Escher, A., Bönzli, P., Otter, A., Neuenschwander, M., Magn. Reson. Chem., 24, 350 (1986).

175. Clark, L.B. and Simpson, W.T., J. Chem. Phys., 43, 3666 (1965).

176. Otter, A., private communication.

177. Wray, V., Ann. Rep. NMR Spectrosc., 14 (1983).

178. Levine, I.N., Physical Chemistry, McGraw-Hill Book Company, New York, 1978.

179. Cvetanovic, R.J., Gunning, H.E. and Steacie, E.W.R., J. Chem. Phys., 31, 573 (1959).

180. Cundall, R.B. and Palmer, T.F., Trans. Faraday Soc., 56, 1211 (1960).

181. Schmidt, M.W. and Lee, E.K.C., J. Chem. Phys., 51, 2024 (1969).

182. Clark, J.H., Leary, K.M., Loree, T.R. and Harding, L.B., Springer Ser. Chem. Phys., 3, (Adv. Laser Chem.), 74 (1978).

183. Graham, D.M., Mieville, R.L. and Sivertz, C., Can. J. Chem., 42, 2239 (1964).

184. Craig, N.C., Piper, L.G. and Wheeler, V.L., J. Phys. Chem., 75, 1453 (1971).

185. Strausz, O.P., Hikida, T. and Gunning, H.E., Can. J. Chem., 43, 717 (1965).

186. Moss, S.J. and Rattanaphani, S., J. Chem. Soc., Faraday Trans. 1, 78, 3053 (1982).

187. Gilbert, J.R., Slagle, I.R., Graham, R.E. and Gutman, D., J. Phys. Chem., 80, 14 (1976).

188. Sanhueza, E. and Heicklen, J., Int. J. Chem. Kinet., 6, 553 (1974).

189. Sanhueza, E. and Heicklen, J., J. Photochem., 4, 1 (1975).

APPENDIX A

Extinction Coefficient Values, ε(10 x cm^{-1} $Torr^{-1}$)

Compound[a]	Wavelength (nm)						
	225	230	235	240	245	250	260
COS	4.10	3.45	2.33	1.32	0.675	0.325	0.110
THT	43.3	38.9	11.2	4.9	2.4	1.6	0.68
$CH_3CF=CH_2$	0.172	0.129	0.100	0.072	0.050	0.029	0.022
FMT	1.18	1.05	1.15	1.31	1.51	1.63	1.69
2,2FPT	6.34	5.12	3.93	2.98	2.07	1.42	0.77
Z-2,1FPT	2.97	1.76	1.31	1.10	0.883	0.700	0.413
DMT's	~2.4[b]	~1.2	~0.6	~0.7	~0.9	~0.9	~1.0
trans-$C_2H_2F_2S$	0.505	0.718	0.802	0.673	0.435	0.191	0.0
cis-$C_2H_2F_2S$	4.07	3.70	3.19	2.61	2.11	1.75	1.30
trans-$C_2H_2Cl_2S$	11.69	12.26	15.58	9.89	6.26	0.977	1.08

a Key to abbreviations: THT=tetrahydrothiophene, FMT=2-fluoro-2-methylthiirane, 2,2FPT=2-fluoro-2-propene-1-thiol, Z-2,1FPT=Z-2-fluoro-1-propenethiol, DMT=2,3-dimethylthiirane

b Values for ε of DMT estimated from UV spectrum of methylthiirane reported in Reference 173.

APPENDIX B-1

Mass Spectral Data for C_3H_5FS Isomers

m/e	Relative Intensity		
	1[a]	2[b]	3[c]
92	83.6	100.0	60.9
59	100.0	94.7	60.9
45	89.1	56.1	80.1
39	39.2	55.4	23.7
71	29.3	16.3	25.0
46	36.1	13.1	29.9
47	28.6	28.7	100.0
72	19.8	12.0	7.6
33	18.1	41.0	14.1
57	14.5	20.5	9.9
60	9.2	4.3	11.0

a Product **1** is 2-fluoro-2-methylthiirane (FMT)

b Product **2** is 2-fluoro-2-propene-1-thiol (2,2FPT)

c Product **3** is Z-2-fluoro-1-propenethiol (Z-2,1FPT)

APPENDIX B-2

Mass Spectral Data for C_4H_8S Isomers

m/e	Relative Intensity	
	trans-DMT	cis-DMT
59	100.0	100.0
88	92.2	91.1
55	84.4	77.2
45	56.8	55.1
60	46.2	48.0
27	41.9	41.5
39	34.3	35.3
29	30.0	28.3
54	20.8	19.0
41	19.0	23.8
73	18.4	18.3
53	18.6	17.7
28	15.7	19.8

APPENDIX B-3

Mass Spectral Data for $C_2H_2F_2S$ Isomers

m/e	Relative Intensity	
	trans-DMT	cis-DMT
45	100.0	100.0
96	99.2	88.0
63	77.4	70.6
32	42.6	19.4
33	38.3	42.2
76	29.0	28.3
77	12.9	30.6
31	14.5	16.4
57	13.4	10.1
64	14.0	13.3
44	11.3	9.3

APPENDIX B-4

Mass Spectral Data for $C_2H_2Cl_2S$ Isomers

m/e	Relative Intensity	
	trans-DMT	cis-DMT
61	11.3	100.0
96	6.2	86.3
45	100.0	35.7
128	91.7	11.5
130	62.4	7.1
132	11.6	
98	3.9	56.5
100	0.6	9.1
63	3.4	31.2
58	42.7	8.7
93	46.4	3.1
87	36.9	
79	18.4	3.5